University of Southampton

Faculty of Medicine

Clinical and Experimental Sciences

Investigating lipid-responsive T cells in tuberculosis; paving the way for new lipid-based vaccines

https://doi.org/10.5258/SOTON/D1977

by

Jennie Suzanne Gullick

ORCID ID 0000-0002-3612-1926

Thesis for the degree of Doctor of Philosophy

September 2021

University of Southampton

Abstract

Faculty of Medicine

Clinical and Experimental Sciences

Doctor of Philosophy

Investigating lipid-responsive T cells in tuberculosis; paving the way for new lipid based vaccines

by

Jennie Suzanne Gullick

Mycobacterium tuberculosis (M.tb), which causes Tuberculosis (TB), remains one of the leading causes of death worldwide. The lack of an effective vaccine and the persistence of multi-drug resistant strains highlights the urgent need for improved therapeutic interventions for TB. Unconventional T cells, including CD1-restricted T cells, represent potential targets for future therapeutics due to the non-polymorphic nature of CD1 and the ability to respond to lipid antigens such as those found in the lipid-rich cell wall of *M.tb.* Although subsets of CD1c-restricted T cells specifically recognise mycobacterial lipids, the majority of T cells restricted by CD1c exhibit autoreactivity as they recognise CD1c bound to self-lipids. Importantly, these autoreactive T cells exhibit dual recognition of both foreign, pathogen derived lipid antigens and self-derived lipids when bound to CD1c. This may indicate a role for CD1c-restricted T cells in TB infection, but their exact function remains unknown. To investigate the hypothesis that "CD1c autoreactive T cells modulate the host-pathogen interaction in human TB infection", I first investigate molecular mechanisms that underpin CD1c recognition by a cognate TCR. I employed methods such as site directed mutagenesis and lipid pulsing to investigate TCR binding footprint and lipid antigen reactivity, respectively. I demonstrate that binding of a CD1c autoreactive αβTCR is likely focused away from the F' roof of CD1c, but further molecular studies are required to unravel exact binding footprint. Furthermore, I identified that this TCR also exhibits promiscuous recognition of various self-derived lipid cargo when bound to CD1c, but recognition is augmented by adjustments in the lipid alkyl chains suggesting a novel mechanism of recognition driven by a degree of fine specificity for lipid alkyl chains. Using CD1c tetramer guided cell sorting, I demonstrate the isolation and cloning of bona fide CD1c autoreactive γδTCRs. New TCRs can be employed in future studies to unravel the molecular mechanisms underpinning their binding to CD1c. Next, I optimised a short-term culture assay to investigate CD1c autoreactive T cells in a small cohort of healthy donors. My results showed that these responses are present in the circulation and they readily expand *in vitro* in response to $CD1c^+$ APC with the majority of expanded cells exhibiting a $CD4^-CD8^-$ phenotype. I then go on to investigate CD1c immunity in the context of *M.tb* infection. I show for the first time using immunohistochemistry that both γδ T cells and $CD1c^+$ cells are present in the lungs of TB patients, but are largely found away from areas of caseous necrosis and reside in inflammatory tissue distal to the infection focus. Moreover, in a cohort of South African TB patients, I demonstrate an increased frequency of CD1c autoreactive αβ T cells in the peripheral blood and CD1c autoreactive $V\delta1^+$ T cells in the lungs when compared to healthy controls. My results also reveal that lung resident $V\delta1^+$ T cells of TB patients express elevated levels of PD1 compared to uninfected controls, suggesting that these cells had become activated and then exhausted in response to antigen. Taken together, my results suggest that *M.tb* drives CD1c mediated responses *in vivo*, indicating an important role for CD1c mediated immune responses in the host pathogen interaction in TB.

I also investigated the hypothesis that “CD1d-restricted iNKTs are associated with disease severity” in the macaque model of infection. I carried out longitudinal studies in the peripheral blood of a small cohort of macaques, pre- and post-*M.tb* challenge, to monitor iNKT numerical and functional changes. My results demonstrate an increase in iNKT frequency at 8 weeks post challenge, however proliferative responses following stimulation with the strong iNKT agonist α-Galactosylceramide (α-GalCer) were impaired. Recovery of the proliferative response at the 4 week time point was observed in some animals, but due to the small cohort size no correlations could be made with lung iNKT frequency, bacteriology and pathology scores at the time of necropsy. Finally, I demonstrate the generation of Cynomolgus macaque CD1c tetramers (mCD1c). In comparison to human CD1c tetramers, positive staining of macaque T cells was observed with the mCD1c tetramer. Further validation of this tool is required in order to utilise these tetramers to study CD1c-restricted T cells in future *M.tb in vivo* challenge studies.

Table of Contents

Table of Tables

Table of Figures

Table of Figures

List of Accompanying Materials

DOI: https://doi.org/10.5258/SOTON/D1977

Research Thesis: Declaration of Authorship

Print name: Jennie Suzanne Gullick

Title of thesis: Investigating lipid-responsive T cells in tuberculosis; paving the way for new lipid-based vaccines

I declare that this thesis and the work presented in it are my own and has been generated by me as the result of my own original research.

I confirm that:

1. This work was done wholly or mainly while in candidature for a research degree at this University;
2. Where any part of this thesis has previously been submitted for a degree or any other qualification at this University or any other institution, this has been clearly stated;
3. Where I have consulted the published work of others, this is always clearly attributed;
4. Where I have quoted from the work of others, the source is always given. With the exception of such quotations, this thesis is entirely my own work;
5. I have acknowledged all main sources of help;
6. Where the thesis is based on work done by myself jointly with others, I have made clear exactly what was done by others and what I have contributed myself;
7. None of this work has been published before submission

Signature: ..... Date: 27th September 2021

Acknowledgements

Firstly, I would like to thank Dr Sally Sharpe and Dr Andrew White for the role they have played in helping me to start my career. I thoroughly enjoyed my time working at Public Health England and I greatly appreciate the ongoing support and opportunities they have provided throughout my PhD.

Secondly, I would like to thank Dr Al Leslie and all of the team at the Africa Health Research Institute in Durban, South Africa for welcoming me into their lab and generously providing me with not only the resources, but also for their support and guidance. I am most grateful for the opportunity to have worked in such a world leading institute.

I'd also like to thank everyone on Level E for their unwavering support and friendship, the encouragement and stimulating discussions have been invaluable to me. Finally, I'd like to thank my supervisors Dr Salah Mansour and Professor Paul Elkington for their consistent encouragement and support. I am incredibly grateful for the opportunities and patience you have offered me and the enthusiasm for the research has been contagious. I feel extremely lucky to have been a part of the CD1-TB group and I could not have asked for better supervisors.

Definitions and Abbreviations

α-GalCer ..... alpha-Galactosylceramide

Ac_2SGL ..... Diacylated Sulfoglycolipid

AIDS ..... Acquired Immune Deficiency Syndrome

AIM ..... Activation Induced Marker

AP-3 ..... Adaptor Protein 3

β_2m Beta-2-microglobulin

BAL ..... Bronchoalveolar Lavage

BCG ..... Bacillus Calmette-Guérin

BSA ..... Bovine Serum Albumin

CD1 ..... Cluster of Differentiation 1

CDR ..... Complementarity-determining Region

CFP-10 ..... 10-kDa Culture Filtrate Protein

CMV ..... Cytomegalovirus

CTV ..... Cell Trace Violet

DC ..... Dendritic Cell

DDM ..... Didehydroxymycobactin

DN ..... Double Negative

ECM ..... Extracellular Matrix

ELISA ..... Enzyme-linked Immunosorbent Assay

ELISPOT ..... Enzyme-linked Immune Absorbent Spot

EPCR ..... Endothelial Protein C Receptor

ESAT-6 ..... 6-kDa Early Secretory Antigenic Target

FACS ..... Fluorescence Activated Cell Sorting

FBS ..... Foetal Bovine Serum

FPLC ..... Fast Protein Liquid Chromatography

GEM ..... Germline-encoded Mycolyl Specific T cell

GM-CSF ..... Granulocyte Monocyte-Colony Stimulating Factor

GMM..... Glucose Monomycolate

GroMM ..... Glycerol Monomycolate

HIV ..... Human Immunodeficiency Virus

HLA..... Human Leukocyte Antigen

HPLC..... High Performance Liquid Chromatography

ICS ..... Intracellular Cytokine Staining

IFN..... Interferon

IL ..... Interleukin

ILT4 ..... Immunoglobulin-like Transcript 4

iNKT..... Invariant Natural Killer T cell

IP-10..... Interferon Gamma-induced Protein 10-kDa

IV..... Intravenous

KO ..... Knockout

LAM..... Lipoarabinomannan

LPA ..... Lysophosphatidic Acid

LPC ..... Lysophosphatidylcholine

LPS..... Lipopolysaccharide

LTBI ..... Latent Tuberculosis Infection

MA ..... Mycolic Acids

MACS ..... Magnetic Activated Cell Sorting

MAG..... Monoacylglycerol

MAIT ..... Mucosal-associated Invariant T cells

MAMPS..... Microbe Associated Molecular Patterns

ManLAM ..... Mannose-capped Lipoarabinomannan

M.bovis ..... *Mycobacterium bovis*

mCD1c..... Macaque CD1c

MDR-TB..... Multidrug Resistant Tuberculosis

MFI ..... Median Fluorescence Intensity

MHC ..... Major Histocompatibility Complex

MICA/MICB ..... MHC Class I-related Chains A and B

mLPA ..... Methyl-lysophosphatidic Acid

M.marinum ..... *Mycobacterium marinum*

MoDC ..... Monocyte-derived Dendritic Cell

MPD..... Mannosyl-β1-phosphodolichol

MPM..... Mannosyl-β1-phosphomycoketide

MR1..... Major Histocompatibility Complex Class I Related Protein

M.tb..... *Mycobacterium tuberculosis*

NHP ..... Non-Human Primate

NMR ..... Nuclear Magnetic Resonance

PBMC..... Peripheral Blood Mononuclear Cell

PBS ..... Phosphate Buffered Saline

PC ..... Phosphatidylcholine

PCR ..... Polymerase Chain Reaction

PD1 ..... Programmed Cell Death Protein 1

PDL1 ..... Programmed Death-ligand 1

PE ..... Phosphatidylethanolamine

PET-CT ..... Positron Emission Tomography-Computed Tomography

PG..... Phosphatidylglycerol

PHE..... Public Health England

PI ..... Phosphatidylinositol

PM ..... Phosphomycoketide

PMA..... Phorbal Myristate Acetate

PPD..... Purified Protein Derivative

PRR ..... Pattern Recognition Receptors

RANTES..... Regulated On Activation, Normal T Cell Expressed And Secreted

RLU..... Relative Light Units

ROI ..... Reactive Oxygen Intermediates

RU ..... Response Units

SDS-PAGE ..... Sodium Dodecyl Sulphate-Polyacrylamide Gel Electrophoresis

SL..... Spacer Lipids

SL-1 ..... Sulfolipid-1

SM..... Sphingomyelin

SPR ..... Surface Plasmon Resonance

TAP-1..... Transporter Associated with Antigen Processing 1

TB ..... Tuberculosis

TCR..... T Cell Receptor

TLR ..... Toll Like Receptor

TNF..... Tumour Necrosis Factor

WHO ..... World Health Organisation

WT..... Wild Type

XDR-TB ..... Extensively Drug Resistant TB

Chapter 1 Introduction

1.1 Tuberculosis

Tuberculosis (TB) is one of the greatest causes of death worldwide from a singular infectious agent, classifying above HIV/AIDS (1). The causative agent of TB, *Mycobacterium tuberculosis* (*M.tb),* is thought to have infected a third of the world's population, with 10 million new cases of TB being reported in 2019 along with an estimated 1.2 million fatalities (1, 2). There is a 5-15% lifetime risk of developing active TB, but for individuals with HIV coinfection, the risk of disease progression is 20 to 30 times more likely (1-3). Of the new TB cases reported in 2019, 25% of these occurred in Africa with South Africa being one of the eight countries contributing to two thirds of the total cases globally (1). Pulmonary TB accounts for 70% of incidences, but extrapulmonary disease affecting the lymph nodes, bones and meninges of the brain can arise through disease dissemination (2). As part of the End TB strategy, the World Health Organisation (WHO) have set a target of a 90% reduction in deaths and an 80% decline in TB incidence by 2030 (1). Additional milestones included a 20% reduction in TB incidence between 2015 and 2020, however on a global scale, the rate of prevalence did not fall fast enough to reach this target as the global cumulative reduction was just 9% (1). The global number of TB related deaths also fell short of the 2020 target of a 35% reduction in fatalities, with just a 14% reduction worldwide (1). Although some individual regions are making good progress towards the 2030 targets, there are still areas which are falling too short of the objectives. TB is a preventable and curable disease, however there needs to be a major breakthrough in measures preventing the progression from latent to active disease in those already infected (1). Control of the TB epidemic has proved challenging due to a combination of the emergence of drug resistant TB, variable efficacy of the only licensed vaccine, and the lack of a rapid and sensitive diagnostic (2). Currently there are only two prevention services: preventative treatment of latent disease progressing to active TB, and the Bacillus Calmette-Guérin (BCG) vaccination which has failed to provide adequate protection. Despite vaccine studies and clinical trials, there has yet to be any successful output contributing to the reduction of the global burden (4, 5).

1.1.1 Mycobacterium tuberculosis

Mycobacterium tuberculosis (*M.tb)* was first identified in 1882 by Robert Koch, who verified that this isolated tubercle bacillus conclusively caused TB (6). The disease is spread from person to person by aerosolisation of the bacteria, coughed out of the lungs in droplets by an individual suffering from the active form of the disease. The bacteria-containing droplets are then inhaled by

another individual, which in most cases will be apprehended by the cells of the immune system leading to either destruction or containment of the pathogen. The successful suppression of *M.tb* can lead to Latent Tuberculosis Infection (LTBI), defined by the WHO as "a state of persistent immune response to *M.tb* without clinically manifested evidence of active disease" (1). However, the disease may become active when the bacteria overwhelm the immune system and the individual starts to exhibit symptoms.

Comprising approximately 40% of the cell envelope weight, the unique combination of lipids within the cell wall contributes to the survival of *M.tb* within the host as well as aiding its pathogenicity (7, 8) (Figure 1). Mycolic acids (MA) in the formation of a bilayer are a distinctive feature of mycobacterial cell envelopes, but the most abundant lipid on the surface is sulfolipid-1 (SL-1) which is only present in pathogenic mycobacterium species (7). The plasma membrane is largely comprised of glycerophospholipids (e.g. cardiolipin, phosphatidylglycerol, phosphatidylethanolamine, phosphatidylinositol), but some are also positioned on the cell envelope which may enable them to interact with cells of the host (8). The lipid composition of *M.tb* is highly adaptable, with cell wall components including phospholipids altering in response to factors such as the host immune response and environmental conditions (e.g. temperature, carbon sources, oxygen levels etc.) in order to survive (8).

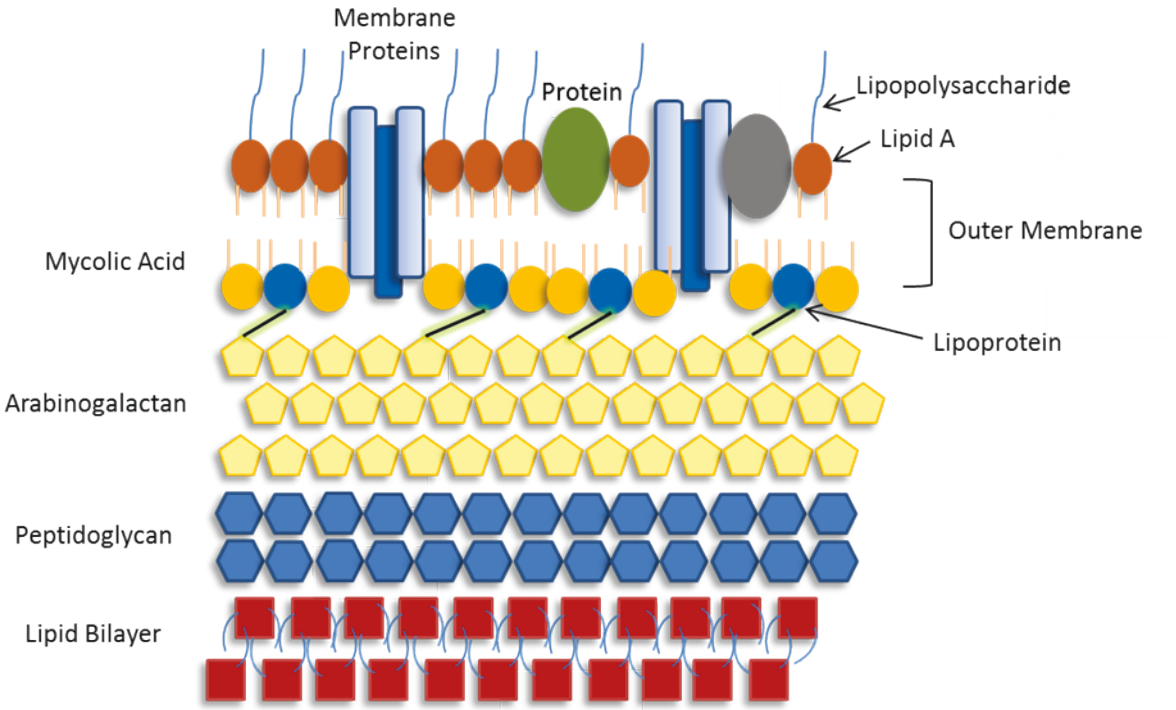

Figure 1: Cell wall of *M.tuberculosis*

The outer membrane of the lipid rich cell wall of *M.tb* is made up of lipoproteins, mycolic acids and lipopolysaccharide. Beneath this lies the arabinogalactan and peptidoglycan layers which sit above the lipid bilayer. Adapted from Ghazaei C. 2018 (7).

M.tb is an obligate human pathogen and survives within phagocytic cells such as macrophages (9). The development of the phagosome around the bacillus and the subsequent fusion to lysosomes increases acidification within the newly formed phagolysosome, leading to destruction of *M.tb* (10, 11). Enhanced immunity has been associated with the ability of infected macrophages to undergo apoptotic cell death, and as they are able to maintain their plasma membrane, release of the intracellular bacilli is prevented (12). However, *M.tb* can avoid this intracellular killing by preventing phagolysosomal fusion, subsequent acidification, and the acquisition of lysosomal markers by the phagosome (13, 14). Lipids within *M.tb* such as isotuberculosinol, mannose-capped lipoarabinomannan (ManLAM), and sulfolipids have been associated with maturation failure of phagosomes, and thus contribute to mycobacterial survival (8). The failure of phagocytes to kill intracellular *M.tb* may lead to necrotic cell death, which allows bacilli to escape and spread from cell to cell (13) (Figure 2).

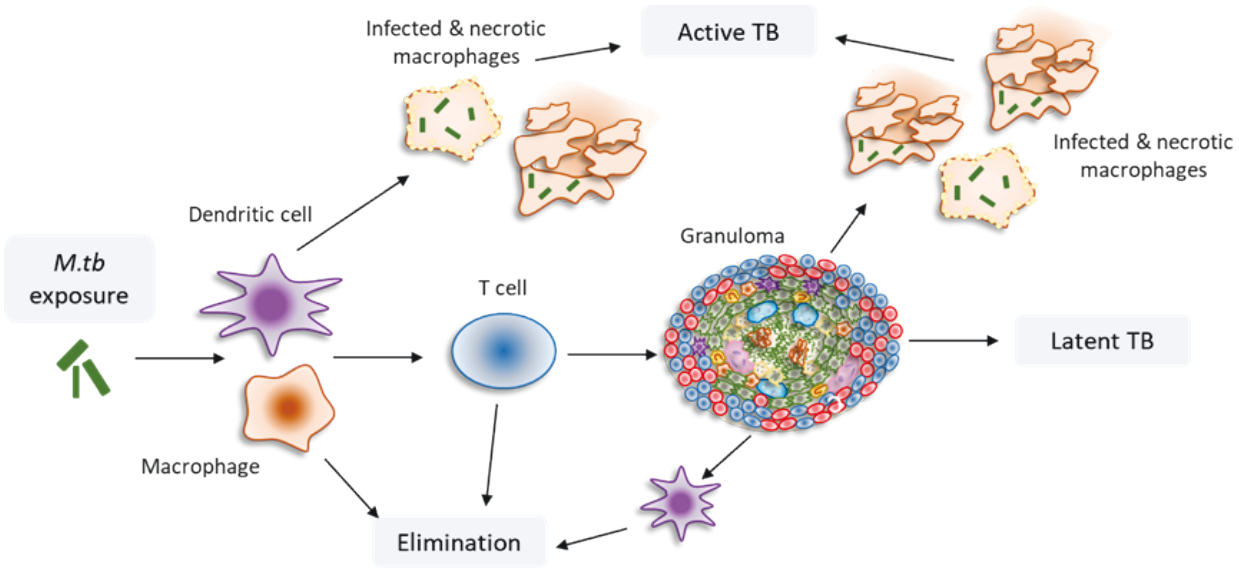

Figure 2: Cycle of TB infection

Inhalation of *M.tb* bacilli can lead to various outcomes: i) *M.tb* are eliminated by phagocytic dendritic cells and macrophages and further infection is prevented, ii) infected phagocytes are overwhelmed, become necrotic and release the pathogen allowing further spread, or iii) macrophages and dendritic cells activate T cells which then either eliminate bacteria or contribute to the formation of a granuloma to contain *M.tb* where it lays dormant (known as latent tuberculosis infection). Granuloma breakdown may occur following an immune system compromising event, in which case the *M.tb* are either eliminated by immune cells or become overwhelmed and active disease initiates.

In an attempt to limit the spread of disease, granulomas can form which are composed centrally of infected macrophages, giant cells, epithelioid cells and foamy macrophages (2, 15). Contributing to the containment of the bacilli are T cells, B cells and fibroblasts which surround the inner cells of the granuloma and aid the prevention of live bacteria coming into contact with immune cells (2, 7, 15). However, this also provides an environment within the granuloma in which the bacteria can survive (16, 17) (Figure 3). In latent disease it has been proposed that bacilli are situated in a central area of hypoxia where their metabolic state is modified by a necrotic caseous core, whereas bacilli in active disease are capable of replication in peripheral oxygenated areas (6, 18).

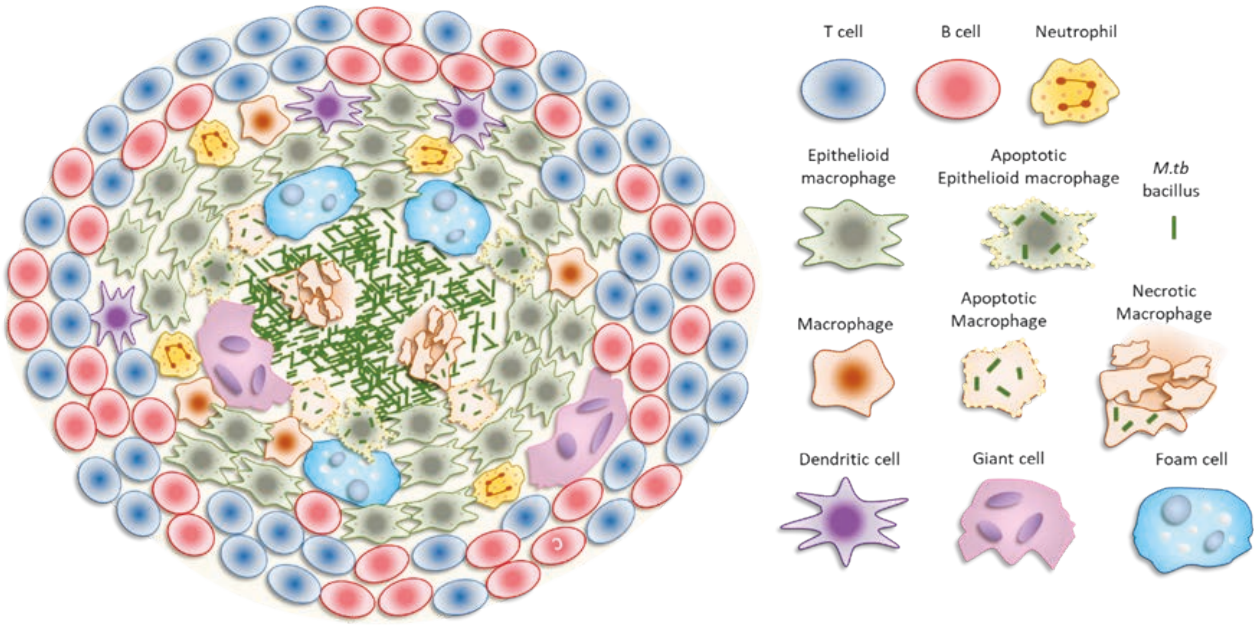

Figure 3: Cellular structure of a tuberculosis granuloma

Cartoon representation of the cellular structure of a granuloma formed following *M.tb* infection. Mycobacterial bacilli are released from necrotic macrophages and become surrounded by epithelioid cells, some of which phagocytose the bacteria and undergo apoptosis. Macrophages may also fuse to become multinucleated giant cells or differentiate into foam cells. More immune cells begin to accumulate including T cells, B cells, dendritic cells and neutrophils. Adapted from Ramakrishnan 2012 (19).

1.1.2 Host response

The host response to *M.tb* infection is extremely complex, and as of yet, is not fully understood. When droplets containing *M.tb* are inhaled that are small enough to evade the physical barriers of the respiratory tract, there are four potential outcomes. The initial immune response may inhibit infection by completely killing and eradicating the bacteria, or may prevent the development of disease by walling off the bacilli in granulomas. This defence however may become compromised and allow for growth and spread of the bacteria causing symptomatic disease, or a complete failure of the immune system to kill or contain *M.tb* in the first instance will lead to primary TB disease. The host response to TB, while appearing to be necessary for containing the infection, may also be a promoter of tissue destruction (3, 9).

During early infection, alveolar macrophages and dendritic cells (DC) in the lower respiratory tract come into contact with *M.*tb (2, 20, 21). Macrophages phagocytose the bacteria through binding to mannose receptors and complement receptors CR1, CR3 and CR4 (21), subsequently attempting to kill the engulfed bacilli through the production of reactive oxygen and nitrogen intermediates in addition to the fusion of phagosomes and lysosomes. DCs that have been

activated by *M.tb* secrete IL-12, stimulating T cells to produce IFNγ in an attempt to control the infection (2, 20). Production of IL-8 by macrophages also recruits T cells to the site of infection in addition to neutrophils and basophils (21). Increased levels of IL-8 have been demonstrated in the supernatant of cultured alveolar macrophages and in bronchoalveolar lavage (BAL) fluid taken from TB patients when compared to healthy controls (22).

The importance of T cells has been illustrated through animal models and studies of human disease. For example, mice defective in $CD4^+$ T cells and/or IL-12 are more susceptible to TB (23), and those with a $CD4^+$ T cell deficiency form granulomas at a slower rate than mice with an intact $CD4^+$ population (24). $CD4^+$ T cells are involved in the recruitment of other immune cells as well as the activation of effector cells at the site of infection. The significance of this T cell population in protective immunity is indicated by the increased susceptibility of HIV^+ individuals to TB, where the $CD4^+$ subset is diminished (25). Furthermore, these cells are crucial in the development of cytotoxic $CD8^+$ T cells (26). $CD8^+$ T cells are thought to contribute to the immune response against TB through secretion of IFNγ and other toxic compounds to induce apoptosis of target cells, as well as direct killing through ingestion of infected macrophages. Killing of *M.tb* infected macrophages has been reported by $CD8^+$ T cells that were CD1-restricted and able to recognise mycobacterial lipid antigens. These cells were demonstrated to function in a Fas-independent manner that resulted in the lysing of infected target cells through exocytosis of granzyme A (27). Although it has been shown that mice deficient in $CD8^+$ T cells and/or the IFNγ producing subset have diminished control over *M.tb* infection (28-30), an intact $CD8^+$ population is not able to compensate for a diminished $CD4^+$ count (2).

Cells of the innate response such as Invariant Natural Killer T (iNKT) and γδ T cells also contribute to antimicrobial immunity by secreting cytokines such as IFNγ and TNFα without the need for prior antigen priming (31). These T cells respond rapidly to foreign antigen invasion and act as the first line of defence by attempting to clear *M.tb* infection. If the bacteria are not eradicated, the host relies on the adaptive immune response to control the infection. The interaction of the host adaptive immune cells and pathogen occurs within the lung extracellular matrix (ECM). The ECM is necessary for regulation of cell survival in TB, but this must be destroyed before *M.tb* can spread (32-34). The use of 3D cell culture methods incorporating ECM components, more closely mimicking human disease than 2D culture, has demonstrated an increase in cell survival during TB infection with integrity of the ECM favouring the host rather than the pathogen (32, 35, 36).

1.1.2.1 Innate immune response

1.1.2.1.1 Macrophages

Upon inhalation, one of the first cells of the immune system to come into contact with *M.tb* are alveolar macrophages residing within pulmonary alveoli (2, 20). The main role of these cells are to phagocytose the pathogen to contain and destroy it before it can invade the host further. Pattern recognition receptors (PRRs) expressed on macrophages such as toll-like receptor (TLR)-2, -4 and -9 recognise *M.tb* microbe associated molecular patterns (MAMPS) and phagocytosis of the bacteria is initiated through the binding of mannose receptor; complement receptors CR1, CR3 and CR4; surfactant molecules and CD209 (21, 37-41). *M.tb* is then subsequently engulfed by the responding macrophage and becomes contained within a phagosome. The phagosome then fuses with lysosomes, increasing acidification in order to kill the engulfed bacilli (10, 11). This is also accompanied by the production of nitric oxide and reactive oxygen intermediates (ROI) to further facilitate the elimination of intracellular *M.tb* (21, 40, 42). Macrophages also recruit and activate additional cells of the immune system, releasing IL-18, Granulocyte Monocyte-Colony Stimulating Factor (GM-CSF), TNFα, IL-1β and IL-6 to summon T cells, neutrophils and basophils to the site of infection (21, 43-45). Infected macrophages, with *M.tb* still contained, may then undergo apoptotic cell death. This feature has been associated with improved protection as the apoptotic macrophages maintain their plasma membrane and so prevent the release of intracellular *M.tb* (12).

In spite of these mechanisms to kill intracellular bacilli and prevent dissemination, macrophages alone are not sufficient for controlling infection and *M.tb* has developed strategies to survive. While TLR-2 is used by macrophages to recognise pathogens and induce subsequent phagocytosis, TLR-2 recognised lipoproteins expressed by *M.tb* can hinder the upregulation of MHC class II in response to IFNγ (46, 47). MHC class I expression by macrophages may also be affected by ESAT-6 and CFP-10 expression by *M.tb*. In addition to the phagolysosome disruption functions of ESAT-6, this protein also combines with CFP-10 to sequester β-2-microglobulin (β_2m), subsequently inhibiting the expression of MHC class I molecules (48). The reduced expression of these antigen presenting molecules then hinders the initiation of the adaptive immune response. *M.tb* is also able to manipulate the internal environment within macrophages, inhibiting the production of ROI and nitrogen radicals and disrupting the phagolysosomal fusion (13, 14, 49, 50). The inability of phagosomes to fuse with lysosomes results in the macrophage undergoing necrosis, with cytolysis of the cell releasing the bacilli and allowing it to spread and infect neighbouring cells (13, 51-54).

1.1.2.1.2 Dendritic cells

Dendritic cells are a major antigen presenting cell population in the response to *M.tb* infection, bridging the gap between innate and adaptive immunity by effectively initiating the T cell response. Interaction between *M.tb* and DCs is a complex process that is not completely understood, however DC present in the airway are able to phagocytose bacilli which induces their maturation and subsequent migration (55, 56). DC infected with *M.tb* then migrate to the lungs and local draining lymph nodes within 8-12 days following exposure, facilitated by IL-12(p40)2 and IL-12p70 (57-59).

Once in the lung draining lymph nodes, DC carry out their most important function: initiating the activation of naïve T cells (20, 58, 60, 61). DC abundantly express both MHC and CD1 antigen presenting molecules, and two pathways have been suggested for the subsequent presentation of antigen to T cells: one involves the direct loading of MHC with antigens following *M.tb* entering into the DC cytosol, and the second suggests that cross-priming occurs after DC phagocytose apoptotic macrophages with *M.tb* antigens contained within vesicles (62-65). In addition to the production of inflammatory cytokines such as TNFα, IL-1α and IL-1β, activated DC secrete IL-12 to drive the development of a Th1 response (62, 66-69). The importance of IL-12 has been demonstrated by numerous studies; in humans the lack of IL-12p40 or IL-12 receptor gene is associated with poor DC migration and reduced IFNγ production by T cells (58, 59, 70, 71). Antibody based depletion has also highlighted the role of DC, with elimination of these cells being associated with faulty priming of $CD4^+$ T cells and elevated susceptibility to infection (61).

Although a number of studies report a positive role for DC in *M.tb* infection by initiating and strengthening the immune response (58, 62, 72), there are also reports of *M.tb* inhibiting their functions (56, 73). Evidence demonstrates that the migratory and stimulatory functions of DC are more efficient following *M.tb* exposure (57, 58, 74) and DC infection with *M.tb* does not reduce surface expression of MHC class II molecules (62, 63). There are even studies reporting an upregulation of MHC in response to infection, in addition to expression of CD54, CD58, CD80 and CD40, indicating DC activation (62, 75). In complete contrast, there is also evidence that CD209-facilitated entry of *M.tb* into DC interferes with the maturation process (56, 76) and their ability to activate T cells through the suppression of IL-12 and upregulation of IL-10 (56, 73, 77, 78). Additionally, *M.tb* may also interfere with the ability of DC to present antigen to T cells following migration to the lungs, further suppressing DC-mediated activation of the immune response (20, 79, 80).

Due to the level of contradictory reports regarding how *M.tb* affects the DC populations, it is still unclear exactly how DC function in response to infection but most studies agree that they are required for stimulation of the T cell response.

1.1.2.1.3 Neutrophils

Neutrophils are abundant in the airways of *M.tb* infected individuals and have been found to be the most predominantly infected cell type (81). However, despite some evidence suggesting neutrophils participate in protective immunity, their exact role is disputed and poorly understood. Neutrophils have been implicated in anti-*M.tb* immunity as both apoptotic neutrophils and neutrophil-derived granules have shown to reduce the viability of mycobacteria (82). *M.tb* infected macrophages are able to phagocytose neutrophils which then exert their protective functions from within, such as the release of antimicrobial granules which improve killing of intra-phagosomal bacilli (82, 83). Infected macrophages may also die by apoptosis which are then taken up by macrophages by efferocytosis, possibly contributing to control of infection (84). Stimulation of neutrophils also results in the production of TNFα, ROI and antimicrobial peptides, in addition to the recruitment of additional immune cells and boosting the priming of T cells (82, 85, 86).

Several studies have reported protective functions of neutrophils. Blomgran and colleagues have demonstrated that depletion of neutrophils hinders the migration of DC to lung draining lymph with a subsequent delay in $CD4^+$ T cell priming, while apoptotic neutrophils may facilitate this process (85, 86). Furthermore, a study involving contacts of TB patients reported that following neutrophil depletion, there was a substantial reduction in the release of antimicrobial peptides in response to *M.tb* and the ability to reduce mycobacterial viability was limited (87). In spite of this, neutrophils have been associated with advancement of pathology and disease progression through excessive antimicrobial protein production (88). Animal models used to investigate the role of neutrophils have revealed that destructive inflammation in the lungs and susceptibility to infection is influenced by an excessive accumulation of neutrophils, but depletion of these cells can improve outcomes in mice (89-91). In studies of human *M.tb* infection, neutrophils are found to express high levels of PDL1 which induces the loss of function of PD1 expressing T cells and therefore impairing the lymphocyte response (92). The conflicting evidence in addition to the difficulty in studying these cells *in vitro* indicates that our current knowledge of the role of the neutrophil in the immune response to *M.tb* infection is severely lacking. Further research is needed to uncover the predominant role of these cells during anti-*M.tb* immunity.

1.1.2.2 Adaptive immune response

1.1.2.2.1 Conventional $CD4^+$ T cells

$CD4^+$ T cells have long been implicated as one of the most important players in the host defence against *M.tb* infection. The dependency upon these cells has been consistently demonstrated in both humans and animal models of *M.tb* infection. Depletion or a complete absence of $CD4^+$ T cells in mice results in a slower rate of granuloma formation and markedly increased levels of fatality (23, 24, 93). Furthermore, depletion of $CD4^+$ T cells has been associated with reactivation in latent-like infection and an elevated mycobacterial burden in the lungs (94). This effect has also been observed in the Non-Human Primate (NHP) model, with antibody mediated depletion of $CD4^+$ T cells resulting in poor control of the disease following reactivation of latent infection (95). The link between an intact $CD4^+$ T cell population and the development of active TB disease is also observable naturally in humans, as HIV mediated depletion of $CD4^+$ T cells increases the susceptibility of HIV^+ individuals to contracting and succumbing to TB (25).

M.tb specific $CD4^+$ T cells are activated by mycobacterial-derived antigens presented by MHC class II molecules expressed by macrophages and DC. The presence of MHC class II molecules has been shown to be critical for the $CD4^+$ T cell mediated immune response to *M.tb* infection. MHC class II knockout mice have been reported to have reduced survival time and more severe lung pathology than those with intact MHC class II genes (24, 96). Furthermore, Srivastava and colleagues demonstrated the importance of the direct contact of $CD4^+$ T cells with infected APCs. Myeloid cells with a knockout of MHC class II were found to harbour a much greater bacterial load compared to wild type myeloid cells within the same lung (97). The hypothesis that contact between $CD4^+$ T cells and APCs is required for an effective response against *M.tb* was further supported by an increased bacterial load within both wild type and MHC class II knockout myeloid cells following $CD4^+$ T cell depletion (97). It has however been reported that antigen presentation by MHC class II in macrophages and the subsequent $CD4^+$ T cell mediated response is impaired following infection with *M.tb* in a Toll-like receptor 2-dependent manner (98-100). This represents one of the many mechanisms *M.tb* uses in order to evade eradication by the host immune response.

In addition to antigen-mediated activation, $CD4^+$ T cells also respond to IL-12 production by macrophages and DC and are polarised to a Th1 phenotype (70, 101). The interaction of CD40L expressed by $CD4^+$ T cells with $CD40^+$ DC is indicated as an essential event for the development, function and survival of antigen-specific $CD4^+$ T cells and has also been suggested to play a role in the maintenance $CD8^+$ T cell effector/memory functions (70, 102-105). Moreover, depletion of $CD11c^+$ DC has been shown to result in reduced control of *M.tb* infection through impaired $CD4^+$ T

cell priming, further demonstrating an important link between these two cellular compartments (61).

Perhaps the most important known function of $CD4^+$ T cells in the TB immune response is the production of IFNγ. Activated $CD4^+$ T cells produce copious amounts of IFNγ which in turn facilitates macrophage activation and phagosome maturation, resulting in the recruitment of more lymphocytes and elimination of phagosome-confined *M.tb* (70, 100, 106). In animal models, intracellular growth of *M.tb* appears to be unobstructed until IFNγ secreting $CD4^+$ T cells arrive in the lungs (93, 107). Increasing numbers of activated $CD4^+$ T cells are observable in the lungs of mice within 2-4 weeks of *M.tb* infection and display an effector/memory profile, suggesting interaction with APCs (108, 109). The importance of these cells during early infection has been demonstrated by $CD4^+$ T cell knockout mice presenting with reduced levels of IFNγ in the first few weeks post-challenge. IFNγ levels recovered by the 3 week mark following contribution by $CD8^+$ T cells, however the delay in reaching levels comparable to wild type mice was not sufficient to prevent development of TB disease (24, 110).

Although IFNγ clearly plays a critical role in the TB specific immune response, $CD4^+$ T cells have demonstrated to have control over *M.tb* infection in the absence of IFNγ production, but as of yet the exact mechanism of this is unknown (111, 112). Effector $CD4^+$ T cells are capable of producing a range of cytokines including IL-2 and TNFα in addition to IFNγ. Multifunctional T cells have been observed in individuals with latent TB infection and BCG vaccinated infants and has been associated with a protective response (113-115). On the other hand, monofunctional $CD4^+$ T cells producing solely TNFα have been linked to the development of active disease (116). It has also been suggested that migratory capabilities of $CD4^+$ T cells may be comparably, if not more important, than the secretion of IFNγ. Adoptive transfer of intravascular- or lung parenchyma-derived $CD4^+$ T cells into infection matched mice demonstrated the migration of parenchymal cells back to the lung. These cells displayed an activated phenotype and were associated with improved control of *M.tb* infection (117). In contrast, this migratory and protective behaviour was not observed in intravascular derived $CD4^+$ T cells, suggesting that the ability of T cells to home to the site of infection strongly correlates with protection (117).

1.1.2.2.2 Conventional $CD8^+$ T cells

While $CD4^+$ T cells are believed to have a leading role in the immune response to *M.tb* infection, evidence demonstrates that $CD8^+$ T cells are also vital for effective control. $CD8^+$ T cells recognise peptide antigens presented by MHC class I molecules expressed on the surface of professional APCs (118). Similar to $CD4^+$ T cells, mycobacteria-specific $CD8^+$ T cells have been reported to appear in the lung draining lymph nodes of *M.tb* infected mice after approximately one week,

with peak lung frequencies observed at the 5-8 week time point (108, 109, 119). MHC class I-restricted $CD8^+$ T cells specific for mycobacterial antigens have been isolated from *M.tb* infected, or BCG immunised hosts and analysis has revealed several peptides recognised by these T cells including 19-kDa, 38-kDA and 65-kDA heat shock protein (120-122). Furthermore, $CD8^+$ T cells specific for CFP-10 and ESAT-6 derived epitopes have been identified in *M.tb* exposed or *M.tb* infected individuals at relatively high frequencies within the total $CD8^+$ T cell population (1/700) (123-126).

Two of the principal effector functions of $CD8^+$ T cells in TB are to produce cytokines such as IFNγ, TNFα and IL-2 and to induce direct killing of infected cells (118, 127). Following activation, $CD8^+$ T cells can directly lyse infected cells through the production of perforin and granulysin (128-130). The secretion of perforin creates pores, lysing infected macrophages and allowing for the influx of granulysin which is then responsible for the death of intracellular bacteria (131, 132). Although $CD4^+$ T cells are the predominant producers of IFNγ, $CD8^+$ T cells also contribute substantially. Mice deficient in $CD4^+$ T cells initially present with diminished IFNγ levels early on in *M.tb* infection, but recovery of this cytokine is largely due to the production by $CD8^+$ T cells following a short delay (24).

This IFNγ contribution by $CD8^+$ T cells may be vital, as mice deficient in IFNγ producing $CD8^+$ T cells have impaired control over *M.tb* infection (29, 30, 110). The requirement for conventional MHC class I-restricted $CD8^+$ T cells for optimal control of infection has been demonstrated by numerous studies (30, 132, 133). Mouse models with a knockout of β_2m or the class I heavy chain have revealed that infected mice have a substantially reduced survival time and increased bacterial burden was observed within granulomas when compared to wild type mice, demonstrating the role of $CD8^+$ T cells in *M.tb* control (30, 70). The importance of the ability of $CD8^+$ T cells to recognise MHC class I presented peptides has also been demonstrated by TAP-1 knockout models. TAP-1 is necessary for the loading and presentation of antigens by MHC class I molecules after acquisition from the cytoplasm, facilitating the presentation to $CD8^+$ T cells in as little as 12 hours post infection (109, 134). However, mice with a knockout of TAP-1 display increased susceptibility and rapid progression of disease due to a lack of a $CD8^+$ T cell mediated response (132, 134). Long term protection has also been associated with an intact $CD8^+$ T cell population, as depletion during the chronic stage of infection results in a greater bacterial burden in mice, demonstrating that $CD8^+$ T cells are critical for sustained control (29).

Despite evidence indicating the requirement of $CD8^+$ T cells for an effective immune response, they do not compensate for a lack of $CD4^+$ T cells alone. This is supported by the susceptibility of HIV^+ patients to coinfection with TB, in addition to studies demonstrating that $CD4^+$ T cell

knockout mice are unable to control infection despite all other IFNγ producing cells being intact and present (2, 135). Furthermore, $CD4^+$ T cells have been indicated as being crucial for the development of cytotoxic $CD8^+$ T cells, with MHC class II deficient mice exhibiting a suboptimal $CD8^+$ T cell response due to the inability of conventional $CD4^+$ T cells to activate in response to antigen and subsequently support $CD8^+$ T cell functions (26).

1.1.2.3 Unconventional T cells

Conventional T cells bear an αβ T cell receptor (TCR) and recognise a vast array of peptide antigens presented by MHC class I and II proteins. The highly polymorphic nature of these antigen presenting molecules subsequently leads to highly varied, donor-specific T cell populations directed against diverse antigenic peptides (136, 137). In contrast, unconventional T cells recognise non-peptidic antigens and use invariant or semi-invariant TCRs that are highly conserved among the human population (136, 138, 139). Unconventional T cells include CD1-restricted T cells, mucosal-associated invariant T cells (MAIT), iNKT and γδ T cells and together they make up approximately 10% of peripheral blood T cells which have a tendency to accumulate in non-lymphoid tissues (136, 140).

While conventional T cells require a relatively long antigenic priming period of days to weeks in order to reach an appropriate quantity of effector T cells from clonal expansion, naïve unconventional T cells by comparison display faster antigen-responding kinetics and mount a response within hours to days of exposure (119, 136, 141, 142). The importance of the conventional T cell response has been demonstrated in the context of HIV infection, as the reduction in $CD4^+$ T cells is associated with a substantially increased risk of developing active TB, and $CD8^+$ T cell knockout mice are unable to control *M.tb* infection subsequently leading to a reduced survival time (70, 143-145). However, unconventional T cells have also been shown to be critical in the control of infection with adoptive transfer of γδ T cells or MA specific, CD1b-restricted T cells conferring protection against *M.tb* (146-148). Furthermore, MR1 or CD1d knockout mice have demonstrated subsequent deficiencies in MAIT and iNKT cells which is associated with reduced control and poorer outcomes following *M.tb* infection (141, 149, 150). The ability of unconventional T cells to quickly respond to antigenic challenge, interact with other cells of the immune system, and display some memory-like functions have led to these cells being often described as bridging the gap between innate and adaptive immunity (151).

1.1.2.3.1 iNKT cells

Immunity to *M.tb* requires the interplay between both the innate and adaptive immune system, with control of the disease being associated with a type 1 cytokine response. iNKT cells have been

implicated as critical players of the innate response in tackling disease effectively, despite making up a mere <0.01-1% of the circulating T cell population (152). These unconventional αβ T cells express a semi-invariant TCR comprised of a Vα24-Jα18 chain paired with a Vβ11 chain (153). In humans iNKTs are mainly located in adipose and the liver, with smaller populations found in the spleen, peripheral blood, lymph nodes and thymus (154). iNKTs develop in the thymus from common lymphoid progenitors and, unlike conventional T cells, are selected by $CD4^+$ and $CD8^+$ double positive thymocytes expressing CD1d presenting lipid antigens (153, 155). Upregulation of the transcription factors Egr2 and PLZF are induced through strong TCR signalling which are required for iNKT cell development (156-159).

iNKT cells can be classified into different subsets based on their co-receptor expression; $CD4^+$, $CD8^+$ or DN, or their cytokine profile in which they can be classified as NKT1, NKT2 or NKT17 (160-162). The NKT1 subsets exhibit a Th1 like profile, secreting IFNγ and TNFα, while NKT2 are more similar to Th2 cells by their secretion of IL-4 and IL-13. In contrast, NKT17 cells characteristically express IL-17a, IL-21 and IL-22 (160, 162). Unlike conventional αβ T cells, iNKT cells recognise lipid antigens presented by CD1d including host-derived lipids such as sulfatide and phosphatidylinositol (PI) (163). The most well characterised CD1d-presented ligand for iNKTs however is α-galactosylceramide (α-GalCer), a sphingolipid isolated from the marine sponge Agelas mauritianus (164). CD1d presented α-GalCer is commonly used as a potent agonist for iNKTs, inducing the production of a number of Th1 (e.g. IFNγ and TNFα) and Th2 cytokines such as IL-4, IL-5, IL-13 and IL-10 (165, 166). The role of iNKTs also extends to promoting DC maturation; specific, adaptive T cell responses; and providing B cells with help signals (167, 168)

It has been documented by multiple studies that the iNKT population is decreased in patients with active TB disease (169-171). The deficiency of iNKTs in those with both pulmonary and extrapulmonary TB has been found to correlate with a decreased proliferation response to the well-known iNKT agonist α-GalCer (171). The reduction in iNKT levels during infection with *M.tb* may be due to an increased expression of the programmed cell death maker PD1. Expression of PD1 has been shown to be elevated on iNKT cells, with blockade of this marker enhancing the response to α-GalCer (171). Additionally, CD1d expression on peripheral blood monocytes was also found to be significantly lower in patients with pulmonary TB compared to healthy controls (171). This is important as anti-mycobacterial activity of iNKTs is dependent upon CD1d expression, as demonstrated by CD1d knockout mice failing to control mycobacterial disease (149, 150). In contrast, CD1d expression has been shown by Gansert *et al* to be prominently expressed in the centre of granulomas in the affected lymph nodes of TB patients (172). The expression of granulysin at the site of disease supports the possible interaction of iNKTs with CD1d at the location of activity (172). The production of cytokines by iNKTs provides them with the ability to

augment host antimicrobial immunity. In the presence of infected macrophages secreting IL-12 and IL-18, iNKTs become activated and secrete IFNγ. However, control of *M.tb* infection *in vivo* has been found to be independent of IFNγ and TNFα (149). In the same study, it was discovered that iNKT antimicrobial activity both *in vitro* and *in vivo* was due to CD1d dependent release of GM-CSF, and the blockade of this cytokine abolished the iNKT restriction of bacterial growth (149).

Animal models have demonstrated the importance of iNKTs in fighting infection. Culture of splenic iNKTs from uninfected mice with *M.tb* infected macrophages suppressed bacterial replication, and also reduced the bacterial burden in the lungs of *M.tb* challenged mice (150). Challenge and vaccination studies of different species of macaque have revealed that there is an association between increased $CD8^+$ iNKTs and better clinical outcomes (31). In both *M.tb* infected Chinese Cynomolgus and Indian Rhesus macaque populations, animals with increased $CD8^+$ iNKTs had lower total disease pathology, decreased lung lesion number and less weight loss than those with lower $CD8^+$ iNKT frequencies (31).

1.1.2.3.2 γδ T cells

γδ T cells, comprising heterodimeric γ and δ TCR chains instead of the more abundant α and β, are a small subset of unconventional T cells making up just 1-10% of peripheral lymphocytes (173-175). Although serving as a first line of defence, γδ T cells are thought to bridge the gap between the innate and adaptive immune response. Similar to αβ T cells, γδ T cells expand upon activation and demonstrate various effector functions including the secretion of multiple cytokines (TNFα, IFNγ, IL-17) and chemokines (RANTES, IP-10, lymphoactin) (174, 176, 177). γδ T cells also carry out potent antimicrobial cytolytic functions through the production of granulysin, granzymes and perforin (178-182) in addition to activating other immune cells such as monocytes, neutrophils, DC and B cells (183-185). The two most abundant subtypes of γδ T cells are those with TCR δ variable region genes TRDV1 and TRDV2 encoding the Vδ1 and Vδ2 chains, respectively (174, 186). Vδ2 T cells predominantly reside in the peripheral blood where they mainly pair with a Vγ9 chain, whereas Vδ1 are largely localised to mucosal tissues and comprise only 10-30% of circulating γδ T cells (174). Each subset has their own individual functions in homeostasis and in response to infection or malignancy, but both of these main γδ T cell populations exhibit TCR and NKG2D induced cytotoxic functions (181, 182).

In contrast to αβ T cells, far less is known about stimulatory ligands for γδ T cells but they have been reported to include stress-inducible antigens (186). Recent evidence demonstrates however that γδ T cells recognise a variety of antigens that aren't limited to MHC presented peptides, including CD1-lipid complexes and metabolites presented by MR1 (187). The most characterised

ligands for γδ T cells are prokaryotic and eukaryotic phosphoantigens which are recognised by the Vγ9Vδ2 subset, but it has been unknown until recently whether these antigens are presented or sensed (188-191). Harly and colleagues demonstrated the critical role of the butyrophilin isoform BTN3A1 in the activation of Vγ9Vδ2 T cells by phosphoantigens (191). Further investigations by several groups has suggested that unlike the CD1 activation of γδ T cells by way of lipid presentation, BTN3A1 mediated phosphoantigen stimulation of γδ T cells is through an 'inside out' signalling mechanism with the phosphoantigen binding to the intracellular B30.2 domain of BTN3A1 (192, 193).

Other ligands that have been identified, particularly as inducible stress ligands, are MHC Class I-related chains A and B (MICA and MICB), endothelial protein C receptor (EPCR) and annexin A2. Recognition of MICA/MICB has been found to be solely by T cells with a Vδ1 TCRδ chain and, unlike conventional MHC class I, do so without association with peptides (194). Expression of these molecules and their subsequent recognition by a Vδ1 clone was also reported to be stress induced, with a large increase in mRNA expression upon heat shock of intestinal epithelial cells (194).

EPCR, another reported stress induced ligand, has been found to be upregulated on epithelial tumour cells and Cytomegalovirus (CMV) infected cells, and specifically activates Vγ4Vδ5 T cells (195). Although EPCR is able to bind lipids as in CD1d, recognition of EPCR by the TCR has been reported not to involve the lipid binding surface of the molecule or discrimination of the bound lipid (195). Instead, the interaction is thought to occur through identification of defined residues and structural components in EPCR's β-sheet (189, 195).

The ability of γδ T cells to respond to stress antigens, recognise lipids in complex with CD1 molecules and their innate and adaptive-like functions suggest a role for these T cells in response to infection. The first report suggesting an involvement of γδ T cells in response to *M.tb* infection was by Janis and colleagues who noted a substantial increase in γδ T cells compared to αβ T cells in the draining lymph nodes of mice inoculated with Freund's adjuvant (196). Studies involving a γδ T cell knockout mouse model have demonstrated the inability of the mice to control *M.tb* infection and develop more severe disease compared to mice with intact γδ TCR genes (68, 106). In addition, γδ T cells have been reported to be involved in the development of granulomas through production of IL-17 (197, 198).

Analyses of substituents of the γδ population have revealed that the distribution of individual subsets is altered in some disease states, including in TB (199). The abundant circulating γδ T cell population, Vγ9Vδ2, has been reported in several studies to decrease in the peripheral blood in response to active TB disease compared to healthy controls or patients with unrelated pulmonary

granulomatous disease (199-201). Furthermore, remaining Vγ9Vδ2 cells have been reported as refractory to *in vitro M.tb* antigens (199), when, under normal circumstances, these secrete large quantities of TNFα and IFNγ in response to antigen challenge (202). Lower frequencies of Vγ9Vδ2 cells in the blood of TB patients was also found by Szereday *et al* compared to healthy volunteers, and more specifically, a lower ratio of these cells were found in TB patients who had a negative reaction to the tuberculin test (173). In contrast to these studies, results from both human and NHP models of *M.tb* infection have revealed an increase in the peripheral Vδ2 γδ T cell population in BCG vaccinated individuals, while an elevated Vδ2 subset is also associated with those sharing accommodation with active TB patients (203-206). Activated Vδ2 T cells in response to BCG stimulation, characterised by upregulation of CD69, CD25 and HLA-DR, have been reported to increase expression of granzyme B and Th1 cytokines in a DC and αβ $CD4^+$ T cell dependent manner (207, 208). A protective role for Vδ2 T cells has also been demonstrated by an adoptive transfer study in the NHP model. During *M.tb* infection, adoptively transferred γδ T cells were found to migrate back to the lungs and were associated with reduced bacterial burden and attenuation of infection (209).

The predominantly tissue-rich Vδ1 T cell population has also been implicated in the response to infection. An accumulation of Vδ1 γδ T cells in the lungs have been reported in patients with pulmonary sarcoidosis (210) and in leprotic lesions (211), but now adaptations in the Vδ1 T cell subset have also been associated with TB. Szereday and colleagues reported the observation that Vδ1 T cells were increased in the blood of TB patients as early as radiological stage 1 of the disease, but interestingly this was only noted for patients that had negative tuberculin reaction (173). Furthermore, it was also reported that tuberculin negative patients presented with more advanced disease than those with a positive test, suggesting that the distribution and numbers of individual γδ T cell subsets are important in disease progression and severity (173). An increase in the Vδ1 T cell population in the peripheral blood of active TB patients compared to healthy controls has also been reported by Negash *et al*. These circulating Vδ1 T cells were found to express the activation marker CD38 as well as the exhaustion marker PD1, indicating that they had responded to antigen (212). Despite the majority of this γδ T cell subset residing in tissues, the investigation into Vδ1 T cells at the site of TB disease in the lungs is only just starting to be explored. Ogongo and colleagues have recently documented a high degree of γδ T cell clonal expansions, dominated by the Vδ1 subset, within the lungs of TB patients (200). These Vδ1 clonotypes were found to be non-overlapping with those in circulation, suggesting that within the lungs, the Vδ1 subset undergo expansion in response to antigen exposure (200). Taken together, the evidence points towards γδ T cells functioning to combat *M.tb* at the site of infection in the lungs.

1.1.2.3.3 MAIT cells

Mucosal-associated invariant T cells (MAIT) recognise small non-peptide metabolites presented by MHC-I-related molecule 1 (MR1) (213). Typical MAIT cells comprise an invariant TCR α chain (TRAV1-2/TRAJ33, TRAJ20 or TRAJ12) associated with an oligoclonal TCR β chain, frequently TRBV6 or TRBV20, and predominantly express a $CD8^+$ or DN phenotype (214, 215). Despite making up approximately 5% of peripheral blood T cells, MAITs are abundant in organs such as the liver, intestines and lungs (167, 216-218) and produce a number of cytokines upon activation including IL-2, IFNγ, IL-17 and TNFα (214-216). MAIT cells recognise a range of Vitamin B metabolites from bacteria and yeast generated during synthesis of riboflavin such as 5-OP-RU (219-223). These metabolites are presented by MR1 which, similar to CD1, is composed of a non-polymorphic heavy chain molecule non-covalently associated with β_2m but resembles MHC class I molecules in its almost ubiquitous tissue distribution (224, 225).

Thymic and circulating MAIT cells have demonstrated the ability to produce TNFα and kill *M.tb* infected lung epithelial cells *in vitro* despite a lack of prior exposure (217, 226).The presence of *M.tb* infection has been reported to augment the distribution of MAIT cells *in vivo*. Several studies have reported the reduction of MAIT cells in the peripheral blood of TB patients but a concurrent increase within the lungs (217, 218). The accumulation of MAIT cells in the lung following infection is reported to occur in less than 10 days and the production of cytokines such as IFNγ, TNFα and IL-17 in response to BCG infected macrophages has been observed to occur in as little as 4 days (141, 227, 228). Despite having lower circulating frequencies, MAIT cells from TB patients are reported to produce a significantly greater frequency of cytokines in response to *ex vivo* BCG stimulation compared to healthy controls (227). However, conflicting studies report that MAIT cells from TB patients fail to produce IFNγ in response to stimulation and a lower circulating frequency is associated with upregulated expression of PD1, both of which are reversed upon PD1 blocking treatment (227, 229). Due to inconsistent observations, our understanding of the function of MAIT cells in response to *M.tb* infection remains incomplete and further work to unravel their role is required.

1.2 CD1

T cells are able to detect and respond to various self- and foreign antigens, reacting to repertoire changes brought on by events such as inflammation or infection. While the Major Histocompatibility Complex (MHC) presents peptide fragments to T cells, a related set of molecules are able to present lipid antigens on the surface of antigen presenting cells (APC). CD1 molecules are a set of MHC-like cell surface glycoproteins which bind and present lipids to

unconventional CD1-restricted T cells. CD1 is expressed as a glycosylated membrane-anchored heavy chain, noncovalently associated with β_2m (165, 230). In contrast to the uniquely expressed MHC, allelic variation of CD1 is rare, meaning an identical set of glycoproteins are expressed by almost all humans (139, 231). Due to this, CD1 reactive T cells are an attractive target for therapeutics and novel vaccines (232).

The CD1 heavy chain is comprised of various domains: an extracellular antigen binding domain, a transmembrane domain and an intracellular tail (233). The heavy chain constitutes three alpha helices (α1, α2, α3), with the α1 and α2 helices forming the antigen binding groove (165, 231). The α3 helix associates with the base of the molecule formed by an anti-parallel six stranded β-sheet platform (165, 233, 234). CD1 molecules are expressed on a variety of professional antigen presenting cells such as DC, macrophages and B cells (165). Hydrophobic channels formed by the α1 and α2 domains within the molecule are deeper than that of the MHC and allow for the binding of lipid alkyl chains (165, 233). While the tail of the antigen is buried within the CD1 molecule, hydrophilic head groups of the lipid ligand remain exposed at the surface of the extracellular domain which allows for direct contact with the TCR.

There are five human CD1 proteins; CD1a, CD1b, CD1c, CD1d and CD1e, which vary in terms of their tissue distribution and intracellular trafficking processes. The five isoforms can be divided into groups according to their amino acid sequence homology: Group 1 includes CD1a, CD1b and CD1c, Group 2 is just CD1d and CD1e is in Group 3 (230, 235). While Groups 1 and 2 are involved in antigen presentation, the role of the exclusively intracellular CD1e is thought to only extend to lipid processing and trafficking (165, 230). CD1 glycoproteins are expressed mainly by professional APC such as myeloid DC (139). Expression of group 1 proteins is not continuous but is instead stimulus-dependent, with expression inducible by bioactive IL-1β, IL-4 and GM-CSF (139, 166, 235)**.** This effect is demonstrable *in vitro*, with DC differentiating from $CD14^+$ monocytes following the addition of GM-CSF and IL-4, producing an observable increase in their CD1a, CD1b and CD1c expression (139, 166)**.**

All of the four main isoforms (CD1a, CD1b, CD1c, CD1d) contain binding pockets within their ligand binding grooves termed A' and F'. The size of the antigen binding groove varies between the isoforms, the largest belonging to CD1b and the smallest to CD1a (230) (Figure 4). The positioning of the α1 and α2 helices as well as the distance between the alpha helices and beta sheet platform determines the overall shape of the antigen binding groove (165). The A' pocket within the antigen binding groove of both group 1 and 2 isoforms is separated from the surface of the molecule by the A' roof (165, 235). The solvent exposed surface of CD1 is connected to the hydrophobic groove by a portal formed by the F' pocket (165). CD1 usually binds lipids of low

aqueous solubility despite the antigen binding groove being directly exposed to aqueous solvent (139).

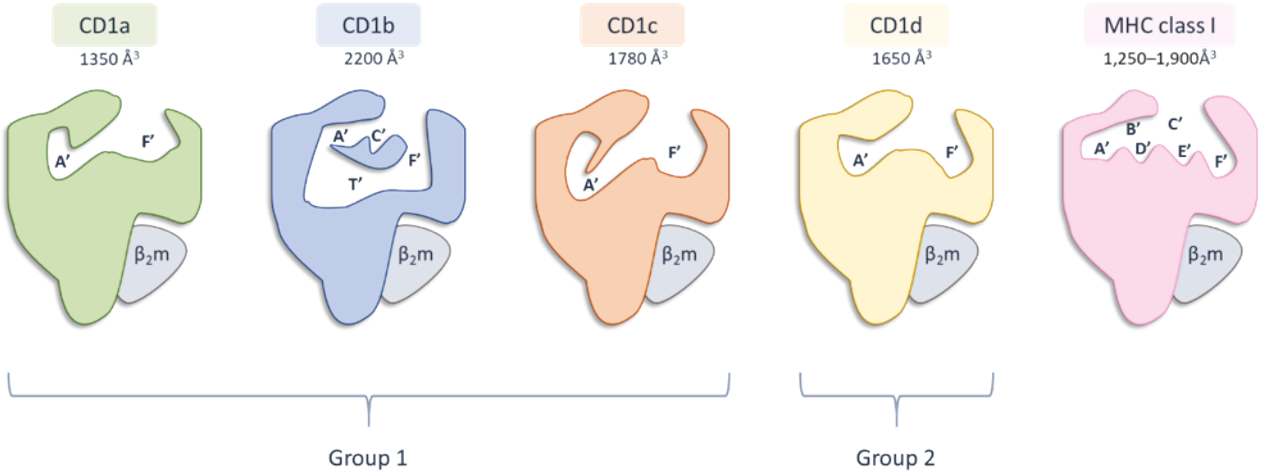

Figure 4: Structure and binding pockets of CD1 molecules

Cartoon representation of Group 1 (CD1a, CD1b and CD1c) and Group 2 (CD1d) CD1 proteins compared to MHC class I molecules. Differences in shape and capacity of antigen binding grooves of each CD1 molecule allows for the binding and presentation of a range of lipid antigens. Adapted from Adams 2014 and Moody 2017 (232, 236).

The majority of lipids that are bound by CD1 are amphiphilic in nature, such as lipopeptides or glycolipids, and contain specific hydrophobic moieties that are bound within the CD1 antigen binding groove (165). The head group of the lipid antigen, which is usually hydrophilic, is exposed on the surface of CD1 and can be recognised by the TCR (165, 167). The first lipid antigen discovered to be presented to CD1 reactive T cells was MA, which is specifically bound and presented by CD1b (165). It is also now known that CD1 molecules can bind antigens in the presence of what is known as 'spacer lipids'. These are endogenous diacylglycerides or deoxyceramides which vary in length and aid in the generation of stable CD1-antigen complexes. These lipids help to prevent the collapse of the molecule which may occur when antigen binding grooves are left empty (165, 167, 230).

1.2.1 CD1a

Expression of CD1a is almost exclusively by Langerhans cells and monocyte-derived dendritic cells (MoDC) (237-239). Unlike CD1b, CD1c and CD1d, CD1a does not contain a tyrosine based sorting motif on its cytoplasmic tail and therefore recycles only through early endosomes (238-242). CD1a has been indicated to accumulate mainly at the cell surface but similar to MHC class I, can be internalised through an AP-independent pathway (238, 240). With an estimated volume of ~1350Å^3, CD1a has the smallest antigen binding groove of all the CD1 isoforms (243). The A'

pocket of CD1a has a hook-shaped structure, with Val28 blocking the pocket from completely encircling the A' pole as in CD1b and CD1d (243). It is estimated that this volume allows for a lipid tail of ~C36 to be accommodated within the A' groove and the A' roof blocks this pocket from being directly open to solvent (243). In contrast, the F' pocket is more shallow than the A' pocket and is open to solvent with antigens most likely to enter this groove through the F' portal (243).

CD1a is known to bind a diverse array of endogenous lipids, but the first documented CD1a-self lipid complex was with sulfatide, a glycolipid highly expressed by the kidney, pancreas and neuronal cells (244-247). Additionally, CD1a has also been shown to present the *M.tb* derived lipopeptide didehydroxymycobactin (DDM) which may indicate a role for this CD1 isoform in the immune response to microbial infection (248). Structures of CD1a in complex with synthetic lipopeptide resembling DDM demonstrate that the alkyl chain was placed within the A' pocket while the peptidic moiety was accommodated in the F' pocket (249-251). Similar to CD1c, spacer lipids have also been found within the F' pocket of CD1a when presenting DDM (251).

1.2.2 CD1b

CD1b proteins are predominantly expressed on MoDC and those migrating to lymph nodes (252, 253). As with CD1c and CD1d, the cytoplasmic tail of CD1b contains a tyrosine based motif, which, upon binding to adaptor protein 3 (AP-3), allows for sorting of CD1b to the late endosomal and lysosomal compartments (238, 239, 242, 254, 255). Endosomal cofactors and acidic pH aids the regulation of lipid availability, although it has also been demonstrated that CD1b can also bind lipid antigens at the cell surface under neutral pH (256, 257).

CD1b has the largest and most complex antigen binding pocket of all the CD1 isoforms, with an approximate volume of ~2200Å^3 made up of four interconnecting pockets termed A', C', F' and T' (258). Crystal structures of CD1b in complex with ganglioside GM2 or PI have revealed that the T' tunnel, only found within CD1b, is situated deep within the molecule and laterally connects the vertically positioned A' and F' pockets to form the A'T'F' superchannel, with the C' portal allowing access of lipid tails to solvent underneath the α2 helix (258, 259). This large antigen binding pocket allows CD1b to bind a variety of lipid antigens up to ~C80 in length (256). CD1b was the first CD1 isoform revealed to bind mycobacterial lipids, with Beckman and colleagues first identifying MA as a ligand for CD1b (260). Following this discovery, a range of *M.tb* derived lipids have been identified as being presented by CD1b including lipoarabinomannan (LAM), glucose monomycolate (GMM) and glycerol monomycolate (GroMM) (261, 262). The structure of CD1b in complex with GMM demonstrates that the A' pocket accommodates the β-hydroxyl chain of the lipid which passes through the T' tunnel and up into the F' pocket, with the tail end egressing into

the solvent. The α-alkyl chain of GMM passes down through the C' pocket and exits into the solvent through the C' portal (263). While CD1b is able to present chains of up to C80 atoms, lipids with shorter alkyl chains (~C32) have been found to load into the molecule at a faster rate and it is possible that any empty space within the antigen binding groove may be taken up by spacer lipids (258, 262).

1.2.3 CD1c

As well as its inducible expression on MoDC with other group 1 proteins, the majority of CD1c expression is found on marginal zone B cells and myeloid DC (139, 264)**.** The toroid A' pocket of CD1c's binding groove is open to solvent and encircles a pole, allowing lipids to pass through the cavity**;** but the conformation of this molecule can adapt and change to accommodate different ligands (231, 235). In other isoforms, the F' pocket is usually closed to solvent, but it has been reported that the F' roof in CD1c can adopt either an open or closed conformation (167, 231, 265, 266)**.** The state of the F' roof has been discussed and contradicted by a few studies, but the general consensus is that CD1c is highly adaptable. For example, whilst the structures of CD1c-phosphomycoketide (PM) and CD1c-mannosyl-β1-phosphomycoketide (MPM) show the F' roof is open to solvent (231, 267), the roof is demonstrated to be closed when CD1c is accommodating spacer lipids (referred to as CD1c-SL) (265). Another difference between these lipid bound CD1c structures is the presence of up to three different portals. The D' portal located underneath the α1 helix allows for the binding of branched antigens within the A' channel such as MPM (87, 167, 231). An additional opening within the molecule connects the F' pocket to the exterior underneath the α1 helix and is referred to as the E' portal (167, 231). This portal has been described in CD1c-PM and CD1c-MPM but was found to be absent in CD1c-SL (167, 231, 265, 267). However, despite the lack of the E' portal in CD1c-SL, a different portal was found to exist in this structure, which was referred to as the G' portal (265).

CD1c is able to bind a wide variety of different lipids including those from pathogenic bacteria, synthetic lipids and host derived lipids. Different classes of lipids have been reported to be bound by CD1c, but many share a common feature of containing only one hydrocarbon tail (266). One class contains methylated mono-alkyl chains which are present in lipids derived from bacteria such as *M.tb* and includes phosphodolichols and PM (166, 266). A second type are N' terminally acylated lipopeptides, which are also known to be presented by CD1a (266). Cholesteryl esters, which are commonly found in foamy macrophages observed during infection with *M.tb*, have also recently been demonstrated as possible ligands for CD1c (265). More recently, it has been demonstrated using mass spectrometry that CD1c can bind endogenous lipids such as monoacylglycerol (MAG), sphingomyelin (SM) and phosphatidylcholine (PC) (268).

1.2.4 CD1d

The only group 2 isoform, CD1d, is more broadly expressed than the other CD1 molecules. As well as being located on DCs and B cells, it is also expressed by macrophages, thymocytes, hepatocytes, stellate cells, intestinal epithelial cells and adipocytes (139, 230)**.** The antigen binding groove of CD1d is the second smallest of the four main isoforms, accommodating lipids up to 43 carbons in length, but unlike CD1b and CD1c it doesn't contain any accessory portals (230, 235). CD1d can present a variety of different ligands including glycosphingolipids, diacylglycerols, phospholipids, lipopeptides and ether lipids, but the most well-known ligand for this isoform is α-GalCer (230). The A' channel of CD1d is occupied by the fatty-acyl chain of α-GalCer while its sphingosine chain is accommodated within the F' pocket (230, 233) (Figure 5). This positioning allows for protrusion of the galactosyl head group out of the groove onto the surface of the molecule, making it accessible for TCR recognition (230, 233). The presentation of this lipid has greatly contributed to the understanding of CD1d-reactive T cells and in particular, the biology of iNKTs which are stimulated by CD1d presented α-GalCer (230). The study of iNKTs has revealed that the semi-invariant TCR docks onto the F' pocket of the CD1d-α-GalCer complex, with most of the contact stemming from the Vα chain (167). However, despite the wealth of information garnered from CD1d binding α-GalCer, this lipid is not a physiological ligand.

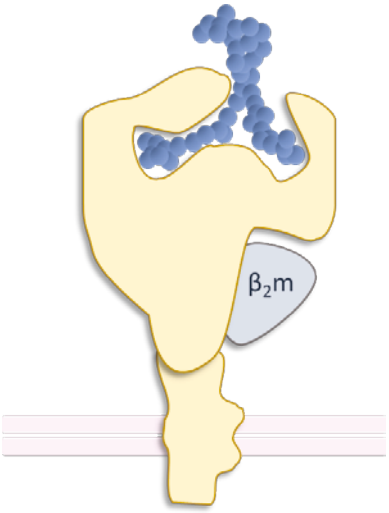

Figure 5: CD1d presenting α-Galactosylceramide

Cartoon representation of CD1d presenting α-Galactosylceramide with alkyl chains residing within the A' and F' channel and the galactosyl headgroup protruding out of the binding cleft.

Many different ligands have been identified for CD1d, including host derived PI, glycophosphatidylinositol, PC and sulfatide; and bacteria derived α-glucuronosylceramide from *Sphingomonas* species and phosphatidylinositol mannosides (269) from *M.tb* (270). However, although these complexes have proved capable in stimulating iNKTs and other CD1d-restricted T

cells, a physiological ligand that stimulates these cells as potently as α-GalCer is yet to be discovered. Thus, the role of CD1d and CD1d-presented ligands in disease still remains elusive.

1.2.5 Molecular recognition of CD1 by the T cell receptor

An important factor in the initiation of an adaptive immune response is the recognition of antigen by T cells. The antigen binding site formed by the α and β chains, or the γ and δ chains, of the TCR determines the antigen specificity of the T cell. The contact points between the TCR, an antigen presenting molecule and/or its bound ligand are key factors in forming an immune response. The TCR of T cells responding to MHC molecules are highly specific, but structural studies have revealed that binding modes between TCR-MHC-peptide complexes vary considerably. There appear to be few shared contact positions between different complexes, which raises the question of whether the position of TCR binding is dictated by chain usage, ligands bound within the antigen presenting molecule, or a combination of factors. Understanding the structural mechanisms underpinning T cell-antigen recognition will allow for the design of both agonists and antagonists to modify T cell responses to prevent disease and improve outcomes.

To investigate the molecular recognition underpinning the TCR-antigen presenting molecule complex, mutational and structural studies can be carried out to determine how the components of the complex interact with one another. Alanine scanning is a widely used technique that investigates the functional impact of amino acid residues within a molecule. Selected residues are mutated to alanine using site directed mutagenesis, as this amino acid is chemically inert and does not induce electrostatic effects or changes in the arrangement of the main protein chain (271). This technique has been useful in determining the contribution of each complementarity determining region (CDR) loop within specific TCRs, and the effect on affinity can be assessed through surface plasmon resonance (SPR). By mutating residues within the α and β chains of the 2C TCR, it was discovered that the CDR1 and CDR2 loops of Vα and Vβ contribute the majority of the energy in the interaction with pMHC ligand L^d bound to the QL9 peptide (272, 273). This is in contrast to another TCR, LC13, in which the CDR1 and CDR2 loops provide little energetic contribution (274). Alanine scanning involving thirty nine mutants across all CDR loops from both TCR α and β chains revealed that the CDR3 loops, particularly CDR3α, dominated the interaction with the FLR ligand bound to HLA-B8 (274). However, it has also been discovered that energetic interactions can vary between ligands. The diverse interaction profiles of different MHC-restricted TCRs lead to the investigation into whether the same principles apply to the CD1 system.

Conserved αβ TCRs of the germline encoded mycolyl lipid-reactive (GEM) (275) T cells are known to specifically recognise CD1b presenting the mycobacterial antigen GMM, but the role CDR3β

plays in the fine specificity of CD1b recognition was only discovered after mutating specific residues within CD1b. Out of the fourteen individual mutations to the α1 and α2 helices of CD1b, there were four residues that were critical to affinity between CD1b-GMM and two GEM TCRs, GEM42 (TRBV6-2^{+}) and GEM21 (TRBV30^{+}), designating a shared hotspot (276). However, mutated residues near the F' pocket of CD1b had differing effects on the interaction with the GEM42 and GEM21 TCR. The residues in question were mapped to the site of interaction with the CDR3β loops of both GEM TCRs, indicating that this loop is involved in fine tuning the CD1b interaction (276). Differences in TCR footprint also occurs between CD1 isoforms. Mutations of both CD1d and iNKT TCR (Vα24-Jα18, Vβ11) and subsequent SPR analysis has revealed that the largest contributions from the Vβ chain were from the CDR2β loop contacting CD1d, whereas it was the CDR3α loop which had the greatest contact with both CD1d and the antigen α-GalCer (277).

While alanine scanning mutagenesis provides information on the functional roles of protein residues, further techniques are needed to provide detailed structures of molecular interaction. X-ray crystallography can be used to determine 3D structures of TCR-CD1 complexes whilst also providing information on residue functions, bonding and interactions (278). Three dimensional structures can be solved by processing the diffraction patterns of x-ray beams that have been directed at protein crystals and modelled using computer graphics software. Crystal structures of CD1b in complex with either ganglioside GM2 or PI have provided information on the complexity of the antigen binding pockets which in turn allows this isoform a greater level of adaptability to lipids with differing alkyl tails (258). These crystal structures have since been used in molecular replacement techniques to model the crystal structure of CD1b binding GMM (263).

Ternary crystal structures of TCR-CD1-antigen complexes have provided a deeper understanding of the differences in TCR footprints and docking orientations. The crystal structure of the GEM42 TCR binding to CD1b-GMM demonstrates a central docking position over the CD1 α1 and α2 helices, with extensive contacts of both CD1b and GMM by the TCRα chain (276). This is in contrast to the structure of the BK6 TCR which directly contacts the A' roof of CD1a without any interaction with bound ligands including endogenous lipids (CD1a-endo) or lysophosphatidylcholine (LPC) (279). Differing docking orientations of TCRs have also been demonstrated on the same CD1-antigen molecule using this method. For example, whereas the PG90 TCR forms an O-ring like seal on CD1b-phospholipid to surround the protruding antigen from the F' portal, the α chain of the BC8B TCR predominantly contacts the neck region of the phospholipid which emerges on the A' roof of CD1b (280).

Despite the benefits of X-ray crystallography, technical challenges and rate limiting steps hinder the use of this technique. Highly variable growing conditions further increase the difficulty, and

poor resolution may occur from crystals that are too small or not structurally consistent (278). Nuclear magnetic resonance (NMR) spectroscopy has been used to determine the docking footprints of TCRs through chemical shift mapping. NMR is reported to have improved detection sensitivity for weak binding over other techniques and has been found to be highly accurate compared to crystal structures of the same complex (281, 282). The interaction of the 2C TCR and the H-2L3-QL9 ligand has been mapped and defined as a footprint on the presenting H-2L^d MHC molecule by analysing NMR shift patterns (282). The chemical shift patterns of labelled pMHC in complex with TCR compared to labelled pMHC alone identify which residues are involved in complex formation. NMR experiments can be used to complement X-ray crystallography as they can provide information on conformational dynamics of the recognition site whereas crystal structures provide visual detail of direct interaction and structural rearrangement within the complex (282, 283). However, investigations by NMR spectroscopy are hindered by the requirement of large quantities of protein but with a smaller size to reduce spectral complexity. To acquire maximum information about the structure and interaction of a complex, it is necessary to utilise a combination of these techniques in order to fully understand the molecular mechanisms at play.

1.2.6 CD1 tetramers

Perhaps one of the most useful tools developed in the past few decades to identify, characterise and quantify antigen-specific T cells is the tetramer. Before the invention of tetramers by Altman and Davis in the 1990's, the standard method of quantitative analyses of antigen-specific T cells was the combination of flow cytometry and limiting dilution analysis (284, 285). Although this enabled enumeration of T cells expressing a particular surface antigen, lower-frequency populations of antigen specific cells or those with low proliferative potential may be drastically underestimated or even missed entirely. TCR specificity was also not a factor in previous methods, further reducing the ability to interpret results (286). The avidity between the TCR and antigen complexes is inherently low, meaning that the identification of antigen specific T cells remained challenging. Multimerisation of soluble proteins therefore allows for the binding of multiple TCRs on one cell and therefore extends the interaction half-life and increases avidity (287). The first tetramers constructed were composed of four biotinylated MHC-peptide complexes which, after binding to phycoerythrin (PE) labelled deglycosylated avidin, could be detected by flow cytometry and thus allowed for the detection of peptide specific T cells (285). MHC molecules however are highly polymorphic in nature which limits their application in a genetically diverse population. In contrast, CD1 molecules are non-polymorphic and are therefore not subject to individual variation. The use of CD1 in place of MHC in tetramer complexes has provided evidence of a

ternary interaction between the TCR and CD1 presented lipid antigens and has been instrumental in demonstrating CD1 restriction by T cells of both αβ and γδ lineage (139).

An advantage of using tetramers in the characterisation of CD1-restricted T cells is their ability to enable the recovery of cells post flow cytometry analysis. Unlike methods such as the Enzyme-linked Immune Absorbent Spot assay (ELISPOT) or PCR, tetramer studies allow specific populations of cells to be sorted for further culture and characterisation (288). This has permitted the downstream investigation into the specificity of different TCRs in addition to their functional response and molecular recognition patterns of CD1 molecules. The first CD1 tetramers generated were that of CD1d loaded with α-GalCer in order to investigate mouse iNKT populations (289, 290), but since then tetramers have been produced for human CD1d as well as all group 1 molecules using oxidative refolding chromatography (291).

Tetramers of group 1 CD1 molecules have been instrumental in demonstrating the existence of CD1-restricted T cells that are specific for mycobacterial lipids. CD1b tetramers loaded with mycobacterial GMM or MA have been used to successfully demonstrate a small sub-population of T cells in TB patients that are lipid specific and CD1b-restricted, and have subsequently enabled the characterisation of the CD1b-restricted GEM and LDN5-like T cell lines (292-294). CD1c-restricted T cells specific for mycobacterial antigens have also been identified using lipid loaded tetramers. CD1c tetramers loaded with mycobacterial PM or MPM have enabled the isolation of both CD1c-restricted αβ and γδ T cells, the latter of which having until recently been difficult to characterise (174, 267).

Perhaps more importantly, CD1 tetramers have been invaluable in demonstrating the existence of self-lipid reactive CD1-restricted T cells. For example, tetramers comprising CD1a loaded with wax esters, CD1b loaded with PG or CD1c loaded with PC have demonstrated populations of T cells in the peripheral blood of healthy humans that recognise CD1 molecules loaded with host-derived lipids (295-297). Further to this, CD1 tetramers have been generated in the absence of any specific lipid and have thus been used to isolate CD1-restricted T cells specific for the CD1 molecule itself. Our group has previously demonstrated that CD1c refolded with spacer lipids (CD1c-SL), incorporated either within the *E.coli* expression system or during the refolding process, is recognised by a subset of T cells in healthy humans (265). The CD1c-SL tetramers were used to isolate a CD1c autoreactive T cell clone, NM4, which upon further analysis was demonstrated to recognise CD1c itself as bound ligands were sequestered within the molecule away from TCR interaction (265).

Tetramers of group 1 CD1 molecules harbouring endogenous lipids (CD1-endo) have also been produced using the mammalian expression system and have contributed to our knowledge of CD1

autoreactive T cells. CD1a-endo tetramers harbouring ~100 different endogenous lipids were utilised by Cotton and colleagues to reveal that CD1a autoreactive T cells recognise CD1a itself regardless of the bound lipids which were positioned away from the TCR binding site (298). CD1b autoreactive T cells have also been characterised following isolation using CD1b-endo tetramers. The use of these tetramers have been valuable in demonstrating that binding patterns of CD1b autoreactive T cells to CD1b are highly variable between different TCRs. T cells expressing either an αβ or γδ TCR that have been isolated using CD1b-endo tetramers show that while some are highly promiscuous for a variety of self-phospholipids or SM, some have more specific requirements of the endogenous lipids that are presented by CD1b (280, 299). Finally, characterisation of a CD1c autoreactive TCR isolated using CD1c-endo tetramers reveals a similar mechanism of self-recognition to the CD1c autoreactive TCR cloned by our group using CD1c-SL tetramers. The 3C8 CD1c autoreactive TCR demonstrated extreme lipid polyspecificity which was attributed to bound lipids being sequestered within CD1c and TCR interaction occurring with the closed F' roof of CD1c (268).

Despite these immunological advancements enabled by CD1 tetramers, their generation and use involve some technical difficulty. Optimal staining of the desired population can be affected by numerous factors including temperature, protein concentration, exposure to light and the risk of blocking by the use of co-receptor antibodies (287). However, careful handling, preparation and experimental planning can mitigate these factors. However, factors such as the hydrophobicity of the desired lipid ligands are likely to cause aggregation in aqueous solutions during the construction process which poses a challenge when attempting to load the antigen into the CD1 proteins (232, 286). Following lipid loading and tetramerisation, another issue posed is the ability of tetramers to bind low affinity T cells, particularly autoreactive T cells which are known to bind CD1 molecules with an even lower affinity (287, 300). The ability of tetramers to bind low affinity T cells has been improved by the use of higher order multimers. Dextramers are constructs of a fluorescently labelled dextran backbone that can bind up to 20 or more CD1 monomers, with the premise that there will be more CD1-lipid epitopes for greater TCR binding (139, 301). CD1b dextramers loaded with mixed lipids have indicated improved staining ability when compared to tetramers (301). The interaction half-lives of dextramers with the T cell surface are longer than that of tetramers, thus improving staining intensity (287). However due to the expense of producing and/or purchasing the dextran backbones required for dextramer production, it may not be feasible to use this method of T cell population identification.

1.2.7 CD1-restricted T cells

1.2.7.1 CD1-restricted αβ T cells

The first evidence of T cells that were not activated by MHC molecules but instead recognised CD1 proteins was reported in 1989 (302). The phenotype of CD1-restricted T cells was found to be diverse, expressing single CD4 or CD8 co-receptors, but could also be negative for both (27, 302, 303). It was not until 1994 that specific lipid antigens presented by CD1 to CD1-restricted T cells were identified. MA derived from the cell wall of *M.tb* were observed to activate CD1b-restricted T cell line, DN1, in a CD1b-dependent manner (260). Activated CD1-restricted T cells have been observed to develop a Th0 or Th1 phenotype, producing IFNγ and TNFα and inducing lysis of *M.tb* infected target cells through Fas-Fas ligand interactions or the release of granulysin (27, 248, 304-306).

Since the discovery of lipid-specific, CD1-restricted T cells, a range of pathogen and self-derived lipids have been revealed to be presented by each of the group 1 CD1 isoforms, but lipid antigens derived from *M.tb* have been particularly numerous. Although recent evidence has shown that the majority of ligands for CD1a are sequestered within the molecule and do not interact with the TCR, Moody and colleagues had previously identified that a family of DDM derived from *M.tb* are presented by CD1a (249). DDM is an intermediate metabolite produced during the synthesis of mycobactin, an essential component in a larger pathway promoting the *in vivo* growth of *M.tb* (301). Activation of the mycobacteria-specific, CD1a-restricted αβ T cell line CD8-2 was observed following stimulation with DDM in a CD1a-dependent manner (249). Furthermore, activation was specific for the acyl and peptidic structural components of the bound CD1a-bound ligands (249). These observations complement previous work reporting anti-mycobacterial functions of CD1a-restricted T cells (27, 248).

Out of all the CD1 isoforms, CD1b has so far been found to present the largest array of *M.tb* derived lipid antigens including MA, LAM, GMM, GroMM, phosphatidylinositolmannan (269) and diacylated sulfoglycolipid (Ac_2SGL) (260, 261, 307-309). The presence of mycobacterial lipid-specific, CD1b-restricted T cell responses in humans appears to be dependent upon exposure to *M.tb* or BCG vaccination, but does not necessarily correlate with TB disease state (261, 307, 310, 311). CD1b-restricted T cells specific for Ac_2SGL or MA appear to only be present in subjects with prior exposure to *M.tb* (307, 311), whereas GroMM specific T cells were also found to be present in both infected and uninfected, BCG vaccinated individuals (261). Stimulation of these CD1b-restricted T cells with cognate lipid antigen resulted in the production of IFNγ and IL-2 and *M.tb* infected target cells were lysed (307, 311). Further to this, responding T cells displayed memory

markers and those acquired from individuals that had undergone successful TB treatment demonstrated recall expansion upon *ex vivo* stimulation with MA (310, 311).

T cells restricted to CD1c were first reported in 1996 and, in a similar manner to CD1b, were initially reported to present lipid antigens derived from *M.tb* (312). Double negative (DN) T cells acquired from healthy donors were cultured in the presence of $CD1^+$ APCs and *M.tb* sonicate before depleting $CD4^+$, $CD8^+$ and γδ T cells to derive the *M.tb* specific αβ T cell line DN6 (312). Restriction of DN6 to CD1c was demonstrated by the inhibition of *M.tb* antigen-induced T cell proliferation upon anti-CD1c mAb treatment of $CD1^+$ monocytes, and more recently has been shown to recognise the *M.tb* cell wall lipid PM in the context of CD1c (264, 312). $CD8^+$ αβ T cells specific for *M.tb* antigens have also demonstrated restriction by CD1c and have been shown to display a cytotoxic Th1 response following stimulation with CD1c expressing C1R cells and *M.tb* extract (248). In 2000, the presence of mycobacterial lipid-specific, CD1c-restricted T cells in *M.tb* exposed individuals was demonstrated for the first time. Moody *et al* reported that the previously isolated CD1c-restricted $CD8^+$ αβ T cell line, CD8-1, recognised CD1c presented isoprenoid glycolipids derived from *M.tb* (313). Furthermore, CD1c-restricted T cell responses specific for mannosyl-β1-phosphodolichols (MPD), which are structurally related to *M.tb* derived MPM, were observed in *M.tb* exposed donors but were absent in the peripheral blood of healthy control subjects (313).

Despite a growing body of research into the lipid antigen recognition of CD1-restricted T cells and their function in the context of both disease and the normal immune system, the understanding of how these T cells develop remains a relative mystery. This is in part due to the lack of appropriate small animal models, but humanised CD1 transgenic mice may be a useful tool in trying to unravel the CD1-restricted T cell developmental pathway. One recent study using humanised mice expressing the CD1b-restricted T cell line HJ1 suggests that cortical thymocytes could be the predominant cell type involved in HJ1 selection as CD1b was not expressed on mature thymocytes but that CD1b-expressing haematopoietic cells were necessary for positive selection of these T cells (314). HJ1 T cells from the CD1 transgenic mice were found to express PLZF, a transcription factor expressed by other unconventional T cells such as iNKTs during their developmental pathway which is responsible for their innate-like functions (156, 158, 314, 315). The selection process for lipid-specific CD1-restricted T cells is still unknown, but unlike MHC-restricted T cells, those autoreactive to self-lipids are not removed. Autoreactive CD1-restricted T cells are found in high frequencies in both umbilical cord blood and peripheral blood with the former predominantly expressing a naïve $CD45RA^+$ phenotype (304). In adult humans, autoreactive CD1-restricted T cells have been found to express either a naïve ($CD45RA^+$) or effector memory phenotype ($CD45RO^+$), but their exact function is still unknown (304, 316).

1.2.7.2 CD1-restricted γδ T cells

While the majority of CD1-restricted T cell populations characterised express an αβTCR, a growing body of evidence shows that CD1 molecules are also recognised by some subsets of γδ T cells. Except for Vδ2 γδ T cells which predominantly recognise phosphoantigens, Vδ1 and Vδ3 γδ T cells have demonstrated reactivity to CD1, although the latter has not been well explored. Vδ1 T cells have shown to have prominent reactivity to CD1d, CD1c and more recently, CD1b (174, 175, 299, 317). The first CD1d-restricted Vδ1 T cells were isolated using CD1d tetramers loaded with sulfatide, an abundant self-lipid found in the GI tract, kidney and brain (318). Structural analysis of the interaction between the Vδ1 TCR and CD1d-lipid complex determined that the CDR3δ loops of the TCRδ chain interacted with both the sulfatide head group and the α1 helix of CD1d (319). Similarly, the interaction of the TCR with CD1d when presenting α-GalCer showed dominance of the germ-line encoded Vδ1 chain, but the main interaction with α-GalCer involved the CDR3γ chain (319, 320). This emphasises conclusions from previous reports, that the CDR3 sequences are critical for the recognition of antigens (321-323).

Until recently, it was thought that Vδ1 T cells only recognised CD1d and CD1c. However, a recent report has detailed the recognition of CD1b by multiple γδ T cells harbouring a Vδ1 chain, with each demonstrating different mechanisms and requirements of binding (299). CD1b tetramers carrying an undetermined array of endogenous lipids incorporated within the mammalian expression system were used to identify and isolate CD1b-restricted γδ T cells from healthy human donors. These Vδ1 T cells activated and produced IFNγ upon stimulation with CD1b in the absence of exogenous lipid, but each TCR with varying Vγ and Vδ1 nucleotide sequences demonstrated differential recognition patterns when exposed to individual phospholipids (299). Chain swapping experiments further highlighted that the specificity for the CD1 isoform was mediated by the δ chain whereas the γ chains had a lesser role (299).

Despite CD1c being the first described ligand for γδ T cells (302), the mode of interaction and specificity for presented lipid antigens are incompletely understood. Recognition of CD1c by γδ T cells has been documented by various groups, reporting that γδ T cell clones are activated following stimulation with CD1c, subsequently lysing $CD1c^+$ target cells using perforin- and Fas-mediated cytotoxicity in addition to producing Th1 cytokines (179, 302, 324, 325). More recently, CD1c tetramers presenting mycobacterial PM have been used to identify a population of CD1c-restricted Vδ1 T cells in healthy human donors. The authors cloned a panel of CD1c-PM tetramer isolated Vδ1 T cells which were all activated when stimulated with PM (174). Interestingly, some of these TCRs demonstrated promiscuous reactivity and responded to CD1c loaded with MPM or various self-lipids such as sulfatide and LPC. Further analysis again revealed that although

different Vδ1 TCRs had preferential lipid requirements and docking mechanisms, the CDR3 loop of the Vδ chain played a key role in CD1c recognition, with the γ chain fine tuning the interaction (174). The ability of Vδ1 T cells to recognise each CD1 isoform in complex with either pathogen or host derived lipids, particularly in a stress-regulated manner, may identify them as a key player in autoimmune processes as well as in response to infectious diseases and cancer.

1.2.8 CD1 and autoreactivity

CD1 molecules are well known for presenting foreign lipids from pathogens to T cells. However, there is a large body of research documenting the presentation of self-lipids to T cells, which are termed 'autoreactive T cells'. These autoreactive T cells may be involved in immunoregulatory processes, but on the other hand they may contribute to the pathogenesis of disease or influence autoimmune destruction.

Perhaps the most well documented CD1-restricted autoreactive T cells are those restricted to CD1a. CD1a is expressed abundantly by Langerhans cells and a large proportion of skin T cells have been demonstrated to be autoreactive to CD1a (298, 316). Lipid ligands for CD1a has been found to include squalene and wax esters, these headless antigens are found to reside within the CD1a molecule after displacing inhibitory lipids with large head groups (295). These lipid antigens constitute sebaceous oil that coats the skin, indicating that CD1a autoreactive T cells may play a role in normal skin barrier immunity (295, 298, 316). Lipid antigen recognition by CD1a autoreactive T cells has been further probed by Cotton *et al*. CD1a produced by the mammalian recognition system was intrinsically loaded with over 100 self-lipids, and following tetramerisation, it was observed that CD1a autoreactive T cells recognised CD1a regardless of the bound lipids (298). Further analysis demonstrated that TCR recognition mapped to areas of CD1a distal to the antigen exit portal, indicating that autoreactivity was directed towards CD1a itself (298). CD1a autoreactive T cells have been found to display diverse TCRs and a large proportion express the $CD4^+$ co-receptor (316, 326, 327). Observations have suggested that CD1a autoreactive T cells are a normal mechanism of skin homeostasis, including the expression of homing receptors CLA, CCR6, CCR4 and CCR10, as well as the secretion of IL-22 (316, 326, 327). IL-22 production following interactions of CD1a autoreactive T cells with Langerhans cells may promote epithelial matrix remodelling without initiating immunopathology and has additional roles in stimulating the production of antimicrobial peptides and increased proliferation (316, 328, 329). However, overproduction of IL-22 has been linked to the promotion of immunopathology in psoriasis through the stimulation of further cytokines including IL-2, IL-13 and IFNγ, suggesting that CD1a autoreactive T cells may in some circumstances function in a deleterious way (330).

Out of the three group 1 CD1 molecules, T cells autoreactive to CD1b have been the most difficult to identify. In 2009, Felio and colleagues generated humanised CD1 transgenic mice and generated an array of group 1 CD1-restricted T cell lines, the majority of which were found to be autoreactive (331). Interestingly, one CD1b-restricted T cell line, HJ1, was able to lyse CD1b expressing target cells in the absence of exogenous antigen and therefore demonstrates one of the earliest examples of a CD1b autoreactive T cell line (331). The HJ1 CD1b autoreactive T cell line has since been used alongside CD1 to generate humanised transgenic mice expressing both the CD1b molecule and cognate autoreactive T cells. Li and colleagues observed that HJ1 T cells in transgenic mice display an activated phenotype and secrete pro-inflammatory cytokines upon stimulation with $CD1b^+$ DC (314). Subsequent studies have endeavoured to uncover whether these CD1b autoreactive T cells play a protective role against disease or are involved in the development of immunopathology. Humanised transgenic mice again expressing both group 1 CD1 molecules and the HJ1 T cell line were used to investigate the role of CD1 autoreactive T cells in the context of the anti-tumour response. HJ1 T cells were observed to recognise CD1b-presented self-phospholipids from both lymphoma cells and normal cells, but the response was greater to lipids extracted from tumour cells with autoreactivity enhanced following treatment with toll-like receptor agonists (332). Furthermore, adoptive transfer of HJ1 T cells induced protection against T cell lymphoma in CD1b expressing mice, demonstrating a role for CD1b autoreactive T cells in the anti-tumour response (332).

In contrast to these observed protective responses, CD1b autoreactive T cells have been implicated in the worsening of psoriatic skin conditions. In another transgenic mouse model, phospholipids and cholesterol were found to accumulate in the diseased skin of ApoE-deficient mice. Activated HJ1 T cells secreting IL-17A were observed in mice that developed psoriasiform skin inflammation in addition to increased production of IL-6 by $CD1b^+$ DC which was associated with hyperlipidemic serum (333). Moreover, the frequency of CD1b autoreactive T cells was increased in human psoriatic patients compared to healthy controls, further demonstrating that under hyperlipidemic conditions CD1b autoreactive T cells may play a detrimental role (333). These transgenic mouse studies demonstrate both a protective and pathogenic role for CD1b autoreactive T cells during lipid-altering disease states, however they do not explain how they function under normal conditions. T cells reactive to MHC presented antigens are processed thoroughly and undergo thymic selection to minimise reactivity toward self-peptide antigens (334), but our understanding of how T cells avoid reactivity to endogenous antigens presented by CD1 is poor.

It has been proposed that CD1 restricted T cells ‘see’ many self-lipids presented by CD1 but are only activated when they encounter a rare antigen (297, 335). An example of this is

Phosphatidylglycerol (PG) which is expressed at low concentrations in mammalian mitochondria but is more abundant in bacteria (297, 301). It is thought that T cells may only come into contact with endogenous PG in incidences causing mitochondrial stress, and is otherwise unavailable for recognition (301). Shahine *et al* demonstrated the recognition of PG by two cloned TCRs (PG10, PG90) with their autoreactivity to CD1b expressing target cells augmented by the addition of micromolar quantities of PG (297). The recognition of this less abundant antigen was shown to be preferential over more common membrane lipids such as PC and phosphatidylethanolamine (297). A study by Van Rhijn *et al* also revealed that four CD1b-restricted T cell lines showed reactivity to both mitochondrial and bacterial produced PG (301). Their work showed that although lipid recognition was necessary for binding of $\alpha\beta$ TCRs to CD1b-phospholipids, the data did not indicate structural differences between self- and foreign-lipids determining resultant T cell responses (301). These studies suggest that while CD1b autoreactive T cells recognise both host and bacterial phospholipids, those in the host may be below the threshold of detection and only display an activated phenotype when lipids are in abundance, such as during infection (297).

Together with the work undertaken by Bagchi *et al* reporting the pathogenic role of CD1b autoreactive T cells in hyperlipidemic conditions, this may indicate a harmful role for these T cells in the context of *M.tb* infection. The inhibition of phagosomal acidification and prevention of phagolysosomal fusion are evasion mechanisms utilised by *M.tb* (13, 336). This in turn may lead to the inability of CD1 molecules to present antigens, as CD1b in particular requires a low pH for lipid loading. However, Shamshiev *et al* discovered that several self-glycosphingolipids were readily bound by CD1b at the cell surface even at neutral pH, and could be recognised without internalisation and processing of the molecule (257). These results may indicate that CD1b autoreactive T cells influence tissue damage through recognition of lipids shared by both the host and pathogen which are presented on the cell surface at neutral pH, and therefore unaffected by blockade of phagosomal acidification.

Autoreactive T cells to the final member of the group 1 CD1 molecules, CD1c, are estimated to comprise 0-7% of circulating $\alpha\beta$ T cells, but as of yet are poorly understood (266, 304). De Lalla and colleagues screened libraries of $CD4^+$ and $CD4^-CD8^-$ DN T cells and found that a large proportion of both were CD1 restricted self-reactive T cells with diverse TCRs, predominantly recognising CD1a and CD1c (304). CD1c autoreactive T cells of both αβ and γδ lineage have been discovered, some of which promiscuously recognise CD1c bound to either host lipids or mycobacteria-derived lipid antigens. For example, CD1c expressed by K562 cells has been shown to consistently activate a population of αβ T cells in the absence of exogenous antigen *in vitro* (337). These T cells were observed to preferentially express the TRBV4-1 chain in addition to the CD4 co-receptor (337). Furthermore, Wun and colleagues discovered that CD1c tetramers

carrying endogenous lipids consistently stained a large percentage of $CD3^+$ cells in healthy donors (268). Their study of the autoreactive $\alpha\beta$ TCR, 3C8, transduced into the J76 Jurkat T cell line revealed an upregulated expression of CD69 when in the presence of CD1c expressing APCs but in the absence of exogenous antigen. Interestingly, mutagenesis patterns of this TCR showed commonalities with CD1c-reactive TCRs that specifically recognise mycobacterial PM (268). Dual reactivity of CD1c autoreactive αβ T cells has been described by Vincent *et al*. $CD8^+$ CD1c-restricted αβ T cell clones with diverse CDR3 regions were derived from donor samples exposed to microbial antigen. They discovered that these T cells responded to CD1c in the absence of exogenous antigen, but displayed an enhanced response when exposed to microbial antigen (300).

Dual reactivity of CD1c autoreactive function has also been described for γδ T cells. CD1c tetramers loaded with the *M.tb* lipid PM have been used to isolate CD1c-restricted γδ T cells which display an activated phenotype upon restimulation with PM (174). Interestingly, some of these CD1c-PM isolated T cell lines also responded to self-lipid antigens, demonstrating dual reactivity of CD1c-restricted γδ T cells to both host and pathogen derived lipids (174). This supports previous work by Spada and colleagues demonstrating that an enriched γδ T cell population expanded in the presence of *M.tb* derived antigens also proliferated in response to $CD1c^+$ DC in the absence of exogenous antigens. These proliferated cells were shown to produce inflammatory cytokines and were able to lyse CD1c expressing target cells (179).

It has been suggested that CD1c autoreactive T cells may have a protective role in the context of disease. CD1c autoreactive T cells, recognising the self-lipid methyl-lysophosphatidic acid (mLPA), have been demonstrated to lyse $CD1c^+$ leukaemia cells in which this lipid accumulates (338). In contrast, nontransformed T cells were poorly recognised by CD1c autoreactive T cells, demonstrating that an abundance of the self-lipid mLPA in transformed cells may have triggered the targeted response (338). Further to this, it has been suggested that CD1c autoreactive T cells may play a role in autoimmune pathology. Myeloid DC expressing CD1c have been found to infiltrate inflamed tissues in various autoimmune disorders including rheumatoid arthritis, vitiligo and thyroiditis (339, 340). Autoimmune tissue destruction as an effector function of CD1-restricted T cells has been demonstrated in Graves and Hashimoto's disease of the thyroid (339). Although not detected in peripheral blood, CD1c-glycolipid specific T cells have been found in lymphocytes isolated from affected thyroid glands and were able to lyse target cells expressing CD1c or CD1a (339). APC expressing CD1c were also found to infiltrate the thyroid gland, suggesting that CD1c autoreactive T cells were present and could lyse target cells leading to tissue destruction in this area. Despite autoreactive CD1-restricted T cells being implicated in adverse immunological events, the response of these T cells to CD1c expressing cells may be

immunoregulatory as has been seen with CD1d (339, 341), suggesting that autoreactivity doesn't necessarily lead to autoimmunity.

Strongly induced expression of CD1c has been observed on foam cell macrophages, which are characterised by their intracellular accumulation of cholesteryl esters (342). Foam cell macrophages, with CD1c antigen presenting capabilities fully retained, are commonly observed in inflammatory lesions of atherosclerosis but are known to also be present in tuberculous lesions (343). Presentation of cholesteryl esters by CD1c, similar to those accumulating in foam cell macrophages, has been shown to be recognised by self-reactive T cells (265). This demonstration of T cell autoreactivity to cholesteryl esters may implicate them in promoting tissue inflammation where foam cell macrophages are known to congregate, i.e. in TB and autoimmune conditions. However, the role of CD1c autoreactive T cells, whether this is a protective or pathological role, in the context of TB disease has yet to be explored.

Autoreactivity has now been demonstrated for subsets of circulating T cells restricted to each of the group 1 CD1 molecules. However, the absence of autoimmune related tissue destruction in healthy humans indicates that there must be mechanisms in place to avoid continued activation of self-lipid specific CD1 autoreactive T cells. The development of MHC restricted T cells occurs in the thymus where they undergo the process of positive and negative selection in order to promote self-tolerance and prevent activation in response to self-peptides. It is however less clear how CD1 autoreactive T cells are prevented from responding to $CD1^+$ APCs presenting self-lipid. Mechanisms to restrict activation of CD1 autoreactive T cells have been suggested to include: modification of expression and spatial separation of CD1 molecules on the cell surface, cytokine mediated augmentation of T cell activation and enzymatic regulation of antigen availability (168). For example, in contrast to CD1d which is constitutively expressed on most APC, upregulated expression of group 1 CD1 molecules is induced on monocytes in response to stimulation with GM-CSF, IL-4 or mycobacterial lipids (339, 344, 345). On the other hand, expression of group 1 molecules have been found to be inhibited by the binding of IgG to FcγRIIa on DC, as well as by factors found within human serum such as cardiolipin and lysophosphatidic acid (LPA) suggesting that CD1 expression in the peripheral blood is highly regulated (346, 347). This indicates that in the circulation of healthy humans, there is a lack of availability of CD1 and/or specific lipids to activate cognate autoreactive T cells. Disease states such as in the context of infection with *M.tb* may then induce the availability of ligands for CD1 autoreactive T cells which in turn may lead to protective or pathological consequences.

1.3 Animal models of TB

1.3.1 Mouse

Understanding the host immune response to TB infection is crucial for the development of new diagnostics, treatments and vaccines. Animal models have been invaluable in evaluating the immune response to mycobacterial challenge in numerous settings, allowing for a complete picture of pre-infection through to post-infection to be interrogated which is not feasible in human participants. The most frequently used animal model in *M.tb* infection is the mouse (348), providing a low cost and less spatially demanding host in which to study the course of infection (349). A large resource of mouse-specific immunological tools and reagents are available, in addition to a variety of different strains which vary in terms of their susceptibility, pathological response and survival times (349). For example, BALB/c mice are less resistant to *M.tb* infection than C57BL/6 mice (350), but unlike most strains, C3HeB/FeJ mice are able to develop necrotic granulomas following infection (351). The simple handling and containment procedures along with the presence of good cellular immunity makes the mouse a preferred model for the rapid evaluation of new drug and vaccine candidates (348). However, despite having comparable immune responses to humans, the physiology and pathology of the mouse makes it less directly applicable to human disease (352, 353). Lung pathology in *M.tb* infected mice differs substantially to that of humans, with the majority of mice failing to develop the hallmark caseating granulomas typically seen in human TB and the granulomas that do develop are poorly organised and lack fibrosis (2, 354-356). Furthermore, in contrast to human TB where mycobacteria tend to be extracellular within necrotic lesions, bacilli within the mouse model are found to primarily reside intracellularly in the lungs which also tend to develop non-necrotic lesions (357, 358). Finally, mice lack some human proteins which are deemed important in TB immunity including CD1a, CD1b, and CD1c.

While the mouse is the predominant model used in TB research, they lack the group 1 CD1 molecules seen in humans (359). The only naturally expressed CD1 molecule in the mouse is CD1d, which has been extensively investigated through knockout and adoptive transfer studies, revealing that CD1d is an important player in the immune response to *M.tb* infection (132, 149, 150, 360). However, until recently this frequently used animal model has not been useful for studying the role group 1 CD1 molecules play in response to infection. The development of the humanised CD1 transgenic mice by Felio and colleagues has allowed for the investigation of CD1a, CD1b and CD1c in the context of *M.tb* infection. The expression pattern of these molecules resembled that of human group 1 CD1 and CD1-restricted T cell responses were induced in response to vaccination with BCG or *M.tb* challenge (331). Further investigations from this group

of CD1 transgenic mice that also expressed a human MA-specific, CD1b-restricted TCR demonstrated that following *M.tb* challenge, CD1-restricted T cells are primed in the mediastinal lymph node and were associated with protection after adoptive transfer (148). The development of the humanised CD1 transgenic mouse model has opened up the possibility of using knock-out studies to further delineate the role of these proteins in response to *M.tb* infection, but the physiological and pathological differences between human and mouse still pose an issue.

1.3.2 Guinea pig and Rabbit

Another popular model for *M.tb* infection which was also the primary model used by Robert Koch in the identification of the tubercule bacillus is the guinea pig (361). Unlike the mouse model, guinea pigs display more comparable aspects of *M.tb* pathology to humans such as necrotic lesions and caseation (348, 362). Guinea pigs are highly susceptible to *M.tb* infection and are predominantly used for drug safety and efficacy studies (348, 363). However, despite presenting a similar lung pathology to humans, guinea pigs have poor cell mediated immunity and there is a distinct lack of immunological reagents available to study cellular response. An improvement upon the guinea pig system may be the rabbit model which also produces necrosis, caseation and cavitation in response to *M.tb* infection but has the added benefit of better cell mediated immunity (348, 364). This model has been primarily used for research into *M.tb* transmission, drug penetration and distribution and also rarer forms of TB such as meningeal, cutaneous and bone infections (348, 365). Similar to the guinea pig, the rabbit is also subject to a lack of immunological reagents for research, but clinical symptoms in this model are also more inconspicuous (348).

The first animal model utilised to study the role of group 1 CD1 molecules was the guinea pig. Guinea pigs express a range of human-like CD1 isoforms including four CD1b molecules, three CD1c and at least one CD1a like molecule (366). The presence of CD1-restricted T cells in the guinea pig model has been demonstrated by Hiromatsu *et al*, showing that CD1-restricted $CD8^+$ T cells are induced upon inoculation with Mycobacterial lipid antigens (367). Guinea pig CD1b and CD1c molecules presented glycolipid antigens derived from *M.tb* and antigen-specific $CD8^+$ T cells demonstrated cytotoxic activity against *M.tb* lipid pulsed $CD1^+$ bone marrow derived DC (367). Vaccination of guinea pigs with mycobacterial lipids including Ac2SGL or PIM2 has been associated with a reduction in both pathology and bacterial burden in the lungs, suggesting that lipid-specific CD1-restricted T cells may play a protective role (368, 369). Their use in *M.tb* infection studies as well as their natural expression of group 1 CD1 molecules makes the guinea pig an attractive model for lipid-vaccine research.

1.3.3 Macaque

More recently, the development of a macaque model of TB has emerged in the field, being utilised in investigations studying susceptibility, treatment and vaccination. The close evolutionary relationship in addition to the similarity of macaque pathology, physiology and immunology to that of humans makes them an ideal model in which to better progress onto efficacy testing in humans (370). There is considerable overlap between TB disease presentation in macaques and humans, with macaques developing a range of granulomas with necrosis, caseation and cavitation (348, 370-374). Different species have shown to have a range of susceptibilities and resistance to *M.tb* (370-374). For example, the various subspecies of Cynomolgus macaque can develop a range of disease presentations in addition to a latent-like disease due to their relative resistance to *M.tb* compared to the Rhesus macaque which are more susceptible (375). Chinese Cynomolgus and Indonesian Cynomolgus macaques demonstrate good control of infection whereas Mauritian Cynomolgus present lower disease resistance (371-373). Furthermore, various granuloma types have been observed not only between macaques, but within each organ (2). Ultra low dose aerosol infection of *M.tb* has further highlighted the differences between species, with Rhesus macaques presenting with a more progressive disease while Cynomolgus macaques demonstrated a reduced burden of disease (372). The differences in immunological response to infection between the species of macaque in addition to their similar pharmacokinetic profiles to that of humans, makes this model an invaluable tool when assessing multiple parameters such as drug and vaccine efficacy, treatment strategies and progression from infection to disease (348). In spite of these advantages, drawbacks of this model include substantial requirements in terms of lab space, expense, maintenance and experimentation which adds to their low availability for use in TB research.

However, a significant advantage for the NHP model is the retention of CD1 genes. Both the Rhesus and Cynomolgus macaque express group 1 and group 2 CD1 molecules and are extremely similar to the human orthologues (376, 377). The group 1 molecules in fact are so similar that macaque CD1b is recognised by and activates human CD1b-restricted T cells (377). The macaque model of the CD1 system has already produced interesting findings. It was previously assumed that *M.tb* derived GMM was only presented by CD1b and recognised by CD1b-restricted T cells, however it has recently been demonstrated that CD1c-restricted T cells from both humans and macaque can recognise GMM, but are specific to CD1c (376, 378). Layton and colleagues also revealed cross-species recognition of macaque and human derived CD1c proteins, further indicating that the NHP model may be the most relevant for investigating this system for their role in disease (376).

1.3.4 Zebrafish

An alternative model for TB pathogenesis as well as drug and vaccine development is the zebrafish (348). Despite little anatomical similarities, zebrafish harbour comparable immunological components to humans including the development of structurally similar granulomas (379-381). Zebrafish represent an ideal model for large scale screening studies due to their ease of care, small requirements for lab space and ability to quickly produce numerous offspring (~300 eggs per week) (379, 382, 383). Although zebrafish are unable to be infected with *M.tb*, challenge with *Mycobacteria marinum* (*M.marinum*) produces a range of human-like infection states such as systemic disease, latent infection, formation of histologically similar granulomas and secondary reactivation (380, 384, 385). Both embryos and adult zebrafish are able to be infected, allowing for a full lifecycle analysis of disease, in addition to being transparent which permits the use of high resolution microscopy (386, 387). The use of the zebrafish model in drug development has been key in revealing the role of mycobacterial efflux pumps in acquiring tolerance to antibiotics, with the addition of the efflux pump inhibitor verapamil suppressing this tolerance and increasing treatment efficacy (388). However, important drawbacks of the zebrafish model of TB infection include their inherent lack of T cells, enabling only interactions of *M.tb* with macrophages to be studied (389). Furthermore, while zebrafish express MHC molecules, they do not harbour CD1 genes, thus preventing a more complete analysis of mycobacterial antigen presentation and CD1-restricted immune responses (390, 391).

Every animal model of TB has limitations, but when choosing a model for vaccine research, it is appropriate to consider all aspects of the immune response including unconventional T cells and antigen presenting molecules.

1.4 Vaccination

The BCG vaccine is the first and currently only licensed vaccination against TB. Since its first use in 1921, the BCG has become the most widely administered vaccination worldwide and is a standard part of national childhood immunisation programmes in over 150 countries (1, 392, 393). The BCG is a live, attenuated vaccine generated by subculture of *Mycobacterium bovis* (*M.bovis*) (394) which, due to variances in culture conditions over time, has been developed into 14 different strains varying in both phenotype and genotype (395, 396). Four strains of the BCG make up more than 90% of the prepared doses worldwide and include BCG Pasteur 1173P2, BCG Japan 172, BCG Glaxo 1077 and BCG Danish 1331 (397). BCG vaccination has been shown to protect against primary disease in children as well as disseminated forms such as TB meningitis and miliary TB with an efficacy as much as 70-80% (1, 3, 398-400). However, the protective effects of the vaccine

are reported to provide a maximum of 20 years of protection (269, 401) and has failed to show adequate prevention of pulmonary disease and secondary reactivation in adults (1, 3, 398). The efficacy of the BCG is reported to vary greatly from between 0 and 80% (402) and correlations have not been found between the cytokine profile of *M.tb* specific T cells in BCG vaccinated newborns and protection from the development of TB (403). Thus far, the global rate of TB incidence is not falling fast enough to hit the WHO's End TB Strategy targets of an 80% reduction in incidence by 2030 (1) and it has been reported that the BCG in its current administration programme is not having a significant impact on this goal (404).

Studies have been conducted into whether the route of BCG administration impacts the protective response. Aerosol delivery of BCG to Rhesus macaques has been reported to induce a Th1 and Th17 cytokine response, with polyfunctional CD4+ T cells detected in the BAL fluid following vaccination (405). However, more strikingly is the improved protection generated in the macaque model following intravenous (IV) delivery of the BCG vaccine. In two studies, IV injection of BCG was found to provide superior protection over the standard intradermal delivery with disease pathology significantly reduced and an improved survival of macaques challenged with *M.tb* (372, 406). Compared to intradermal or aerosol BCG delivery, IV injection induced larger frequencies of antigen specific CD4+ and CD8+ T cells in BAL fluid and peripheral blood, with some animals even displaying an absence of detectable infection using positron emission tomography-computerised tomography (PET-CT) (372, 406). However, despite these positive results, the BCG vaccine may still be unsuitable for the entire population. Safety testing of IV BCG has yet to be carried out in humans, and in the current regime, the BCG is only suitable for those without prior sensitisation to mycobacteria which presents a major issue in countries with high incidences of LTBI in adults (407). Despite improved protection demonstrated in animal models in response to *M.tb* challenge following IV BCG, the demand for a more efficacious vaccine that can provide protection for all remains high.

Since August 2019, there are more than 14 alternative vaccines against active TB that have been under investigation in clinical trials including live attenuated or recombinant vaccines, viral vector and protein adjuvants (1, 397). One candidate currently undergoing a phase Ib/IIa trial in South Africa is MTBVAC, a live, genetically attenuated vaccine and is the only potential TB vaccine derived from the clinical isolate of *M.tb* (408-410). A phase I trial observed a comparable safety level to the BCG vaccine and found that all vaccinated participants were IGRA negative at the 2 year follow up (411). The intention behind this vaccine is to replace the BCG for newborns and to serve as a booster vaccine for adults, however the same concerns regarding prior mycobacterial sensitisation exist for MTBVAC as for BCG (397). A second potential candidate is the viral vector vaccine ChAdOx1 85A-MVA85A developed by Oxford University. This vaccine combines the

chimpanzee adenovirus ChAdOx1 with the modified vaccinia Ankara virus MVA85A which both express the *M.tb* antigen Ag85A and uses a prime-boost strategy to induce CD8+ and CD4+ T cell responses (412, 413). Following promising results in the mouse model, the ChAdOx1 85A-MVA85A vaccine candidate underwent a phase I in 42 healthy BCG vaccinated adults. The ChAdOx1 85A prime induced $CD4^+$ and $CD8^+$ T cell responses but was not boosted by a second dose. However these responses were boosted upon administration of MVA85A. The prime-boost candidate was well tolerated and immunogenic, but the results were not overwhelming (414).

Another promising candidate is the H56:IC31 protein adjuvant vaccine constituting the *M.tb* derived early secretory proteins ESAT-6 and Ag85B and the latent infection associated protein Rv2660C in combination with adjuvant IC31. This potential vaccine is intended to protect against new infections with *M.tb* in addition to preventing reactivation of LTBI (415). H56:IC31, when used in the NHP model, has demonstrated to significantly reduce lung pathology while inducing a robust memory response when compared to the BCG (416). Furthermore, H56:IC31 vaccinated Cynomolgus macaques with latent *M.tb* infection did not show evidence of reactivation upon anti-TNF antibody treatment (416). Phase I trials, which included HIV negative adults with LTBI or patients with drug susceptible TB that had undergone treatment, concluded that the vaccine was safe and produced good immunogenicity at all trial doses (415, 417, 418). Phase II trials investigating the ability of H56:IC31 to reduce TB recurrence in HIV negative individuals post-treatment for TB in South Africa and the United Republic of Tanzania is currently ongoing.

Of all the vaccine candidates currently undergoing investigation, the protein adjuvant vaccine M72/AS01 has appeared as a front-runner. Developed by Glaxo-SmithKline, recombinant fusion proteins Mtb31 and Mtb39 are combined with adjuvants AS01b, AS02a or AS01E and are designed to promote BCG induced immunity (419). The vaccine has performed well in animal models of *M.tb* infection, inducing greater protection than BCG alone in mice, guinea pigs and macaques (420, 421). Phase IIb trials conducted in Kenya, South Africa and Zambia revealed the vaccine induced significant protection against TB in individuals with LTBI, with an acceptable safety profile in addition to inducing robust humoral and cellular immune responses (1, 397). Vaccine efficacy was estimated at 54% over 2 years of follow up, which in terms of TB vaccine research, is a clinically significant result (1).

However, despite advances in the search for an improved TB vaccine, the innate and unconventional T cell responses to *M.tb* infection have yet to be thoroughly investigated or exploited. T cells specific for lipids presented by molecules of the CD1 system are induced following infection with *M.tb*, suggesting that lipid based vaccines may be an ideal target. Humanised transgenic mouse models expressing group 1 CD1 proteins and a CD1b-restricted, MA-

specific TCR (DN1) were assessed for their response to *M.tb* challenge (148). Activated DN1 T cells displayed a polyfunctional phenotype and were found to accumulate in lung granulomas but protected against *M.tb* infection (148). A further study investigating the protective response of lipid-based vaccines comprising *M.tb* derived Ac2SGL or PIM2 found that vaccinated guinea pigs had a reduced bacterial burden in the spleen compared to unvaccinated animals following challenge with *M.tb* (369). Furthermore, a reduction in the number of lesions and severity of immunopathology was observed in the lungs of the vaccinated group (369). This is in support of previous studies which observed an induction of lipid-specific, CD1-restricted T cell responses following inoculation of guinea pigs with mycobacterial lipid mixtures or *M.tb* total lipids and a reduction in pathology and bacterial burden following *M.tb* challenge (367, 368). These studies represent a promising beginning to the exploitation of the CD1-restricted T cell response by way of lipid-based vaccines, but further work is needed to fully understand the host-pathogen interaction upon *M.tb* infection.

1.5 Summary

Despite efforts to reduce the global burden of Tuberculosis, the rate of incidence and mortality is simply not falling fast enough to meet the goals of the END TB Strategy set out by the WHO. The emergence of multidrug-resistant TB (MDR-TB), extensively drug-resistant TB (XDR-TB) and totally drug resistant TB highlights the growing need for improved methods of prevention, diagnosis and treatment. As the only licensed vaccine for the prevention of TB has such a variable rate of efficacy, a new vaccine is urgently needed and could prevent many of the new cases of TB reported each year. Unfortunately, despite extensive research, the immunology underpinning infection control versus disease is still incompletely understood, thus stalling the development of new vaccines.

Unconventional CD1-restricted T cells are fast becoming a target of *M.tb* immunology research. As *M.tb* has a high lipid content and mycobacterial lipid specific CD1-restricted T cells have been demonstrated, there is strong evidence that these T cells play an important role during infection. In addition to this, it has been observed that plasma lipidomics of TB patients is altered when compared to healthy controls. Several studies have documented decreased levels of LPC in those with active TB (422-424) but a simultaneous increase in PC and PG has also been reported (422). However, it is unclear whether the alteration in these lipid levels have an effect on the frequency and function of CD1-restricted T cells, or if these T cells are protective or deleterious in the context of TB. Therefore, in order to target these responses in TB, we need to understand the basic molecular mechanisms that govern the interaction between T cells and CD1-lipid complexes.

In addition, phenotypical and functional characterisation of CD1 restricted T cell subsets in human TB are required in order to shed light on the T cell subsets that play important roles in host immunity to infection. Important T cell subsets can be dissected for their "friend" or "foe" function in TB by studying T cell function in sophisticated 3D cell culture models and via *in vivo* models. Hence, a better understanding of unconventional CD1 mediated immunity in the host pathogen interaction in TB may provide the platform for the generation of improved future vaccines and better therapeutics for TB.

1.6 Hypotheses and Aims

1.6.1 Hypotheses

The overarching hypothesis of my research is that *Lipid-CD1 reactive T cell immune responses play a central role in the host immune response to tuberculosis infection*.

To investigate my overarching hypothesis, I will investigate unconventional CD1 mediated immune responses in the context of TB in humans and in the macaque model of infection with the following species specific hypotheses:

1) *CD1c autoreactive T cells modulate the host-pathogen interaction in human TB infection*
2) *CD1d-restricted iNKT responses in macaque TB infection are associated with disease severity and outcomes*

1.6.2 Aims

I will address the above hypotheses with the following specific aims:

<u>Human</u>

I. Examine the molecular basis underpinning CD1c-lipid recognition by TCR through mutational analyses; involving the generation of CD1c alanine mutants and the interrogation of their interaction with TCR by FACS analysis and SPR.
II. Establish CD1c autoreactive T cell lines and clone respective TCRs onto Jurkat T cell lines to determine reactivity to CD1c through combined tetramer binding and functional studies.
III. Explore CD1c mediated immune response in healthy subjects through optimisation of short term expansion methods
IV. Determine expression of CD1c and γδ T cell receptors in human TB granulomas by Immunohistochemistry.

V. Investigate numerical and phenotypical characteristics of CD1c mediated responses in the peripheral blood and lungs of human TB patients.

Macaque

VI. Investigate numerical and functional changes of iNKT and CD1c-restricted T cell repertoire from peripheral blood and tissues of animals pre- and post-*M.tb* challenge in longitudinal studies.

VII. Determine iNKT phenotype in blood and lung biopsy samples with pathological and bacteriological readouts.

VIII. Generate macaque CD1c tetramers and investigate their binding to T cells in order to explore these responses in future *M.tb in vivo* challenge studies.

Chapter 2 Materials and Methods

2.1 Human

2.1.1 Protein production and purification

2.1.1.1 Site directed mutagenesis of CD1c

Mutant CD1c proteins were generated using a hybrid CD1c protein ($CD1c^h$), a construct of the extracellular α1 and α2 domains of CD1c and the α3 domain of CD1b, cloned into the pET-23d vector (Novagene). Alanine substitutions of residues within the F' roof of CD1c were performed using the QuikChange Lightning Site Directed Mutagenesis kit (Agilent) and custom primers purchased from Eurofins Genomics (Table 1).

Table 1: Primer sets for site directed mutagenesis, amplification and sequencing of soluble CD1c

Site Directed Mutagenesis Primer Sets		
E>A F	Forward	CTT TGG ATT AAC TCG GGC GAT TCA AGA CCATGC AAG
E>A R	Reverse	CTT GCA TGG TCT TGA ATC GCC CGA GTT AATCCA AAG
H>A F	Forward	CTC GGG AGA TTC AAG ACG CTG CAA GTC AAGATT ACT C
H>A R	Reverse	GAG TAA TCT TGA CTT GCA GCG TCT TGA ATCTCC CGA G
L>A F	Forward	GGC CCA AAG TGT CTG TCA TGC ACT CAA TCATCA GTA TGA AG
L>A R	Reverse	CTT CAT ACT GAT GAT TGA GTG CAT GAC AGACAC TTT GGG CC
Y>A F	Forward	CAT CTA CTC AAT CAT CAG GCT GAA GGC GTCACA GAA AC
Y>A R	Reverse	GTT TCT GTG ACG CCT TCA GCC TGA TGA TTGAGT AGA TG
CHOP N>T F	Forward	CAA TAA TTT TCC TGC ATA CCT GGT CCA AGGGCA ACT TC
CHOP N>T R	Reverse	GAA GTT GCC CTT GGA CCA GGT ATG CAG GAAAAT TAT TG
CHOP R>Q F	Forward	CTA CCT CTT TGG ATT AAC TCA GGA GAT TCAAGA CCA TGC AAG
CHOP R>Q R	Reverse	CTT GCA TGG TCT TGA ATC TCC TGA GTT AATCCA AAG AGG TAG
CHOP H>R F	Forward	CTG TCA TCT ACT CAA TCG TCA GTA TGA AGGCGT CAC
CHOP H>R R	Reverse	GTG ACG CCT TCA TAC TGA CGA TTG AGT AGATGA CAG
Amplification Primer Sets		
CD1c_FL_Fwd	Forward	GCG CCC TAG GCG CCA CCA TGC TGT TTC TGC AGT TTC TGC TGC TAG CTC
CD1c_FL_Rev	Reverse	GCG CGC GTC GAC TCA CAG GAT GTC CTG ATA TGA GCA GTG CTT CT
Sequencing Primer Sets		
CD1cLV_Mid_Fwd	Forward	CTG ATG GGA CAT GGT ATC TTC
CD1cLV_Mid_Rev	Reverse	CAG GAA AAT TAT TGT GCC TGA
CD1cLV_Start_Fwd	Forward	ATG CTG TTT CTG CAG TTT CTG
CD1cLV_End_Rev	Reverse	TCA CAG GAT GTC CTG ATA TGA GC

F' roof residues mutated to alanine included TYR155, LEU150, HIS87, and GLU83. Other mutations located within the α1 and α2 helices included ASN55 to THR55, HIS153 to ARG153, and ARG82 to GLN82. The PCR programme utilised can be found in Table 2. The CD1c DNA and polypeptide sequence and the location of the mutants can be found in Figure 6. Mutated DNA was transformed into ultra-competent XL10-Gold cells, following the protocol supplied by Agilent. Plasmid DNA was generated from the CD1c mutant colonies using a QIAprep Spin Miniprep Kit (Qiagen), and the DNA sequence of each was confirmed to contain the correct mutation by the Source Bioscience Sanger sequencing service. Recombinant mutant proteins, as well as wild type (WT) CD1c, were purified, cleaned and subsequently refolded with β_2m in the presence of PC (Avanti Polar Lipids). Following biotinylation and re-purification, mutant CD1c-lipid complexes were conjugated to Streptavidin-R-phycoerythrin (Invitrogen) to generate fluorescently conjugated mutant CD1c tetramers.

Table 2: PCR programmes for site directed mutagenesis and CD1c insert amplification

Site Directed Mutagenesis PCR		
Temperature (°C)	**Time (hh:mm:ss)**	**Number of Cycles**
95	00:02:00	1
95	00:00:20	18
60	00:00:10	
68	00:00:30	
68	00:05:00	1
Insert Amplification PCR		
Temperature (°C)	**Time (hh:mm:ss)**	**Number of Cycles**
98	00:00:30	1
98	00:00:10	35
72	00:00:15	
72	00:10:00	
4	Hold	

Extracellular Hybrid CD1c Sequence

```
                                                    atgggcaacgcggat
                                                     M  G  N  A  D
gcgtcccaggaacacgtgtccttccatgtcatccagatcttctcatttgtcaaccaatcc
 A  S  Q  E  H  V  S  F  H  V  I  Q  I  F  S  F  V  N  Q  S
tgggcacgaggtcagggctcaggatggctggacgagttgcagactcatggctgggacagt
 W  A  R  G  Q  G  S  G  W  L  D  E  L  Q  T  H  G  W  D  S
gaatcaggcacaataatttcctgcataactggtccaagggcaacttcagcaatgaagag
 E  S  G  T  I  I  F  L  H  N  W  S  K  G  N  F  S  N  E  E
ttgtcagacctagagttgttatttcgtttctacctctttggattaactcgggagattcaa
 L  S  D  L  E  L  L  F  R  F  Y  L  F  G  L  T  R  E  I  Q
gaccatgcaagtcaagattactcgaaatatccctttgaagtacaggtgaaagcgggctgt
 D  H  A  S  Q  D  Y  S  K  Y  P  F  E  V  Q  V  K  A  G  C
gagctgcattctggaaagagcccagaaggcttctttcaggtagctttcaacggattagat
 E  L  H  S  G  K  S  P  E  G  F  F  Q  V  A  F  N  G  L  D
ttactgagtttccagaatacaacatgggtgccatctccaggctgtggaagtttggcccaa
 L  L  S  F  Q  N  T  T  W  V  P  S  P  G  C  G  S  L  A  Q
agtgtctgtcatctactcaatcatcagtatgaaggcgtcacagaaacagtgtataatctc
 S  V  C  H  L  L  N  H  Q  Y  E  G  V  T  E  T  V  Y  N  L
ataagaagcacttgcccccgatttctcttgggtctcctggatgcagggaagatgtatgtg
 I  R  S  T  C  P  R  F  L  L  G  L  L  D  A  G  K  M  Y  V
cacagacaagtgaagcctgaggcctggctgtccagtggccccagtcctggacctggccgt
 H  R  Q  V  K  P  E  A  W  L  S  S  G  P  S  P  G  P  G  R
ctgcagcttgtgtgccatgtctcaggattctacccaaagcccgtgtgggtgatgtggatg
 L  Q  L  V  C  H  V  S  G  F  Y  P  K  P  V  W  V  M  W  M
cggggtgagcaggagcagcagggcactcagctaggggacatcctgcccaatgctaactgg
 R  G  E  Q  E  Q  Q  G  T  Q  L  G  D  I  L  P  N  A  N  W
acatggtatctccgagcaaccctggatgtggcagatggggaggcggctggcctgtcctgt
 T  W  Y  L  R  A  T  L  D  V  A  D  G  E  A  A  G  L  S  C
cgggtgaagcacagcagtttagagggccaggacatcatcctctactggggtccgggatcc
 R  V  K  H  S  S  L  E  G  Q  D  I  I  L  Y  W  G  P  G  S
ggtggtggtctgaacgatatttttgaagctcagaaaatcgaatggcattaa
 G  G  G  L  N  D  I  F  E  A  Q  K  I  E  W  H  -
```

Figure 6: DNA and polypeptide sequence of the extracellular portion of hybrid CD1c

The α3 domain of CD1b has been shown to preserve functionality of CD1c whilst improving stability (265). Residues to be mutated within the F' roof are highlighted in yellow while blue highlighting denotes the location of the mutants outside this region.

2.1.1.2 CD1c-lipid monomer production

Recombinant proteins of the CD1c heavy chain and β_2m were generated as inclusion bodies in Rosetta strain E.*coli* (Novagen). After establishing protein concentration in 8M Urea, inclusion bodies were washed and solubilised in a denaturing buffer of 6M guanidine-HCL. The oxidative *in vitro* refolding of CD1c and β_2m was carried out in the presence of 200µg of specific lipids solubilised in vehicle (150mM NaCl and 0.5% Tween 20) including PC, PG, and phosphatidylethanolamine (PE) (Avanti Polar Lipids) as previously described (425), or with vehicle alone. Briefly, the denatured proteins were reduced with 20mM DTT before adding to a refolding buffer (1mM EDTA, 100mM Tris, 300mM L-arginine, 1M urea, 3mM reduced glutathione, 3mM oxidised glutathione) and allowed to stir at 4°C. 1ml of vehicle buffer composed of 150mM NaCl and 0.5% Tween 20, or 1ml of vehicle buffer containing 200µg/ml solubilised lipid were added to

the refolding mixture. The refolding was optimised either in the presence or absence of the chaperone proteins GroEL, DsBA and PPI (291, 425). Proteins were concentrated before purification of the stable complexes through a fast protein liquid chromatography (FPLC) system using size-exclusion chromatography columns such as the preparatory grade (SD75 26/60) and the analytical grade (SD75 GL 10/300) columns (GE Healthcare). Subsequently, some proteins were further purified by anion exchange chromatography using the MonoQ 4.6/100 PE column (GE Healthcare).

2.1.1.3 CD1 tetramers

Biotinylation of the CD1c-lipid monomers was carried out *via* an engineered BirA motif on the C terminus of CD1c using the BirA ligation kit (Avidity) and then repurified by size exclusion chromatography. The eluted protein was then subjected to anion exchange column (MonoQ 4.6/100 PE) (GE Healthcare) to further refine protein purity. Five individual protein fractions were collected before conjugation to Streptavidin-R-phycoerythrin, Streptavidin-Allophycocyanin, Streptavidin-BV421 or Streptavidin-BV605 (All Biolegend) to generate CD1c tetramers.

2.1.2 Flow cytometry

2.1.2.1 Staining of Jurkat T cells

J.RT3-T3.5 Jurkat cells were washed in cold MACS buffer before the addition of 0.3μg tetramer and incubated on ice for 25 minutes. The cells were further stained with anti-CD3-APC antibody (Biolegend) and incubated on ice for a further 20 minutes before washing again in cold MACS buffer. Propridium Iodide (Sigma) was added to the cells before acquisition by the FACSCalibur (BD Biosciences) and analysed using FlowJo VX (FlowJo LLC).

2.1.2.2 CD1c tetramer staining

Staining of $CD4^+$ T cells: $CD4^+$ T cells were purified using a CD4 MACS purification kit (Miltenyi). $CD4^+$ T cells were washed in cold MACS buffer before incubating with 50nM Dasatinib (Sigma) for 30 minutes at 37°C. The samples were stained with 0.3μg tetramer and with human specific antibodies anti-CD3-FITC (Biolegend) and anti-CD4-APC (Biolegend) before incubating on ice for 45 minutes. Samples were stained with Propridium iodide following washing with MACS buffer and acquired by the FACSCalibur (BD Biosciences). CD1c-lipid specific $CD4^+$ T cells were identified by gating on the live $CD3^+$ lymphocyte population and analysed using FlowJo VX.

Staining and sorting of Vδ1 T cells (Southampton): Peripheral blood mononuclear cell (PBMC) samples were washed in cold MACS buffer before incubating with 50nM Dasatinib (Sigma) for 30 minutes at 37°C before staining with 0.3μg tetramer. Cells were then stained with the human specific antibodies anti-CD3-FITC and anti-Vδ1-APC (Miltenyi) before incubating on ice for 45 minutes. Samples were washed in MACS buffer before staining with Propridium iodide. Samples were acquired by the FACSAria and cells that were positive for both tetramer and Vδ1 were bulk sorted into 3ml FACS tubes for culture.

Staining and sorting of CD1c tetramer$^+$ γδ T cells (King's College London): Cells from three γδ T cell enriched cell lines and one *ex vivo* PBMC sample were resuscitated in complete media and rested at 37°C for 1 hour. Cells were washed in PBS before incubating with 50nM Dasatinib (Axon) for 30 minutes at 37°C. The samples were stained with two tetramers, CD1c-SL-PE and CD1c-PG-BV421, before staining with anti-CD3-BV786, anti-αβTCR-APC, anti-γδTCR-PE/Cy7 and anti-Vδ2-FITC and incubating for 45 minutes on ice. The cells were washed in PBS before acquiring on a FACS Aria Fusion (BD Biosciences) and sorting single cells into 5μl PBS in PCR plates. The PCR plates were chilled on dry ice, centrifuged at 600g for 1 minute and subsequently frozen at -80°C.

2.1.2.3 γδTCR transduced Jurkat T cells

An aliquot of NFAT-Gluc Jurkat cells transduced with different γδTCRs was washed in cold MACS buffer before staining with anti-CD3-FITC (Biolegend) and anti- Vδ1-APC (Miltenyi) antibodies and incubated on ice for 45 minutes. After washing in MACS buffer, the cells were acquired by a FACS Aria IIu (BD Biosciences). The percentage of TCR expression was analysed and TCR positive cells were bulk sorted into complete RPMI media for expansion in culture to obtain a cell population with 100% TCR expression.

γδTCR transduced NFAT-Gluc Jurkat cells were washed in cold MACS buffer before staining with 0.3μg of various tetramers: CD1c-SL, CD1c-endo, and CD1c-SL/endo proteins pulsed with citrate buffer only, 0.5% CHAPS only, PG 16:0 and PC 18:0. Another aliquot of NFAT-Gluc Jurkat cells were also stained with 1.8μg CD1c-SL dextramer. Cells were further stained with anti-CD3-APC antibody (Biolegend) and incubated on ice for 45 minutes. Cells were washed in cold MACS buffer before acquisition by FACS Aria IIu (BD Biosciences) and analysed using FlowJo VX (FlowJo LLC).

2.1.2.4 Activation induced marker assay (AIM)

T cells expanded in a short term culture and stimulated overnight with either THP1-CD1c or THP1 Knockout (THP1-KO) cells were resuspended and washed in sorting buffer (HBSS, 1% human AB serum, 10mM HEPES, 2mM EDTA) before staining with an antibody cocktail for co-receptors and activation markers: anti-CD3-FITC, anti-CD4-PerCP/Cyanine5.5, anti-CD8-BV510, anti-CD69-PE,

anti-CD25-PE/Cyanine7, anti-CD137-APC (Biolegend) and LIVE/DEAD Near IR (Invitrogen). THP1 cells were gifted to us by Immunocore, Oxford, and are knockouts for the β_2m and CIITA genes. The lack of β_2m prevents the natural formation of MHC class I and CD1 molecules, and the absence of CIITA prevents upregulation of MHC class II molecules upon TCR engagement. This allows for the determination of CD1c-mediated activation of T cells in THP1 cells transduced with CD1c whilst lacking MHC and other CD1 molecules. T cells were acquired by BD FACS Aria IIu (BD Biosciences) and analysed using FlowJo XV (FlowJo LLC). The remaining incubating T cells were continued in culture and re-stimulated with THP1 cells and IL-2 every 7 days. On day 25, the cells were stained as above and $CD69^+CD137^+$ T cells were sorted into T cell media. Sorted cells were cultured overnight in 96 well plates with 1µg/ml PHA, 100U/ml IL-2 and $2x10^5$ irradiated autologous PBMCs. On day 4 after initiation of the culture, cells were stimulated with 100U/ml IL-2 and were re-stimulated in this manner every other day.

2.1.2.5 Staining of CD1c-restricted T cells in South African TB patients

Peripheral blood staining: PBMC were resuscitated and washed in RPMI 1640 (Lonza) media containing 10% Foetal Bovine Serum (FBS) before resting for 1 hour at 37°C. Cells were washed in PBS before blocking with a 50% human serum, 0.2% Bovine Serum Albumin (BSA) solution for 10 minutes at 4°C. The cells were washed twice in PBS before incubating with 50nM Dasatinib (Sigma) for 30 minutes at 37°C. Cells were stained with 0.1µg of each CD1c-SL tetramer-PE and CD1c-SL tetramer-BV421/BV605 before staining with 25µl LIVE/DEAD Fixable Near-IR Dead Cell Stain (Invitrogen) diluted to 1:200 in PBS. Cells were then stained with human specific antibodies anti-CD3-PE CF594 (BD Biosciences), anti-CD19-BUV496 (BD Biosciences), anti-Vδ1-APC (Miltenyi) and anti-TCRα/β-Alexa Fluor 488 (Biolegend) and incubated on ice for 45 minutes. Samples were washed in PBS and acquired by the FACSAria Fusion and data was analysed using FlowJo VX (FlowJo LLC)

Lung and PBMC staining: PBMC and Lung samples from *M.tb* infected donors were handled within a Biosafety Level III (BSLIII) laboratory. The samples, previously harvested and processed by collaborators at the Africa Health Research Institute (AHRI), Durban, were resuscitated in R10 media (RPMI, 10% FBS) and rested at 37°C for 20 hours. Cells were washed in PBS and incubated with FACS block (PBS, 50% human AB serum, 0.2% bovine serum albumin) for 10 minutes at 4°C before washing twice. Samples were incubated with 50nM Dasatinib for 30 minutes at 37°C before staining with two CD1c-SL tetramers conjugated to PE and BV421. The cells were then stained for 45 minutes on ice following staining with an antibody cocktail comprising anti-CD3-BV785, anti-αβTCR-FITC, anti-γδTCR-PerCP/Cy5.5, anti-Vδ2-BV711, anti-CD103-BV605, anti-PD1-AF700, anti-CD19-PE/Cy7, anti-CD14-PE/Cy7 and anti-CD11b-PE/Cy7 (Biolegend), anti-CD69-

BUV395 (BD), anti-Vδ1-APC (Miltenyi). Cells were washed in PBS and acquired using a FACS Aria Fusion at BSLIII. Data was analysed using FlowJo VX (FlowJo LLC). Single cells that were CD1c-SL Tetramer^{+} Vδ1^{+} were sorted into 5µl PBS in 96 well PCR plates before centrifuging at 600g for 1 minute and freezing at -80°C for TCR sequencing at a later date.

2.1.3 Investigating T cell reactivity

2.1.3.1 Surface plasmon resonance

Surface plasmon resonance (SPR) experiments were carried out by our collaborating colleague Johanne Pentier at Immunocore, Oxford. Streptavidin (~5000RU) was amine-coupled to a BIAcore CM-5 chip (BIAcore AB) and 50µg/mL biotinylated CD1c-SL complexes were loaded on individual flow cells until the response measured ~1000RU. Recombinant NM4 TCRs were serially diluted and flowed over the protein-loaded flow cells at a rate of 5 or 50µL/min for determination of equilibrium binding. Responses were recorded in real time on a BIAcore 3000 machine at 25°C, and data were analysed using the BIAevaluation software (BIAcore).

2.1.3.2 CD1c-mediated activation of Jurkat T cells

Optimisation of T2 and NM4 Jurkat T cell co-cultures: Two types of Jurkat cell lines, J.RT3-T3.5 and NFAT-Gluc, expressing a self-reactive, CD1c-restricted TCR (NM4) were seeded into wells of a 96 well plate at a concentration of $1x10^5$ cells/well in complete media. T2 lymphoblast cells, either expressing WT CD1c (T2-CD1c) or parental (T2-negative), were added to wells containing Jurkat cells in 4 different concentrations: $5x10^4$ cells/well, $1x10^5$ cells/well, $1.5x10^5$ cells/well and $2x10^5$ cells/well. As a positive control, $1x10^5$ Jurkat cells were stimulated with 50ng/ml PMA and 1µM Ionomycin. Cells were incubated for increasing lengths of time: 1 hour, 2 hours, 3 hours, 4 hours, 8 hours, 16 hours and 24 hours. Prior to washing in MACS buffer, the supernatant of each NFAT-Gluc co-culture was transferred to a separate plate and frozen at -20°C for later use in fluorescence assays (Luciferase). Washed cells were stained with anti-CD3-FITC (Biolegend) and anti-CD69-PE (Biolegend) before incubating on ice for 45 minutes. Samples were washed in MACS buffer before staining with Propridium iodide and acquired by the FACSCalibur.

Culture of γδTCR Jurkat T cells and CD1c expressing APC: γδTCR transduced NFAT-Gluc Jurkat T cells were plated in 96 well plates at $2.5x10^5$ cells/well in complete media. THP1 or T2 cells, with or without expression of CD1c, were added to the Jurkat T cells at $1.25x10^5$ cells/well. Jurkat T cells stimulated with 10ng/ml PMA and 500ng/ml Ionomycin, and un-stimulated Jurkat T cells acted as positive and negative controls, respectively. Cells were incubated at 37°C 5% CO_2 for 20 hours before washing in MACS buffer. Cells were stained with anti-CD69-PE and anti-CD3-APC

(Biolegend) before acquiring by a BD FACS Aria IIu (BD Biosciences). Frequency of CD69 and CD3 expression was analysed using FlowJo VX (FlowJo LLC).

2.1.3.3 Plate bound CD1c assay

Wells of a Nunc-immuno Maxisorp 96 well plate (Thermo Scientific) were coated with 1µg CD1c-PC or 0.5µg CD1c-PC in 50µl PBS, or with 50µl PBS only. Plates were incubated at 4°C for 20 hours, before washing three times with 200µl sterile PBS to remove unbound protein. Jurkat T cells, of either the J.RT3-T3.5 or NFAT-Gluc cell line, were added to each well at a concentration of $1x10^5$ cells/well and were incubated at 37°C for 24 hours. Following incubation, supernatants were removed from each culture and transferred to a separate plate and frozen at -20°C for later use in fluorescence assays (Luciferase). Cells were washed in MACS buffer prior to staining with anti-CD3-FITC (Biolegend) and anti-CD69-PE (Biolegend) for 45 minutes on ice. Cells were washed in MACS buffer and stained with Propridium iodide before acquiring on the FACSCalibur.

2.1.3.4 Lipid loaded CD1c

Stable refolded CD1c monomers were loaded with defined ligands which included; GD1a (860055 Avanti), PC (850375 Avanti), SM (860584 Avanti), Liver PI (840042 Avanti), Lyso Liver PI (850091 Avanti) and a range of PG analogues including 16:0-18:1 (840457 Avanti), 18:0-18:1 (840503 Avanti), 18:0 (840465 Avanti), 16:0 (840455 Avanti) and 18:1 (Δ9 cis) (840475 Avanti). 16µg of lipid was sonicated in 23µl of 0.5% CHAPS (Sigma) in 50mM sodium citrate buffer (pH 7.4 or 6.5) for 30 minutes at 37°C. 10µg of CD1c monomers, which had been refolded solely with vehicle, was added to the solubilised lipids before incubating at 37°C overnight. As a control, 0.5% CHAPS in 50mM sodium citrate buffer (pH 7.4 or 6.5) or sodium citrate buffer alone was added to vials without lipid and sonicated in the same way before the addition of CD1c monomer. The following day, 17µl PBS was added to each vial of CD1c to bring the protein concentration to 0.2mg/ml in 50µl. The CD1c monomers were then tetramerised with Streptavidin-PE (Biolegend). J.RT3-T3.5 Jurkat cells, both parental TCR negative and NM4 TCR expressing lines, were stained with 0.3µg of lipid-pulsed CD1c tetramer, followed by anti-CD3-APC antibody (Biolegend) and incubated on ice for 45 minutes. The cells were washed in cold MACS buffer and stained with Propridium Iodide (Sigma) before acquisition by the FACSCalibur (BD Biosciences) and analysed using FlowJo VX (FlowJo LLC).

2.1.3.5 Luciferase activity

γδTCR transduced NFAT-Gluc Jurkat T cells were plated in 96 well plates at $2.5x10^5$ cells/well in complete media. THP1 or T2 cells, with or without expression of CD1c were added to the Jurkat T cells at $1.25x10^5$ cells/well. Jurkat T cells stimulated with 10ng/ml PMA and 500ng/ml Ionomycin,

and un-stimulated Jurkat T cells acted as positive and negative controls, respectively. Cells were incubated at 37°C 5% CO_2 for 20 hours before washing twice in PBS. Cells were lysed and the cell extract was mixed with luciferase substrate as per Luciferase Reporter Gene Assay kit instructions (Roche). Luciferase activity for each parameter was measured in triplicate by a Glomax Discovery plate reader (Promega) with a 10 second integration time and no filter.

2.1.4 Cell purification, isolation and preparation

2.1.4.1 Human PBMC isolation

Blood samples were obtained from a range of donors which included those who had no evidence of active or latent TB, and those who were clinically assessed to have latent TB. Approximately 50ml of blood was collected from each donor in heparin containing tubes and diluted 1:1 with PBS before layering over Ficoll-Paque (GE Healthcare) and centrifuged at 2000 rpm for 20 minutes with the brake off. The buffy coat was harvested and washed twice in PBS. Unused cells were cryopreserved in FBS + 10% DMSO.

2.1.4.2 Magnetic activated cell sorting (MACS)

Cells were washed and resuspended in MACS buffer (PBS, 0.5% BSA, 0.4% 0.5M EDTA) to a concentration of $1x10^7$ cells/80µl buffer before incubating with 10µl of CD14 or CD4 microbeads (Miltenyi) for 15 minutes at 2-8°C. After washing cells in MACS buffer, cells were resuspended in 500µl buffer and run through an MS MACS column to collect $CD14^+$ monocytes or $CD4^+$ T cells labelled with the microbeads. Enrichment of γδ T cells was carried out by labelling cells with a biotin-antibody cocktail (Miltenyi) to bind cells not expressing the γδ TCR. Cells were then incubated with anti-biotin microbeads and run through an MS MACS column in the same fashion to collect the unlabelled γδ T cells. Cells from each MACS separation were counted before use in the following assays.

2.1.5 Establishing T cell lines

2.1.5.1 DC stimulation of T cells

MACS (Miltenyi) was used to isolate $CD14^+$ monocytes and $CD4^+$ T cells from donor PBMC. T cells were cryopreserved in FBS +10% DMSO while monocytes were incubated in RPMI 1640 media (Lonza) containing 1% Penicillin/Streptomycin-Glutamax (Gibco) and 10% FBS (Sigma) (Complete media). The media was supplemented with 20ng/ml GM-CSF and 20ng/ml IL-4 to differentiate the monocytes into MoDCs. MoDCs were cultured for 5 days, changing the media every 2 days, before pulsing overnight with 50ng/ml of specific lipids which included PC, PG and PE (Figure 7).

Maturation of DC was induced with 50ng/ml Lipopolysaccharide (LPS) before addition of thawed autologous $CD4^+$ T cells. DC and T cells cultured together for 2 weeks before staining for analysis by flow cytometry.

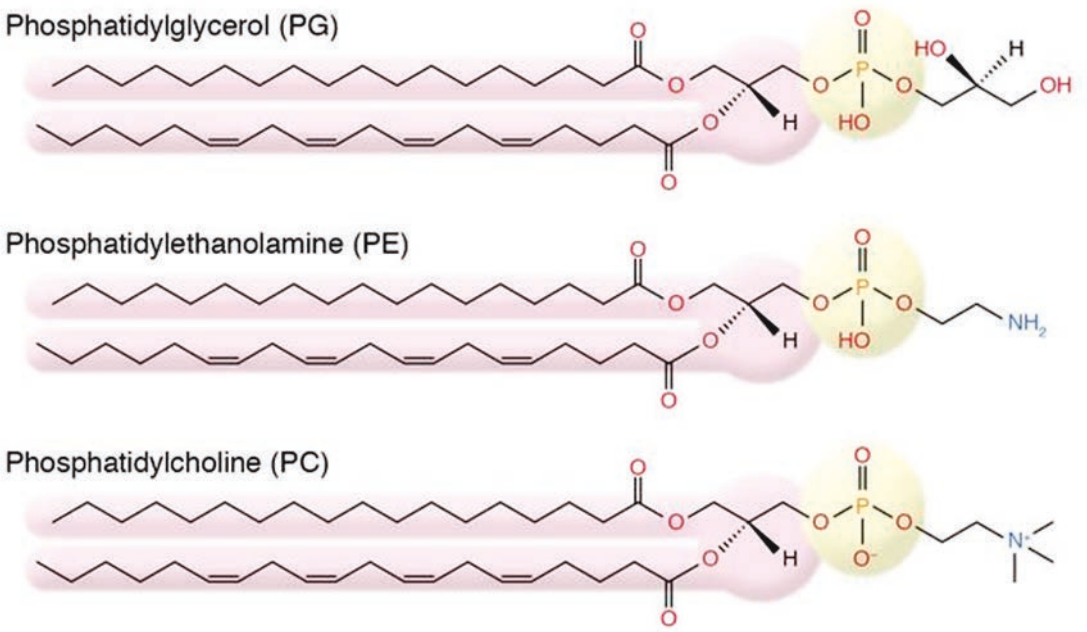

Figure 7: Structures of phosphatidylglycerol (PG), phosphatidylethanolamine (PE) and phosphatidylcholine (PC)

Adapted from O'Donnel 2018 (335).

2.1.5.2 Preparation and culture of *ex vivo* sorted lines

MACS sorting (Miltenyi) was used to isolate γδ T cells from human PBMCs prior to staining for sorting by flow cytometry. Cells were sorted into RPMI 1640 (Lonza) media containing 1% Penicillin/Streptomycin-Glutamax (Sigma), 10% human AB serum (Sigma), 1X amino acids (Sigma), 1X non-essential amino acids (Sigma), 11mM Hepes buffer (Sigma) (T cell media), supplemented with 1.6μg/ml PHA (Sigma), and cultured with $1.5x10^5$ irradiated feeder cells per well of a 96 well plate. Cells continued to be fed and expanded for 21 days, with T cell media supplemented with 100U/ml IL-2 (Miltenyi). After 3 weeks, the cells were stained for analysis and sorting by flow cytometry.

2.1.5.3 Plate bound anti-γδ T cell expansion

Wells of a 6 well plate were coated with 0.3μg/ml, 3μg/ml or 30μg/ml LEAF purified anti-γδ TCR antibody (Biolegend) in PBS and incubated at 4°C overnight. Coated plates were seeded with $2x10^6$/ml human PBMCs in RPMI 1640 (Lonza) media containing 1% Penicillin/Streptomycin-Glutamax, 1mM sodium pyruvate (Sigma) and 5% human AB serum (Sigma) (γδ media) and

incubated overnight at 37°C. The following day, PBMCs were stimulated with 100U/ml IL-2. Cultures were expanded into T25 flasks and fed every 2 days with γδ media supplemented with 100U/ml IL-2 for 21 days. PBMCs were stained for analysis by flow cytometry at day of plating (day 0), day 14 and day 21. In a second method, 30µg/ml of LEAF purified anti-γδ TCR antibody was bound to two wells of a 6 well plate in the same manner. One of these wells was also coated with 10µg CD1c-SL protein in a total volume of 1ml PBS with the anti-γδ TCR antibody. A third well was coated with just 10µg CD1c-SL protein in 1ml PBS. PBMCs were added in the same concentration and expanded under the same conditions.

2.1.5.4 Short term culture for the Activation Induced Marker (AIM) assay

PBMCs were isolated by density gradient centrifugation from whole blood taken from both healthy donors and those with *M.tb* exposure. $CD3^+$ T cells were isolated using a Pan T cell isolation kit (Miltenyi) and stained with Cell Trace Violet (Invitrogen) according to the manufacturer's instructions. $CD3^+$ T cells were then resuspended in T cell media (RPMI 1640, 1X Penicillin/Streptomycin-Glutamine, 1X non-essential amino acids, 1X sodium pyruvate, 5% human AB serum) to $2x10^6$ cells/ml and plated in 24 well plates. THP1 cells, with or without CD1c expression, were irradiated with 80Gys before adding $3x10^5$/ml to the plated T cells. Two wells of T cells without THP1 cells were used as controls, one stimulated with 10ng/ml PMA and 500ng/ml Ionomycin, and one left unstimulated. The T cell cultures were then incubated at 37°C, 5% CO_2. On day 4, 10U/ml IL-2 was added to each well of cells (Aldesleukin, Chiron). On day 8, the cultured T cells were re-stimulated with $3x10^5$ irradiated THP1 cells, with some wells originally cultured with THP1-CD1c being re-stimulated with THP1-KO as a control for CD1c-mediated activation. On day 9, supernatant was removed from each T cell culture and frozen at -20°C.

2.1.6 Immunohistochemistry

Paraffin-embedded lung tissue taken from human TB patients and controls with adenocarcinoma was acquired from the histology archive at University Hospital Southampton in line with the ethical approval obtained for this project (REC Reference: 13/SC/0043). Sections of tissue were cut to 4µm thick and mounted onto APES coated glass slides by colleagues in the Histochemistry Research Unit as part of the provided histology service. Tissue sections were dewaxed in two tanks of TISSUE-CLEAR (Sakura) for 10 minutes each and rehydrated in graded alcohols (2x absolute alcohol, then 70% alcohol) for 5 minutes each. Endogenous peroxidase was inhibited by incubating sections in freshly made 0.5% hydrogen peroxide in methanol for 10 minutes. Tissue sections were subsequently washed 3 times for 2 minutes in TBS buffer pH 7.2-7.6 before performing heat-induced epitope retrieval by microwaving for 25 minutes on 50% power in 330ml

10mM citrate buffer pH 6 for CD1c or 330ml 1mM EDTA pH 8 for TCRδ. Sections were cooled in running water and washed three times for 2 minutes in TBS before coating in avidin solution for 20 minutes (Vector Laboratories Ltd). Following 3 washes in TBS, the sections were coated in biotin solution (Vector Laboratories Ltd) for a further 20 minutes. Blocking solution composed of Dulbecco's modified eagle medium with 10% FCS and 2% BSA was then applied to each slide following a further three TBS washes and incubated for 30 minutes. Primary antibody was then applied to the appropriate sections, including anti-CD1c 1:500 (EPR23189-196 Abcam) and anti-TCRδ 1:100 (H-41 Santa Cruz), followed by overnight incubation at 4°C. After washing in TBS, sections were coated in secondary antibody for 30 minutes; goat anti-rabbit 1:800 (2B Scientific) for CD1c and goat anti-mouse 1:800 for TCRδ (2B Scientific). Avidin-Biotin complex to amplify signal detection (2B Scientific) was prepared, constituting 1:1:75 parts of Reagent A, Reagent B and TBS, respectively. Following a TBS wash, slides were coated with the avidin-biotin complex for 30 minutes. DAB chromagen solution, constituting 1ml DAB substrate buffer, 32µl DAB chromagen (Launch Diagnostics) and 50µl 15% sodium azide, was freshly prepared and applied to each section following a TBS wash step. Following a 5 minute incubation, sections were washed once in TBS before washing under running water for 5 minutes. Sections were subsequently counterstained in Mayer's haematoxylin for 30 seconds to 1 minute before washing for a further 5 minutes in running water. Slides were mounted and a cover slip applied using XTF mounting medium (CellPath). Sections were allowed to dry and subsequent imaging was carried out by David Johnston using an Olympus BX51, CC12 (dotSlide) as part of an imaging service provided by the Biomedical Imaging Unit at University Hospital Southampton. Section images were analysed using Olympus OlyVIA.

2.1.7 TCR Sequencing

2.1.7.1 Single cell PCR and sequencing

Single CD1c tetramer$^+$ CD3$^+$ Vδ1$^+$ cells sorted into 96 well plates were thawed on ice and incubated for 5 minutes at 65°C before returning to ice. The reverse transcription PCR was performed using the qScript XLT One-Step RT-PCR Kit (Quanta Biosciences) in a 20µl reaction with 500nM total concentration of each forward and reverse external primer (Table 3). The PCR reaction was then diluted 1:5 before performing a second round of PCR using Phusion High-Fidelity DNA Polymerase (NEB) and sets of internal primers for the γ and δ chains (Table 4). The subsequent PCR product was separated by electrophoresis on a 1.5% agarose gel before purifying the selected bands with the QIAquick Gel Extraction Kit (Qiagen) and sending for Sanger sequencing using custom primers at Source Bioscience.

Table 3: PCR and sequencing primer sets for analysis of single sorted cells

External primer sets		
hGV23458-ext_F	Forward	TGCCAGTCAGAAATCTTCCAAC
hCgamma-Xba_R	Reverse	atattctagaTTATGATTTTTCTCCATTGCAGCAG
Vd1-ext_F	Forward	atatctcgaggccgccaccATGCTGTTCTCCAGCCTGCTG
Cd_R	Reverse	atatgcggccgcTTACAAGAAAAATAACTTGGCAGTCAAGAG
Internal primer sets		
hGV23458-int_F	Forward	atatcctgcaggCACTGGTACCTACACCAGGAGG
hGC12-int_R	Reverse	atatggcgcgccGGAGGAGGTACATGTAATATGCAGAG
hDV1-int_F	Forward	atatggcgcgccGGTACAAGCAACTTCCCAGCAAAG
hDC-int_R	Reverse	atatgcggccgcGGCAGCTCTTTGAAGGTTGC
Sequencing primers		
hGammaC-Seq_R	Reverse	GCAGTAGTGTATCATTTGCATC
hDeltaC-seq_R	Reverse	GGTTTTACGTGATCTGTAGAATCTGTC

Table 4: PCR programmes for single sorted cells

1st PCR		
Temperature (°C)	**Time (hh:mm:ss)**	**Number of Cycles**
50	00:20:00	1
94	00:03:00	1
94	00:00:15	35
64	00:00:30	
72	00:01:30	
72	00:02:00	1
4	Hold	
2nd PCR		
Temperature (°C)	**Time (hh:mm:ss)**	**Number of Cycles**
98	00:03:00	1
98	00:00:20	35
64	00:00:15	
72	00:00:15	
72	00:02:00	1
4	Hold	

2.1.8 Transduction of γδTCRs onto Jurkat T cells

The sequences of six γδTCRs identified from tetramer-guided sorting of patient samples and cell lines were cloned into the pELNS Lentivector by Genscript. Another γδTCR clone previously identified in collaboration with our colleagues at King's College was also cloned into the pELNS

Lentivector (TCR7). HEK 293T cells were plated in 100mm tissue culture dishes in 7ml DMEM (Lonza) supplemented with 10% FBS (Sigma) and 1X Penicillin-Streptomycin-Glutamine (Gibco) (complete DMEM), and cultured overnight at 37°C 5% CO_2. The following day, media was removed from the plates and the cells were gently washed in 4ml PBS. The DNA media was prepared in 300µl DMEM and constituted 1µg/µl Pol/Gag, 1µg/µl pRSV.REV, 0.5µg/µl pVSV-g and 1µg/µl Lentiviral plasmid containing γδTCR DNA. The DNA media was vortexed before adding 20µl TurboFect Transfection Reagent (Thermo Scientific) and incubating at room temperature for 10 minutes. 3ml complete DMEM was mixed into the DNA media before adding dropwise onto the adherent HEK cells and incubating at 37°C for 3 hours. DNA media was then removed from the cells before gently washing with 4ml PBS. 6ml fresh complete DMEM was then added to the cells before incubating overnight at 37°C. The following day, NFAT-Gluc Jurkat T cells to be transduced were plated in 6 well plates at densities of $5x10^5$ and $1x10^6$ cells per well in 3ml complete DMEM each, and incubated overnight at 37°C. On day 4, the media was removed from the HEK cells and transferred into a tube for centrifugation at 37°C for 5 minutes at 1500rpm. 6ml fresh complete DMEM was added to the HEK cells and continued incubation at 37°C. The centrifuged supernatant was passed through a 0.45µm PES filter (Sartorius) before adding in two concentrations, neat or 1:2, to each density of NFAT-Gluc Jurkat T cells that had been cultured from the previous day. The NFAT-Gluc Jurkat T cells were then centrifuged at 2000rpm for 90 minutes at 37°C before incubating overnight. The transduction procedure was then repeated the following day after removing the media from the NFAT-Gluc Jurkat T cells before incubating for a further week.

2.1.9 Statistical Analysis

2.1.9.1 Clinical data

The statistical significance of the frequency of T cell subsets and CD1c tetramer staining between healthy controls and TB patients was tested using the Mann-Whitney test. Correlations between the CD4 count of the HIV^+ TB patients and the frequency of T cell subsets and CD1c tetramer staining was tested by using Spearman's correlation. The Wilcoxon test was used to calculate the statistical significance of T cell subset frequencies between matched lung and PBMC samples from donors in each group.

2.1.9.2 T cell activation assays

The statistical significance of CD69 and CD3 expression by Jurkat T cells expressing γδTCRs between those stimulated with APCs expressing CD1c, parental CD1c negative APC (-KO) or Jurkat T cell only cultures was tested using the Mann-Whitney test. This test was also used to analyse the statistical significance of AIM expression by all donor T cells cultured with THP1-CD1c, THP1-

KO or cultured alone. The Wilcoxon test was used to assess statistical significance of AIM expression by each set of donor T cells between time points, T cell subsets, or culture conditions.

2.2 Macaque

2.2.1 Experimental animals

The three animals used for the iNKT study were Rhesus macaques of Indian origin, bred in the Public Health England (PHE) UK colony at Porton Down in 2013 (~5 years old at the time of study). Confirmation of absence of exposure to mycobacterial antigens was established by a negative tuberculin skin test prior to the beginning of the study. Macaques were challenged with *M.tb* Erdman strain K 01 with a presented dose in the range of <10-50 CFU via aerosol exposure. Clinical parameters were monitored throughout the duration of the study which included behaviour, weight, temperature, axillary and inguinal lymph node scores and haemoglobin concentration. Animals were sedated at two weekly intervals following *M.tb* challenge for blood collection. At 7-8 weeks post challenge, the macaques were humanely euthanized and biopsies were taken from each lung lobe at random.

2.2.2 Disease burden

Disease burden of the iNKT study animals was assessed using bacteriology analysis and pathology scoring of lung tissue samples. Gross pathology of lung tissue was assessed using a previously described scoring system (371) that is based on the number and extent of observed lesions (Table 5). The scores assigned to each lobe were combined to give a total pathology score for the lungs. Standard bacteriology scores were produced by collecting samples of each lung lobe with and without lesion as described previously (426). Homogenised lung lobe samples were either directly plated onto Middlebrook 7H11 oleic acid-albumin-dextrose-catalase (OADC) selective agar, or serially diluted prior to plating. Agar plates were incubated at 37°C for 3 weeks before counting colonies. A second type of sampling was applied for bacteriology analysis using a randomised punch biopsy method as detailed by Luciw *et al* (427) before plating out in the same way.

Table 5: PHE scoring system to assess pathology within the lungs

Lung (per lobe)	Score
No visible lesions	0
1 lesion, <10mm	1
2-5 lesions, <10mm	2
>60 lesions, <10mm; or 1 lesion, >10mm	3
>1 lesion >10mm	4
Coalescing lesions	5

2.2.3 Cell purification and isolation

2.2.3.1 Macaque PBMCs

Blood samples from macaques challenged with *M.tb* were handled at Containment Level 3, whereas samples prior to infection were handled at Containment Level 2. Whole blood samples from three Rhesus macaques were received fortnightly in 20ml heparin containing universal tubes. PBMCs were isolated in accupsin tubes (Greiner) containing Ficoll-Paque. Following centrifugation of blood at 800 RCF for 15 minutes, the buffy coat was harvested and washed in RPMI 1640 (Sigma) with 1% Penicillin-Streptomycin (Sigma), 1% L-glutamine (Sigma) and 2% FBS (Lab Tech International) (R2 media). Red blood cells were lysed by incubation with ACK lysis buffer (Gibco) for 5 minutes before further washing with R2 media. Unused cells were cryopreserved in FBS + 10% DMSO.

Lung biopsy samples were digested by agitation at 37°C in Earle's Balanced Salt Solution (Gibco) supplemented with 350U/ml DNase (Sigma) and 715U/ml collagenase (Sigma). Lung samples were homogenised using a GentleMACS dissociator (Miltenyi) before layering over Ficoll and centrifuging at 400 RCF for 30 minute with the brake off. The buffy coat was harvested and washed in R2 media before red cell lysis with ACK lysing buffer.

2.2.4 Flow cytometry

2.2.4.1 iNKT staining

Infected samples were handled and stained at Containment Level 3. PBMCs and lung biopsy samples from each macaque were washed with PBS before staining with 0.3μg CD1d-α–GalCer tetramer. Macaque cross-reactive antibodies were then added: anti-CD3-APC (BD Biosciences) and anti-Vα24-FITC (Beckman Coulter) followed by 1:50 diluted LIVE/DEAD Fixable Red Dead stain (Life technologies) in water. Following incubation for 30 minutes, cells were washed in PBS before fixing in 2% paraformaldehyde for 15 minutes. Cells were acquired by the LSRFortessa and

analysed using FlowJo VX. The iNKT cells were identified as Vα24 and CD1d tetramer double positive cells from within the live $CD3^+$ lymphocyte population.

2.2.4.2 CD1c-restricted T cells

Cryopreserved PBMCs from two Rhesus macaques and ten Cynomolgus macaques were resuscitated and washed in complete media before resting at 37°C for approximately 2 hours. Cells were washed in MACS buffer before staining for 45 minutes on ice with anti-CD3-FITC antibody and either negative control tetramers or 0.3µg human CD1c-SL-PE and –APC tetramers. Cells were acquired by the FACSAria IIu and analysed using FlowJo VX.

In a separate experiment, PBMCs isolated from three Cynomolgus macaques and three Rhesus macaques were washed in cold MACS buffer before incubating with 50nM Dasatinib (Axon) for 30 minutes at 37°C. The samples were then stained with either Streptavidin-R-Phycoerythrin alone or one of two tetramers; mCD1c-SL or human CD1c-SL. Cells were subsequently stained with anti-CD3-APC (SP34-2 BD), and Live/Dead Aqua (Invitrogen) for 45 minutes on ice. Following washing with MACS buffer, the cells were acquired by a FACS Aria IIu (BD Biosciences) and data analysed using FlowJo VX (FlowJo LLC).

2.2.4.3 Staining of Jurkat T cells

J.RT3-T3.5 Jurkat cells expressing the human CD1c-restricted TCR, NM4 (TRAV22, TRBV6.2), as well as the parental TCR negative Jurkats, were washed in cold MACS buffer before the addition of 0.3µg mCD1c-SL tetramer and stained with anti-CD3-APC. The cells were incubated on ice for 45 minutes before washing in MACS buffer. The cells were acquired on a FACSCalibur (BD Biosciences) and the data analysed using FlowJo VX (FlowJo LLC).

2.2.5 T cell culture

2.2.5.1 iNKT expansion

Macaque PBMCs in T cell media (with 10% FBS instead of human AB serum) were seeded onto 24 well plates at $3x10^5$ cells per well. Half of the wells for each animal were supplemented with 200µg/ml α-GalCer (Avanti Polar Lipids). After 14 days in culture, PBMCs were stained to investigate iNKT frequency and determine the fold expansion, defined as the frequency of iNKTs in 14 day culture over *ex vivo* iNKT frequency.

2.2.5.2 Expansion of CD1c-restricted T cells

Heparinised blood samples from three naïve Rhesus macaques were processed to harvest PBMCs before isolating $CD3^+$ T cells using an NHP Pan T cell Isolation kit (Miltenyi). T cells were stained with Cell Trace Violet (Invitrogen) before aliquoting into 24 well plates at $2x10^6$ T cells per well in Macaque T cell media (Mq media) (RPMI, 10% FBS, 1X Penicillin-Streptomycin-Glutamine, 1X non-essential amino acids (Sigma), 10mM HEPES (Sigma) 1mM sodium pyruvate (Sigma)). THP1 cells, with or without expression of CD1c, were irradiated with 80Gys before adding $3x10^5$ cells in Mq media to each well of T cells. On day 8, the T cells co-cultured with THP1-CD1c were re-stimulated with $3x10^5$ irradiated THP1-CD1c cells, and the T cells co-cultured with THP1-KO were re-stimulated with $3x10^5$ irradiated THP1-KO cells. The following day, cells were washed in Mq media before incubating with 50nM Dasatinib for 30 minutes at 37°C. The cells were then either stained with an antibody cocktail of anti-CD137-APC, anti-CD25-PE (Biolegend), anti-CD3-AF488 (SP34-2 BD) and Live/Dead Near IR (Invitrogen), or with 1µg CD1c-SL tetramer, anti-CD3-AF488 and Live/Dead Near IR. Cells were stained for 45 minutes on ice before washing in Mq media and acquiring by FACS Aria IIu (BD Biosciences) and analysed using FlowJo VX (FlowJo LLC).

2.2.6 Production of mCD1c tetramers

2.2.6.1 Macaque CD1c cloning

The extracellular portion of Cynomolgus macaque CD1c (mCD1c) was synthesised by GeneArt Gene Synthesis (Thermo Scientific) and held within the pMK-RQ vector. The mCD1c pMK-RQ plasmid was propagated through transformation into XL10-Gold ultracompetent cells (Agilent) and DNA extracted using an Endofree Plasmid Maxi Kit (Qiagen). The plasmid was digested with restriction enzymes NcoI and BamHI (New England Biolabs) and the mCD1c insert of approximately 850bp was extracted from a 1% agarose electrophoresis gel using a Qiaquick Gel Extraction Kit (Qiagen). The mCD1c insert was ligated with the pet23d vector, which had also been digested with NcoI and BamHI, using a 1:3 vector:insert calculation and T4 DNA Ligase (New England Biolabs). The ligation reaction was incubated at 4°C overnight before incubating at 65°C for 10 minutes to inactivate the ligase. The ligation mixture was then transformed into MAX Efficiency Stbl2 competent cells (Thermo Scientific). Picked colonies were grown in LB broth before extracting DNA using QIAprep Spin Miniprep kit (Qiagen). The mCD1c plasmid DNA was digested with NcoI and BamHI (New England Biolabs) to visually examine the presence of the mCD1c insert within the pET23-d vector and the sequence was confirmed by Sanger Sequencing (Source Bioscience).

2.2.6.2 Protein production and purification

mCD1c was generated as inclusion bodies in Rosetta strain *E.coli* (Novagen) and solubilised in 6M guanidine-HCL. The mCD1c inclusion bodies were run on a 12% SDS-PAGE gel with 4x reducing dye (200mM Tris pH 6.8, 40% Glycerol, 8% SDS, 0.4% Bromophenol blue, 400mM DTT) to ascertain whether the protein was of the expected molecular weight prior to refolding. Oxidative refolding of mCD1c and β_2m, following reduction with 20mM DTT, was carried out *in vitro* with a vehicle buffer composed of 150mM NaCl and 0.5% Tween 20 added to the refolding buffer (1mM EDTA, 100mM Tris, 300mM L-arginine, 1M urea, 3mM reduced glutathione, 3mM oxidised glutathione). The refolding mixture was allowed to stir for 3 days at 4°C before concentrating using a vivaflow (Sartorius) and spin columns (Sartorius). The refolded mCD1c protein was then purified using an FPLC system constituting a size exclusion chromatography column SD75 26/60 (GE Healthcare) and anion exchange column MonoQ 4.6/100 PE (GE Healthcare). Biotinylation of the mCD1c monomers was then carried out via an engineered BirA motif on the C terminus of CD1c using a Biotin-Protein Ligase kit (Genecopoeia) and then purified further using an analytical grade chromatography column (SD75 GL 10/300) (GE Healthcare). The resultant purified protein was conjugated to Streptavidin-R-Phycoerythrin (Biolegend) to generate mCD1c tetramers.

Chapter 3 Investigating the molecular basis underpinning TCR recognition of CD1c-lipid complexes

3.1 Molecular Mechanisms of Recognition by a CD1c autoreactive αβ TCR

In order to utilise CD1c-restricted T cells in the development of potential new vaccines for TB, we first need to understand the molecular mechanisms that underpin recognition of CD1c by its cognate TCRs. We aim to understand the binding mechanism of a previously cloned TCR through a combination of CD1c surface residue mutagenesis and lipid loading studies to provide information on crucial contact points and how recognition of CD1c can be modulated by bound lipid cargo. For these studies, we will investigate the binding mechanisms of a previously cloned human CD1c restricted $\alpha\beta$ TCR, NM4.

3.1.1 Understanding TCR binding footprint

How the TCR interacts with CD1c and its bound ligands is critical for the development of suitable vaccines and therapeutics that can effectively activate or inhibit CD1c-restricted T cells. Interestingly, most CD1c restricted TCRs are autoreactive because they recognise CD1c complexes bound to self-lipid cargo. Until recently, a ternary structure of TCR bound to a CD1c-lipid complex had not been solved. The general mode of recognition was predicted to be that of the absence of interference model as demonstrated for CD1a (232). The first crystal structure of an αβ TCR (3C8) bound to CD1c presenting self-lipids provided a three dimensional image of this complex, but the specific docking footprint was revealed through the use of alanine scanning mutagenesis (268). This technique has been invaluable in deciphering various docking mechanisms of different TCRs on CD1b, and has revealed a range of fine specificities (276, 280). Our group has previously demonstrated that the human self-reactive NM4 TCR binds a conformation of CD1c whereby the F' roof region is closed (265). We hypothesise that this region is critical for the recognition of CD1c by self-reactive TCRs. To investigate this hypothesis, alanine substitutions were carried out within the F' roof region of the α1-α2 domain using site directed mutagenesis.

To investigate the important contact points in the recognition of CD1c by TCR, seven residues in the α1-α2 domain of the extracellular portion of CD1c were mutated. Four residues within the F'

roof location; HIS87, TYR155, LEU150, GLU83, were substituted for alanine. A further three amino acids were mutated; ASN55 positioned on the loop joining the α1 helix to the β-sheet, HIS153 on the α2 helix and ARG82 on the α1 helix were altered to THR55, ARG153 and GLN82, respectively. These three amino acid mutations were chosen in collaboration with the Children's Hospital of Philadelphia as they are the most frequent mutations found to occur in paediatric autoimmune disease patients, and were initially used to optimise this method (Figure 8).

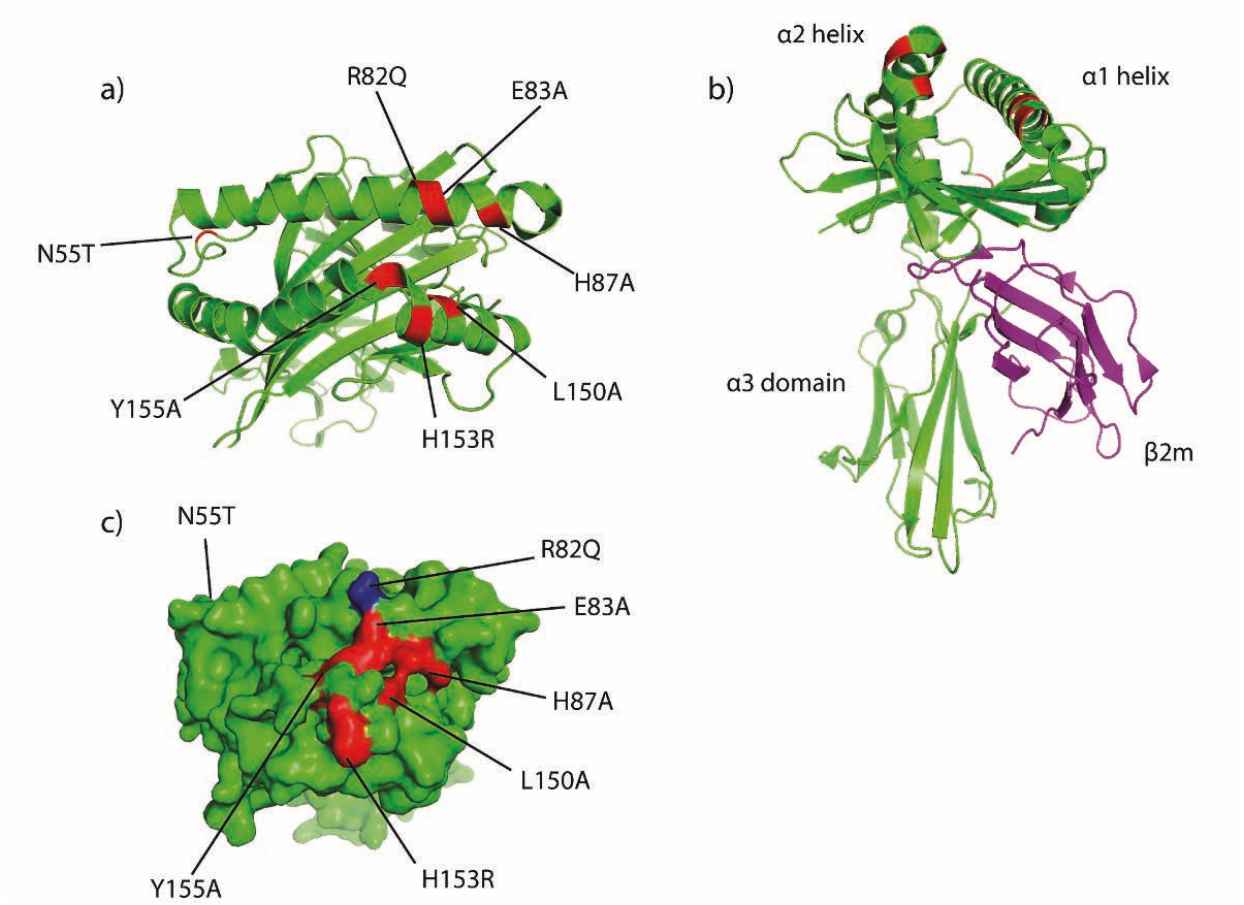

Figure 8: Overview of CD1c structure and location of residue mutations

a) Cartoon representation of CD1c with residues selected for mutation highlighted in red and blue. b) Cartoon representation of the CD1c structure. c) Orthogonal view of CD1c with red and blue highlighted residues for mutation.

Mutant CD1c proteins were expressed as inclusion bodies before purification and refolding. Following tetramerisation of stably refolded protein monomers with Streptavidin-PE, the binding of these mutant CD1c tetramers, in concentrations ranging from 0.1 to 0.5μg, to NM4 TCR expressing Jurkat T cells were investigated in a dose response experiment. Analysis of the first three tetramerised mutants, R82Q, H153R and N55T, demonstrated varying degrees of binding as measured by median fluorescence intensity (MFI). R82Q and N55T exhibited reduced binding at all tested tetramer concentrations compared to the WTCD1c tetramer. N55T had the greatest

effect on binding to the NM4 TCR, demonstrating an 87% reduction in MFI compared to WT CD1c when staining with 0.3-0.5µg of tetramer, and a 94% and 92% reduction when using 0.1µg and 0.2µg N55T tetramer, respectively. The R82Q tetramer also showed reduced binding capacity, with MFI decreased by >40% for each dose of tetramer, with the exception of 0.3µg which has a reduction of 29% compared to the MFI of the WT CD1c tetramer. In contrast, the H153R tetramer had an improved binding capacity over WT CD1c, ranging from a 14% increase with the lowest concentration of tetramer to a 69% increase with 0.4µg of tetramer. This work demonstrates that although not an absolute requirement for TCR binding, arginine and asparagine residues away from the F' roof at positions 82 and 55 of CD1c, respectively, are of significant importance for effective interaction. On the other hand, histidine at position 153 adjacent to the F' roof appears to reduce the interaction, as the mutation to arginine increased binding.

In addition, four F' roof mutations have been refolded and tetramerised. Both Y155A and E83A demonstrated reduced binding to the NM4 TCR in comparison to WT CD1c. E83A exhibited a 77% to 91% reduction in MFI compared to WTCD1c, whereas Y155A demonstrated a lesser but still substantial reduction of 73% to 82% (Figure 9). The L150A tetramer had a very similar staining profile to WT CD1c at each concentration of tetramer. However, variation in MFI from that of WT CD1c increased with tetramer concentration, with the L150A tetramer demonstrating minimally greater binding (1.9%) than WT at 0.1µg but 18.02% less binding with 0.5µg of tetramer. The H87A tetramer had an overall reduced level of binding compared to WT CD1c, demonstrating a 43% to 55% reduction in staining over the range of tetramer concentrations. The reduced level of tetramer staining introduced by the majority of these mutations indicates a crucial role of the F' roof in the binding of CD1c to the NM4 TCR, at least through this analysis revealed by this tetramer assay.

a)

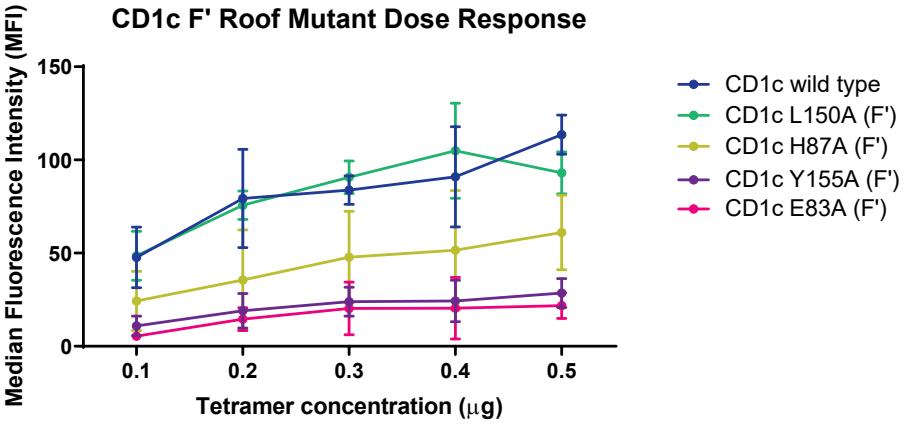

b)

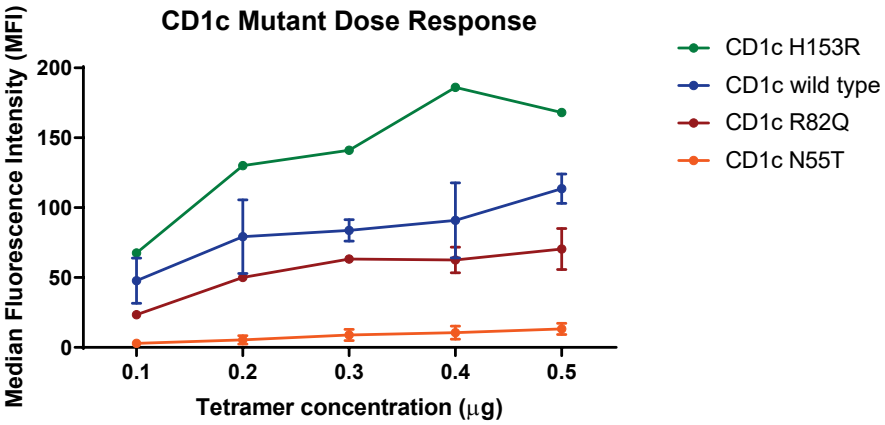

Figure 9: Dose response of CD1c mutant tetramers

Graphs representing average staining intensity (n=3) of NM4 Jurkat T cells stained in a dose-response by CD1c mutant tetramers, with data suggesting that several mutants may disrupt TCR binding to CD1c. a) Staining intensity of CD1c tetramers with mutations within the F' roof region, b) staining intensity of CD1c tetramers with mutations outside the F' roof region.

3.1.2 Surface plasmon resonance

To further investigate the NM4 TCR binding footprint, the binding affinity of the NM4 TCR was analysed by SPR. Despite differences in tetramer staining of NM4 by the seven CD1c mutants being observed over a range of tetramer concentrations, the equilibrium binding constant (K_D) was not markedly different for each of the CD1c mutants compared to WT CD1c. Mutants L150A and R82Q had K_D values of 5.7μM and were most similar to that of WT CD1c (5.8μM) (Figure 10 and 11). These two mutants were also the most similar to WT CD1c in terms of tetramer binding.

However, K_D values for the remaining CD1c mutants did not closely match the tetramer staining profiles when compared to WT CD1c. Mutant Y155A which had poor binding of NM4 in tetramer studies, but had the highest affinity (4.9µM) with the TCR when analysed by SPR. H153R also had a greater affinity with the TCR than WT CD1c, however the difference in K_D was negligible and a greater affinity was expected as it had greater staining in tetramer studies. The remaining mutant proteins all had lower affinities than WT CD1c, but these results did not correlate to tetramer studies.

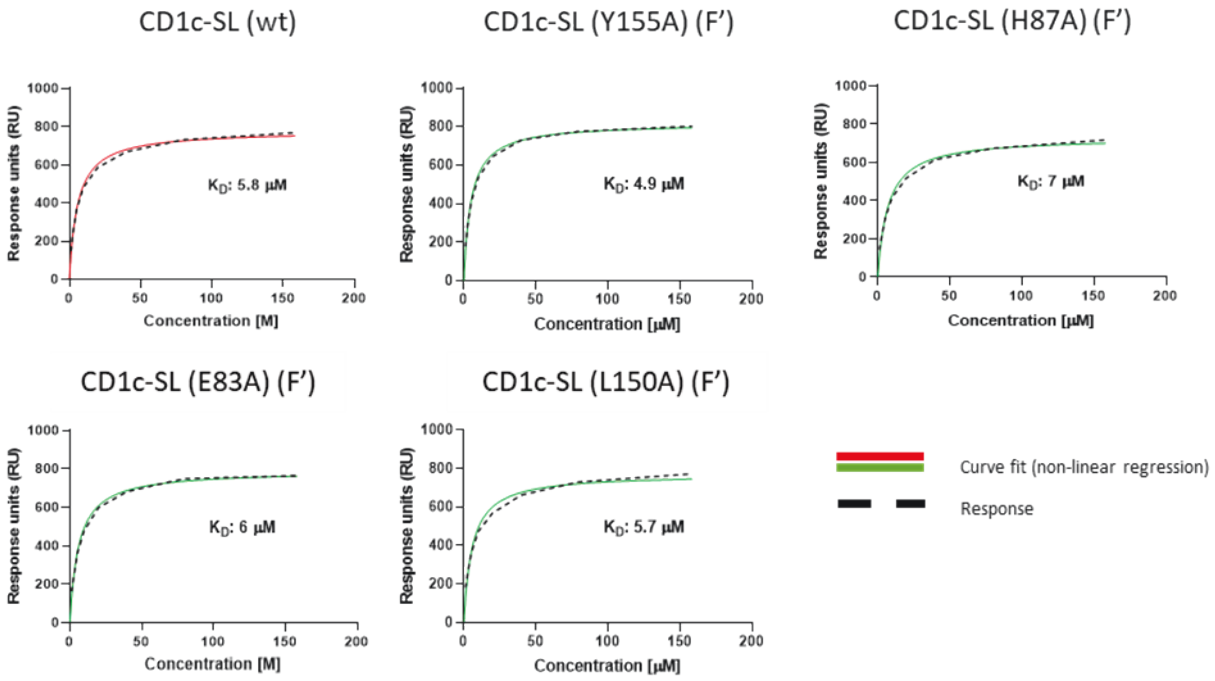

Figure 10: CD1c-SL F' roof mutant binding to NM4 TCR

Surface plasmon resonance measurements for binding of NM4 TCR to immobilised CD1c-SL wild type (WT) and F' mutant (each complex indicated in the above plots) complexes at equilibrium. K_D, calculated dissociation constant; RU, response units.

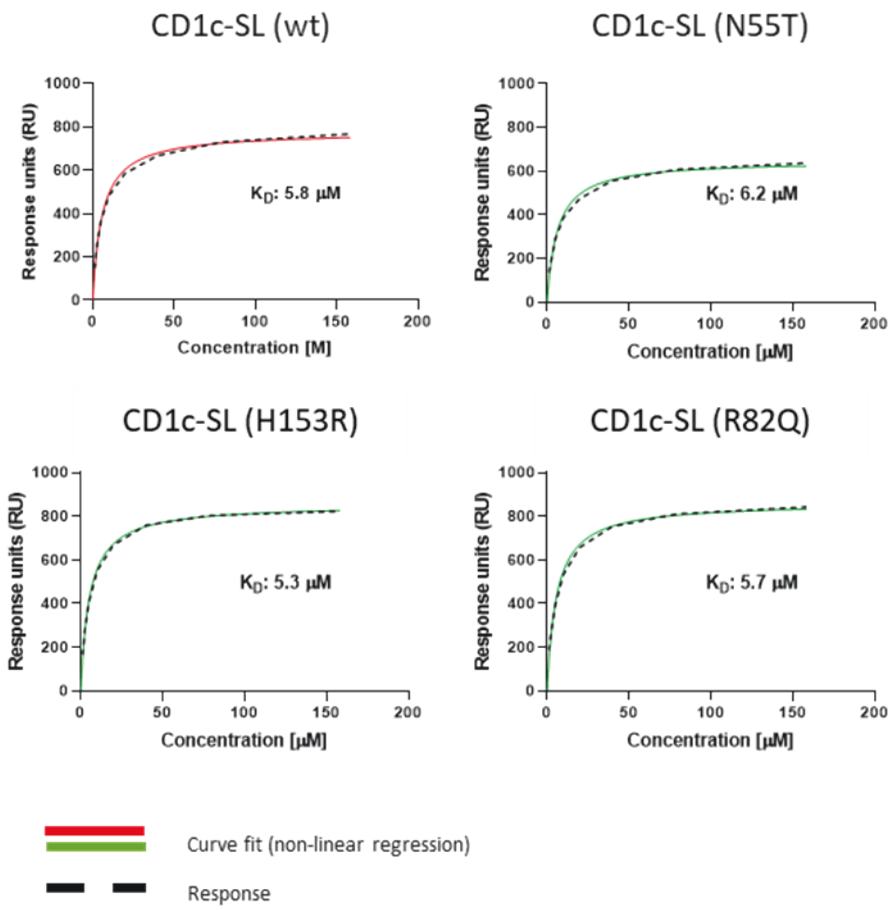

Figure 11: CD1c-SL mutant binding to NM4 TCR

Surface plasmon resonance measurements for binding of NM4 TCR to immobilised CD1c-SL wild type (WT) and mutant (each complex indicated in the above plots) complexes at equilibrium. K_D, calculated dissociation constant; RU, response units.

3.1.3 Optimising Jurkat T cell activation assays

In order to investigate recognition of WT CD1c by the NM4 TCR and subsequent T cell activation, we sought to optimise an activation assay through culture of T2 lymphoblast cells expressing wild-type CD1c with NM4 Jurkat T cells. Two NM4 Jurkat T cell lines were used: the J.RT3-T3.5 parental Jurkat T cell line and J.RT3-T3.5 cells harbouring the NFAT-inducible luciferase reporter cassette (termed NFAT-Gluc Jurkat T cells). Jurkat T cells were cultured in 96 well plates at a concentration of $1x10^5$ cells per well with either parental WT T2 cells (T2-negative) or T2 expressing CD1c (T2-CD1c). The effect of increasing concentrations of T2 cells, from $0.5x10^5$ to $2x10^5$ cells per well, and the duration of culture on T cell activation was investigated in order to optimise this assay. T cell activation was measured by frequency (%) of live lymphocytes expressing CD69 and CD3. Fold change in CD69 expression and the percentage downregulation of CD3 expression between Jurkat T cells cultured with T2-CD1c and T2-negative was then analysed. From 2 hours of incubation, there was a positive fold change in CD69 expression by both Jurkat T cell lines cultured with T2-

CD1c cells compared to T2-negative cells (Figure 12). Generally, a greater fold change in CD69 expression was observed following longer duration of cultures with T2 cells, with J.RT3-T3.5 cells having greater fold change at 24 hours. NFAT-Gluc T cells were also observed to have greatest fold change at 24 hours for those cultured with $0.5x10^5$ and $1x10^5$ T2s, but for the higher T2 concentrations, the greatest fold change in CD69 expression was observed at 16 hours of culture. Overall, we observed that NFAT-Gluc Jurkat T cells expressing the NM4 TCR had a greater fold change in CD69 expression over the range of culture conditions compared to J.RT3-T3.5 Jurkat T cells.

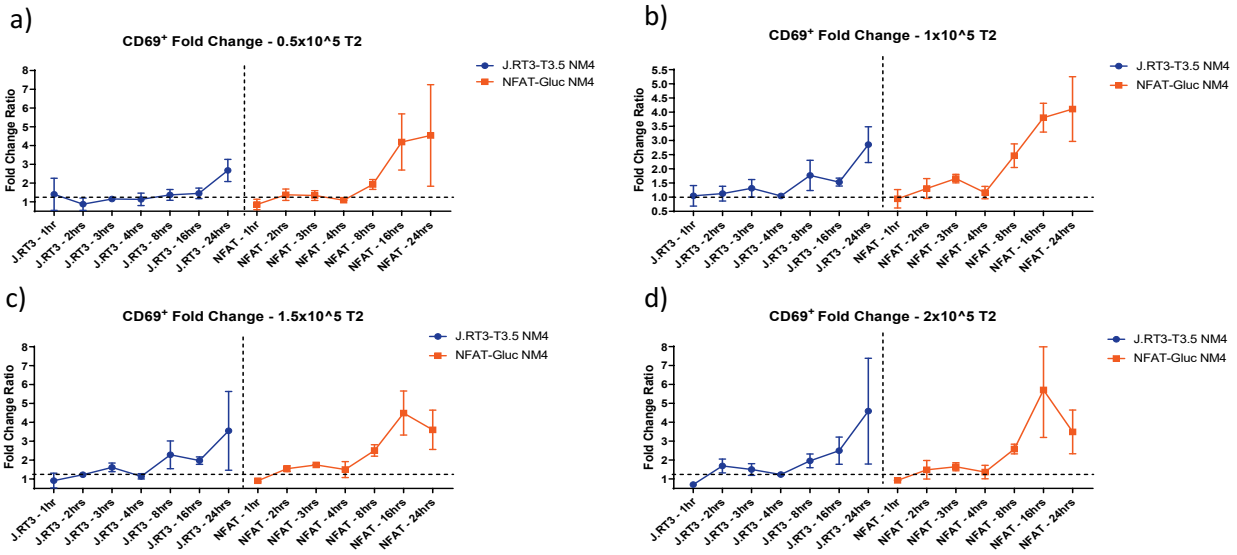

Figure 12: CD69 expression by Jurkat T cells stimulated with CD1c

Flow cytometry analysis of two Jurkat T cell lines, J.RT3-T3.5 and NFAT-Gluc, cultured for various lengths of time with T2 cells at concentrations of a) $0.5x10^5$ T2, b) $1x10^5$ T2, c) $1.5x10^5$ T2 and d) $2x10^5$ T2. Results are presented as fold change ratios calculated from the average $CD69^+$ Jurkat T cells cultured with T2-CD1c cells (n=3) / average $CD69^+$ Jurkat T cells cultured with parental CD1c negative T2 cells (n=3).

In addition to CD69 expression, another indicator of T cell activation is downregulation of the TCR, measured here by CD3 expression. Generally, from 3 hours of culture we observed a downregulation of CD3 for both Jurkat T cell lines cultured with T2-CD1c compared to T2-negative cells (Figure 13). An increase in percentage downregulation was observed with increasing concentrations of T2 cells, with NFAT-Gluc Jurkat T cells demonstrating an overall slightly greater level of CD3 downregulation than J.RT3-T3.5 Jurkat T cells. For both Jurkat T cell lines, the greatest percentage of CD3 downregulation was observed to be at 8 hours of culture, however NFAT-Gluc Jurkat T cells also demonstrated greater TCR downregulation at 16 and 24 hours.

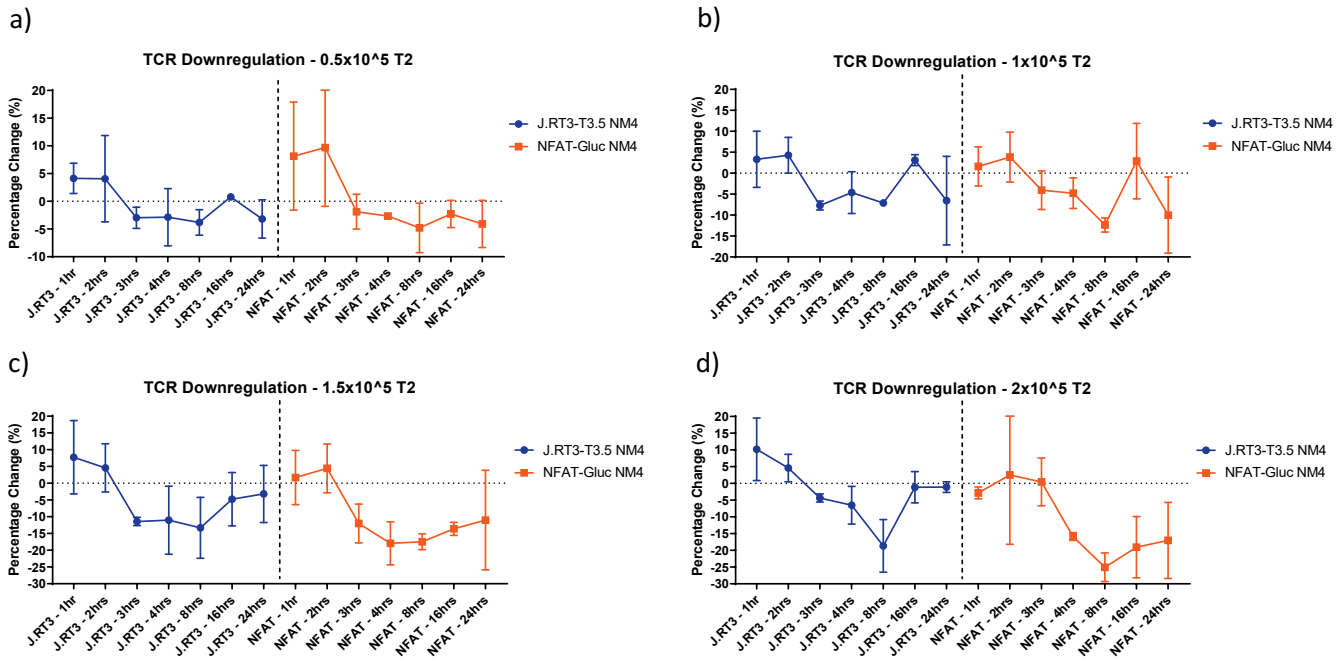

Figure 13: TCR downregulation by Jurkat T cells stimulated with CD1c

Flow cytometry analysis of two Jurkat T cell lines, J.RT3-T3.5 and NFAT-Gluc, cultured for various lengths of time with T2 cells at concentrations of a) $0.5x10^5$ T2, b) $1x10^5$ T2, c) $1.5x10^5$ T2 and d) $2x10^5$ T2. TCR downregulation was calculated by the percentage change in average CD3 expression by Jurkat T cells cultured with T2-CD1c cells (n=3) from the average CD3 expression by Jurkat T cells cultured with parental CD1c negative T2 cells (n=3).

Although the percentage downregulation of CD3 was similar between NFAT-Gluc and J.RT3-T3.5 Jurkat T cells, we observed a clearly greater response from NFAT-Gluc T cells in the context of CD69 expression. Taken together, both NM4 expressing Jurkat T cell lines are clearly activated in the presence of CD1c. However, in addition to the greater response of NFAT-Gluc Jurkat T cells in the presence of CD1c, this cell line contains a luciferase reporter cassette which enables activation to also be measured by the secretion of luciferase into the supernatant. Subsequently, NFAT-Gluc Jurkat T cells are a better tool when measuring antigen-specific activation of T cells.

3.1.4 Plate bound CD1c assay

With the aim of investigating the recognition of soluble CD1c by the NM4 TCR and the subsequent T cell activation, a plate bound CD1c assay was utilised. In order to optimise this experiment, soluble WT CD1c was bound to wells of a 6 well plate at concentrations ranging from 0.5 to 2μg per well, with protein-free PBS as a negative control. NFAT-Gluc Jurkat T cells expressing the NM4 TCR were added to each protein coated well at a concentration of $1x10^5$ cells per well. Following incubation of the cells for 24 hours at 37°C, frequency of CD69 and CD3 expression by NFAT-Gluc

Jurkat T cells were analysed by flow cytometry. There were negligible differences in CD69 expression between Jurkat T cells cultured with plate bound CD1c or the PBS negative control, but while a small increase in CD69 expression was observed in cultures with 0.5µg and 1µg of CD1c, lower frequencies of CD69 were observed with 1.5µg and 2µg of CD1c. Expression of CD3 was also minimally affected by the presence of CD1c, although a trend for decreasing average CD3 expression with increasing concentration of plate bound CD1c can be observed (Figure 14).

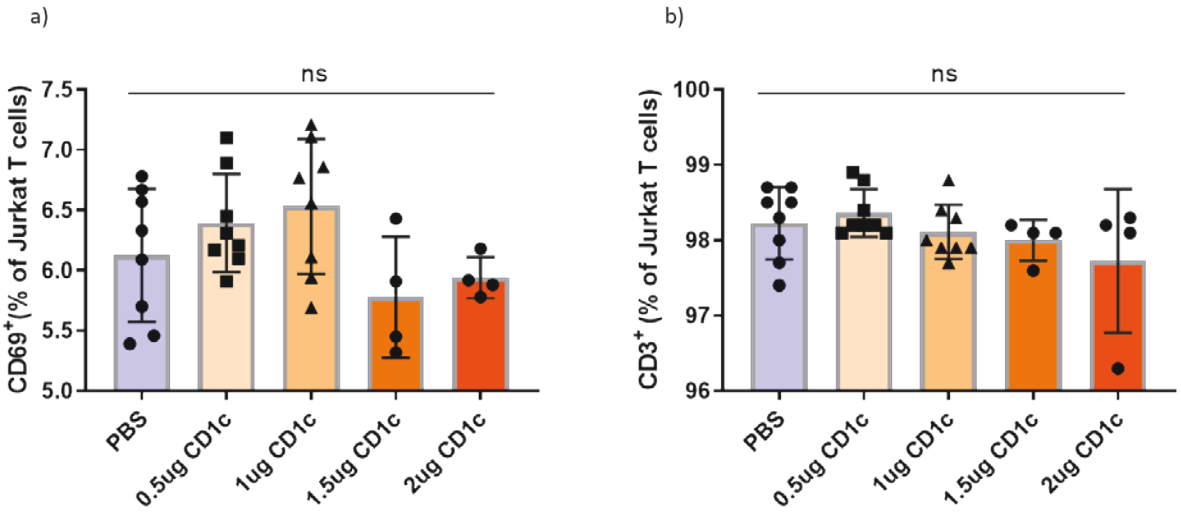

Figure 14: Activation of Jurkat T cells stimulated with plate bound CD1c

Flow cytometry analysis of NFAT-Gluc Jurkat T cells cultured with different concentrations of plate bound CD1c monomers for 24 hours at 37°C. Activation of Jurkat T cells was measured by the frequency of a) $CD69^+$ Jurkat T cells and b) $CD3^+$ Jurkat T cells. Data is represented as the mean ± SD for each concentration of CD1c (n=3).

Although there are trends for small changes in the average CD69 and CD3 expression of the Jurkat T cells cultured with CD1c monomer (n=3), greater levels of activation were expected. High concentrations of protein may have led to more aggregation, or the assay itself may not have been sensitive enough to see a consistent effect. If this method is to be used to further analyse CD1c-specific activation of T cells, further optimisation is required.

3.1.5 Understanding lipid reactivity of the NM4 TCR

CD1c is a widely expressed antigen presenting molecule that is commonly expressed on marginal zone B cells and myeloid DC. T cells restricted to CD1c presenting specific lipids have been identified, including the pathogen-derived lipid PM (264). However, CD1c autoreactive T cells are known to circulate in high frequency in the peripheral blood and our group has previously isolated and identified a self-reactive CD1c-restricted TCR (NM4) using a tetramer comprised of CD1c

containing only spacer lipids (CD1c-SL). It has been demonstrated that there are CD1b-restricted T cells that are promiscuous in nature, recognising CD1b loaded with a range of self-phospholipids and sphingolipids, but are still specific for CD1b itself (280). Additionally, recognition of both CD1a and CD1c harbouring sequestered lipids has been observed, whereby the TCRs recognise the CD1 protein itself but not the bound lipids (268, 295). We aimed to investigate whether CD1c could be loaded with self-lipids ranging in head group size, lipid tail length and saturation, and hydrophobicity. Lipids were solubilised in 50mM sodium citrate buffer pH 6.5 + 0.5% CHAPS and incubated with refolded CD1c-SL monomers overnight. The lipid-pulsed proteins were then tetramerised and used to stain our CD1c-restricted TCR clone, NM4, in order to investigate whether recognition and binding to CD1c was augmented by loaded self-lipids. As a control, CD1c-SL protein was also incubated with citrate buffer alone, and citrate buffer 0.5% CHAPS. CD1c in citrate buffer alone showed positive staining of NM4 but when incubated with buffer supplemented with 0.5% CHAPS, staining was almost abolished. Addition of each lipid demonstrated improved staining when compared to protein incubated with citrate buffer + 0.5% CHAPS alone, but with variable levels of staining. CD1c pulsed with PG 16:0-18:1 demonstrated the greatest level of staining followed by Liver PI, while SM, PC (18:1 Δ9 cis) and GD1a also produced positive staining but to a lower extent (Figure 15). This indicates that NM4 is a highly promiscuous TCR with no requirement for a specific lipid. To assess whether lipid tail variations affected the recognition of CD1c by NM4, analogues of the lipids were tested. CD1c tetramers pulsed with Lyso Liver PI which is a monoacyl lipid, were found to have substantially poorer staining of NM4 than Liver PI, suggesting that both lipid tails are required for recognition of CD1c by this TCR.

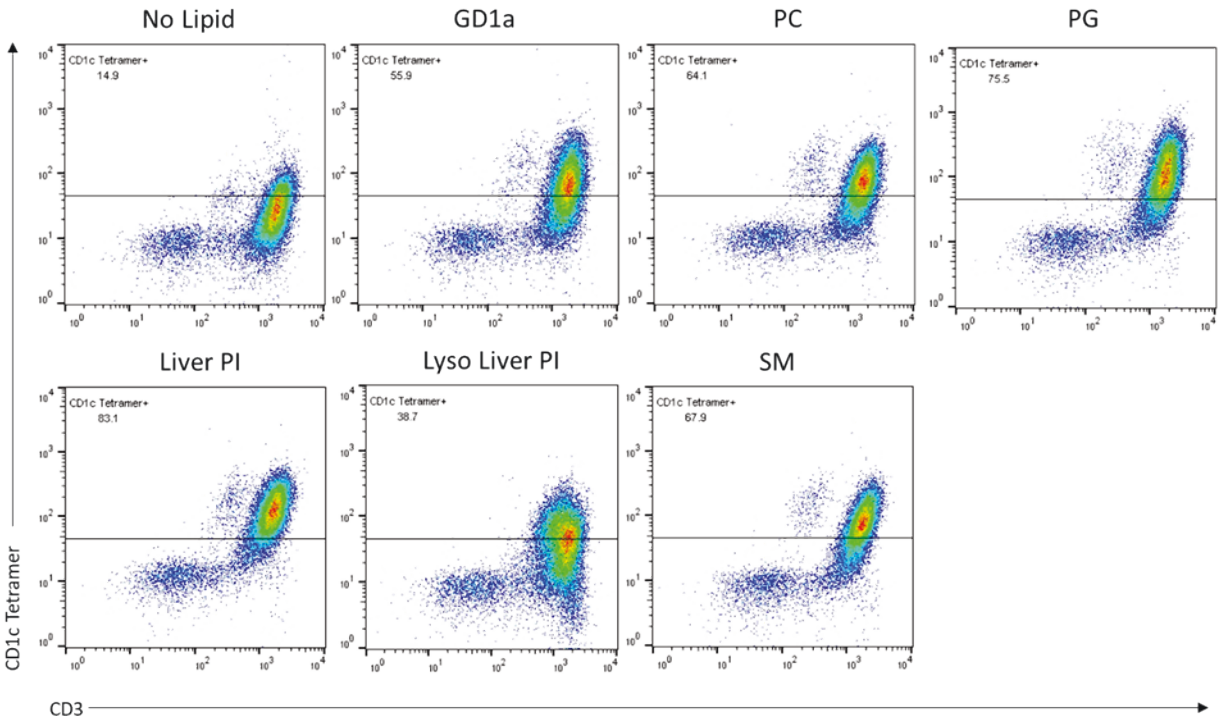

Figure 15: Staining of the NM4 TCR with lipid pulsed CD1c tetramers

Flow cytometry dot plots showing the staining of NM4 Jurkat T cells stained with tetramers composed of lipid-pulsed CD1c monomers and anti-CD3 antibody. CD1c tetramers pulsed with vehicle (0.5% CHAPS sodium citrate buffer) served as a control for lipid loading. Loaded lipids are solubilised in vehicle and are indicated above each plot. Lipids loaded into CD1c included GD1a, PC, PG, Liver PI, Lyso Liver PI and SM.

Four further analogues of PG were tested: 18:0, 16:0, 18:0-18:1 and 18:1 (Δ9 cis). Tetramers loaded with fully saturated lipid tails, PG 18:0 and 16:0, were consistently recognised the strongest by NM4, surpassing PG analogues 18:0-18:1 and 16:0-18:1 with one unsaturated bond, despite observable positive staining with these tetramers (Figure 16). PG analogue 18:1 (Δ9 cis) had little to no staining of NM4 and was observed to have poorer functionality than CD1c treated with citrate buffer + 0.5% CHAPS alone. This suggests that while other PG analogues are recognised, the conformation of this lipid tail may have altered the ability of NM4 to recognise CD1c. However, the PC analogue tested also had the same level of unsaturation and tail conformation, which may suggest that both head group and lipid tail conformation may be important in recognition of CD1c by this TCR. In conclusion, these studies, which were repeated at least four times per tetramer, indicate that the NM4 TCR recognises CD1c when bound to a range of self-lipid ligands, including those with head groups. In addition, our data suggests a role for lipid backbone structure in NM4 mediated recognition of CD1c which warrants future investigation.

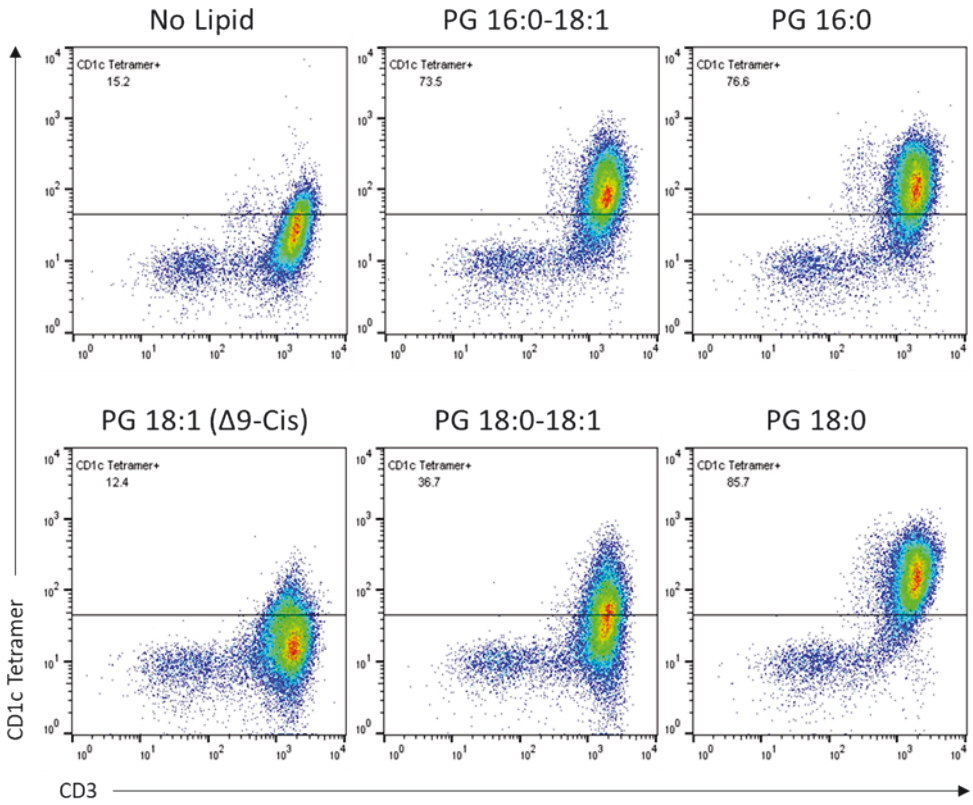

Figure 16: Staining of NM4 Jurkat T cells with CD1c tetramers loaded with phosphatidylglycerol (PG) lipid analogues

Flow cytometry dot plots showing the staining of NM4 Jurkat T cells with CD1c tetramers loaded with PG analogues. The head groups of the PG analogues are the same but comprise different structural variants within their lipid chains. CD1c tetramers pulsed with vehicle (0.5% CHAPS sodium citrate buffer) served as a control for lipid loading. Loaded lipids are solubilised in vehicle and are indicated above each plot.

3.2 Deriving CD1c-restricted T cells

A growing body of evidence suggests a functional role for CD1c and its restricted T cells in human TB. Furthermore, many CD1c-restricted T cells recognise CD1c in the absence of foreign lipid antigen, suggesting their recognition of CD1c when bound to host derived self-lipids. However, the molecular mechanisms underpinning CD1c recognition by T cells are not well understood. Here, our overarching aim was to clone new CD1c autoreactive TCRs and compare their CD1c recognition mechanism to that of αβ NM4 TCR. To this end, we first sought to expand T cells by several methods before employing CD1c tetramer guided cell sorting to clone T cells or their TCRs by flow cytometry. In order to clone T cells, we attempted to enrich CD1c restricted T cell populations using two methods before tetramer guided T cell cloning. In the first method, we used self-lipid loaded $CD1c^+$ MoDC as APC which were co-cultured with autologous $CD4^+$ T cells. In another method, we specifically expanded Vδ1 T cells within PBMC using a plate bound anti-γδ antibody assay. We also attempted to derive a clonal CD1c-restricted T cell population from donor blood through *ex vivo* tetramer guided cell sorting.

3.2.1 DC-T cell co-culture

The first method employed to generate enriched CD1-restricted T cell lines was the co-culture of DC with autologous T cells. MACS isolated $CD14^+$ monocytes were cultured with 20ng/ml IL-4 and 20ng/ml GM-CSF for 5 days to generate $CD1^+$ DC (428) before pulsing overnight with 50ng/ml of one of the following lipids: PC, PG or PE. Before adding autologous T cells in a ratio of 10:1 (T cells:DC), half of the DCs were matured with 50ng/ml LPS to observe whether matured DC would affect expansion of T cells in comparison to T cells stimulated with immature DC. After 2 weeks of culture, T cells were stained with CD1c tetramers (Figure 17).

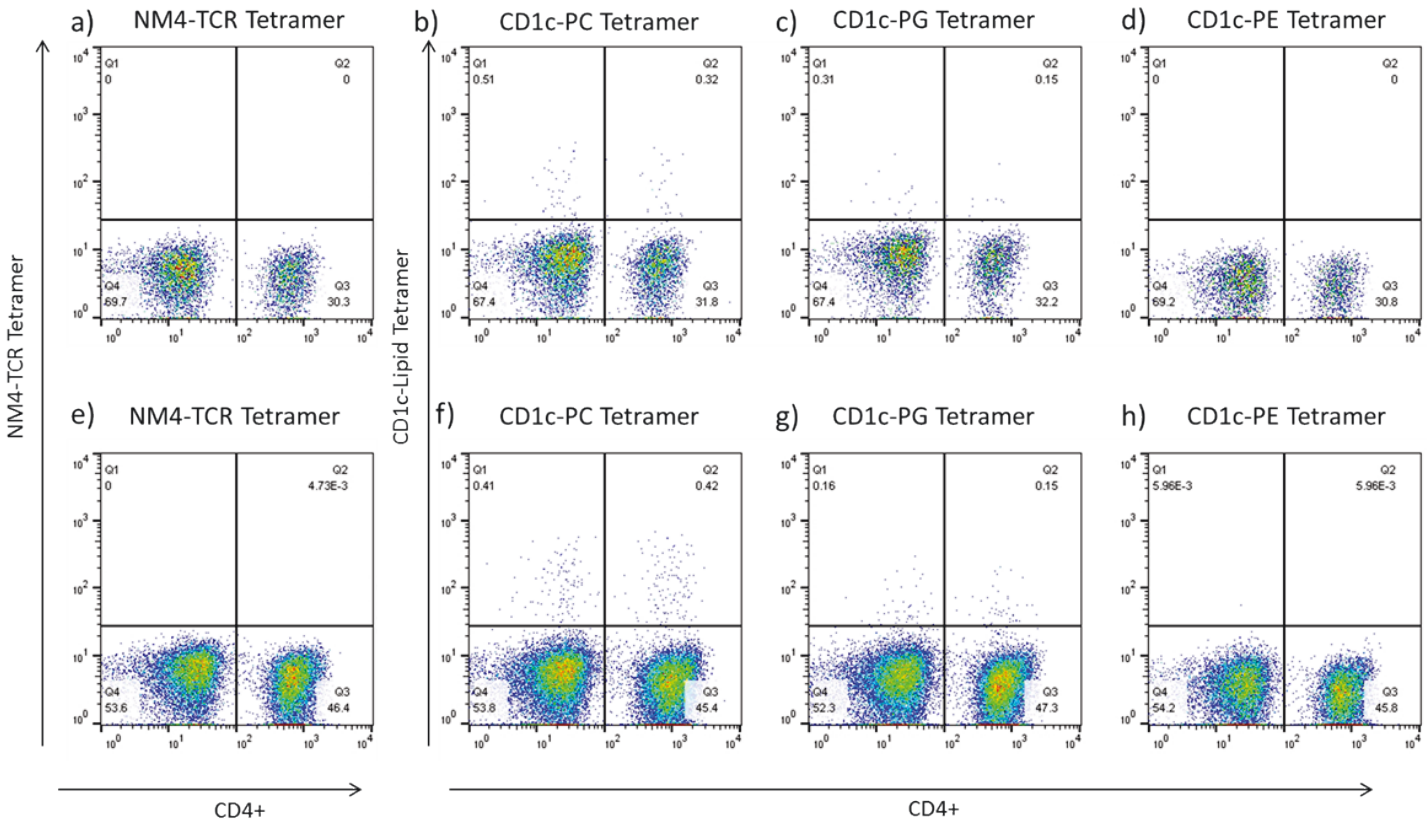

Figure 17: CD1c-lipid tetramer staining of DC expanded T cell lines

Representative dot plots of CD1c-lipid tetramer stained T cells stimulated with mature (top row) or immature (bottom row) DC that had been pulsed with phosphatidylcholine (PC). T cell lines were pre-gated on Live $CD3^+$ T cells and stained with anti-CD4 antibody and the following tetramers: a) control NM4 TCR tetramer, b) CD1c-PC tetramer, c) CD1c-PG tetramer, d) CD1c-PE tetramer, e) control NM4 TCR tetramer, f) CD1c-PC tetramer, g) CD1c-PG tetramer and h) CD1c-PE tetramer. Data representative of three individual T cell cultures pulsed with three different lipids.

We found that for each of the cultures, T cells cultured with immature DC compared to those with mature DC had a greater number of cells stained with each of the CD1c-lipid tetramers, regardless of whether the CD1-lipid tetramer complex matched the lipids added to each culture (Figure 18).

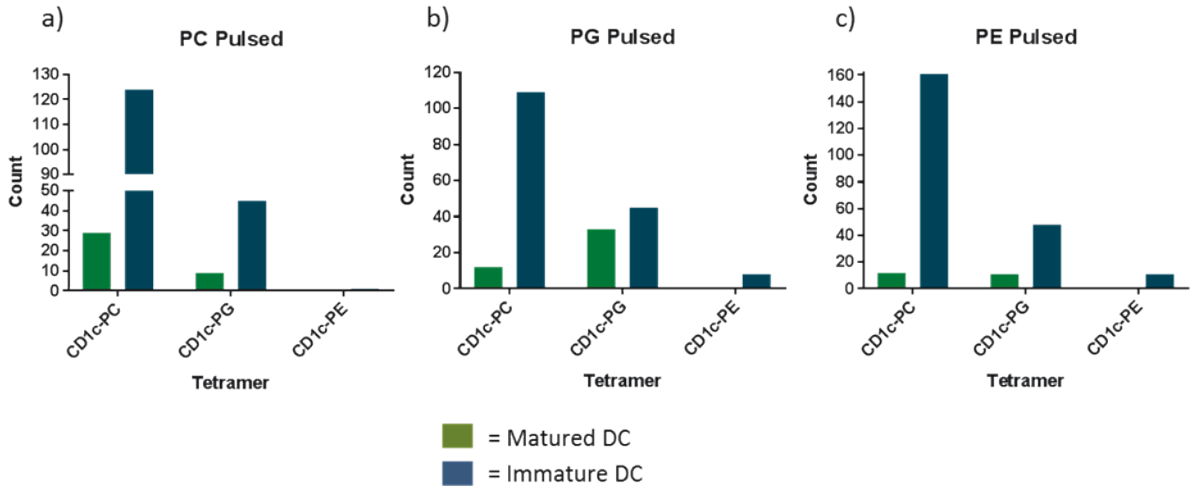

Figure 18: Tetramer staining of DC stimulated T cell cultures

Graphs showing numbers of tetramer positive T cells within T cell lines cultured *in vitro* with immature or mature DC. a) T cells cultured with phosphatidylcholine (PC) pulsed DC, b) T cells cultured with phosphatidylglycerol (PG) pulsed DC and c) T cells cultured with phosphatidylethanolamine (PE) pulsed DC.

T cells cultured with immature DC contained large numbers of T cells that were stained by CD1c-PG tetramers and even greater numbers of T cells stained with CD1c-PC tetramers, regardless of which lipid was added to culture. This may suggest that CD1c tetramers may exhibit non-specific binding for T cell lines generated by immature DC. However, this may also suggest the presence of expanded CD1c autoreactive T cells which can be cloned for further analyses. Staining with CD1c-PE tetramers was low to absent, even when cells were exposed to PE in culture. The level of staining with this tetramer was comparable to staining with the NM4-TCR tetramer used as a negative control. These results suggested that the CD1c-PE tetramer may not have been functional at the time of this experiment, and was investigated against a freshly made CD1c-PE tetramer. CD1c-PE tetramers used to stain expanded cultures failed to stain a CD1c-restricted NM4-TCR expressing Jurkat T cell line, compared to a freshly made CD1c-PE tetramer which showed clear binding to NM4 Jurkat T cells (Figure 19). However, the tetramer staining was not sufficiently bright when bound to NM4 Jurkat T cells which prompted us to revisit the CD1c refolding and purification procedures to improve tetramer staining efficiency.

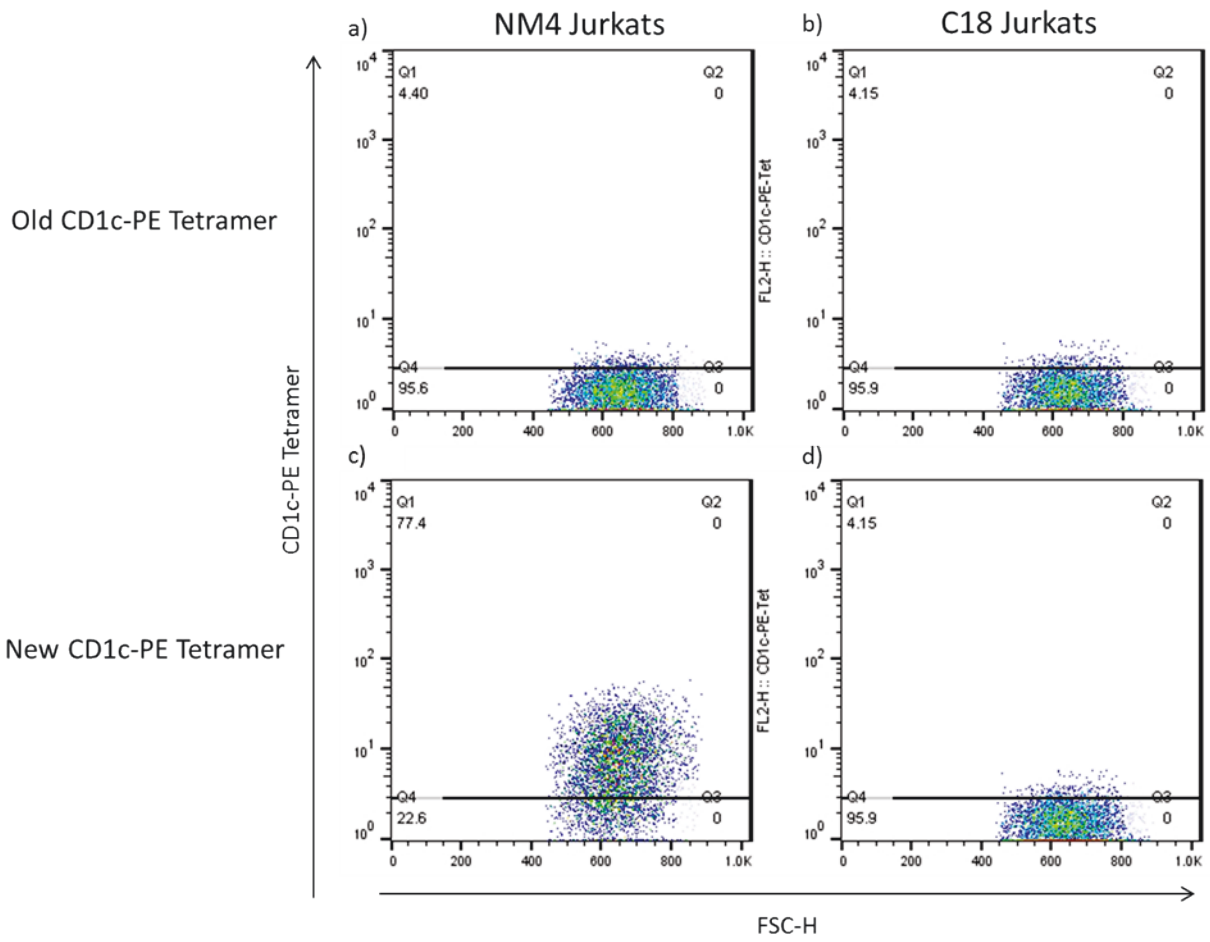

Figure 19: Comparing newly refolded CD1c-PE tetramers with those used in T cell staining

Flow cytometry dot plots showing a) CD1c-restricted NM4 Jurkat T cells stained with old CD1c-PE tetramer, b) CD1b-restricted C18 Jurkat T cells (negative control) stained with old CD1c-PE tetramer, c) NM4 Jurkat T cells stained with new CD1c-PE tetramer, d) C18 Jurkat T cells stained with new CD1c-PE tetramer.

3.2.2 Improving CD1c tetramer quality

In order to improve tetramer staining efficiency, we attempted to improve the purification procedure of our refolded CD1c lipid complexes. Refolded CD1c lipid complexes are usually purified by several rounds of size exclusion chromatography. We introduced another purification step involving anion exchange chromatography. The addition of an anion exchange column to the purification of the CD1c protein enabled us to analyse whether different fractions eluted from the column corresponded to higher quality monomers and thus an enhanced staining profile when tetramerised. Five CD1c protein fractions were eluted from the anion exchange column and these were subsequently tetramerised with Streptavidin-PE before staining the NM4 Jurkat T cells. The tetramer staining revealed that Fraction 2 had a significantly brighter staining than the pre-anion

exchange fraction and all other anion exchange fractions, indicating that this method of purification enabled separation of optimally refolded protein from lower quality monomers (Figure 20).

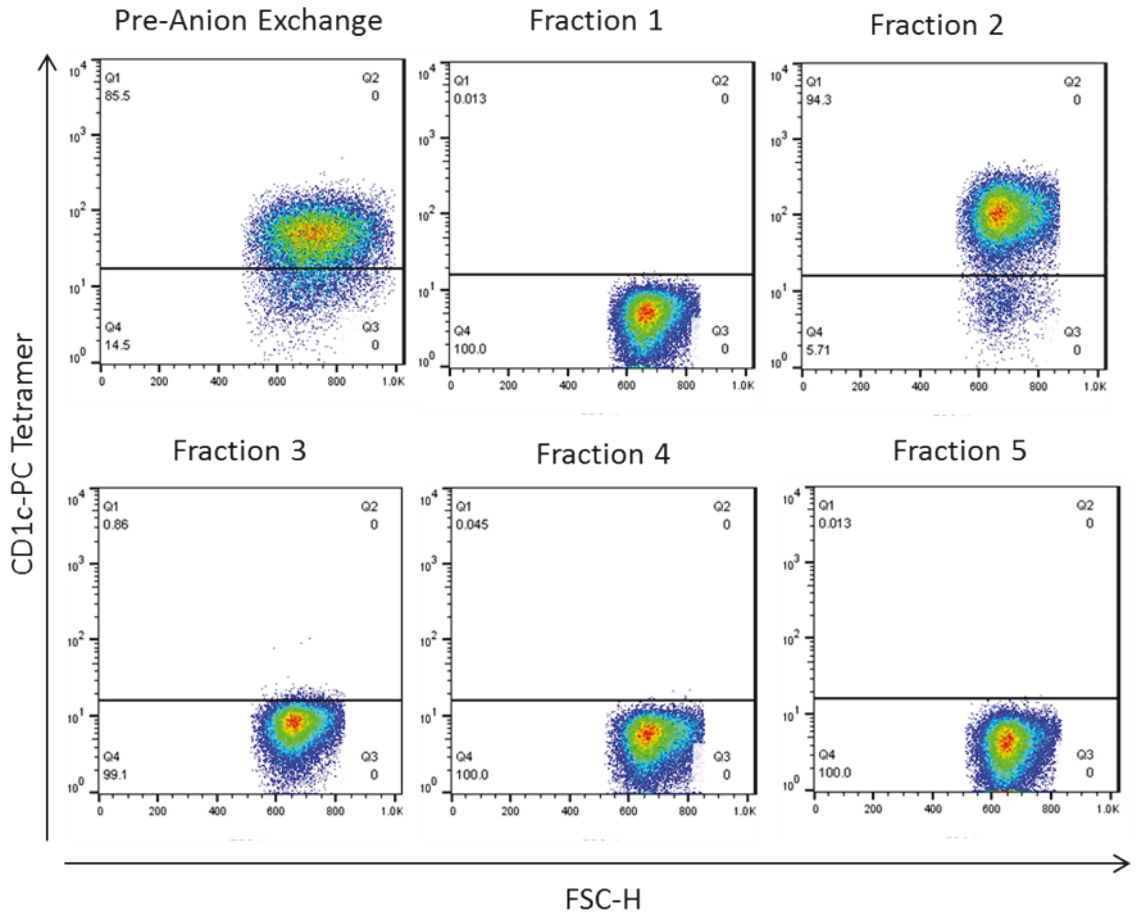

Figure 20: Comparing tetramer staining of different CD1c protein fractions

Flow cytometry dot plots of CD1c-restricted NM4 Jurkat T cells stained with tetramers composed of CD1c-PC protein that was eluted from the anion exchange column at increasing concentrations of salt. Only pre-anion exchange fraction and fraction 2 stained Jurkat T cells.

The refolding of CD1 proteins is frequently carried out in the presence of a refolding matrix. A ternary refolding matrix is comprised of a minichaperone and two isomerases, known as foldases. The minichaperone GroEL binds to unfolded polypeptides and is understood to prevent improper protein folding and aggregation (425). The two foldases, protein disulphide isomerase DsbA and peptidyl-prolyl cis-trans isomerase PPI, are included in the ternary matrix to assist in the formation of disulphide bridges and catalysis of cis-trans isomeration of peptidyl-proline bonds, respectively (425). Previous data has shown that the use of a ternary refolding matrix increases solubilisation of the sample and decreases protein aggregation, leading to enhanced sample recovery following High Performance Liquid Chromatography (HPLC) (291, 425). For CD1a and

CD1b, it has been shown that if the ternary matrix lacks one component, the β_2m light chain remained solubilised in solution but the CD1 heavy chain precipitated (291). However, it has also been shown that CD1a is able to refold in the absence of the ternary matrix if ligand is present (291). To investigate whether a ternary matrix was crucial for the refolding of CD1c and whether exogenous ligand was required, we refolded CD1c and β_2m in the absence of matrix either in the presence of vehicle (0.5% Tween 20, 150mM NaCl) as a control, or in the presence of vehicle with solubilised PC lipid antigen. Surprisingly, both these refolding experiments gave rise to stable protein complexes, producing tetramers that stained NM4 Jurkat T cells (Figure 21). These data suggested that CD1c can be refolded in the absence of the refolding matrix, but also that components of vehicle can successfully stabilise the protein. This suggests that during the CD1c-PC refold, PC may not have been incorporated into CD1c. We had previously crystallised CD1c following refolding with vehicle which gave rise to CD1c-SL (265). Henceforth, we shall employ our improved CD1c-SL tetramers for T cell staining.

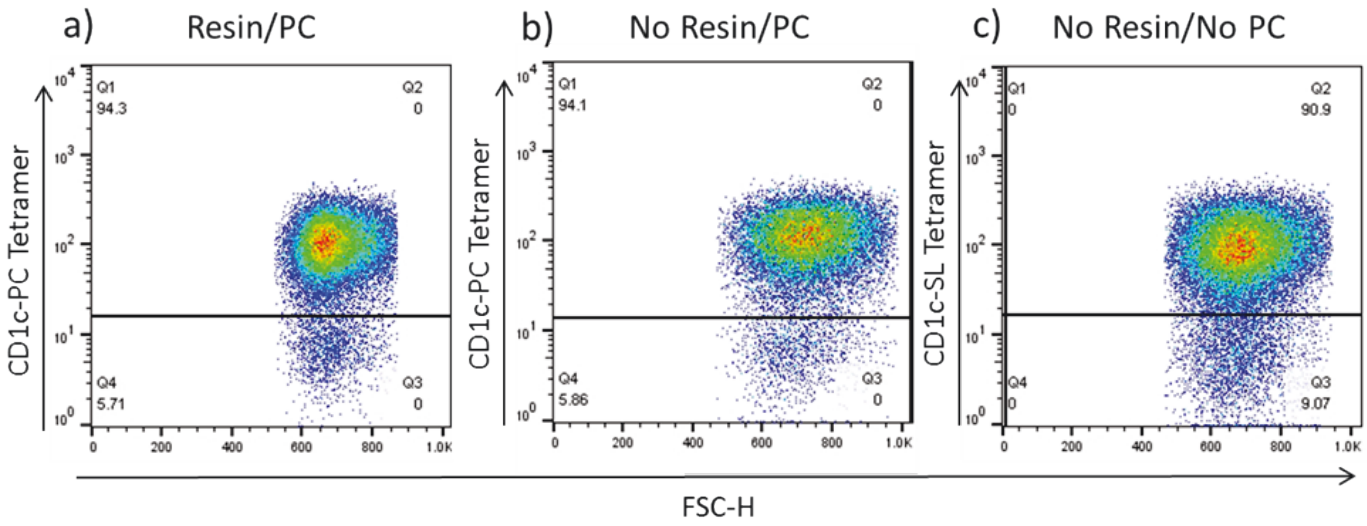

Figure 21: Comparing tetramers refolded with/without refolding matrix "resin" and with/without specific lipid

Flow cytometry dot plots of CD1c-restricted NM4 Jurkat T cells stained with a) CD1c tetramers refolded in the presence of Phosphatidylcholine (PC) and resin, b) CD1c tetramers in the presence of PC but without resin, C) CD1c tetramers refolded in the absence of both PC and resin.

3.2.3 *Ex vivo* sorting

In parallel to the DC mediated expansion method, we also employed tetramer guided cell sorting from *ex vivo* PBMC in order to clone CD1c-restricted T cells. In addition to sorting directly from PBMCs, several strategies were employed to enrich specific T cell populations prior to tetramer staining, including the enrichment of $CD3^+$ T cells and γδ T cells by MACS sorting. Tetramer sorted populations were cloned by a recently published method for the cloning of CD1b-restricted T cells (429). Generally, we sorted three different tetramer positive populations from several donors. These included CD1c $tetramer^+$ $CD3^+$ T cells, CD1c $tetramer^+$ $CD3^+$ $CD4^+$ T cells and CD1c $tetramer^+$ $CD3^+$ $V\delta1^+$ T cells. Our *ex vivo* staining revealed a clear CD1c $tetramer^+$ population in comparison to control TCR tetramers and streptavidin-PE alone (Figure 22). Tetramer positive populations were sorted in bulk, seeded into 8 wells of a 96 well plate and cultured with $1.5x10^5$ irradiated feeder PBMCs. Cells were stimulated overnight with 1.6µg/ml PHA before supplementing the next day with 100U/ml IL-2. After two weeks of T cell expansion, T cells were stained again with CD1c tetramers to investigate the fold expansion of CD1c-restricted T cells. However, we found that the frequency of CD1c $tetramer^+$ T cells was reduced after this initial round of expansion. Nevertheless, similar to recent CD1b tetramer guided cloning methods (301, 429), we performed several rounds of sorting and expansion for several lines. Despite a lack of expansion, a modest enriched population of T cells staining with CD1c tetramers was observed (Figure 23). Taken together, these results demonstrate that we were not successful in cloning CD1c restricted T cells using this method.

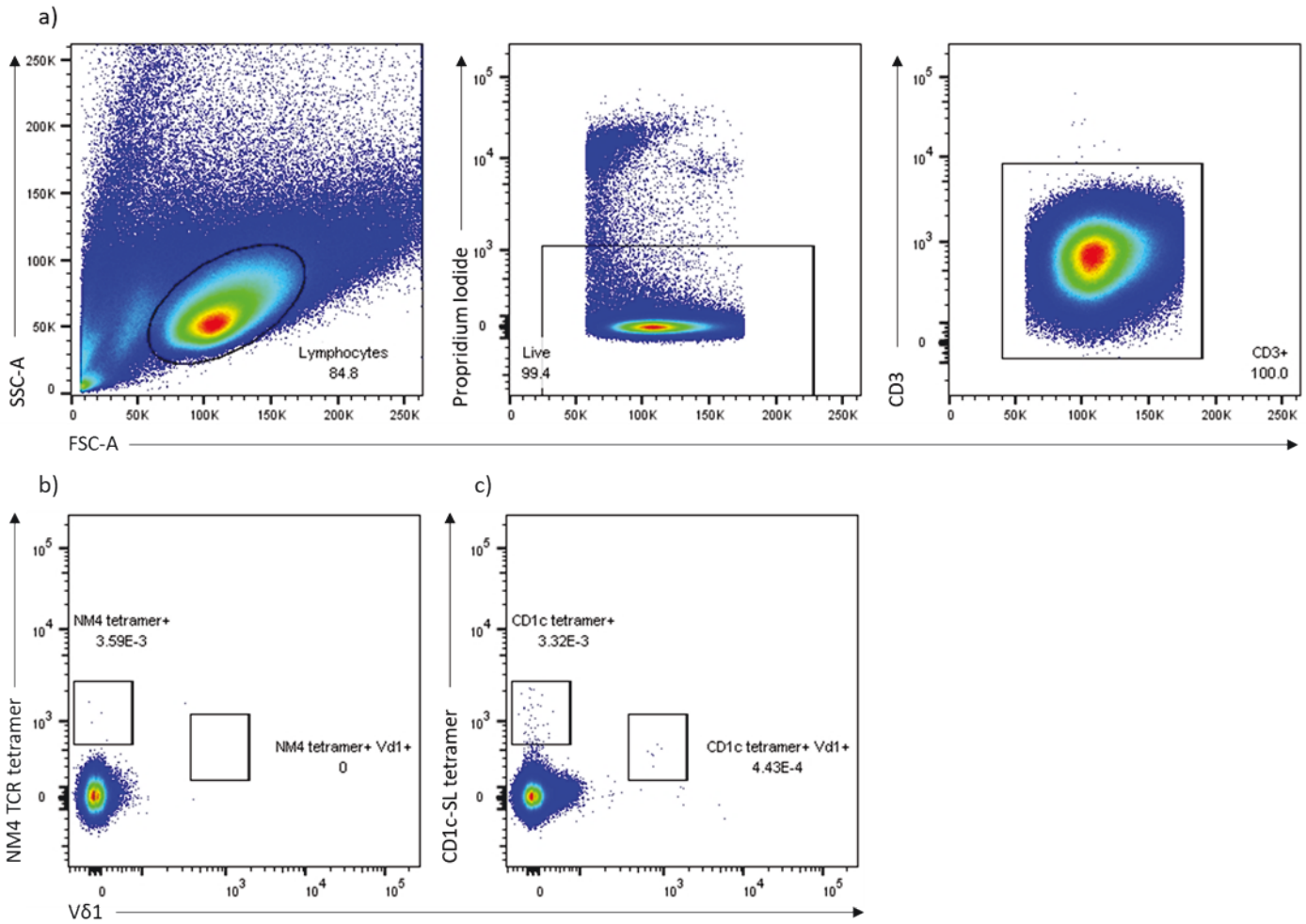

Figure 22: *Ex vivo* sorting of CD1c-SL tetramer$^+$ Vδ1$^+$ T cells from PBMC of a healthy donor

Representative flow cytometry dot plots showing tetramer staining of donor PBMCs for *ex vivo* sorting of CD1c-SL tetramer$^+$ Vδ1$^+$ T cells. a) Gating strategy of donor PBMCs including gating on lymphocytes, live cells (Propridium iodide$^-$) and CD3$^+$ T cells, b) Donor PBMCs stained with negative control NM4 TCR tetramer and anti-Vδ1. No cells were sorted from this sample. C) Donor PBMCs stained with CD1c-SL tetramer and anti-Vδ1. Cells staining positive with the CD1c-SL tetramer or tetramer and anti-Vδ1 antibody (indicated gates) were sorted into FACS tubes.

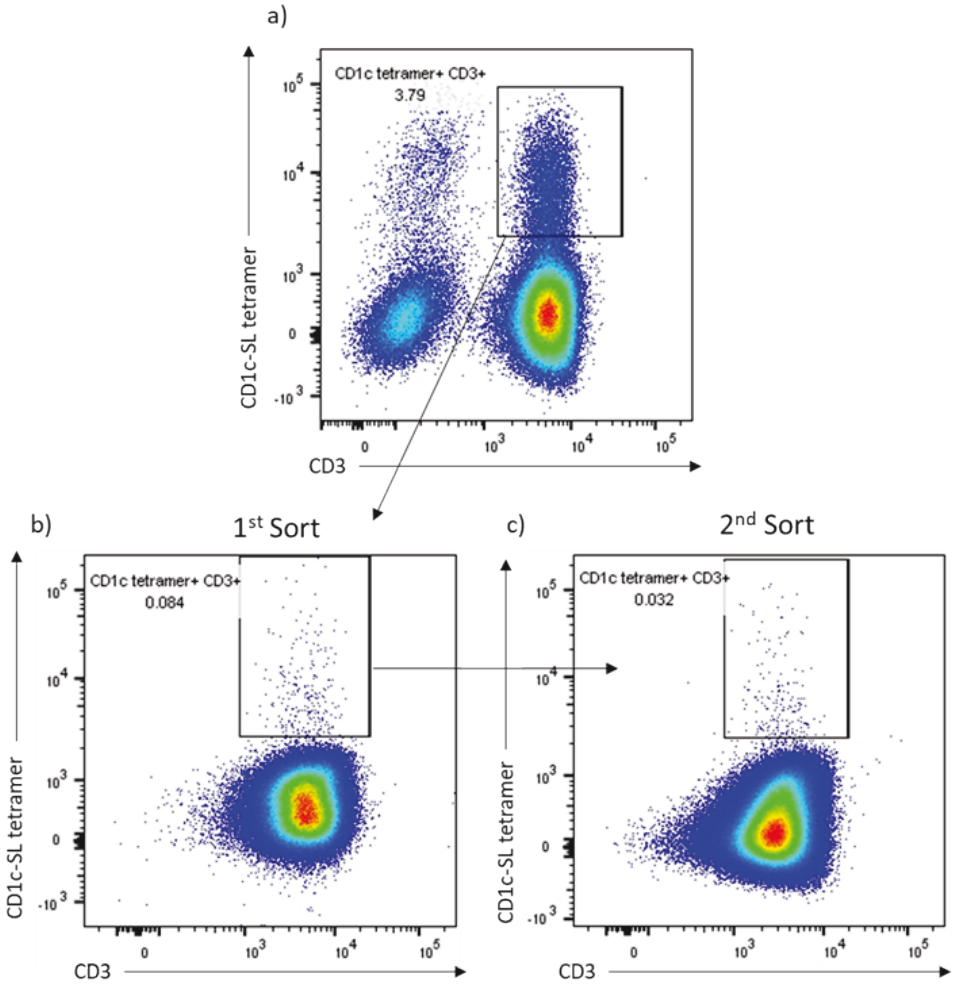

Figure 23: *Ex vivo* sorting of CD1c-SL tetramer$^+$ CD3$^+$ T cells from donor PBMC

Representative flow cytometry dot plots showing *ex vivo* sorting and generation of T cell lines. a) *Ex vivo* sorted donor PBMCs that were CD3$^+$ and CD1c-SL tetramer$^+$, b) Sorted cells were cultured for two weeks before staining and re-sorting tetramer$^+$ CD3$^+$ T cells. There was a reduction in CD1c tetramer staining cells but an expansion of CD3$^+$ T cells. c) Following re-sorting and culture of sorted cells, cells were stained again but there was a further decline in CD1c-SL tetramer$^+$ cells.

3.2.4 Plate bound anti-γδ T cell assay

In parallel to the above mentioned methods, we sought to specifically expand γδ T cell lines using an unbiased method, in order to investigate whether CD1c-restricted T cells expand within these populations. To investigate whether blood derived Vδ1 T cells could be specifically expanded *in vitro*, a plate bound anti-panγδ TCR antibody assay was utilised. PBMCs from healthy donors were suspended in media supplemented with 5% human AB serum. The PBMCs were seeded at a concentration of 2x10^6/ml in wells of a 6 well plate coated with one of three concentrations of anti-γδ TCR antibody: 0.3μg/ml, 3μg/ml or 30μg/ml. Initial screening of donor PBMCs revealed a

low frequency of Vδ1 T cells at 0.61%, compared to a higher population of Vδ2 T cells at 4.33% (Figure 24). The PBMCs were cultured in the presence of 100U/ml IL-2 for 21 days, and cells were stained with anti-Vδ1 at day 14 and 21 to observe expansion levels. Staining at day 14 revealed a large increase in the frequency of Vδ1 cells for samples cultured with each of the three concentrations of anti-panγδ TCR antibody. Cells cultured in the presence of 0.3μg/ml of antibody revealed the lowest expansion of Vδ1 at 1161%, whereas cells cultured with 30μg/ml showed an expansion of 2556%. At day 21, the frequency of $V\delta1^+$ T cells cultured with 0.3μg/ml and 3μg/ml of anti-panγδ TCR antibody increased by 19% and 13%, respectively. In contrast, there was a 6% decrease in the frequency of $V\delta1^+$ T cells cultured with 30μg/ml antibody (Figure 25). The reduction in expansion and lower frequency may have been due to prolonged time in culture, leading to slowed growth and cell death. These results indicated that stimulation with 30μg/ml of anti-panγδ TCR antibody produced the greatest fold expansion of $V\delta1^+$ T cells but came at the cost of cell death. The cells were also stained with CD1c tetramers at each time point to identify CD1c-restricted T cells. However, minimal staining was observed and was attributed to the use of poor quality tetramers used at the time of this experiment.

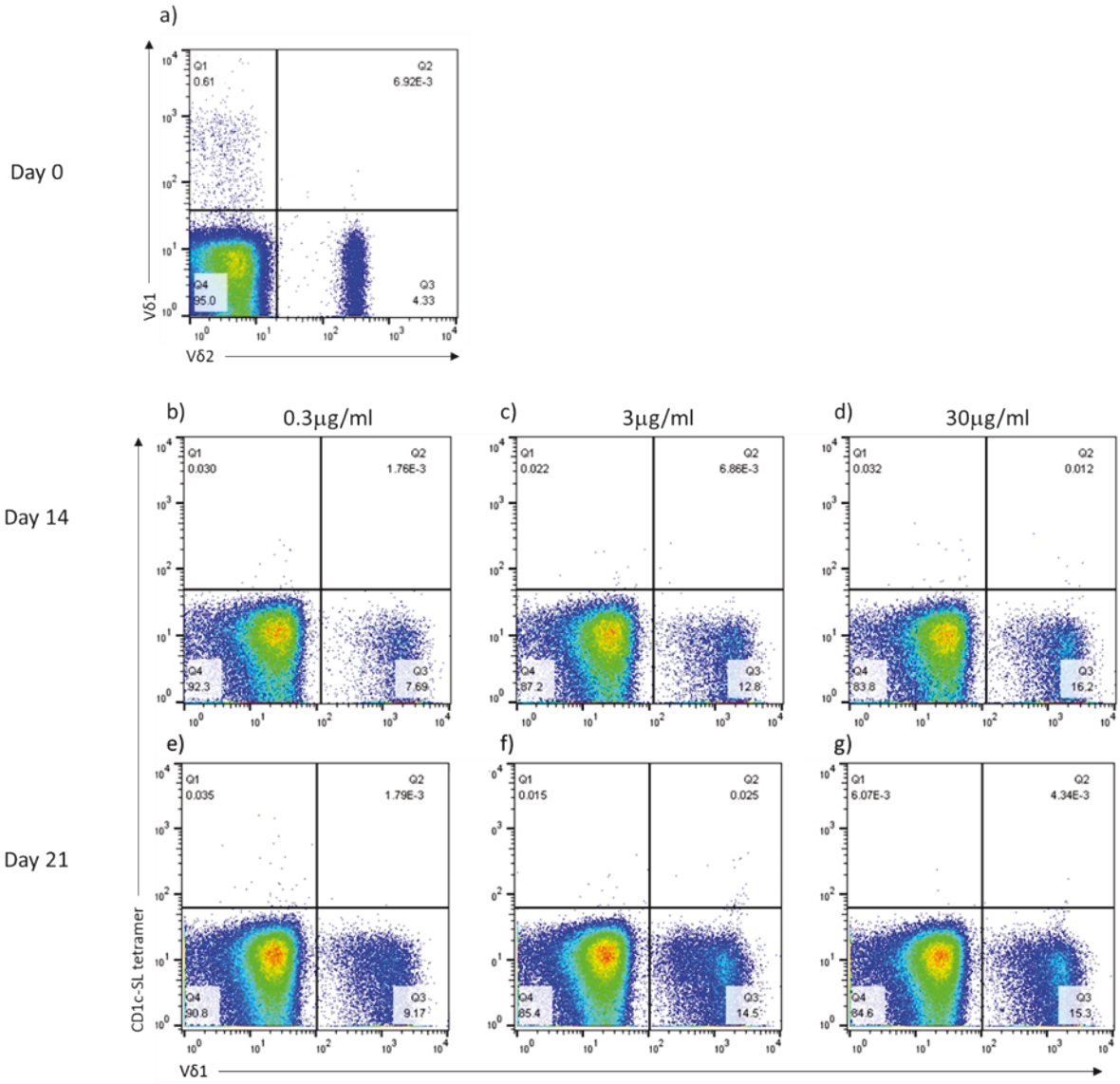

Figure 24: Comparing Vδ1⁺ T cells in response to increasing concentrations of anti-γδ TCR antibody

Flow cytometry dot plots of T cells stained with CD1c-SL tetramer and anti-Vδ1 antibody following incubation with different concentrations of plate bound anti-γδ TCR antibody. a) *Ex vivo* stain of PBMC demonstrating initial frequency of Vδ1⁺ T cells. Vδ2⁺ T cells were also stained, b) day 14 staining of cells cultured with 0.3µg anti-γδ TCR antibody, c) day 14 staining of cells cultured with 3µg anti-γδ TCR antibody, d) day 14 staining of cells cultured with 30µg anti-γδ TCR antibody, e) day 21 staining of cells cultured with 0.3µg anti-γδ TCR antibody, f) day 21 staining of cells cultured with 3µg anti-γδ TCR antibody, g) day 21 staining of cells cultured with 30µg anti-γδ TCR antibody.

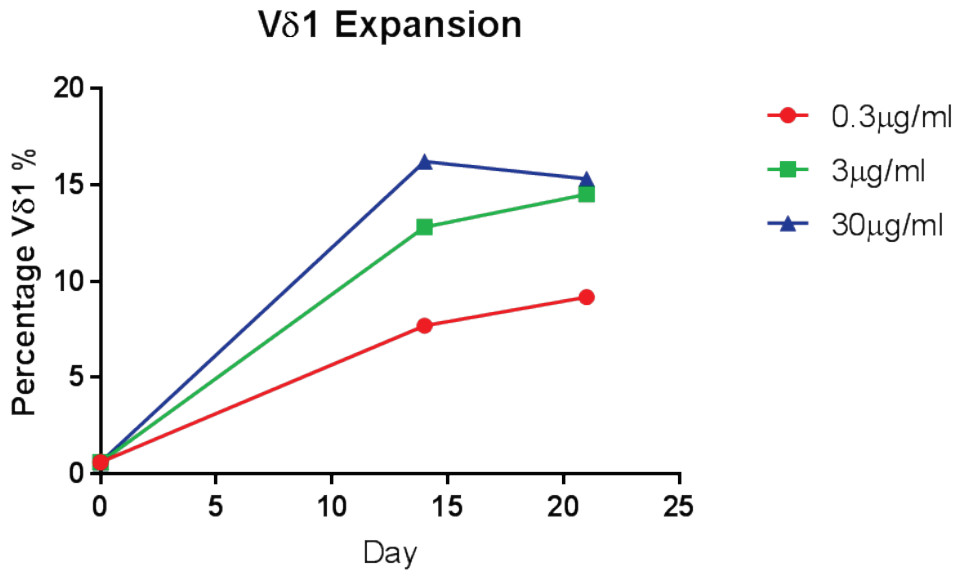

Figure 25: Expansion of Vδ1⁺ T cells between day 0 and day 21

Graph representing the expansion of Vδ1⁺ T cells within the donor PBMC fraction that had been cultured with three different concentrations (0.3µg/ml, 3µg/ml, and 30µg/ml) of anti-panγδ TCR antibody over 21 days.

Vδ1⁺ T cells from further healthy donors were subsequently expanded using the single concentration of 30µg/ml of plate bound antibody. Although rates of expansion varied for each donor, the frequency of Vδ1⁺ T cells within the CD3⁺ subset was observed to increase each week. By day 21, frequencies of Vδ1⁺ T cells had increased to as much as 35% of the CD3⁺ population, demonstrating that this method is ideal for rapidly expanding the Vδ1⁺ T cell subset in a variety of donors. These expanded cell lines were also stained with CD1c tetramers to investigate whether CD1c specific Vδ1⁺ T cells also expanded using this method. Staining with CD1c tetramers on Day 0 (i.e. before plate bound antibody expansion) revealed that some donors have a distinct, albeit small population of Vδ1⁺ cells that recognise CD1c. However, following *in vitro* culture with plate bound antibody, the frequency of Vδ1⁺ T cells staining with the CD1c tetramer declined each week for all donors. PBMCs from one donor were cultured under three different conditions to investigate whether the presence of CD1c influenced expansion of CD1c-restricted Vδ1⁺ T cells: PBMCs cultured with either 30µg/ml plate bound anti-γδ antibody or 10µg CD1c monomer; or PBMCs cultured with both CD1c monomer and anti-γδ antibody. Despite a substantial increase in Vδ1⁺ T cells from donor cells cultured in each of the three conditions, an expansion of CD1c-restricted T cells was not observed and in some cases was completely absent (Figure 26). This indicates that the culture conditions may not be suitable for expanding CD1c specific populations. Interestingly however, following cryopreservation of the expanded cell lines and subsequent resuscitation, a large population of Vδ1⁺ T cells recognising CD1c were observed upon staining

with CD1c tetramers (Figure 27). The distinct population observed in some donors following resuscitation was of a greater frequency than the CD1c tetramer$^+$ Vδ1$^+$ T cells observed at day 0. This suggests that this method may indeed expand this particular subset, but that CD1c-specific TCR downregulation may have occurred during culture.

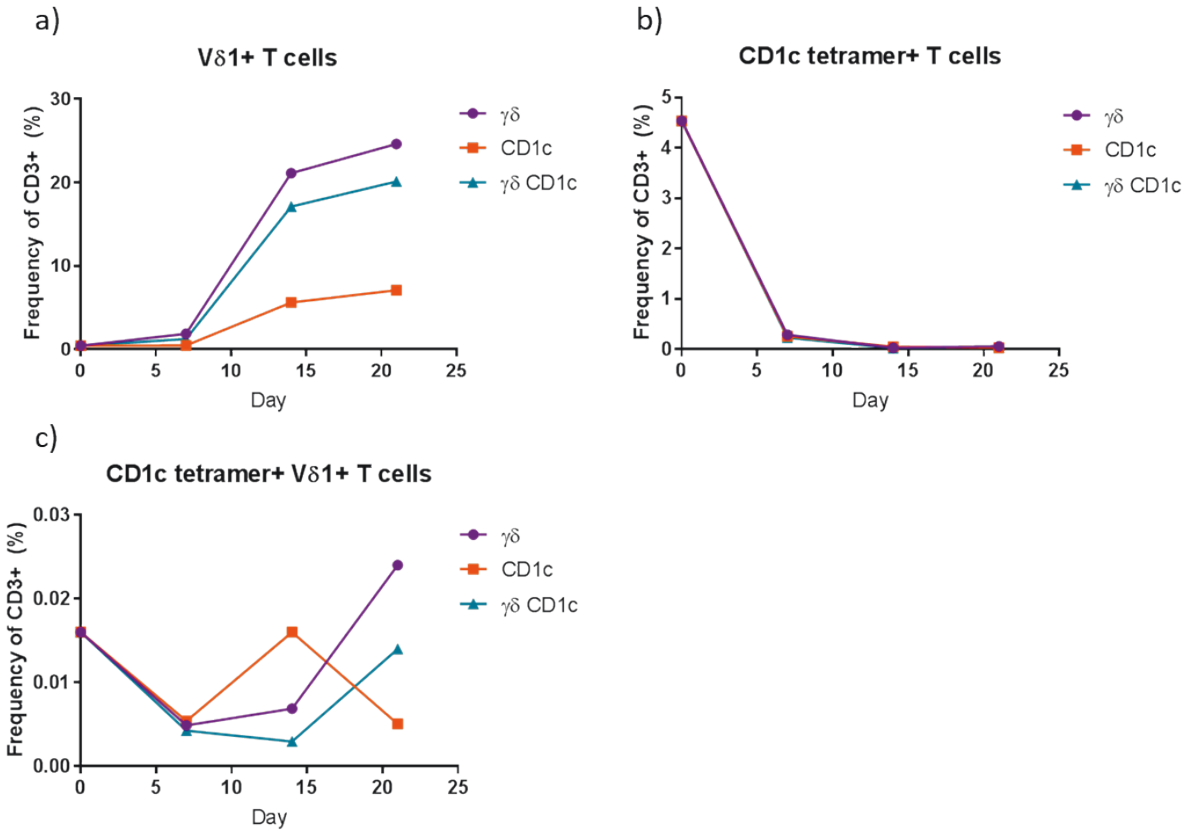

Figure 26: Expansion of T cells cultured with anti-pan γδTCR antibody and/or CD1c-SL monomer
Graphs representing the expansion in T cells following 21 days in culture. a) Expansion of Vδ1$^+$ T cells following incubation with anti-panγδ TCR antibody (γδ), CD1c monomer (CD1c) or anti-panγδ TCR antibody and CD1c monomer (γδ CD1c). b) Expansion of CD1c-SL tetramer$^+$ T cells following culture with γδ, CD1c or γδ CD1c. c) Expansion of CD1c-SL tetramer$^+$ Vδ1$^+$ T cells following culture with γδ, CD1c or γδ CD1c.

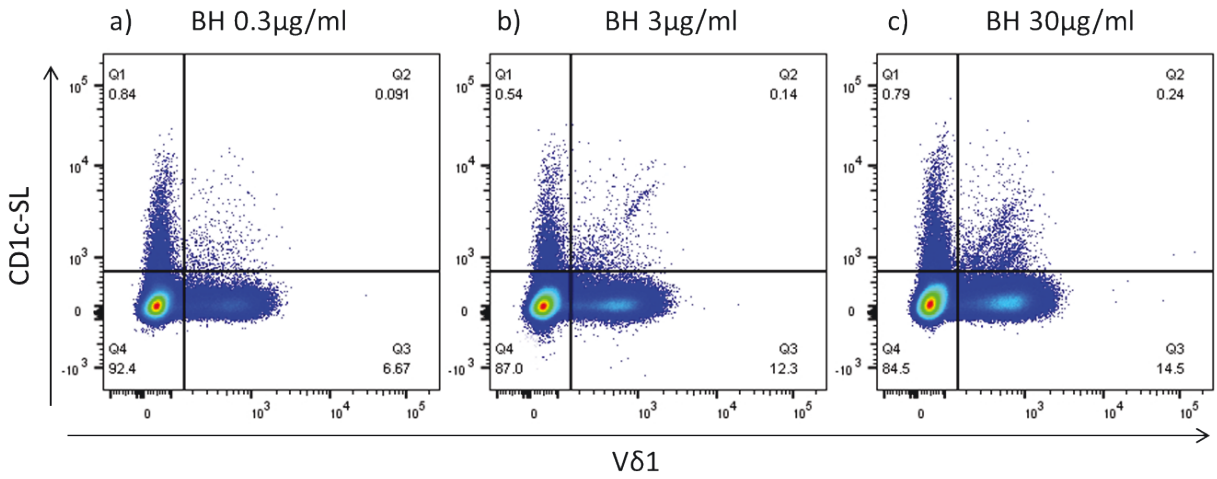

Figure 27: CD1c-SL tetramer staining of resuscitated enriched Vδ1$^+$ T cell lines

Flow cytometry dot plots demonstrating CD1c-SL tetramer and anti-Vδ1$^+$ antibody staining of resuscitated donor cells that had been expanded in culture with plate bound anti-panγδ TCR antibody. a) Cells cultured with 0.3µg/ml anti-panγδ TCR antibody, b) Cells cultured with 3µg/ml anti-panγδ TCR antibody, c) Cells cultured with 30µg/ml anti-panγδ TCR antibody. Data demonstrates the presence of CD1c-SL tetramer$^+$ Vδ1$^+$ T cells within cultures.

3.2.5 Cloning of CD1c tetramer$^+$ TCRs

As the plate bound anti-γδ antibody method appeared to successfully expand convincing CD1c tetramer$^+$ T cell populations, we sought to directly clone the TCRs for further functional and biochemical characterisation. CD1c tetramer$^+$ T cells from the most distinct populations were sorted as single cells by FACS for the specific amplification, separation and sequencing of the γ and δ TCR chains, a method adapted from Melandri *et al* (296). In the first instance, donor cells that were expanded in the first plate bound anti-γδ assay were resuscitated and stained for sorting by flow cytometry. Donor cell lines BH3 and BH30, as well as a γδ T cell enriched population expanded by our group (AL1) and an *ex vivo* PBMC sample from donor Ex.P.1, were stained with two tetramers, CD1c-SL and CD1c-PG, and a cocktail of antibodies including CD3-BV786, αβTCR-APC, γδTCR-PE/Cy7 and Vδ2-FITC. Frequencies of γδTCR$^+$ Vδ2$^-$ cells varied between each donor, but all demonstrated a distinct population of these cells that stained positively with the CD1c-SL tetramer, and/or with the CD1c-PG tetramer. Tetramer$^+$ cells in the Ex.P.1 sample were much more numerous but appeared to be CD3^{lo}γδTCR^{lo}. Single cells that were γδTCR$^+$ Vδ2$^-$ and showed positive staining with either one or both tetramers were sorted into PCR plates containing PBS before freezing at -80°C (Figure 28).

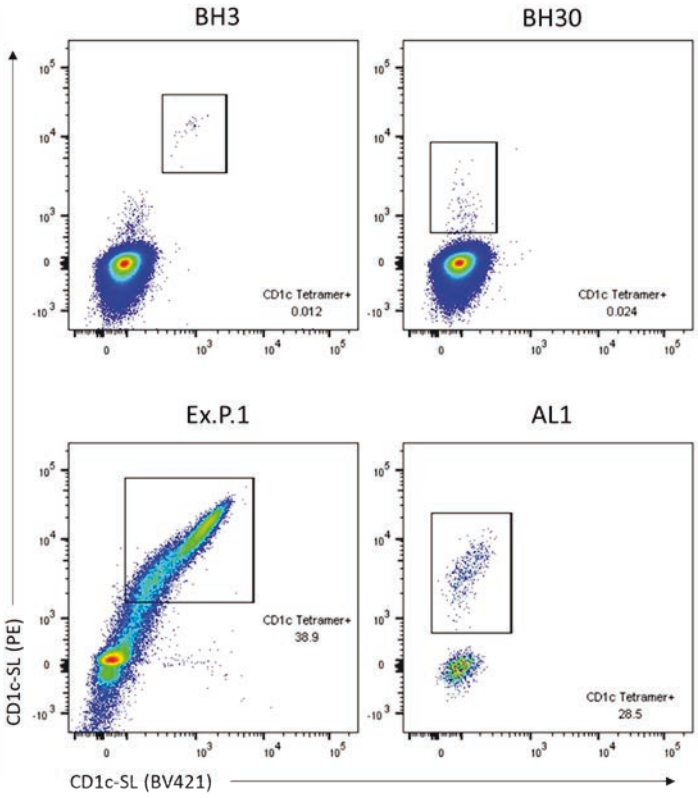

Figure 28: CD1c tetramer guided single cell sorting of Vδ1/Vδ3$^+$ T cells for TCR sequencing
Flow cytometry dot plots representing CD1c-SL (PE) and CD1c-SL (BV421) staining of three γδ enriched T cell lines (BH3, BH30, AL), and one *ex vivo* sample (Ex.P.1). Live lymphocytes were pre-gated and doublets were excluded before gating on αβTCR$^-$ CD3$^+$ T cells and then selecting for γδTCR$^+$ Vδ2$^-$ T cells. CD1c tetramer$^+$ Vδ2$^-$ T cells were sorted as single cells and their individual γ and δ TCR chains were sequenced.

Sorted cells from donors BH3 and Ex.P.1 were thawed and subjected to two rounds of PCR to amplify and separate the γ and δ chains of each T cell clone. PCR products of rows A and B for donor Ex.P.1 and the whole of the plate from donor BH3 of both the individual γ and δ chains were separated by agarose gel electrophoresis (Figure 29). Of the 24 wells analysed for donor Ex.P.1, only two corresponding wells produced bands at the expected molecular weight of 700bp and 550bp for the γ and δ TCR chains, respectively. The majority of the wells from the BH3 γ and δ PCR plates produced bands of the expected molecular weights. Of these, 16 pairs of γ and δ chains were excised from the gel along with the two pairs from donor Ex.P.1, and were sent for Sanger Sequencing. Only one pair of γδ TCR chains from donor Ex.P.1 had a clear read, but the δ chain of the other pair demonstrated the same sequence as the first. Nine γδTCR sequences from donor BH3 had clear sequences and included three Vγ8c2.2Vδ1 TCRs with identical sequences, one Vγ2Vδ3, one Vγ4Vδ3, one Vγ3c2.2Vδ1 and three Vγ4Vδ1 with identical γ chains only. Interestingly, a recurring δ chain was observed in a Vγ4Vδ1 and the Vγ8c2.2Vδ1 sequences.

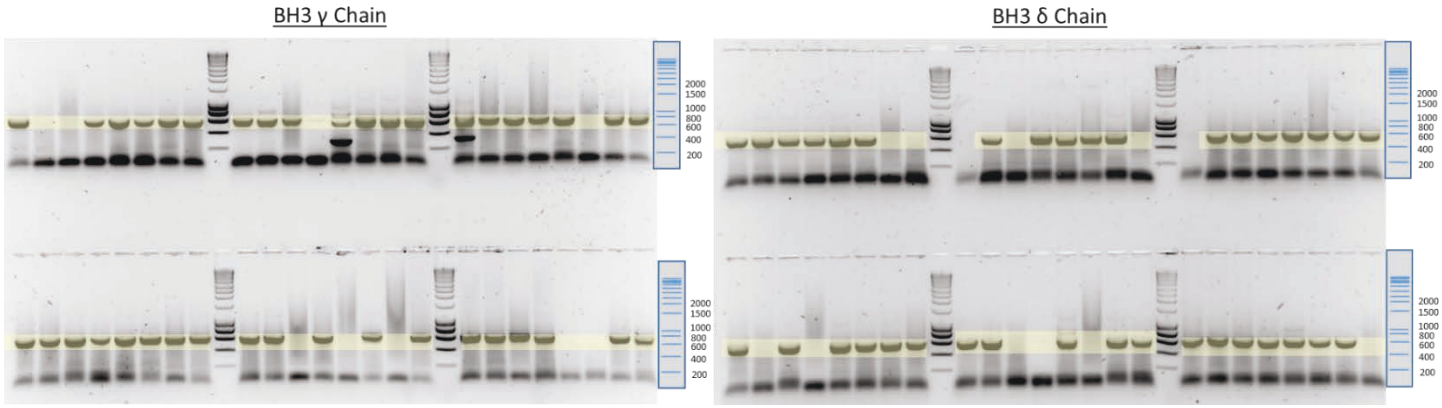

Figure 29: Separation of γ and δ TCR chains of CD1c tetramer^{+} sorted γδ T cells

Representative images of agarose gel electrophoresis separation of γ and δ TCR chains from CD1c tetramer sorted γδ T cells from *ex vivo* and γδ T cell enriched T cell lines. Matched γ and δ chains from 24 wells were analysed following Sanger sequencing. γ and δ TCR bands highlighted in yellow.

3.2.5.1 Synthesis of γδTCR Lentiviral plasmids

Of the sequenced TCR pairs, six were chosen to be transduced into Jurkat T cells to assess their recognition of CD1c (Table 6). This included the three Vγ4Vδ1 pairs and the Vγ8c2.2Vδ1 to investigate whether specificity and affinity for CD1c is dictated by the γ or δ chain. It has previously been reported that for CD1d and CD1b, the δ chain is necessary for specificity and recognition, and in CD1c the γ chain has a fine tuning role in affinity and stabilisation (174, 299, 320). The two Vδ3 TCRs were also chosen as there is little known about recognition of CD1c by γδTCRs with δ3 chain usage.

Table 6: Chain sequences of the γδTCRs chosen for cloning and expression onto Jurkat T cells

T Cell Receptor	γ Chain	δ Chain
TCR1 – Vγ4Vδ1	APQRLLYYDSYTSSVVLESGISPGKYDTYGSTRNNLRLIL RNLIENDSGVYYCATWDGSKKLFGSGTTLVVT	EMIFLIRQGSDEQNAKSGRYSVNFKKAAKSVALTISALQLE DSAKYFCALGTSFLRGIRLASADKLIFGKGTRV
TCR2 – Vγ4Vδ1	APQRLLYYDSYTSSVVLESGISPGKYDTYGSTRNNLRMI LRNLIENDSGVYYCATWDGSKKLFGSGTTLVVT	EMIFLIRQGSDEQNAKSGRYSVNFKKAAKSVALTISALQLE DSAKYFCALGESSLGYWGILADKLIFGKGTRV
TCR3 – Vγ4Vδ1	APQRLLYYDSYTSSVVLESGISPGKYYTYASTRNNLRLIL RNLIENDSGVYYCATWDGSKKLFGSGTTLVVT	EMIFLIRQGSDEQNAKSGRYSVNFKKAAKSVALTISALQLE DSAKYFCALGELLKGDTSVPDKLIFGKGTRV
TCR4 – Vγ8c2.2Vδ1	APQRLLYYDSYNSRVVLESGISREKYHTYASTGKSLKFIL ENLIERDSGVYYCATWDNYKKLFGSGTTLVVT	EMIFLIRQGSDEQNAKSGRYSVNFKKAAKSVALTISALQLE DSAKYFCALGTSFLRGIRLASADKLIFGKGTRV
TCR5 – Vγ4Vδ3	APQRLLYYDSYTSSVVLESGISPGKYDTYGSTRKNLRMI LRNLIENDSGVYYCATCPYYKKLFGSGTTLVVT	SFQFVFYGDNSRSEGADFTQGRFSVKHILTQKAFHLVISPV RTEDSATYYCALPSSKGGFLYTDKLIFGKGTRV
TCR6 – Vγ2Vδ3	APQRLQYYDSYNSKVVLESGVSPGKYYTYASTRNNLRL ILRNLIENDSGVYYCATWDGQFWKLFGSGTTLVVT	SFQFVFYGDNSRSEGADFTQGRFSVKHILTQKAFHLVISPV RTEDSATYYCGVGTGGPFNTDKLIFGKGTRVTVEP
TCR7 – Vγ4Vδ1	APQRLLYYDSYTSSVVLESGISPGKYDTYGSTRKNLRMI LRNLIENDSGVYYCATWDGYKKLFGSGTTLVVT	EMIFLIRQGSDEQNAKSGRYSVNFKKAAKSVALTISALQLE DSAKYFCALGPPLFYVLGYRKLIFGKGTRV

These sequences, along with another Vγ4Vδ1 clone (TCR7) isolated with our collaborators at King's College London using our CD1c dextramers, were attempted to be cloned into a γδTCR backbone gifted to us by collaborators at King's College. The aim was to digest the TCR backbone with restriction enzymes AjuI and BaeI in order to excise and purify the vector backbone (~7.5kb) and IRES (~1.5kb). Forward and reverse oligos of the CDR3 portion of each γ and δ chain (Eurofins Genomics) were then to be 5' phosphorylated using T4 Polynucleotide Kinase before annealing to the digested TCR backbone vector and IRES. The resultant TCR backbone containing the desired CDR3 sequence of the γ and δ pair would then be cloned into the pELNS Lentiviral vector. Unfortunately, there were significant issues with this technique. Digestion of the TCR backbone was not successful with the required restriction enzymes. Some cutting was observed when using XhoI and XbaI but this was inconsistent**.** Due to the inability to remove the vector and IRES from the TCR backbone, this method of cloning was not completed. In order to move ahead with this project, the γδ pairs were synthesised and cloned into the pELNS Lentivector by Genscript for transduction into NFAT-Gluc Jurkat T cells for further investigation.

3.2.5.2 Transduction of γδTCRs into Jurkat T cells

The γδTCR Lentivector DNA was transfected into HEK 293T cells and, following incubation for 2 days, the supernatant of the cell culture was used to transduce into TCR negative NFAT-Gluc Jurkat T cells (J.RT3-T3.5 background) with the neat virus or diluted with two parts culture media. Each of the transduced NFAT-Gluc Jurkat lines were stained with anti-Vδ1 and anti-CD3 antibodies to assess frequency of TCR expression by flow cytometry. Greater TCR expression, as assessed by CD3 and Vδ1 frequency (excluding Vγ4Vδ3 and Vγ2Vδ3), was observed for NFAT-Gluc Jurkat T cells transduced with neat virus compared to 1:2 diluted virus. Approximately one week after transduction, the frequency of TCR expression ranged from 5% for TCR1 to 79% for TCR 3. Cells

that were CD3+ and Vδ1+ (in the case of TCR1-4 and TCR7) were bulk sorted into complete media and expanded in culture to obtain approximately 100% TCR expression (Figure 30 and 31). TCR expression appeared to be stable in the majority of γδTCR Jurkat lines, however it was observed that TCR4 and TCR7 transduced cells were unable to maintain a high level of expression and positive staining with anti-Vδ1 and anti-CD3 antibodies was not observed above ~45%.

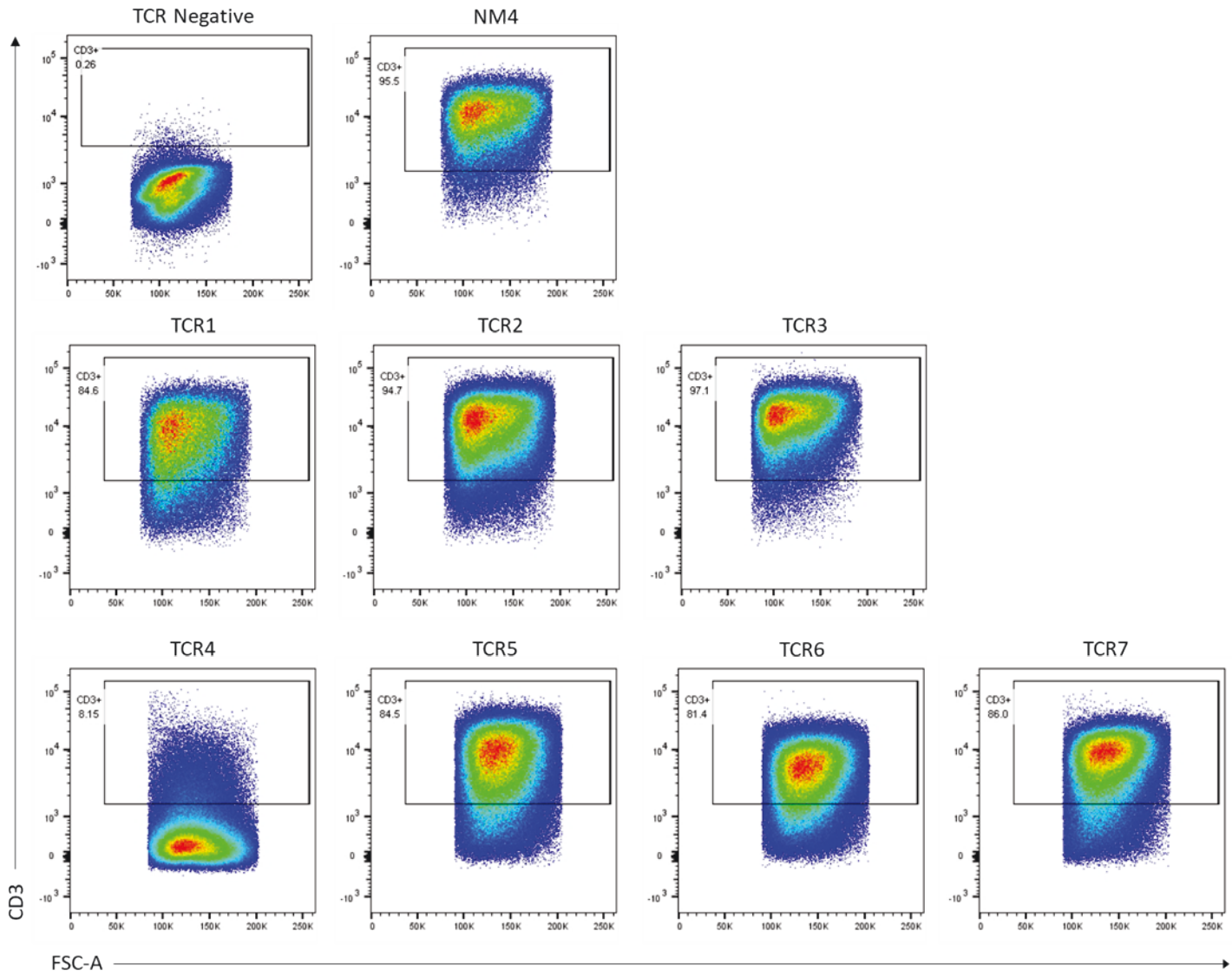

Figure 30: TCR "CD3" expression by γδTCR transduced Jurkat T cells

Flow cytometry dot plots demonstrating $CD3^+$ TCR expression by NFAT-Gluc Jurkat T cells transduced with γδTCRs (TCR1-TCR7). Parental TCR negative NFAT-Gluc and NM4 Jurkat T cells were included as a staining control. The results demonstrate high TCR expression in transduced Jurkat T cells except for TCR4.

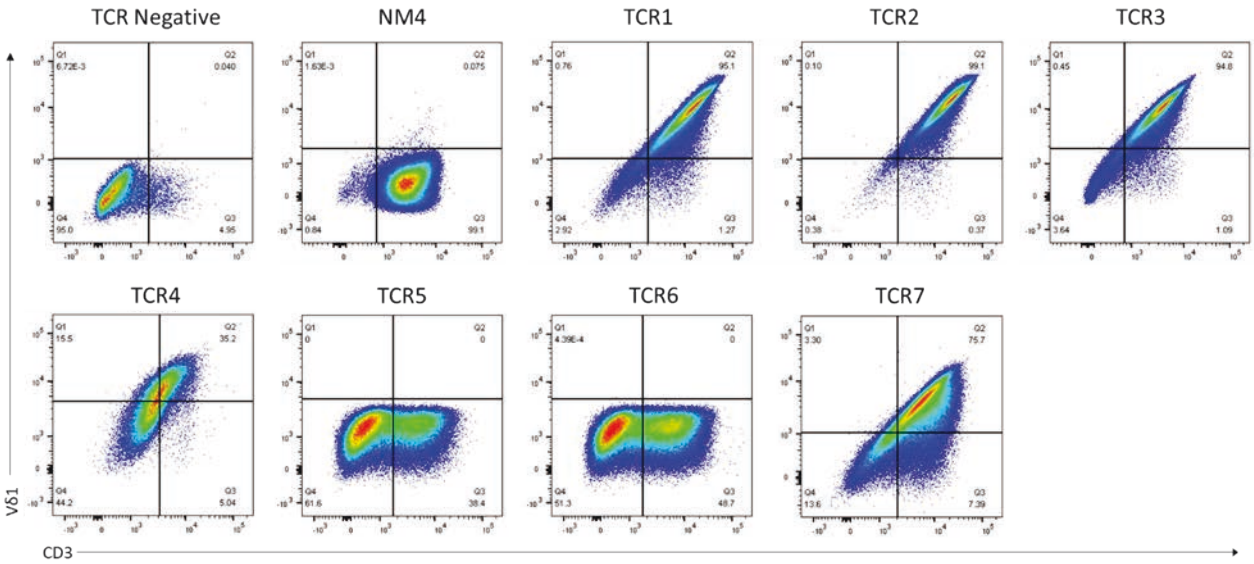

Figure 31: Vδ1 and CD3 expression by γδTCR transduced Jurkat T cells

Flow cytometry dot plots demonstrating TCR expression represented by Vδ1 and CD3 staining by NFAT-Gluc Jurkat T cells transduced with γδTCRs (TCR1-TCR7). Parental TCR negative NFAT-Gluc and NM4 Jurkat T cells were included as a staining control. TCR5 and TCR6 showed negative staining for Vδ1 as these TCRs constitute a Vδ3 chain, while NM4 is an αβ TCR with no Vδ1 chain.

3.2.6 Investigating γδ T cell receptor reactivity

3.2.6.1 CD1c Tetramer assay

To investigate the reactivity of the cloned γδTCRs to CD1c, the transduced NFAT-Gluc Jurkat lines were stained with a CD1c-SL tetramer. The CD1c-restricted αβ TCR, NM4, was also used as a control to ensure functionality of the tetramer. Out of the seven cloned γδTCRs, only TCR4 and TCR7 demonstrated clear staining despite not having 100% TCR expression at the time of this analysis (Figure 32).

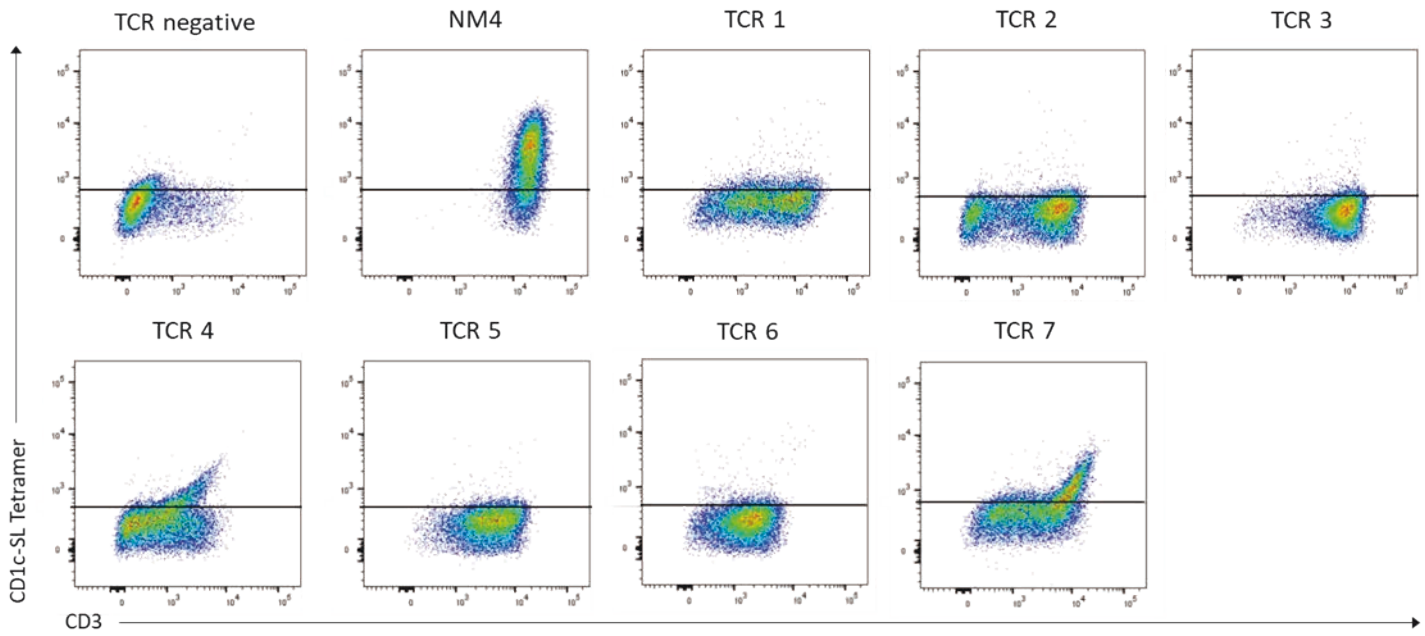

Figure 32: CD1c-SL tetramer staining of γδTCRs

Flow cytometry dot plots depicting CD1c-SL tetramer staining of the seven γδTCR NFAT-Gluc Jurkat T cells, including the parental NFAT-Gluc TCR negative and NM4 Jurkat T cells as controls for tetramer staining. CD1c-SL tetramers bind Jurkat T cells stably expressing the γδTCRs 4 and 7 as well as the αβ TCR NM4.

As the mammalian system is an established method of producing CD1c monomers, we also investigated the reactivity of our cloned γδTCRs to CD1c-endo which has been demonstrated in the literature as a tool to identify autoreactive T cells (268). TCR4 and TCR7 were observed to also have clear staining with the CD1c-endo tetramer, but surprisingly, NM4 Jurkat T cells did not show positive staining (Figure 33). This clearly indicates that while CD1c-SL stained three different human CD1c autoreactive TCR clones, CD1c-endo did not. In addition, in light of these data and studies conducted above, they suggest that the NM4 TCR may have a radically different mechanism of binding to CD1c in comparison to the published autoreactive TCR 3C8, which does indeed positively stain with CD1c-endo tetramers. Finally, we did not observe obvious CD1c tetramer staining of the remaining γδ Jurkat T cells (Figure 33), suggesting that the remaining TCRs may not confer reactivity to CD1c.

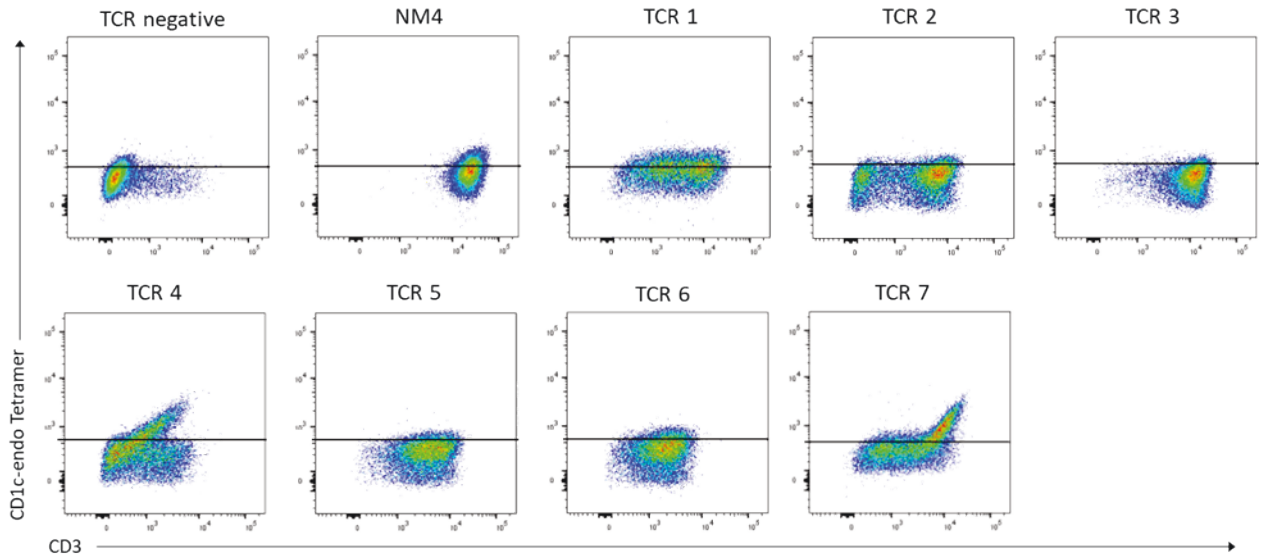

Figure 33: CD1c-endo tetramer staining of γδTCRs

Flow cytometry dot plots depicting CD1c-endo tetramer staining of the seven γδTCR NFAT-Gluc Jurkat T cells, including the parental NFAT-Gluc TCR negative and NM4 transduced Jurkat T cells as controls for tetramer staining. CD1c-endo tetramer bind autoreactive γδTCRs 4 and 7 but not the αβ TCR NM4.

3.2.6.2 Luciferase activity as a measurement of T cell activation

Recognition and subsequent activation of the γδTCR transduced NFAT-Gluc Jurkat T cells by CD1c presenting cells can be monitored by the production and activity of luciferase. The NFAT-Gluc Jurkat cell line is integrated with a firefly luciferase reporter gene which is induced by NFAT activation following engagement of the TCR/CD3 complex by cognate antigen. To investigate whether our cloned γδTCRs are activated by CD1c, we cultured the transduced NFAT-Gluc Jurkat T cells with two antigen negative APC lines, THP1-KO and T2-KO, or the APC lines expressing CD1c (THP1-CD1c and T2-CD1c). Cell culture supernatant was then analysed following cell lysis to measure levels of luciferase by way of luminescence. Initially, all γδTCR lines (TCR1-7) and the parental TCR negative NFAT-Gluc cell line were cultured alone, with THP1-KO, or with THP1-CD1c. All γδTCRs demonstrated a lower level of luminescence when cultured alone than with APCs. Additionally all γδTCRs had a lower level of luminescence following stimulation with THP1-KO than with THP1-CD1c (Figure 34). Issues with the TCR7 Jurkat only condition lead to no activity being recorded for this cell line.

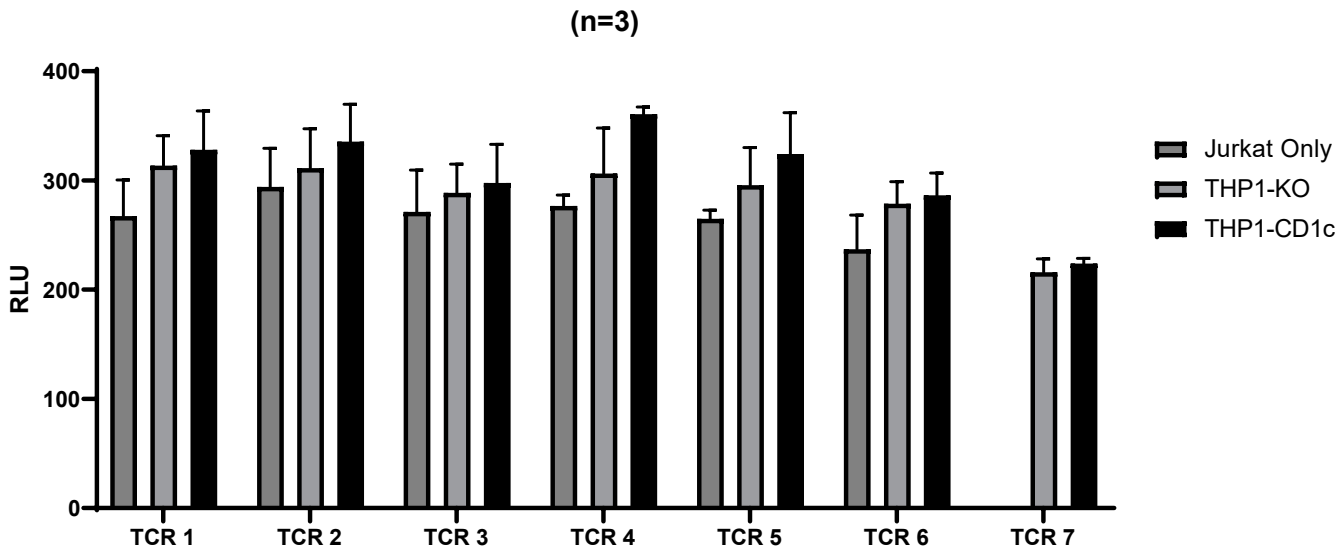

Figure 34: T cell activation via Luciferase activity by THP1 stimulated γδTCR Jurkat T cells
Bars showing the average (n=3) luciferase activity, measured in relative light units (RLU), plotted for each γδTCR transduced NFAT-Gluc Jurkat T cell line following stimulation with THP1-CD1c, THP1-KO or culture alone (Jurkat only).

There was a modest percentage change between Jurkat T cells cultured alone and those cultured with THP1-CD1c. TCR4 demonstrated the greatest increase in luminescence at 30% with the remaining TCR lines demonstrating <25% increase when cultured with THP1-CD1c compared to Jurkat T cells alone (Figure 35). The percentage difference between cells cultured with THP1-KO and THP1-CD1c was observed to be lower. The only cell line to exceed a 10% increase in luminescence with THP1-CD1c compared to THP1-KO was TCR4 with a ~18% increase. Surprisingly, despite TCR7 clearly binding CD1c tetramers, there was only a marginal increase in luminescence when cultured with THP1-CD1c compared to THP1-KO. However, for all TCRs the response in each of the three repeats was modest but consistent.

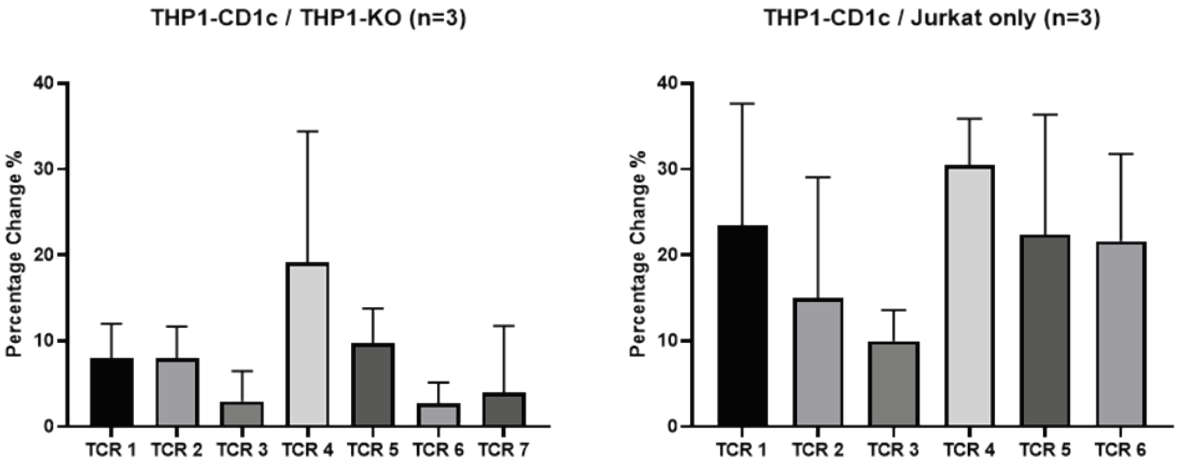

Figure 35: T cell activation as percentage change in luminescence

Graphs depicting the mean percentage change in luminescence for each γδTCR NFAT-Gluc Jurkat T cell line following stimulation with THP1-CD1c and THP1-KO (left), or THP1-CD1c and unstimulated, Jurkat only cultures (right). Graphs represent 3 experimental repeats.

As THP1 cells are known to express other antigen presenting molecules such as HLA-DR, the MHC class II deficient cell line T2 was also used to investigate CD1c recognition by the γδTCRs. In this experiment, only TCR4 and TCR7 were investigated as they were the only cloned γδTCRs to demonstrate recognition of CD1c in the tetramer assay. The CD1c-restricted αβTCR NM4 was also used as a control. When comparing the culture with T2-CD1c relative to T2-KO, all three Jurkat cell lines demonstrated minimal increases in luminescence with NM4 having the greatest increase at 6% (Figure 36). Levels of luminescence were also negligible between γδTCR Jurkat T cells cultured with T2-CD1c compared to those cultured alone without APCs. Despite low signal in some γδTCR lines, consistent activation with the CD1c expressing APCs was observed. The greater changes observed in the cultures with THP1 cells compared to the T cells cultured alone condition may suggest that other molecules expressed on these cells may have contributed to greater levels of luminescence through a co-stimulatory mechanism.

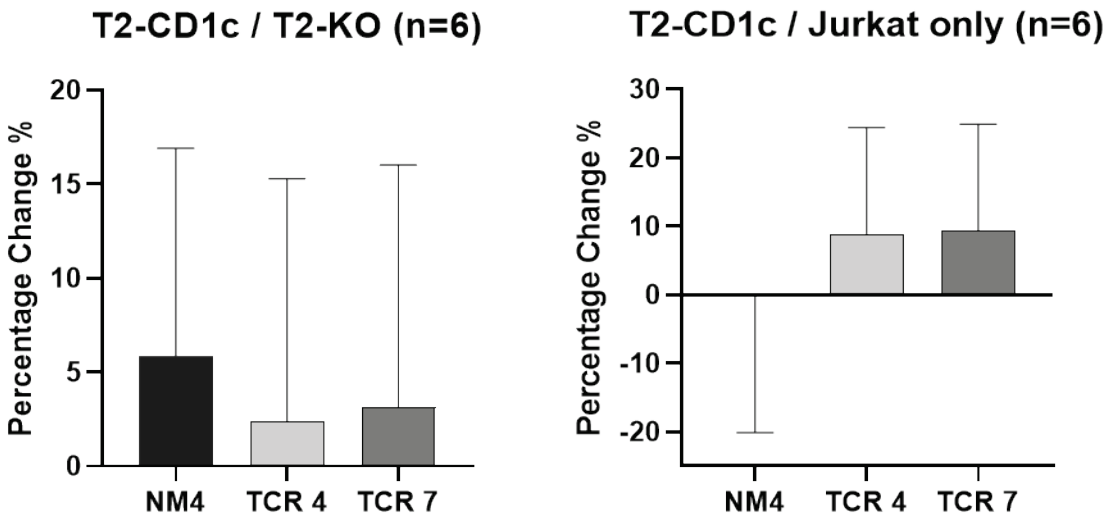

Figure 36: T cell activation as percentage change in luminescence

Graphs depicting the mean percentage change in luminescence for NM4 and γδTCR transduced NFAT-Gluc Jurkat T cell lines TCR4 and TCR7 following stimulation with T2-CD1c relative to T2-KO (left), and T2-CD1c relative to unstimulated, Jurkat only cultures (right). Graphs represent 6 experimental repeats.

3.2.6.3 T cell activation assay via CD69 upregulation and CD3 downregulation

As tetramer studies determined that only TCR4 and TCR7 bound CD1c tetramers, only these TCRs in addition to the CD1c-restricted αβTCR NM4 were included to further analyse CD1c-mediated activation. This variation to the assay was repeated six times. For each of the three Jurkat lines, the average frequency of CD69 expression was found to be greater when in culture with T2-CD1c compared to T2-KO or solitary culture. This was significant for both NM4 and TCR4 but not TCR7. For NM4 and TCR4, CD69 expression was over 150% greater when cultured with T2-CD1c compared to T2-KO, while TCR7 only had a 36% greater expression. Both NM4 and TCR4 had an even greater difference in CD69 expression between the T2-CD1c and Jurkat only culture conditions, showing an average percentage increase in the T2-CD1c culture of 236% and 317%, respectively. In contrast, TCR7 showed a smaller difference in CD69 expression between these two culture conditions, having only a 29% increase in expression in the T2-CD1c culture (Figure 37). Expression of CD3 by each of the γδTCR Jurkat lines was found to be significantly less in the T2-CD1c culture compared to the solitary culture, with TCR4 having the greatest decrease in expression by 70%. This suggests that culture with an APC line induces downregulation of CD3 expression. However, each γδTCR demonstrated a percentage increase in the frequency of CD3

expression of cells cultured with T2-CD1c compared to T2-KO, albeit a small increase of between 17 and 27% (Figure 37).

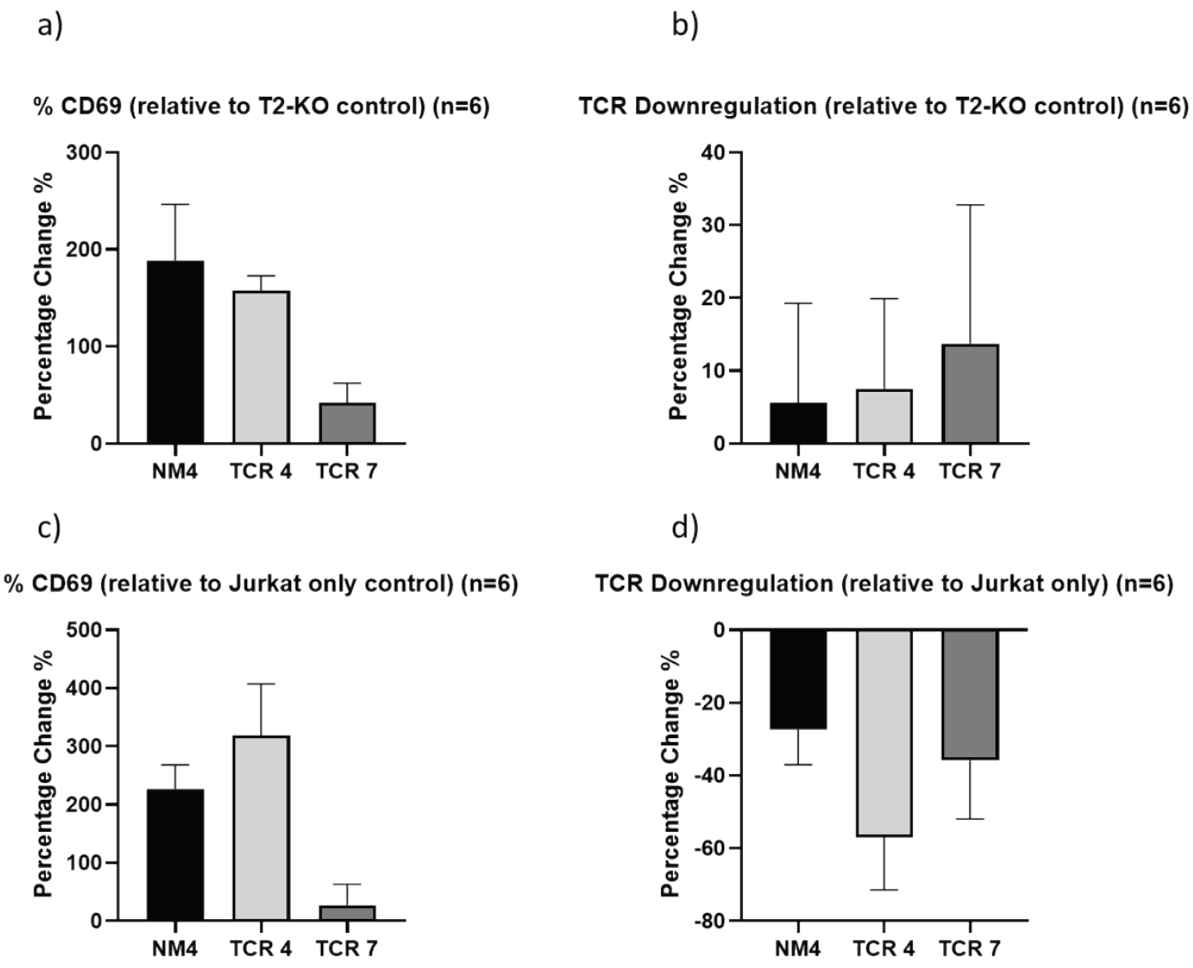

Figure 37: T cell activity as a percentage change in CD69 and CD3 expression

Mean percentage change of 6 experimental repeats in CD69 and CD3 expression by NM4 and γδTCR transduced NFAT-Gluc Jurkat T cell lines TCR4 and TCR7. a) Percentage change in CD69 upregulation by Jurkat T cells stimulated by T2-CD1c relative to control T2-KO cells. b) Percentage change in CD3 downregulation by Jurkat T cells stimulated by T2-CD1c relative to control T2-KO cells. c) Percentage change in CD69 upregulation by Jurkat T cells stimulated with T2-CD1c relative to unstimulated Jurkat T cells. d) Percentage change in CD3 downregulation by Jurkat T cells stimulated by T2-CD1c relative to unstimulated Jurkat T cells.

In conclusion, the combination of these assays assessing CD1c recognition and subsequent activation demonstrate that while some response towards CD1c is demonstrated by all γδTCRs, TCR4 and TCR7 were more consistent across all assays, supporting their reactivity and recognition of CD1c.

3.3 Discussion

3.3.1 Molecular Mechanisms of CD1c Recognition by an autoreactive αβ TCR

3.3.1.1 Understanding the TCR binding footprint

Establishing T cell lines from multiple donors allows for the generation of TCR clones for molecular and functional analysis. The TCRs of sorted single cells from these T cell lines can be sequenced and cloned to determine the mode of binding and recognition of CD1c molecules. The mode of binding is known to vary between different TCRs, as has been demonstrated for numerous TCRs binding CD1b and CD1d (175, 280). Knowing which TCRs are involved in the response to mycobacterial antigens and how the TCR binds to CD1c will enable the development of therapeutics that can utilise the CD1c-restricted T cell system.

We first investigated the binding mechanism of a self-reactive αβTCR clone, known as NM4, to CD1c. It has been reported that CD1c can be "remodelled" by the ligands it binds (231, 267). The formation of an F' roof over the F' channel has been reported, enclosing bound spacer lipids from external solvent (265). This closed position has also been reported by Wun and colleagues, where endogenous lipids bound by CD1c were shielded and the 3C8 TCR (TRAV29-TRBV7-2) docked centrally above this area (268). The position of this F' roof however has been demonstrated to be open when CD1c is bound to mycobacterial lipids PM or MPM, exposing these ligands to solvent (231, 267). This led us to investigate the hypothesis that the F' roof has a vital role in autoreactive TCR interaction.

Mutagenesis of multiple CD1c extracellular residues, four in the F' roof and three in the surrounding areas of the α1-α2 domain highlighted the involvement of these areas in binding to our NM4 TCR. Three of the four F' roof mutants tested, Y155A, E83A, and H87A, contributed to a clear reduction of TCR binding by the CD1c tetramers, adding weight to our hypothesis that the F' roof is crucial in binding to the TCR. The remaining F' roof mutant, L150A, was observed to have a similar staining profile to that of WT CD1c tetramers but with a slight reduction in binding at greater concentrations of tetramer. Alanine scanning of both Y155 and E83 has previously been examined by Wun *et al* and Roy *et al* for their binding to different CD1c-restricted TCRs. Although docking mechanisms for each of the TCRs in these studies varied, the importance of these two residues were highlighted as binding of the TCR and subsequent activation was reduced following mutation to alanine (267, 268). Another of our chosen mutants, L150, was also examined by both these groups, but the importance of this residue in binding was not consistent across the different TCRs investigated (267, 268). However, these data taken together with our observation of

minimally reduced binding of CD1c with L150A mutation to our NM4 TCR further highlights that docking mechanisms differ between TCRs.

Our CD1c mutants R82Q and N55T also led to a reduction in binding of the CD1c tetramers to the NM4 TCR, indicating that a larger area of the α1 helix may be involved in TCR contact and that the loop connecting this helix to the β-sheet may be involved in flexibility or lipid loading of the molecule. Although staining intensity of these mutant CD1c tetramers was minimal, binding was not completely abolished. This suggests that although important for recognition, these residues are not absolute determinants for TCR binding. In comparison, mutant H153R, located on the α2 helix, demonstrated increased levels of binding compared to WT CD1c. Arginine is frequently found at contact points between proteins as its hydrophilic nature allows for the formation of hydrogen bonds and salt bridges (430). This then may have led to improved binding capabilities of CD1c to the NM4 TCR following mutation from histidine which is known to be functionally sensitive to pH (431). To build upon our findings, we plan to generate further CD1c alanine mutants to create a more comprehensive picture of the NM4 TCR binding footprint on CD1c.

The mutant and WT CD1c tetramers tested here were refolded in the absence of specific lipids. CD1c in complex with spacer lipids (CD1c-SL) has been demonstrated to have a closed F' roof and is able bind the NM4 TCR, thus we hypothesised that NM4 is autoreactive to CD1c itself and the F' roof may be an important structure in the binding footprint of the TCR. Wun *et al* also demonstrated an augmentation in T cell activation following culture of their CD1c autoreactive TCR 3C8 with CD1c expressing APC that had F' roof mutations (268). However, Roy *et al* also demonstrated the importance of the aforementioned F' roof mutants when CD1c was loaded with mycobacterial PM (267). Although the importance of these mutants varied between different TCRs, this study highlights that the F' roof positioning, which has been revealed to be open when CD1c is binding PM, may not be a key area in TCR docking. To further investigate the importance of the F' roof in NM4 recognition of CD1c, we need to first optimise the loading of CD1c with specific lipids and then subsequently analyse how these lipids affect recognition of both WT CD1c, and our generated CD1c mutants.

In addition to analysing recognition of CD1c by our NM4 TCR using tetramer studies, we also carried out SPR to analyse binding affinity. Compared to WT CD1c, we observed similar binding affinities of each of the CD1c mutants to the NM4 TCR. Despite the lack of correlation with our tetramer studies, the binding affinity of NM4 to CD1c was seemingly high for an autoreactive TCR (137, 432). The binding affinity of the autoreactive TCR 3C8 to WT CD1c was reported to have a K_D of 40μM, a much weaker interaction than the 5.8μM observed for our NM4 TCR (268). It has been reported that autoreactive TCRs with a high binding affinity have a K_D in the range of 1-50μM, a

value which would normally be considered low affinity when analysing binding of TCRs to microbial antigens (432). However, despite NM4 binding to CD1c with relatively high affinity, SPR did not indicate that mutations to CD1c had any discernible effect on TCR docking.

The lack of corroboration between the tetramer studies and SPR analysis does not enable us to draw solid conclusions from these results. While CD1 tetramers are commonly used to detect and sort CD1-restricted T cell populations by flow cytometry, a number of factors affect their functionality and ability to provide a convincing representation of the target population. Temperature, concentration and light exposure are known to affect functionality of tetramers following their generation and during usage, but also the length of storage can lead to degradation which varies between proteins (287). Furthermore, as autoreactive TCRs generally have lower affinity for cognate antigen than TCRs specific for exogenous ligands, detection by flow cytometry can be more challenging (287). SPR is a more robust technique which can sensitively detect complexes formed with weak affinities and is less affected by concentration than tetramer staining. Greater differences observed between mutant CD1c proteins in tetramer studies may have been due to tetramer degradation, temperature changes, light fluctuations, protein aggregation and poor signal detection due to low affinity. Taken together, due to the contradictory results generated from these studies, we cannot confidently conclude that CD1c mutations affected recognition by the NM4 TCR. However, we can further probe the binding footprint of this TCR by generating more CD1c mutants involving amino acids in other areas of the protein such as the A' roof. The effects of these mutations on recognition of CD1c by the NM4 TCR can be further analysed by carrying out additional studies such as activation markers assays, cytokine release and crystallography.

3.3.1.2 Investigating the impact of CD1c on T cell activity

The successful recognition and binding of CD1c-lipid complexes by the cognate TCR leads to activation of the T cell. This can be measured by numerous methods, including the detection of cytokine secretion, CD3 downregulation, and CD69 upregulation. To establish a baseline level of activation for WT CD1c, we optimised an activation assay involving the culture of T2 cells expressing CD1c and NM4 TCR expressing Jurkat T cells in preparation for future investigations of CD1c mediated TCR activation. The expected outcome of this experiment was that CD69 expression would increase for Jurkat T cells that were cultured with increasing concentrations of CD1c expressing T2 cells, and that this would occur simultaneously with a downregulation in CD3 expression.

CD69 is known to be an early marker of T cell activation, with expression inducible within just 30 minutes of stimulation and peak expression observed between 18 and 48 hours (433, 434). This is

in keeping with our observation that the greatest fold change in CD69 expression between cells cultured with T2-CD1c and T2-negative cells occurred when both Jurkat lines were incubated in culture for 24 hours. The greatest fold change in CD69 expression by the Jurkat T cells was found to be approximately 5.2 when cultured with $2x10^5$ T2 cells for 16 hours. In a study by Guo *et al* which investigated the effect of CD1c APCs on the expression of CD69 by 84 clonotypic TCRs, only 9 of these TCR clones had a comparable level of fold change in CD69 expression to our NM4 TCR, with clones having a fold change above 4.5 being grouped together as the greatest responders to antigen (337). The J76 clone 110 (C110) Jurkat T cells in this study were cultured with CD1c expressing K562 cells for just 6 hours, and approximately half of the TCR transfectants produced a CD69 fold change ratio of at least 1.5. The shorter culture durations producing high levels of activation seen in the study by Guo and colleagues may be due to the cell lines used. K562 cells are known to express the surface adhesion molecules CD54 and CD58 (435) which may lead to increased binding and the subsequent activation of T cells. As well as activating the C110 Jurkat T cells, the K562 cells expressing CD1c were also shown to successfully activate primary $CD4^+$ T cells, but this was measured by upregulation of CD154 (337). Cultures of Jurkat T cells and $CD1c^+$ antigen presenting cells have also been used to evaluate the effect of mutations in CD1c on the level of activation of the responding T cells. Wun and colleagues transduced another self-reactive, CD1c-restricted TCR into J76 Jurkat T cells, known as 3C8 (TRAV29, TRBV7-2) and evaluated the percentage of CD69 expression when in culture with C1R cells expressing WT CD1c compared to those in culture with mutated CD1c (268). The cells were cultured in a 1:1 ratio and found that there were pronounced changes in levels of CD69 expression in comparison to CD1c WT, whereas we observed similar levels of CD69 expression with each concentration of T2 cells (268).

Additionally, our measurements of CD69 expression seemingly coincided with levels of CD3 downregulation, with this association appearing stronger with longer duration of cultures. As downregulation of CD3 is known to be tightly linked with TCR engagement and the subsequent activation of the T cell (436), this indicates that the NM4 TCR did indeed bind CD1c as we observed a downregulation of CD3 expression by as much as 25%. As Jurkat T cells have background expression of CD69, it may be advantageous to measure activation by additional means. T2 lymphoblasts expressing CD1c have been used previously to measure the activation of Jurkat T cells through cytokine secretion. For example, in the Guo study, T2 cells were used as CD1c presenting cells and the activation of T cells was measured by the secretion of IL-2 and TNFα (337). Mansour and colleagues also used T2-CD1c cells in a 1:1, 24 hour culture with NM4 Jurkat T cells, but again the level of activation was measured by cytokine release, including TNFα and IL-10 (265). The use of NFAT-Gluc Jurkat T cells in our work also has the additional benefit over the WT T3.5 cell line of carrying the firefly luciferase reporter gene, allowing response to CD1c to be

measured in terms of luminescence. This feature will be exploited in future experiments investigating antigen-mediated activation of T cells through TCR engagement.

Activation of NM4 TCR expressing NFAT-Gluc Jurkat T cells was also analysed using a plate bound protein method. NFAT-Gluc Jurkat T cells were cultured in 96 well plates that had been coated with the extracellular portion of CD1c. The activation response was then measured by flow cytometric analysis of CD69 and CD3 expression. Minimal changes were observed in CD69 expression between NFAT-Gluc Jurkat T cells cultured with plate bound CD1c or the negative control, which is in contrast to the findings of Guo *et al.* This group demonstrated an increase in positive CD69 staining to 75% when Jurkat T cells were cultured with plate bound CD1c (5µg/ml) compared to the negative control (337). Our findings from this assay are also in contrast with the results of our T2-Jurkat culture which demonstrated a downregulation of CD3 in response to CD1c expressing cells.

The lack of response to the plate bound protein may have arisen due to a variety of factors. Firstly, successful binding of the CD1c monomers to the plate was not confirmed so we cannot be sure as to whether there was any protein available to bind to the Jurkat T cells following washing of the plate. If repeated, successful binding could be confirmed through an ELISA. If protein had coated the plate successfully, we would have expected to observe some level of activation. Our NM4 clone is a CD1c autoreactive TCR and its binding to CD1c without the presence of specific lipid has been confirmed through tetramer and activation studies. Another CD1c autoreactive TCR, 3C8 has been demonstrated to upregulate expression of CD69 in the presence of CD1c but in the absence of exogenous lipid antigens (268). As with our NM4 TCR, 3C8 also binds CD1c with sequestered lipids and a closed F' roof (265, 268). In addition to our findings of CD69 upregulation and CD3 downregulation in the presence of T2 cells expressing CD1c, this suggests that there was a lack of available CD1c in the plate bound assay for sufficient activation of the NM4 TCR. Therefore it would perhaps be useful in future to repeat this experiment with smaller increments in concentration of plate bound CD1c and to confirm successful coating of the plate using an ELISA. Following optimisation, this experiment could then be used to investigate the effect of mutations to CD1c on the recognition by the NM4 TCR and subsequent T cell activation.

3.3.2 Understanding lipid reactivity of the NM4 TCR

CD1c autoreactive T cells are abundant in the peripheral blood of healthy humans (304) but the self-lipid reactivity of these T cells has yet to be understood. We sought to characterise the lipid reactivity of our previously isolated CD1c autoreactive TCR clone, NM4, to further understand the mechanism of CD1c recognition. Refolded CD1c-SL monomers were loaded separately with a

range of phospholipids, SM and a ganglioside (GD1a) and tetramerised to compare binding of the NM4 TCR by flow cytometry. We observed clear staining of NM4 with CD1c-SL tetramers incubated with only citrate buffer (pH 6.5), but a greatly decreased level of staining when CD1c-SL was incubated with 0.5% CHAPS citrate buffer. Precise concentrations of CHAPS have previously been shown to be a requirement of successful lipid loading into CD1 molecules, with higher concentrations observed to be comparably ineffective to the absence of the detergent (437). Upon addition of specific lipids to the 0.5% CHAPS citrate buffer, we observed clear staining of the NM4 TCR with lipid loaded CD1c tetramers. CD1c tetramers loaded with phospholipids PG (16:0-18:1), PC (18:1 Δ9 cis) and Liver PI were observed to have the greatest staining of the NM4 TCR, followed by SM and GD1a. This demonstrates extreme promiscuity of NM4 as each of the classes of lipid vary by their lipid tail, neck region and head group size and constitution.

The ability of NM4 to recognise CD1c loaded with various self-lipids indicates that this TCR has a different binding mechanism to that of the published CD1c autoreactive TCR, 3C8, which displayed a lack of recognition when CD1c was loaded with SM or PC and was only able to form a ternary complex with small head group lipids such as fatty acids (268). Another CD1c autoreactive T cell line described by this group, HD1, which was also derived by CD1c-endo tetramer sorting, was revealed to only recognise CD1c loaded with small head group lipids such as MAG and C16 fatty acids but did not recognise CD1c loaded with PC or SM (268). For this particular CD1c autoreactive T cell line, PC and SM acted as non-permissive ligands but are strongly recognised by our NM4 TCR, further highlighting the differences in TCR binding and recognition mechanisms of CD1c. Interestingly, although mass spectrometry analysis of CD1c-endo revealed bound lipids including C16, C18 and C18:1 fatty acids, MAG, SM and PC, the absence of recognition of SM and PC by the HD1 and 3C8 indicates that while CD1c-endo carries a mixture of lipids, only a fraction of these are permissive for TCR recognition (268). Analysis of CD1b-endo by Shahine *et al* also demonstrated a variety of lipids bound within this complex including phosphatidic acid (PA), phosphatidylserine (PS), PI, PC, PE, and SM (280). Corroborating the differential lipid recognition observed between our CD1c autoreactive TCR and those described by Wun *et al*, Shahine and colleagues observed different patterns of recognition by CD1b autoreactive TCRs derived by CD1b-endo tetramer sorting. While the CD1b autoreactive TCRs showed functional response to CD1b-endo in the absence of exogenous lipid, two TCRs demonstrated cross-reactive recognition of many phospholipids and sphingolipids, three TCRs recognised different classes of phospholipids but were not cross-reactive to any sphingomyelins, and two further TCRs only recognised phospholipids with small headgroups such as PG or LPA (280). These phospholipid specific TCRs may have been derived through recognition of the lipids bound by CD1b-endo. This is in contrast to our NM4 TCR that was previously cloned using CD1c-SL tetramers. CD1c-SL has been revealed

to sequester a C18 stearic acid in the A' channel and two C12 lipids in F' channel, presumed to be lauric acids (265). This may indicate that in contrast to most of the TCRs described by the Shahine and Wun groups, NM4 may be recognising CD1c itself with binding augmented by various classes of loaded self-lipids. In conclusion, this work further highlights that the role of individual lipids and their relationship to the TCR is complex.

We also aimed to investigate whether recognition of CD1c by the NM4 TCR was augmented by differences in the lipid tail. We chose to initially investigate PG as this lipid is abundantly expressed by *M.tb* but is only available in host cells under conditions of stress, such as during microbial infection. It has previously been observed that CD1b autoreactive T cells that recognise PG do not discriminate between mammalian and bacterial PG and display dual recognition of PG from self and foreign origin (301). Van Rhijn and colleagues have also previously demonstrated that T cell responses to mycobacterial MA differ according to modifications of the lipid tail (437). Three MA specific, CD1b-restricted TCR clones demonstrated differential recognition of three different, natural forms (α, keto and methoxy) of C80 MA as well as a synthetic C83 MA (437), demonstrating that lipid tail conformation has a role in lipid-specific TCR recognition. Our group has also previously performed an in depth investigation into how structural changes in meromycolate chains of MA affect the ability of the GEM18 TCR to recognise CD1b (275). The response of this TCR to a panel of 12 synthetic mycolates revealed through activation assays that the fine specificity of the lipid backbone directly impacts TCR recognition (275).

With this in mind, we analysed CD1c tetramers loaded with five analogues of PG, varying in chain length and saturation. We observed greater staining of NM4 with CD1c tetramers loaded with fully saturated lipid tails, of either C16 or C18 in length. Comparable, but slightly weaker staining was observed with CD1c tetramers loaded with PG with one unsaturated bond, indicating that although still permissible, fully saturated chains are preferable by NM4. However, we consistently observed minimal staining with CD1c tetramers comprising PG 18:1 (Δ9 cis). As we observed binding with PG comprising an unsaturated double bond, it may suggest that the cis conformation at position 9 may have an effect on the conformation of CD1c which may not be desirable for binding by NM4. However, we had previously observed tetramer staining of CD1c loaded with PC 18:1 (Δ9 cis) which may suggest that the head group of the phospholipid may have more involvement in TCR recognition of CD1c than we expected. While NM4 has been revealed to recognise a broad range of lipids, the fine specificity of recognition needs to be further elucidated. Shahine and colleagues observed that while three of their cloned CD1b-restricted TCRs recognised a range of self-phospholipids including PC, they were not cross-reactive to SM which has the same head group of PC but differs in the phosphoglycerol neck region (280). These data suggests

binding of some highly specific autoreactive TCRs such as NM4 may still have precise requirements for permissive binding.

Here we have demonstrated that while tetramer studies indicate that mutations to CD1c augment recognition by the NM4 TCR, SPR does not corroborate these results. This may indicate that the chosen mutations are not involved in the TCR binding footprint but may instead have affected conformation of CD1c. Furthermore, while FPLC is a useful tool to purify proteins, it is also possible that the collected CD1c protein fractions may not be of homogeneous quality, thus affecting tetramer production and function. Further work is required to understand how the NM4 TCR binds to CD1c, which will include producing additional CD1c mutants and analysing the subsequent effect on TCR recognition by tetramer studies, SPR and activation assays. We will also further investigate the lipid reactivity of NM4 and dual recognition of self and mycobacterial antigens by loading CD1c with additional phospholipid analogues as well as synthetic mycobacterial lipids. The functional response of NM4 to lipid CD1c can then also be analysed by expression of activation markers and cytokine release.

3.3.3 Establishing CD1c-restricted T Cell Lines

It has been known since the 1990s that CD1 molecules present mycobacterial lipid antigens to T cells (139). In addition, it has been demonstrated more recently that the CD1c isoform may play a role during active TB infection (304, 306, 307, 311-313). Mycobacterial lipids including PM and polyisoprenoids have been shown to be recognised by lipid specific CD1c-restricted T cells (313, 438, 439), as well as lipids that are shared by both *M.tb* and the host such as PI (266). Hence, we wanted to employ our CD1c-lipid tetramers to isolate and clone TCRs to characterise their recognition of human CD1c. Furthermore, we sought to validate our CD1c-SL tetramer as a tool that could identify autoreactive αβ and γδ T cells in healthy humans and in the context of *M.tb*.

3.3.3.1 DC-T cell co-culture

T cell lines have proved useful during the investigation of antigen immunogenicity and TCR specificity, and have also been used in the demonstration of CD1 molecules presenting mycobacterial lipids to CD1-restricted T cells. Phospholipids have been characterised as being presented by both CD1b and CD1c (280, 297, 440), and extreme binding promiscuity of different TCRs to CD1b presenting various phospholipids has been reported (280). It is unknown whether CD1c has a binding preference of ‘rare’ lipids such as PG over the more common PC and PE, or whether binding to CD1c-phospholipid complexes has similarities to that of CD1b. With the ultimate aim of deriving new TCR clones, we first investigated the binding of T cells to different CD1c-lipid complexes, cultured in the presence of lipid pulsed APCs.

The frequency of CD1c-lipid specific T cells cultured with MoDCs that had been pulsed with three lipids, PC, PG and PE, were assessed using CD1c tetramers in complex with each of the three different lipids. PG and PE both contain neutral head groups and are highly expressed in bacterial membranes. On the other hand, in humans PG is considered a 'rare' antigen as it is predominantly found in mitochondrial membranes and is thought to only be released under conditions of stress (297, 301, 441, 442). Due to this, there may have been a lack of PG release and therefore a low frequency of CD1c-PG reactive T cells from the lack of cognate antigen. In contrast to PG and PE, PC has a polar head group and is abundant within human cell membranes, which may indicate that the large frequency of cells staining with the CD1c-PC tetramer were self-reactive T cells. Our data also suggested that the culture of T cells with immature DCs lead to an increased frequency of cells that stained positively with the CD1c tetramers. This could suggest that immature DC influenced the expansion of CD1c-reactive T cells, perhaps due to increased expression of CD1c on the DC in this particular stage of maturation (341, 443). However, to confirm this, both the immature and mature DC's should have been stained with an anti-CD1c antibody to assess levels of expression.

During this experiment, substantial staining with the CD1c-PC and PG tetramers was noted, but the frequency of CD1c-PE tetramer staining was comparable to the negative control. This indicated poor functionality of the tetramer which was later confirmed when tested against a freshly made CD1c-PE tetramer. This highlights the importance of frequently assessing tetramer staining as they are a crucial tool when analysing and sorting CD1c-lipid specific T cells for further experimentation. Multiple issues can occur prior to and during the generation of tetramers including protein aggregation, photobleaching of the conjugated fluorophores and unsuccessful incorporation of specific ligands (444). With this in mind, it would be important to identify whether the CD1c monomers were refolded correctly with the specific lipid of choice following conformation of protein refolding by SDS-PAGE. Comparison of CD1c-PC tetramer staining with that of CD1c-SL tetramers suggests that PC may not have been successfully incorporated into the molecule, indicating that the TCR is interacting solely with CD1c. Pulsing CD1c-SL monomers with lipid prior to tetramerisation may improve the incorporation of the lipid into the CD1c molecule (268). This could subsequently alter the staining profile when compared to CD1c-SL without lipid pulsing. The binding of lipids by CD1c can also be detected by mass spectrometry (440). This would provide more conclusive evidence of the lipids incorporated within the refolded CD1c monomers and therefore allow us to conclude lipid-specificity of tetramer-isolated T cells.

3.3.3.2 *Ex vivo* sorting

CD1 molecules in complex with self-lipids have been used to isolate self-reactive T cells into established T cell lines (268, 297). While this has predominantly been undertaken in samples from healthy donors, this technique can be utilised to reveal the TCR repertoire in TB patients. The majority of research into the role of CD1 in TB focuses on T cells with an αβ TCR, but γδ T cells have also been suggested as playing a role in the immune response against *M.tb* infection (68, 106, 196). T cells expressing a Vδ1 TCRδ chain have been demonstrated to have prominent recognition of CD1c, yet are the least studied subtype of γδ T cells (173-175). Their production of Th1 cytokines such as TNFα and IFNγ (202), as well as the observation that Vδ1 are increased in active TB patients exhibiting anergy (173) makes them an interesting candidate as a key player in *M.tb* immune response. Furthermore, there have been reports that γδ T cells are able to recognise CD1c in the absence of antigen (174, 179). To examine this specific population, we endeavoured to expand and establish CD1c-restricted Vδ1$^+$ T cell lines. Our CD1c-SL tetramer could then be used to sort single cells from these lines with the aim of sequencing and cloning CD1c autoreactive TCRs to investigate specificity, reactivity and diversity within the context of *M.tb.*

Direct *ex vivo* sorting of CD1c-SL tetramer bound T cells from various blood donors was undertaken to establish CD1c-restricted Vδ1$^+$ T cell lines. This technique demonstrated a larger frequency of positive staining with the CD1c-SL tetramer compared with the CD1c-PC tetramer, but the vast majority of these cells were not Vδ1$^+$. However, this was expected as γδ T cells represent no more than 10% of circulating T cells, with only 10-30% of these comprising Vδ1$^+$ T cells (174, 175). Only cells that were double positive were sorted, but this population was minimal. It was expected that CD1c-SL tetramer staining would be a greater, more distinct population, but the absence of this increased speculation that staining capacity of the CD1c-SL multimers was poor. Optimisation of tetramer functionality lead to vastly increased *ex vivo* staining of both CD4$^+$ and Vδ1$^+$ T cells, allowing for greater quantities of CD1c tetramer$^+$ populations to be sorted for expansion in culture. Expansion of cells expressing the CD4 co-receptor or Vδ1$^+$ TCR was successful when culturing these sorted cells with irradiated feeder PBMCs. However, a decrease in CD1c tetramer staining was observed, indicating a loss of CD1c-reactive T cells or perhaps a downregulation of the TCR. This method of expanding CD1-restricted T cell populations has however proved successful for other groups. This process of sorting, culture and re-sorting has demonstrated to yield an expanded population of CD1b- and CD1c-restricted T cells of both αβ and γδ lineage (174, 264, 268, 301). Although we found little success with this method in expanding CD1c-restricted populations, it can be noted that others have utilised anti-

CD3 antibody or CD3/CD28 activation beads in the culture of the sorted cells which may have improved expansion of CD1c-restricted T cells.

3.3.3.3 Plate bound anti-γδ T cell assay

Due to the lack of success in expanding CD1c-restricted T cells that were sorted directly from numerous donors, we attempted to stimulate the expansion of Vδ1 T cells within the PBMC fraction using a plate bound anti-γδ TCR antibody. The results from the initial experiment demonstrated an increasing expansion of Vδ1 T cells with increasing quantities of plate bound anti-γδ TCR antibody, verifying that this method is capable of specifically expanding Vδ1 cells. Although there was an expansion of Vδ1 cells, there were very few which stained positively with the CD1c-SL tetramer. This lack of staining may have arisen from a variety of factors, including the possibility that samples from these particular donors contained a low frequency of circulating peripheral CD1c-restricted Vδ1$^+$ T cells. Another potential reason for this may have been due to the culture conditions, as it has been reported that this population is particularly difficult to grow (174). However, even low levels of T cell staining would be expected, suggesting a possible issue with the CD1c tetramer.

Following enhancement of the CD1c refolding and purification methods, and the subsequent confirmation of improved tetramer staining, a larger population of CD1c-reactive Vδ1$^+$ T cells were identified from resuscitated cells that were expanded using this method in the initial experiment. Despite this more convincing population, expansion of this sorted population in culture with irradiated feeder PBMCs yielded similar disappointing results to the *ex vivo* sorting method as the CD1c-specific Vδ1$^+$ population failed to expand further. Interestingly, following cryopreservation and subsequent resuscitation, there was a much greater population of Vδ1$^+$ T cells that stained positively with the CD1c-SL tetramers. It has been reported previously that there is an observable decrease in T cell staining with MHC/peptide multimers of cells in culture despite normal levels of TCR expression (445). This reduction in multimer staining has been noted following culture of T cells with persistent stimulation, which resembles our method of expansion involving continuous supplementation with IL-2. The effects of cryopreservation and stimulation on T cell expansion has been investigated, and Sadeghi *et al* report that cryopreservation itself has little effect on antigen specificity, but that specificity was ablated following culture with a large dose of IL-2 (446). As the cells in both our plate bound expansion and *ex vivo* sorting methods are cultured with IL-2 supplemented media, this may have contributed to the almost eradicated CD1c tetramer staining despite seemingly normal CD3$^+$ levels and increased Vδ1$^+$ TCR expression.

On the other hand, prolonged stimulation with IL-2 may not have removed antigen specificity but rather downregulated the TCR complex. The binding avidity of tetramers is lower than that of

antibodies and rates of dissociation for tetramers is higher (287). Therefore, following TCR downregulation, staining of the remaining CD1c-restricted TCR complexes will be more observable with anti-Vδ1 antibodies than with CD1c-tetramers. Furthermore, it has been reported that TCRs reactive to molecules presenting self-antigens have a lower affinity than those that are responsive to pathogen-derived ligands (287, 447). As the CD1c tetramers used in our work are refolded in the absence of specific lipid (CD1c-SL), low affinity self-reactive TCRs that are able to bind our CD1c-SL tetramers may not be clearly detected. This may be due to failure of binding in the first instance or fast rates of dissociation. Additionally, as affinity is a crucial factor in staining intensity (287), lower affinity CD1c-restricted self-reactive T cells that have bound the tetramer may appear closer to the negative staining population. This may be evidenced in our work, as distinct populations of cells appearing to bind CD1c tetramers were observed close to the negative population. Nevertheless, our data suggest that some donors had several convincing T cell populations that bound CD1c-SL tetramers that we then exploited for TCR cloning.

3.3.4 Investigating reactivity of CD1c autoreactive γδ TCR clones

CD1c restricted γδ T cells isolated with a CD1c-PM tetramer have been reported to show cross-reactivity to both self- and foreign lipids, with TCR recognition predominantly directed toward CD1c itself (174). We endeavoured to use our CD1c-SL tetramers to isolate and clone CD1c autoreactive Vδ1^{+} T cells from enriched γδ T cell lines. Ten γδ TCR pairs were sequenced following CD1c-SL tetramer guided single cell sorting, six of which were transduced onto NFAT-Gluc Jurkat T cells (of J.RT3-T3.5 background) for further characterisation. One further γδ TCR (TCR7) which was cloned in collaboration with colleagues at King's College London was also included in our analysis as a positive control for CD1c tetramer staining (296). We then proceeded to stain each γδTCR transduced Jurkat T cell line with CD1c-SL tetramers. As expected, TCR7 stained positively but surprisingly, only TCR4 had clear staining out of the six γδTCRs that were cloned. We hypothesised that absence of staining of the remaining TCRs may be due to low affinity interactions with CD1c, as T cell lines used for sorting were pre-treated with Dasatinib to prevent TCR downregulation upon engagement and thus improve tetramer staining of low affinity TCRs (444, 448). In addition to CD1c-SL, we also stained our γδTCR clones and our αβTCR clone NM4 with CD1c-endo tetramer which has been validated by other groups to identify CD1c autoreactive T cells (268). While TCR4 and TCR7 both stained positively with CD1c-endo, surprisingly NM4 did not show reactivity to this tetramer, suggesting that recognition of CD1c by NM4 is inhibited by lipids within the CD1c-endo complex. The lack of reactivity of the other γδTCRs may also imply that the original γδ T cells sorted may have been due to non-specific tetramer binding. Dead and dying cells with compromised membrane integrity are known to cause a high number of non-specific binding

events, however as we included a viability dye this is an unlikely explanation (449). Some cells, such as $CD19^+$ and $CD14^+$ cells, express the ILT4 receptor that has been reported to bind CD1c tetramers (450). Although we did not include antibodies to exclude these cells, we included numerous T cell markers and employed double tetramer staining in order to reduce the possibility of staining other peripheral blood cells. We sought to further characterise the autoreactive recognition of CD1c by γδTCR clones through measurement of luciferase activity and CD69 upregulation/CD3 downregulation as indicators of CD1c-specific activation.

NFAT-Gluc Jurkat T cells contain a firefly luciferase reporter gene which, following engagement of the TCR, is induced and luciferase is secreted by the activated cell. Luciferase present in the cell supernatant can then be detected as luminescence (451). We observed consistently greater differences for all γδTCR transduced Jurkat T cells cultured with THP1-CD1c compared to THP1-KO cultures, with TCR4 observed to have the greatest CD1c-specific response. Interestingly, despite a lack of staining of TCR5 with CD1c tetramers, in the luciferase assay this TCR demonstrated more indicative CD1c-specific activity than TCR7, which had the lowest measurement of luminescence. Antigen-specific activation without observable tetramer staining has also been reported by Reijneveld *et al*, indicating that although tetramer binding is indicative of reactivity, low affinity TCRs are not always detected by this method (299). We also sought to characterise CD1c-specific activation of these seven γδTCR clones can be detected through measurement of CD69 and CD3 expression. In contrast to the luciferase assay, activation as measured by CD69 upregulation by γδTCR Jurkat T cells when cultured with THP1-CD1c compared to THP1-KO was minimal (data not shown). However, there was an observable increase in CD69 expression by TCR1, TCR4 and TCR5 when stimulated with CD1c (data not shown), supporting observations made in the luciferase assay. Low but detectable upregulation of CD69 has been demonstrated previously for CD1c-restricted γδTCRs, as Roy and colleagues reported weak upregulation of this T cell marker by two PM-specific γδTCR clones following addition of PM to culture media despite clear recognition of CD1c-PM tetramers (174). Furthermore, Reijneveld and colleagues also reported a similar finding, with their CD1b autoreactive γδTCR clone BC14.1 clearly staining with CD1b tetramers but CD69 upregulation was minimal (299).

As we had previously optimised an activation assay involving our autoreactive αβ TCR clone, NM4, in culture with the T2 cell line, we chose to repeat investigation of CD1c-mediated activation of our γδTCR clones with this APC line. The cellular origin of APCs may affect their lipidome and surface expression of co-stimulatory molecules, so it is possible that activation may differ between Jurkat T cells cultured with THP1 or T2 cells. The use of two APC lines has been reported by other groups and may be used in order to ascertain antigen-specific activation of TCRs (299). Wun and colleagues analysed activation of CD1c-restricted T cells following stimulation with

either K562 or C1R cells expressing CD1c. They observed that while both CD1c expressing APC lines stimulated production of IFNγ, K562-CD1c induced marginally more IFNγ as measured by ELISPOT (268). Additionally, Reijneveld *et al* sought to measure activation marker upregulation and TCR regulation of CD1b-restricted T cells also in response to K562 and C1R cells. Similar to our results, the authors observed complete TCR downregulation upon stimulation with K562.CD1b but only a partial effect when stimulated with C1R.CD1b (299), indicating that choice of APC line can influence TCR-mediated activation. In contrast to THP1 stimulated Jurkat T cells, we observed that NM4 and both γδTCR Jurkat T cell lines showed a minimal increase in luminescence when stimulated with CD1c expressing T2 cells compared to the CD1c negative parental T2 line. However, when analysed by flow cytometry, all three Jurkat T cell lines showed significant upregulation of T cell activation marker CD69 in the presence of T2-CD1c cells compared to culture in the absence of T2 cells. TCR4 was also observed to have significantly increased expression of CD69 in the presence of CD1c compared to T2-KO; although a similar trend was observed for TCR7, this was not significant. Despite differences in sensitivity of these two assays with each APC line, we consistently observed CD1c-specific responses by TCR4 and TCR7.

It has been reported that the γ and δ TCR chains have different functions with regards to recognition of CD1 proteins. Roy *et al* characterised three CD1c-PM specific γδTCR clones that harboured identical Vδ1 chains but different Vγ chains. Chain swapping experiments revealed that whilst the δ chain was required for specific recognition of CD1c, binding affinity of the protein was augmented by the γ chain, with Vγ3 contributing to greater binding affinity of CD1c-PM than Vγ8 (174). Two of our γδTCR clones, TCR1 and TCR 4, have identical Vδ1 CDR3 sequences but do not appear to recognise CD1c at a comparable level. As these TCRs express the same δ chain, we would expect to see similar levels of activation as the Vδ1 chain has been described as the dominant TCR chain in CD1 docking (174, 299, 319, 320). However, as the γ chain has been shown to significantly affect binding affinity, this may explain why we see CD1c-specific staining and activation of TCR4 but smaller levels of activation and absent tetramer staining of TCR1. Similar to four of our transduced γδTCR clones, the BC14.1 γδTCR clone described by Reijneveld and colleagues also expresses Vγ4Vδ1 TCR chains, albeit with restriction to CD1b (299). In addition to other Vγ4Vδ1^{+} T cells described by Di Marco Barros *et al,* the CD1b-restricted BC14.1 γδTCR clone upregulated CD69 to a greater extent when stimulated with K562 cells expressing butyrophilin like (BTNL) protein 3, BTNL8 and CD1b compared to K562 cells expressing CD1b alone (299, 452). It has been recently proposed that Vγ4^{+} γδTCRs may have dual recognition of CD1c and butyrophilins, taken together with the data on CD1b restricted γδTCR clones, this may suggest that our Vγ4Vδ1 TCRs isolated using a CD1c-SL tetramer may demonstrate increased levels of activation markers in the presence of butyrophilins or BTNLs (296). As TCR1, TCR2 and TCR3 all

have identical Vγ4 chains but differing Vδ1 chains, it would be interesting to further investigate dual reactivity of these TCRs to CD1c and butyrophilins or BTNLs.

In conclusion, we have successfully isolated CD1c autoreactive γδ T cells from healthy human donors using our CD1c-SL tetramers. The combination of tetramer studies with activation assays suggests that the transduced γδTCR clones have a range of binding affinities to CD1c. To further investigate this, we could employ chain swapping experiments and activation assays in the presence of butyrophilins. We aimed to investigate these γδTCR clones in a similar manner to that of NM4, i.e. analysing binding augmentation to CD1c mutants and CD1c loaded specific lipids. However, due to the COVID-19 pandemic and ensuing lockdown, we were unable to complete these experiments. Therefore, these experiments will also be carried out in future to further probe CD1c recognition by these autoreactive γδTCR clones.

Chapter 4 CD1c autoreactive T cells in healthy and *M.tb* infected humans

4.1 Activation Induced Marker (AIM) Assay

We have previously used CD1c tetramers to detect and isolate CD1c-restricted T cells in healthy donors. However, we sought to optimise a tetramer independent assay to detect T cells that respond to CD1c in the absence of exogenously added microbial lipid antigens. The recognition of antigens by the TCR often induces activation of the cell leading to downstream effects. Common methods of investigating cellular activation often include analysis of cytokines including ELISPOT and Intracellular cytokine staining (ICS). However, these methods are often limited and typically only investigate one type of T cell, such as those which are Th1-biased (453, 454). AIM assays overcome this issue by analysing the expression of particular surface markers in response to stimulation with an antigen, thus defining antigen specificity of a range of T cell types (337, 338, 453, 455, 456). To this end, we employed an AIM assay in order to investigate the presence of CD1c autoreactive T cells in a small cohort of healthy human donors. We optimised a short term T cell culture with APC which will also be used in future experiments to investigate the functional phenotype of CD1c autoreactive T cell responses by Luminex. We first isolated CD3+ T cells from a small cohort of six healthy donors, with three of these having prior exposure to *M.tb*. We then cultured $CD3^+$ T cells with parental WT THP1 cells (THP1-KO) or THP1 cells expressing CD1c (THP1-CD1c). No exogenous antigen was added to the cultures in order to drive the expansion and subsequently confirm the presence of CD1c autoreactive T cells. Expression of CD1c on THP1-CD1c cells was confirmed by flow cytometry analysis after staining with anti-CD1c antibody (Figure 38).

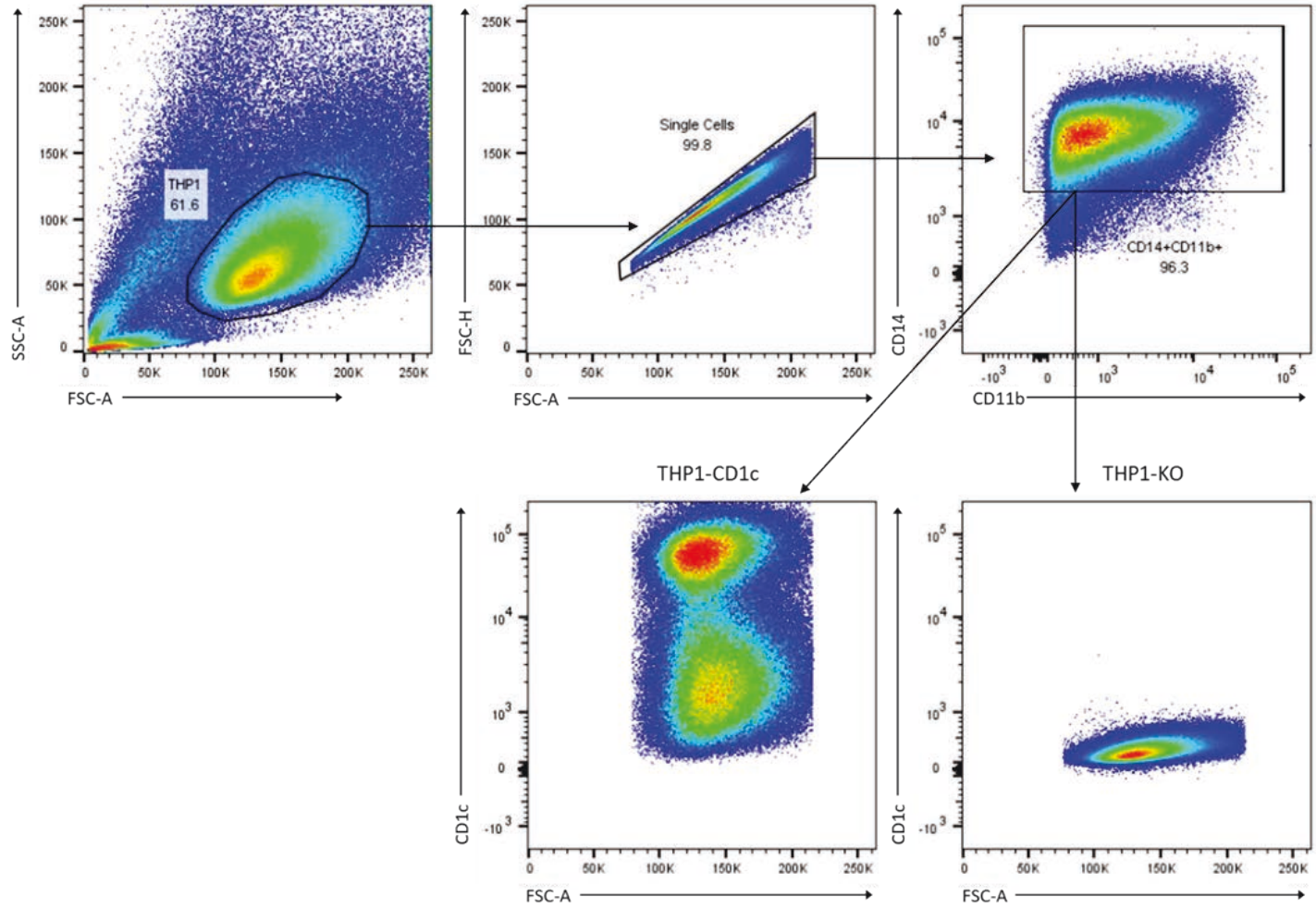

Figure 38: Flow cytometry gating strategy for THP1 cells

The flow cytometry dot plots indicate that cells were pre-gated on lymphocytes and doublets were excluded. $CD14^{+}CD11b^{+}$ cells were then analysed for expression of CD1c. No positive CD1c staining was observed on THP1-KO cells and clear positive CD1c staining was observed on THP1-CD1c cells.

As a control, T cells were also cultured without APCs and were either stimulated with PMA and Ionomycin, or left unstimulated for the duration of the experiment. A schematic depicting the experiment can be viewed in Figure 39. Over the course of 3 weeks, T cells were re-stimulated each week and analysed by flow cytometry for their expression of the activation markers CD137, CD25 and CD69, as well as their proliferative response indicated by the diminishing signal of Cell Trace Violet (CTV). CTV allows for the tracking of cell proliferation as it diffuses into the cell and covalently binds to intracellular amines and subsequently becomes diluted as the cell divides. The fluorescence of CTV is easily analysed by flow cytometry, and diminishing signal is representative of generations of cell division. The gating strategy to analyse the expanded populations of $CD3^{+}$ T cells and the expression of activation markers can be viewed in Figure 40.

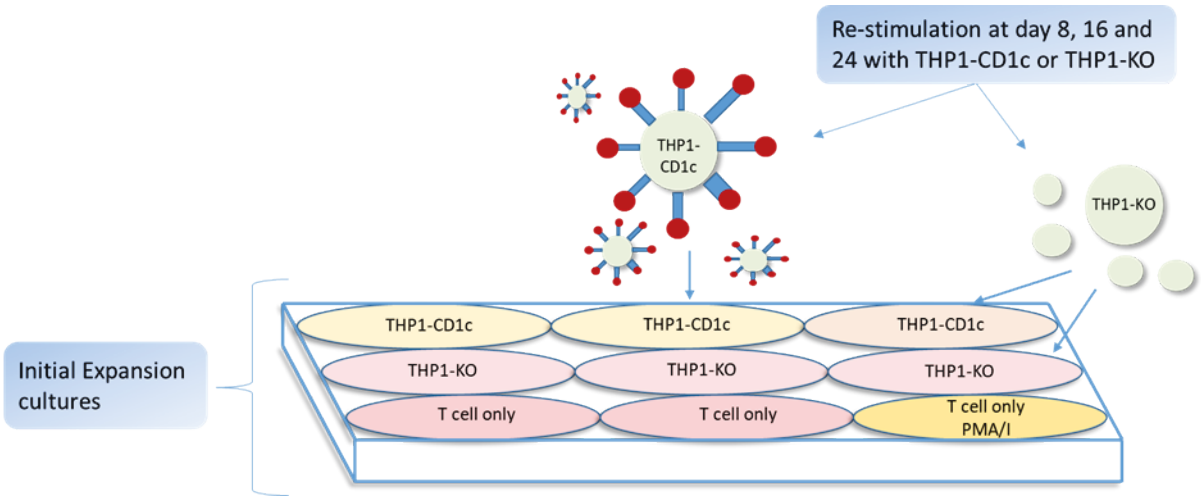

Figure 39: Experimental workflow for short term expansion (AIM) assay

Cartoon schematic representing expansion of T cells in culture with CD1c negative parental THP1 line (THP1-KO), THP1-CD1c, T cells alone, or positive control T cells stimulated with PMA and Ionomycin (PMA/I). At day 8, 16 and 24, T cells were re-stimulated with THP1-KO or THP1-CD1c before analysing expression of activation markers CD69, CD25 and CD137 the following day by flow cytometry.

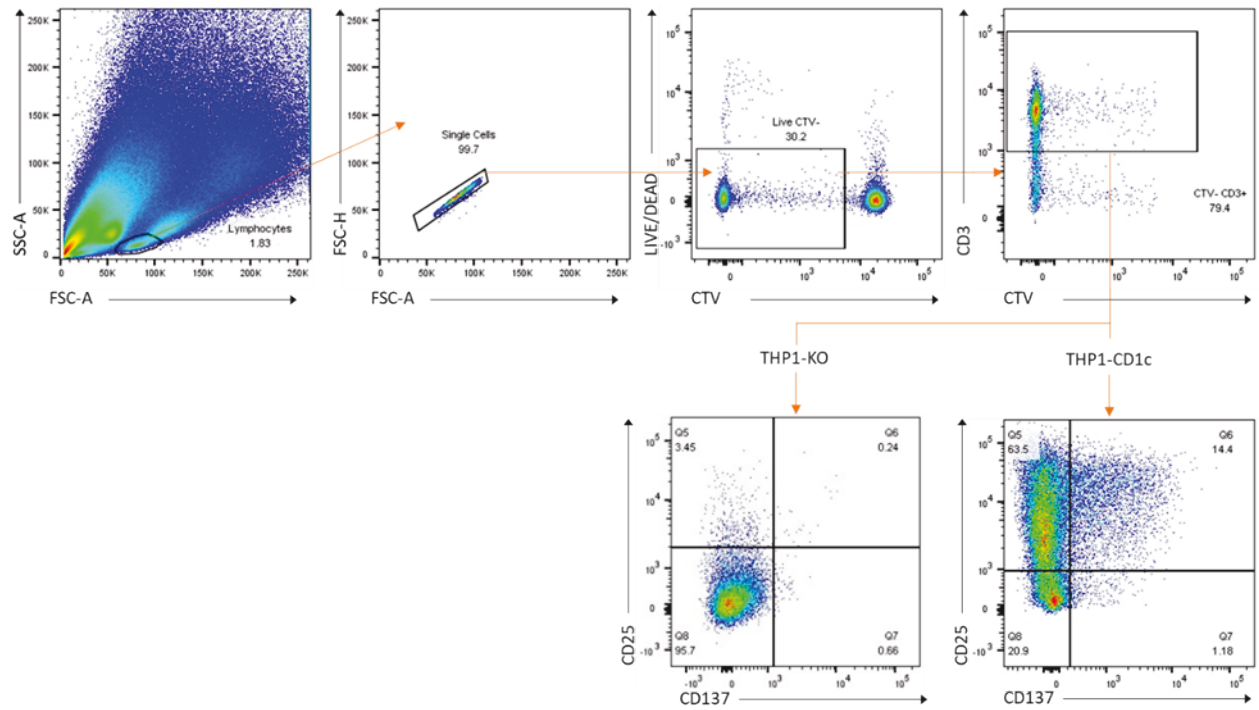

Figure 40: Gating strategy of proliferated T cells and expression of activated induced markers

Representative flow cytometry dot plots showing the gating strategy used to identify proliferated T cells and the identification of CD69, CD25 and CD137 expression. After gating on lymphocytes, doublets were then excluded. Live, CTV^- cells (indicating proliferation) were gated on before selecting $CD3^+$ T cells. $CD69^+CD137^+$ and $CD25^+CD137^+$ double positive T cells were identified.

On day 8, a significantly greater frequency of proliferated T cells as defined by the CTV^- $CD3^+$ population (Figure 41) was clearly evident in the THP1-CD1c stimulated cultures compared to T cells that were cultured alone. Increased proliferation was also observed in the THP1-KO stimulated cultures compared to T cells alone, suggesting that the presence of APCs seemingly drives T cell proliferation. On day 16, most donors (n=5) had an increase in the number of proliferated CTV^- $CD3^+$ T cells. Our data revealed an increase in the number of proliferated CTV^- $CD3^+$ T cells in cultures stimulated with THP1-KO APCs, but this was substantially lower compared to cells cultured with THP1-CD1c APC for most donors. We also observed an increase in the frequency of CTV^- T cells on day 24, but due to cell death and a lack of activation markers at this time point, it was deemed that 2 weeks of culture was seemingly the ideal time point to investigate the expanded T cells.

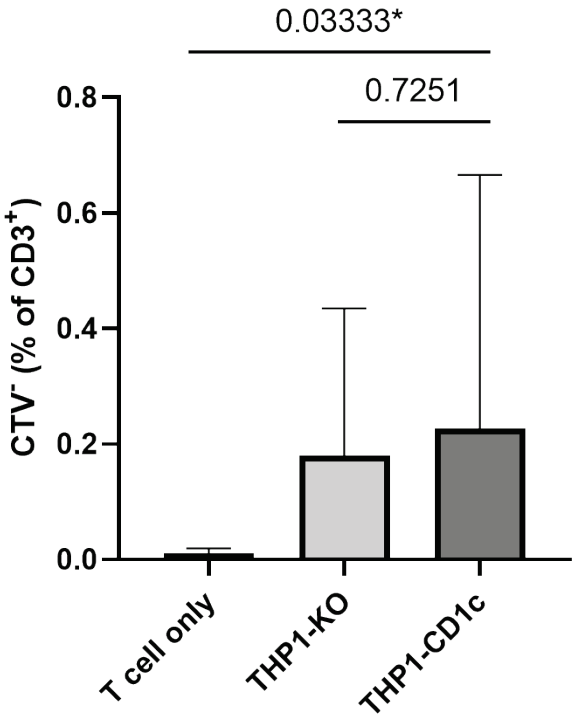

Figure 41: Proportion of CTV^- $CD3^+$ T cells in CD1c stimulated lines

Average frequency (n-6) of CTV^- $CD3^+$ T cells at day 8 after solitary culture or overnight stimulation with THP1-CD1c. Statistical significance calculated using a Mann-Whitney test.

We next sought to investigate the antigen specific responses within our short term T cell cultures. To this end, the frequency of T cells that were double positive for the T cell activation markers CD69/CD137 and CD25/CD137 within the CTV^- T cell population were assessed and compared to that of CTV^+ T cells as an internal control. Antigen specific activation was assessed by comparing T cells stimulated overnight with THP1-KO and THP1-CD1c before analysing activation markers after 24 hours by FACS analysis. Our data revealed that T cells from all donors stimulated with THP1-CD1c had significantly greater frequencies of activated T cells as shown by a greater $CD69^+CD137^+$

and $CD25^+CD137^+$ T cell population within the CTV^- gate than in the CTV^+ gate at day 8 and day 16 (Figure 42) This demonstrates that to understand antigen specific activation, the expanded population indicated by CTV negativity is the population to assess.

On day 8, half of the donors (A.PT.1, A.S.2, A.L.1) had greater frequencies of $CD69^+CD137^+$ when stimulated overnight with THP1-CD1c compared to control THP1-KO APCs, but only A.PT.1 and A.S.2 had greater frequencies of $CD25^+CD137^+$ in the THP1-CD1c stimulated group. However, our results reveal that on day 16 all donors had significantly greater frequencies of $CD69^+CD137^+$ and $CD25^+CD137^+$ when stimulated overnight with THP1-CD1c compared to THP1-KO APCs (Figure 43). This further suggests that two weeks of culture is the optimal time point to investigate activation marker expression. Finally, our data confirm the presence of CD1c autoreactive T cells through their specific proliferation and activation in short term T cell cultures from a small cohort of healthy subjects.

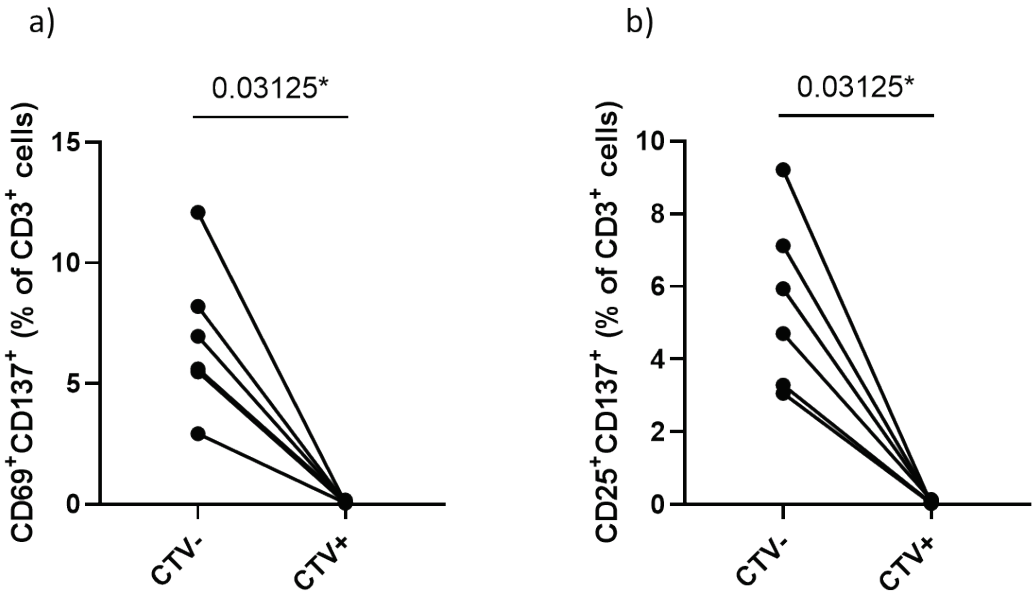

Figure 42: Activation marker expression at day 16 following overnight CD1c stimulation
Frequency of CTV^- and CTV^+ T cells stimulated overnight with THP1-CD1c expressing a) CD69 and CD137, and b) CD25 and CD137. Significantly greater frequencies of $CD69^+CD137^+$ and $CD25^+CD137^+$ T cells observed in the CTV^- gate than the CTV^+ gate. Statistical significance calculated using a Wilcoxon matched pairs signed rank test.

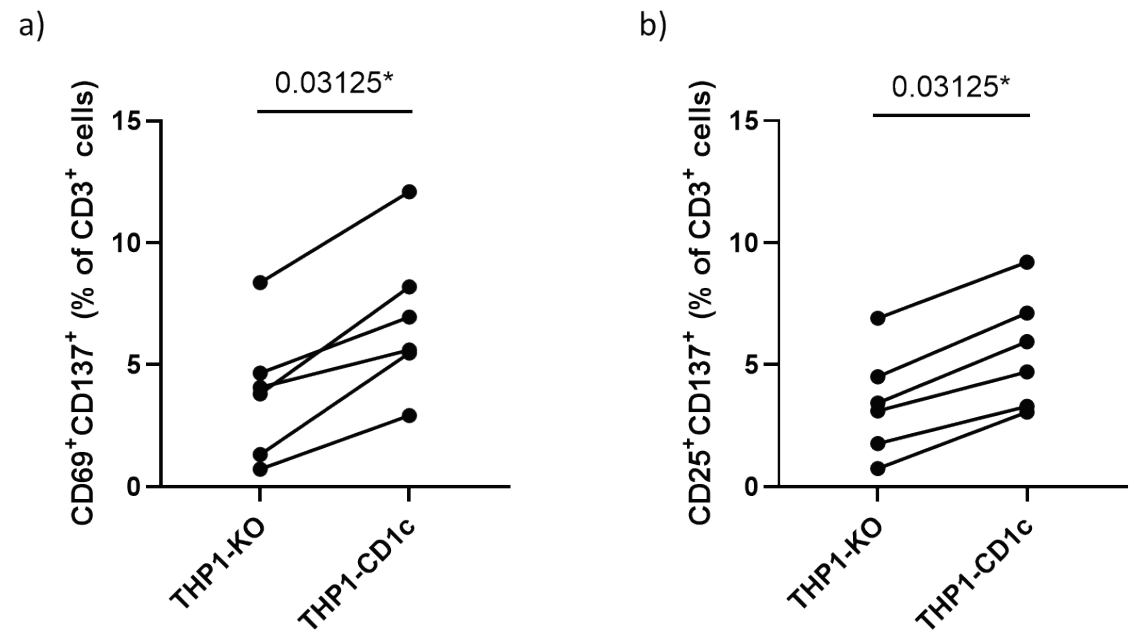

Figure 43: Activation marker expression at day 16 by CTV$^-$ T cells following overnight stimulation
Frequency of CTV$^-$ CD3$^+$ T cells stimulated overnight with CD1c negative parental THP1 line (THP1-KO) or THP1-CD1c expressing a) CD69 and CD137, and b) CD25 and CD137. Statistical significance calculated using a Wilcoxon matched pairs signed rank test.

4.1.1 Co-receptor expression by CD1c autoreactive T cells

To further investigate the phenotype of proliferating cells, we also stained the T cells with anti-CD4 and anti-CD8 antibodies. Between day 8 and day 24, all the THP1-CD1c expanded T cells showed an increase in the CD4$^+$ population despite an observable reduction at day 16 from which T cell frequencies subsequently recovered and increased. The changes in the CD4$^+$ population in the THP1-KO stimulated cultures was not consistent across the cohort, with half decreasing at day 16 and the other half increasing. Generally, we observed a greater frequency of CD4$^+$ cells in the THP1-CD1c stimulated cultures at day 8 and 16 than those stimulated with THP1-KO APCs. A larger frequency of this T cell subset was also seen in the T cell only cultures.

Compared to CD4$^+$ T cells, the CD8$^+$ subset in all culture conditions remained relatively stable over the time course for the majority of donors, with a peak at day 16 seen for only 2 donors. Generally, the greatest frequency of CD8$^+$ T cells was found in the T cell only condition at each time point, with lower frequencies observed in the THP1-CD1c expanded co-cultures. CD4$^-$CD8$^-$ DN T cells cultured with THP1-CD1c were observed to peak in frequency at day 16 before decreasing at day 24 to a similar level observed at day 8. In general, DN T cells cultured with THP1-KO increased in frequency between day 8 and day 24 but were on average lower than those cultured with THP1-CD1c at day 16. Day 16 again appeared to be the most valuable time point

with greater levels of expansion observed for all T cell subsets. At this time point, the DN T cells were, on average, the predominating subset for those cultured with THP1-CD1c and THP1-KO, but $CD8^+$ T cells were the largest fraction in cultures with T cells alone. Figure 44 depicts the overall co-receptor status of T cells stimulated with CD1c antigen compared to control unstimulated T cells.

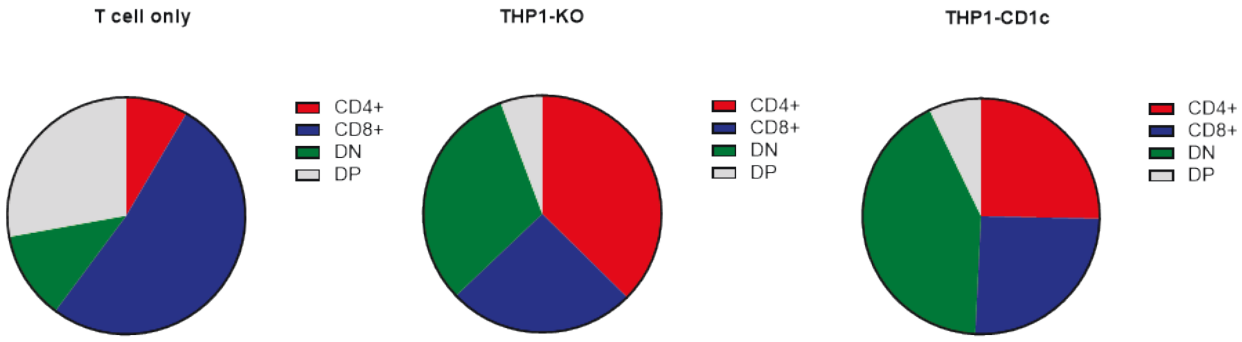

Figure 44: Proportion of T cell subsets at day 16

Proportion of $CD4^+$, $CD8^+$, double negative (DN) and double positive (DP) CTV^- $CD3^+$ T cells at day 16 following overnight stimulation with THP1-CD1c or T cells cultured alone.

We then investigated the co-receptor status of the CD1c-expanded T cells that were activated following overnight CD1c stimulation, hence co-receptor status of CD1c-autoreactive T cells. As previously observed with the overall T cell population, the majority of $CD69^+CD137^+$ and $CD25^+CD137^+$ T cells within each co-receptor subset peaked at day 16. At this time point, the greatest average frequency of $CD69^+CD137^+$ and $CD25^+CD137^+$ T cells was within the DN T cell subset. $CD4^+$ T cells on average were the least activated T cell subset when measured by $CD69^+CD137^+$ expression, but were similar to that of $CD8^+$ T cells when analysing $CD25^+CD137^+$ (Figure 45). Overall, CD1c-specific activation did not differ greatly between the three co-receptor subsets, but activated DN T cells were somewhat more numerous.

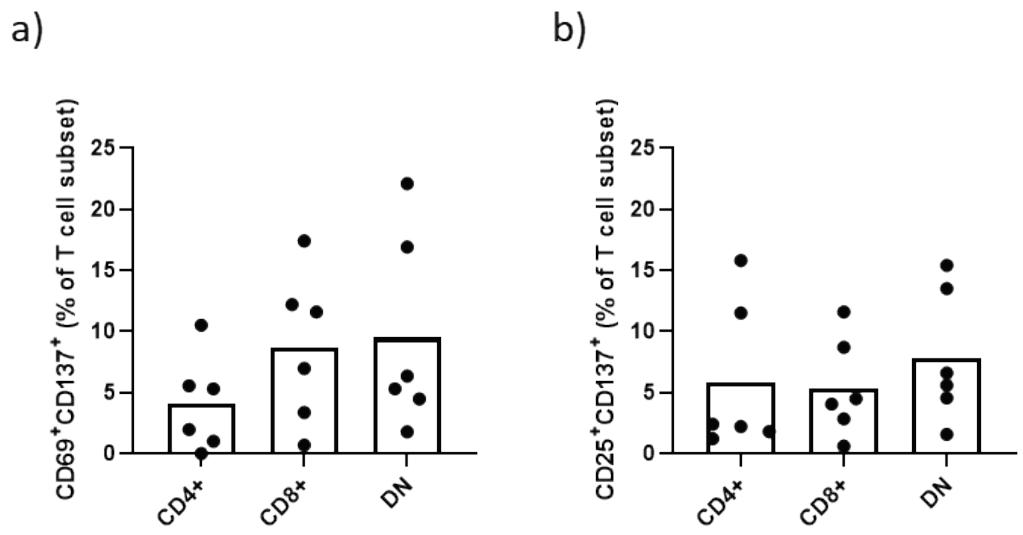

Figure 45: Activation marker expression by CD4$^+$, CD8$^+$ and DN T cells after overnight stimulation
Frequency of CD1c antigen specific CD4$^+$, CD8$^+$ and DN CTV$^-$ T cells at day 16 expressing a) CD69 and CD137, and b) CD25 and CD137 following overnight stimulation with THP1-CD1c.

To investigate the effects of prior *M.tb* exposure on the response of CD1c autoreactive T cells to cognate antigen, we analysed activation markers of T cell subsets stimulated with THP1-CD1c at day 16 for both healthy and TB exposed donors. Generally, the frequency of CD69$^+$CD137$^+$ and CD25$^+$CD137$^+$ CD3$^+$ T cells were similar between the *M.tb* exposed and unexposed groups. The frequency of CD69$^+$CD137$^+$ CD4$^+$, CD8$^+$ and DN cells was observed to be generally higher in the unexposed group than the *M.tb* exposed group, whereas the frequency of CD25$^+$CD137$^+$ cells in the CD8$^+$ and DN subsets were found to be similar between the two groups (Figure 46). Unlike the CD8$^+$ and DN T cell subsets, unexposed healthy donors were observed to have a higher frequency of CD25$^+$CD137$^+$ CD4$^+$ cells, (Figure 46). This could suggest that this subset may respond more avidly to antigen in healthy donors and they might be reduced in TB which warrants further investigation in a larger cohort.

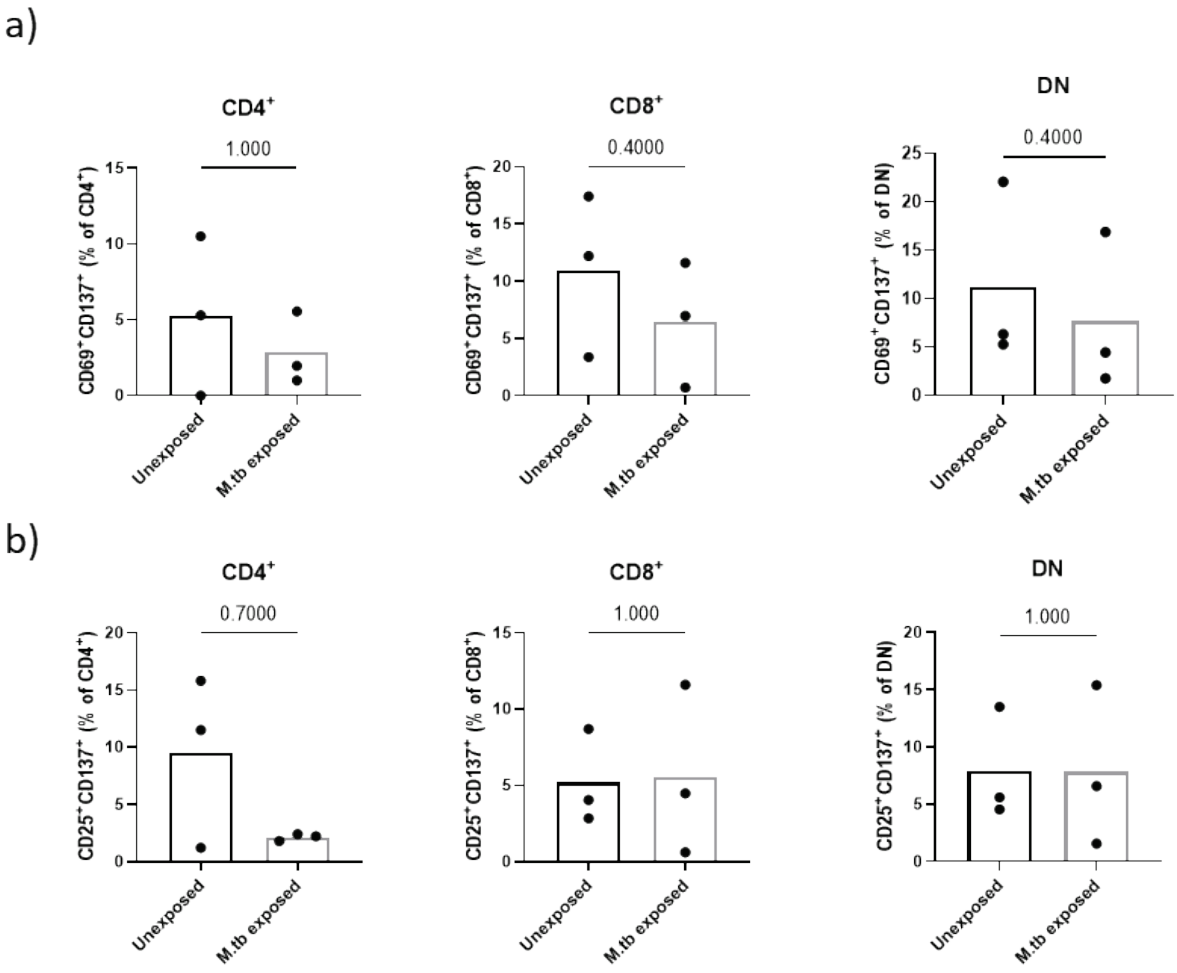

Figure 46: Activation marker expression by CD4$^+$, CD8$^+$ and DN T cells between unexposed and *M.tb* exposed donors

Frequency of CD4$^+$, CD8$^+$ and DN CTV$^-$ T cells overnight at day 16 expressing a) CD69 and CD137, and b) CD25 and CD137 by unexposed and *M.tb* exposed donors following overnight stimulation with THP1-CD1c. Statistical significance calculated using a Mann-Whitney test.

4.2 Immunohistochemistry staining for CD1c and γδ T cells in human TB granulomas

CD1c is known to be expressed on antigen presenting cells such as myeloid DC and a sub-population of B cells (139, 264). Additionally, CD1c has been demonstrated to be strongly induced on foam cell macrophages which are present in inflammatory lesions, such as those in atherosclerosis (342). Foam cell macrophages are also known to be present in TB lesions, as well as B cells which often are found in follicles remote from the inner cells of granulomas (2, 7, 15). The presence of $CD1c^+$ DC in the lung has been demonstrated in the human CD1 transgenic mouse model (331), and an increase in $CD1c^+$ DC in pleural effusions from TB patients has been reported, but as of yet there is no evidence of CD1c expressing cells in human TB lung granulomas. We therefore sought to demonstrate the expression of CD1c within the granuloma using immunohistochemical staining of lung sections taken from five human TB patient biopsies.

Using heat-induced epitope retrieval, expression of CD1c was observed in lung tissue from all five TB patients, but the majority of expression was remote from the granuloma centre, the focus of infection. Areas of positive staining were observed in B cell follicles and inflammatory tissue distal to areas of caseous necrosis (Figure 47), but overall CD1c expression was low relative to the amount of inflammation seen in each patient. Positive staining of CD1c however was observed within a small number granulomas (Figure 48). However, this was localised to specific granulomas in each tissue section and the majority of expression was seen away from the TB granulomas. In control tissue sections, some CD1c expression was identified in the normal airway tissue but no large areas of expression were observed. Negative control stains of the lung sections confirmed the absence of non-specific secondary antibody binding.

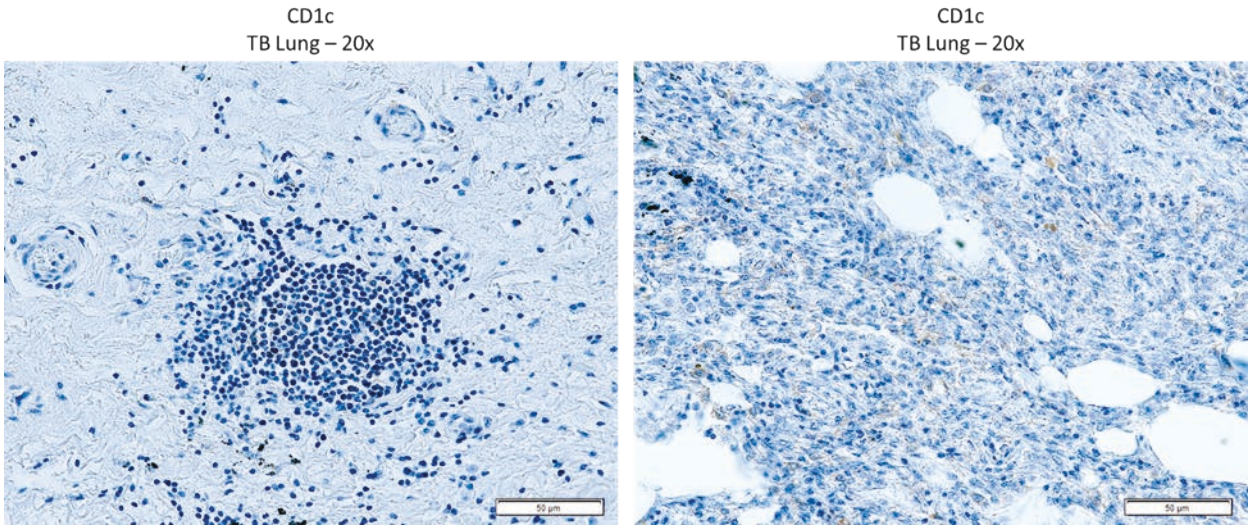

Figure 47: Immunohistochemistry staining of CD1c expression in *M.tb* infected lung tissue

Representative staining of CD1c expression in lung tissue taken from an *M.tb* infected patient. Positive CD1c staining is demonstrated within a B cell follicle (left) and in inflammatory tissue remote from areas of caseous necrosis (right) at 20x magnification. Scale 50µm.

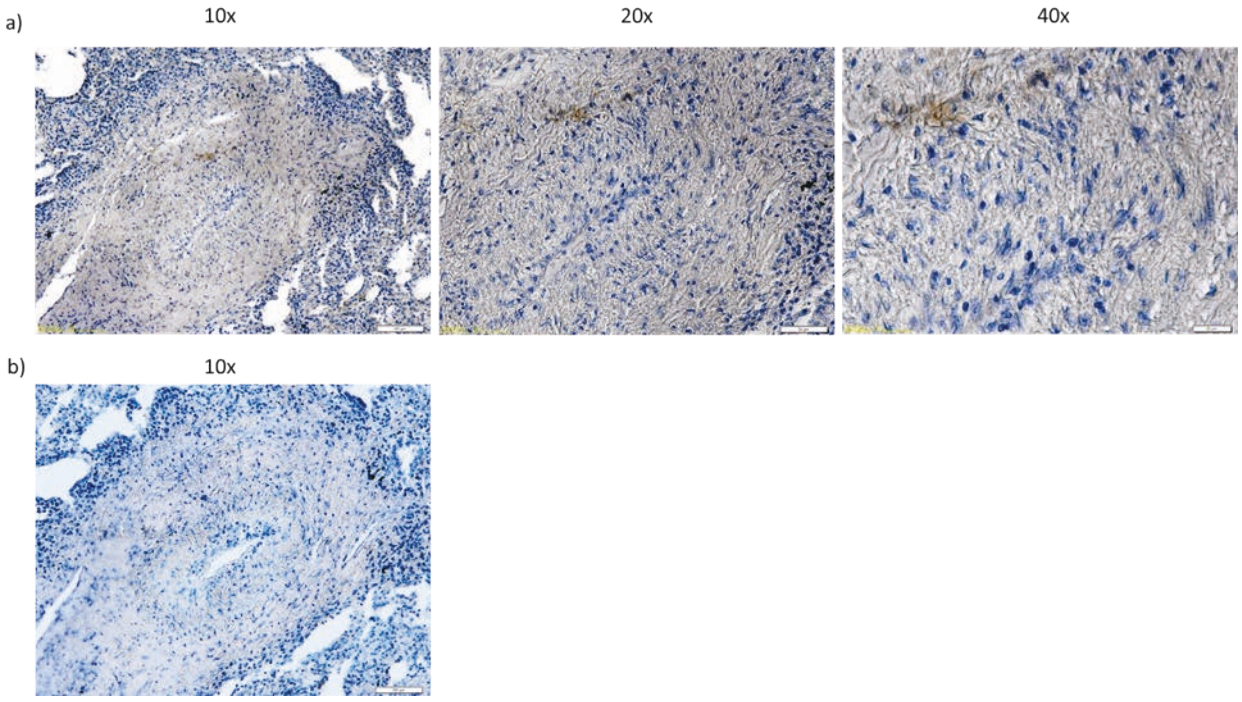

Figure 48: Immunohistochemistry staining of CD1c expressing cells in lung sections taken from an *M.tb* infected patient

Representative staining of CD1c expression within a TB granuloma using a) CD1c antibody at 10x, 20x and 40x magnification and b) Negative control staining using secondary antibody only at 10x magnification. Scale bars in 10x, 20x and 40x magnification depict 100µm, 50µm and 20µm, respectively.

Additionally, we also aimed to demonstrate staining of γδ T cells within the granuloma from these same patients. $V\delta1^+$ are the predominant tissue resident subset of γδ T cells and have been reported to accumulate in the lungs of patients with pulmonary sarcoidosis, a disease which is histologically similar to TB (210, 457). Lung resident populations of γδ T cells dominated by localised clonal expansions of the $V\delta1^+$ subset were recently identified and characterised by Ogongo *et al* (200), but these T cells have also yet to be visually demonstrated in the granuloma. Using anti-TCRδ antibodies, we performed heat-induced epitope retrieval on the five sections of lung tissue from TB patients and the absence of non-specific antibody binding was determined using a negative control stain of secondary antibody only. Four out of five TB lung sections were positive for γδ T cells, with expression differing substantially both between and within each tissue section. Clusters of positive staining for γδ T cells were observed in a small subset of granulomas (Figure 49), but this was not detected in every TB patient. The majority of γδ T cells were observed in inflammatory tissue near areas of caseous necrosis, but expression was scanty and less clustered than in the granuloma. In contrast, no staining of γδ T cells was observed in areas of normal lung tissue from the TB patients, or in normal lung tissue from the control patients (Figure 50).

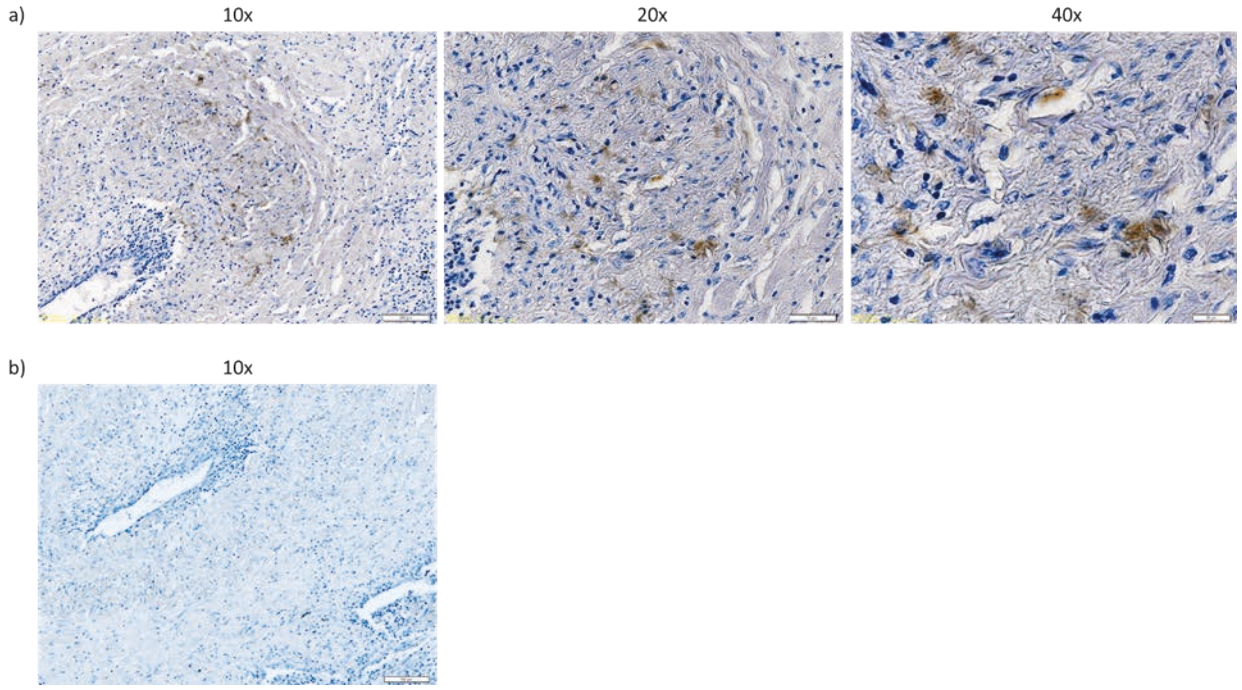

Figure 49: Immunohistochemistry staining of γδ T cells in lung sections taken from an *M.tb* infected patient

Representative staining of γδ T cells within a TB granuloma using a) TCRδ antibody at 10x, 20x and 40x magnification. B) Negative control staining using secondary antibody only at 10x magnification. Scale bars in 10x, 20x and 40x magnification depict 100µm, 50µm and 20µm, respectively.

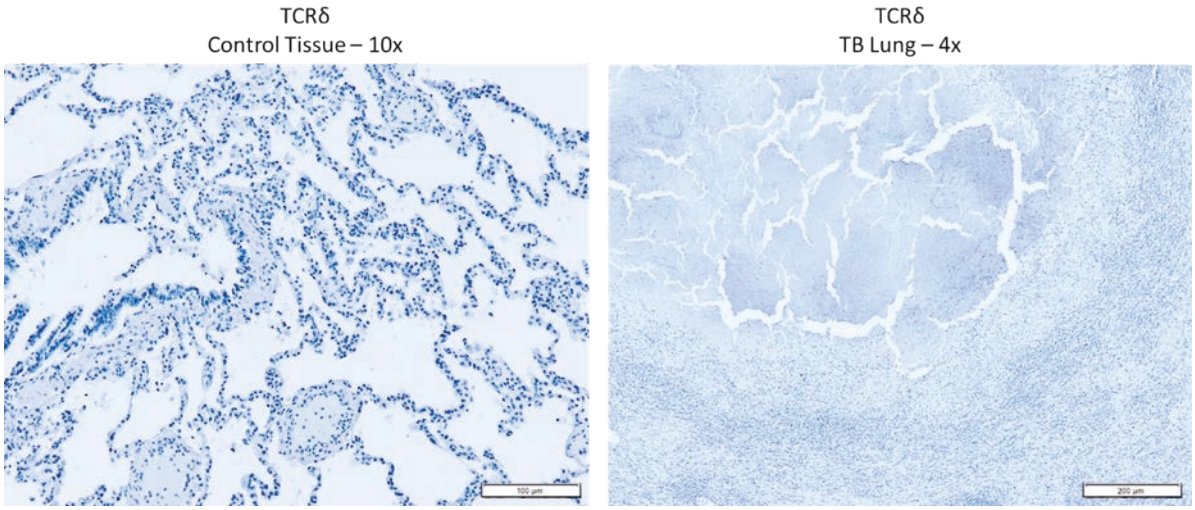

Figure 50: Immunohistochemistry staining of lung sections negative for γδ T cells

Representative staining of *M.tb* uninfected control lung (left) demonstrating a lack of γδ T cells in healthy tissue, and *M.tb* infected lung tissue (right) demonstrating no TCRδ antibody staining at areas of caseous necrosis in TB patients.

These results demonstrate the presence of both CD1c and γδ T cells within *M.tb* infected lung tissue, but the majority of staining was observed to be remote from the area of infection. This suggests that areas of immunopathology may be linked to *M.tb* induced downregulation of CD1c, a phenomena which has been previously documented in several studies (63, 458-460). Suppression of CD1c may also impact on the recruitment and activation of CD1c-restricted γδ T cells, leading to an absence of observable γδ T cells in this area (460).

4.3 The localisation of CD1c mediated immune responses in TB

Over the past few decades, T cells recognising mycobacterial lipids in the context of CD1 group 1 molecules have been characterised. Several lines of evidence suggest that *M.tb*-lipid specific CD1 group 1 restricted T cells contribute to anti-mycobacterial immunity. Analyses of CD1 restricted T cell lines derived from healthy or *M.tb* exposed donors has revealed that these T cells are cytotoxic and release the cytokines TNF-α and IFNγ which are deemed critical for anti-mycobacterial immunity (306, 429, 461). Furthermore T cells from *M.tb* infected donors responded with significantly greater magnitude and frequency to mycobacterial lipid antigen preparations than lymphocytes from uninfected healthy donors (306). *M.tb* lipid specific T cell responses were enriched within the $CD4^+$ T cell fraction and restricted by CD1 molecules. This suggests that CD1-restricted T cells responding to *M.tb* lipid antigens comprise a significant portion of the circulating pool in human TB (306). Of note, CD1b-restricted T cells that are specific for the *M.tb* lipid antigens MA and GMM are elevated in the peripheral blood of donors with active or latent TB (311). Upon recognition of antigen, CD1b restricted T cells produced TNF-α and IFNγ and killed *M.tb* infected cells via cytolysis and granulysin delivery (166, 167, 230, 236, 292, 429).

Furthermore, circulating CD1c mediated T cell responses specific for mycobacterial lipids are also elevated in the peripheral blood of human TB patients (306, 313). CD1c tetramers loaded with the mycobacterial lipid PM have been used to identify mycobacteria-specific T cells in the blood of subjects that had been exposed to *M.tb*, but not in healthy controls (264). CD1c-PM $tetramer^+$ T cells were specifically activated by CD1c only in the presence of the microbial lipid antigen PM. In addition, CD1c-restricted T cell lines derived from subjects with a positive tuberculin skin test (PPD^+) have been shown to have a significantly greater proliferative response to mycobacterial MPD compared to T cell lines derived from naïve controls (313).

However, the majority of CD1c-restricted T cells appear to be autoreactive, whereby they are specifically activated by $CD1c^+$ APCs in the absence of microbial antigens (268, 304, 337). CD1c-autoreactive T cells are abundant in the peripheral blood of healthy humans and they released the cytokines IFNγ, TNF-α and IL-2 upon their recognition of CD1c carrying endogenous self-lipids (268, 304, 337). Despite the knowledge that CD1c-restricted *M.tb* lipid antigen-specific responses are increased in TB, there is as of yet no insight into the role of CD1c-autoreactive T cell subsets in human TB. We hypothesised that CD1c and its autoreactive T cells may contribute to the host-pathogen interaction in human TB infection. To address this hypothesis, we sought to investigate the frequency and phenotype of CD1c autoreactive T cells in human TB patients. Furthermore, it is pertinent that we understand the immune response at the site of infection. While studies

revealed elevated numbers of $CD1c^+$ DC in TB pleural effusions and increased CD1 expression in BAL fluid (139, 462), studies of CD1c and its autoreactive T cells within TB patient granulomas remained elusive due to the technical challenges of studying these cells.

4.3.1 CD1c autoreactive T cells in the peripheral blood of TB patients

Several studies have demonstrated high frequencies of autoreactive T cells in the peripheral blood of healthy human donors and neonates (268, 304, 316, 337). In addition, a recent study used mammalian derived CD1c-endo tetramers, which are loaded with self-lipids, revealing specific tetramer staining of large numbers of circulating CD1c autoreactive T cells in a small cohort of healthy donors (268). Furthermore, studies indicate that an increase in the frequency of autoreactive T cells is a feature of TB. An increase in autoreactive T cell frequencies have been demonstrated in the blood of TB patients (463) and also in the vitreous humour of patients with tuberculosis-associated uveitis, an autoimmune condition that has been shown to occur in individuals with TB (464). In addition, CD1c expressing DCs are also increased in TB patients (462), further suggesting an involvement for CD1c mediated responses in TB immunity.

Human CD1 transgenic mice (hCD1Tg mice) generated by Felio *et al* demonstrated that a large proportion of CD1c-restricted T cell lines generated from *M.tb* infected hCD1Tg mice were autoreactive (331). While *M.tb* specific CD1c-restricted T cell lines were also derived and released cytokine in response to *M.tb* lipid antigens, the majority of T cell lines generated were autoreactive and were able to lyse CD1c expressing DC in the absence of exogenous microbial antigen (331). Interestingly, the authors found that the expansion of CD1c-restricted T cell responses was observed in hCD1Tg mice exposed to *M.tb* or BCG, but not in naïve mice, indicating that *M.tb* drove the *in vivo* expansion of CD1c-autoreactive T cells (331). This work further supports our hypothesis that CD1c autoreactive T cells may play an as of yet unknown functional role in the host pathogen interaction in human TB. As we have previously demonstrated that our CD1c-SL tetramers bind both CD1c autoreactive αβ and γδ T cells, we sought to investigate the frequency and phenotype of CD1c-restricted T cell subsets in the peripheral blood in a cohort of South African TB patients.

4.3.1.1 Patient Cohort Demographics

Cryopreserved PBMCS were obtained from fifteen patients with active TB that were enrolled onto an observational study at the Africa Health Research Institute, Durban, South Africa, between February and May 2014. All TB patients were diagnosed with pulmonary TB and were currently undergoing treatment as per national guidelines. One patient had been diagnosed with diabetes mellitus in 2011 but was not receiving ongoing treatment. One patient had previously completed

6 months of treatment with Rifafour for a previous TB infection, so was therefore removed from the data set. There were eight patients that were seropositive for HIV infection but only four of these were receiving anti-retroviral therapy. All patients receiving anti-retroviral medication were receiving the same three treatments: Efavirenz, Lamivudine and Tenofivir. Eighteen healthy controls were selected at random between September 2018 and February 2019, with PBMCs isolated and cryopreserved at the time of donation. All healthy controls were negative for active TB and HIV. There were no healthy controls that had received previous treatment for TB or had a diagnosis for diabetes mellitus or an autoimmune disease. Demographic and clinical characteristic information can be found in Table 7.

Table 7: Demographics and clinical status of South African TB patients and controls

Characteristic	TB Patients (n = 15)	Healthy Controls (n = 18)
Male (%)	80%	55.56%
Age (Mean ± S.D.)	33.67 ± 7.24	28.11 ± 8.57
Ethnicity	Black African (100%)	Black African (83.33%) White African (11.11%) Indian (5.56%)
Pulmonary TB (%)	100%	0%
Currently on TB treatment (%)	100%	0%
HIV Status (%)	Positive (53.33%) Negative (33.33%) Unknown (13.33%)	0%
Currently on anti-retroviral therapy (%)	50% (of HIV^+ patients) 26.67% (Of total group)	0%
Smoker status	Current (20%) Former (60%) Non-smoker (20%)	Non-smoker (100%)

4.3.1.2 Flow cytometry staining methodology

In order to stain CD1c-restricted T cells in our patient cohort, we employed a similar staining and gating strategy to previously published reports (174, 267, 268). To reduce non-specific staining, we first blocked the PBMCs with 50% human serum and 0.5% BSA. Following washing, the cells were then incubated with 50nM Dasatinib to inhibit downregulation of the TCR upon engagement. To further reduce non-specific binding to our tetramers, we also included a doublet exclusion gate and a CD19 and CD14 exclusion gate in order to remove cell populations known to express the ILT4 receptor which have been reported to bind CD1c (450). The cells were then stained with two CD1c-SL tetramers conjugated to the fluorophores PE and BV421 before staining

with an antibody cocktail including anti-CD3, anti-αβTCR and anti-Vδ1. The gating strategy for this cohort can be viewed in Figure 51.

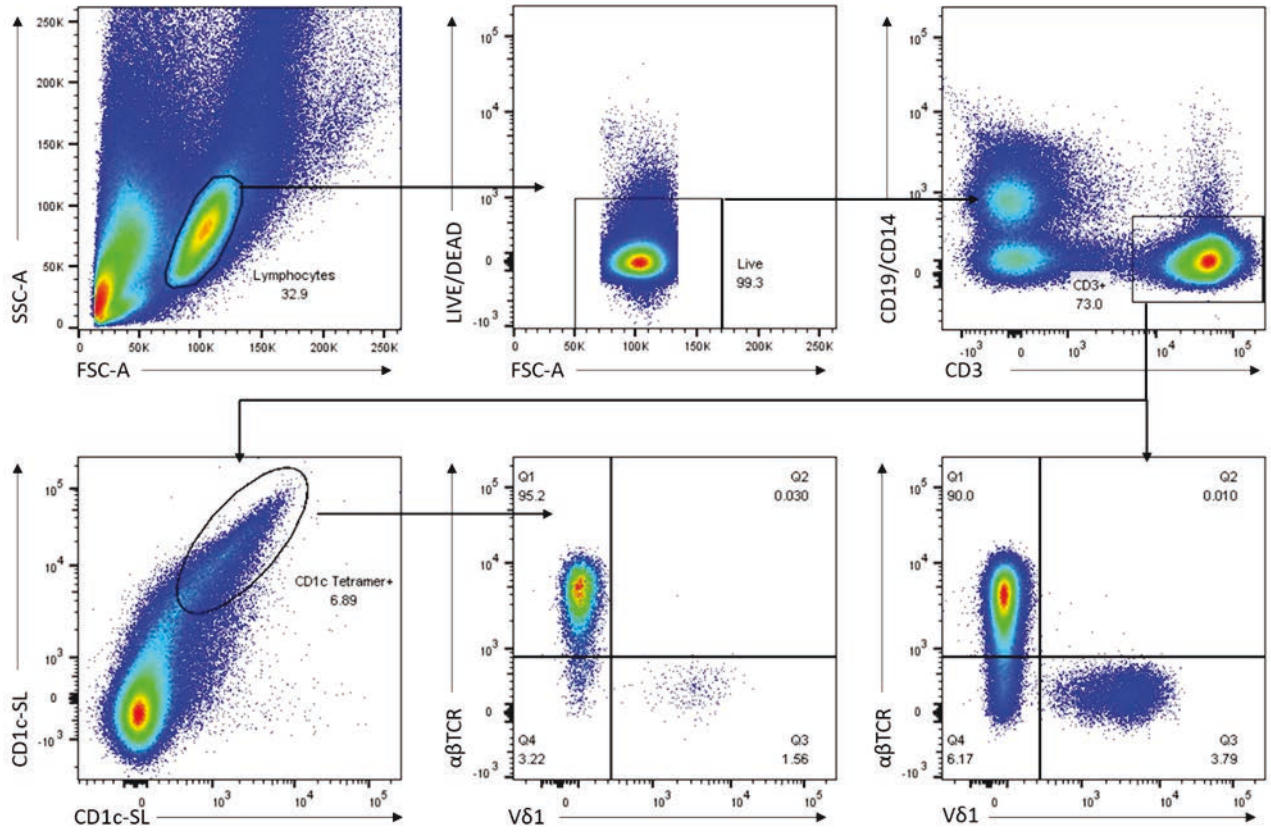

Figure 51: Gating strategy of T cell subsets

Representative flow cytometry dot plots depicting the gating strategy used to identify live $CD3^+$ T cells within the lymphocyte gate. $\alpha\beta TCR^+$ T cells and $V\delta1^+$ T cells within live $CD3^+$ T cells are shown. Live $CD3^+$ PE and BV421 conjugated CD1c-SL tetramer double positive T cells and their corresponding $\alpha\beta TCR^+$ and $V\delta1^+$ T cells are also shown.

4.3.1.3 T cell subsets

Following analysis of the data, one donor from the healthy control group was a clear outlier. It was noted that cells from this donor were of poor viability and were thus removed from all subsequent analysis and data presentation. Although we observed non-significant trends towards a decreased frequency of total circulating T cells and $\alpha\beta TCR^+$ T cells in active TB patients, our results revealed a significant increase in the frequency of circulating $V\delta1^+$ γδ T cells in active TB patients compared to healthy controls (p = 0.0277*) (Figure 52). Our analysis of CD1c $tetramer^+$ populations revealed a non-significant trend towards an increased frequency of CD1c $tetramer^+$ T cells in TB patients (Figure 53). Within the CD1c $tetramer^+$ population, we observed a significantly greater frequency of $\alpha\beta TCR^+$ T cells in TB patients (p = 0.0254*) but also a significantly decreased

αβTCR$^-$ Vδ1$^-$ T cell subset (p = 0.0041**) compared to healthy controls. Furthermore, although not significant, we observed a trend for an increased CD1c tetramer$^+$ Vδ1$^+$ T cell subset in TB patients. Overall, these results suggest an increase in circulating Vδ1$^+$ T cells and CD1c autoreactive T cells in human TB infection.

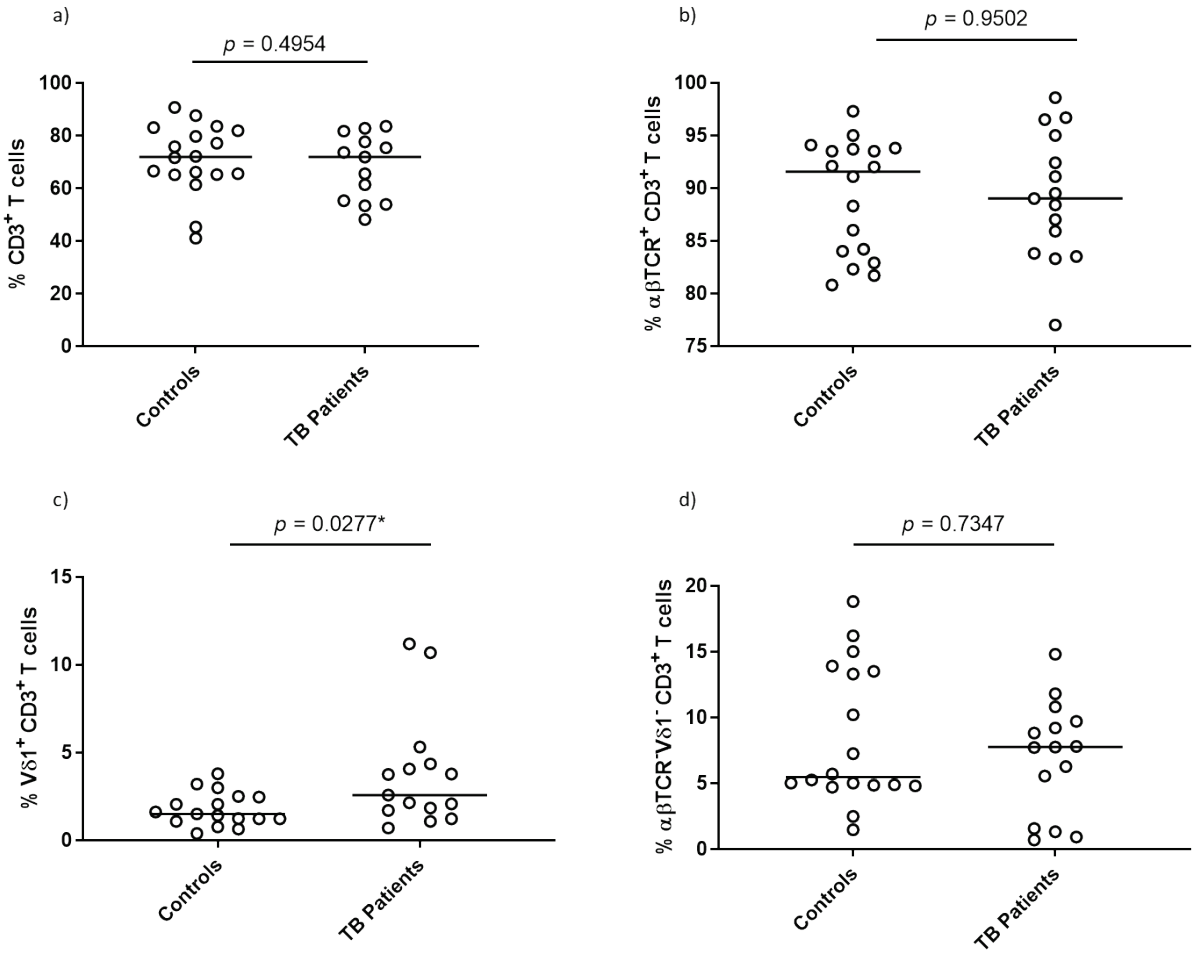

Figure 52: Comparison of T cell subsets between healthy controls and active TB patients in the circulation

Cumulative staining data showing frequency of a) CD3$^+$ T cells, b) αβTCR$^+$ T cells, c) Vδ1$^+$ T cells and d) αβTCR$^-$Vδ1$^-$ T cells in the Live CD19$^-$CD14$^-$ and Live CD19$^-$CD14$^-$ CD3$^+$ population in healthy control and active TB patients. Statistical significance calculated using a Mann-Whitney test.

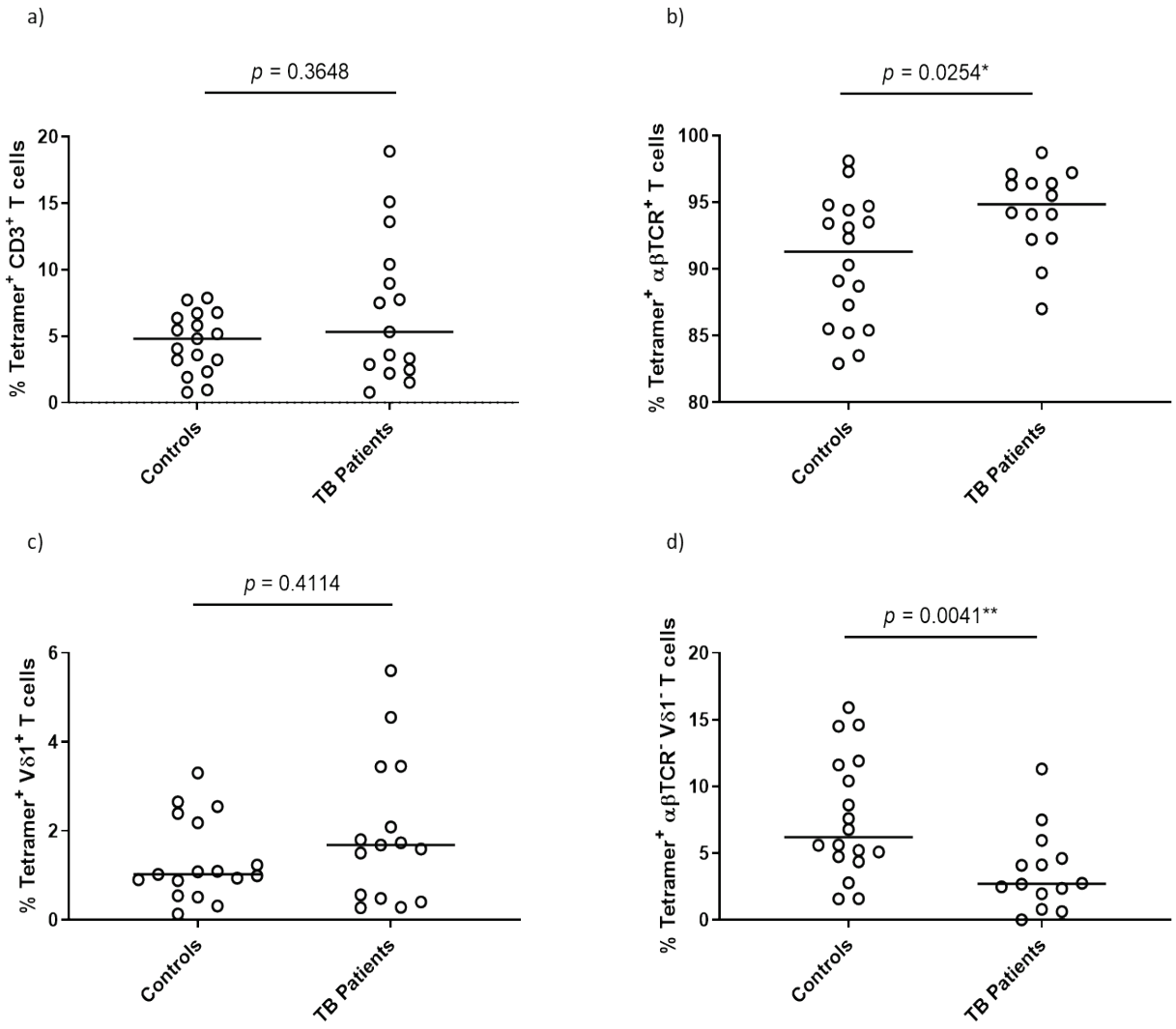

Figure 53: Comparison of CD1c tetramer$^+$ T cell subsets between healthy controls and active TB patients in the circulation

Cumulative staining data showing frequency of a) CD1c tetramer$^+$ CD3$^+$ T cells, b) CD1c tetramer$^+$ αβTCR$^+$ T cells, c) CD1c tetramer$^+$ Vδ1$^+$ T cells and d) CD1c tetramer$^+$ αβTCR$^-$Vδ1$^-$ T cells in the Live CD19$^-$CD14$^-$ and Live CD19$^-$CD14$^-$ CD3$^+$ population in healthy controls and active TB patients. Statistical significance calculated using a Mann-Whitney test.

4.3.1.4 CD1c-restricted T cells in the context of HIV status

Following the categorisation of the TB group by HIV status and the exclusion of two patients whose co-infection status was unknown, the T cell subsets were re-analysed. We categorised the TB group into those that were HIV^+ and HIV^- and analysed the overall T cell frequency between these groups. Our results did not reveal statistically significant differences in the total frequency of $CD3^+$ T cells between each TB patient group and the healthy controls, although a trend towards a decreased $CD3^+$ frequency in both HIV^+ and HIV^- groups is still observable. Within the $CD3^+$ T cell population, there was a trend towards a decreased $\alpha\beta TCR^- V\delta1^-$ T cell subset in HIV^+ TB patients compared to HIV^- TB patients and healthy controls (Figure 54). For CD1c $tetramer^+$ populations, we observed a trend towards increased CD1c $tetramer^+$ T cells in the HIV^+ TB patients. Of CD1c $tetramer^+$ T cell population, TB patients of both HIV^+ and HIV^- status showed a trend towards an increased $\alpha\beta TCR^+$ T cell subset, but a decreased $\alpha\beta TCR^- V\delta1^-$ T cell subset, with a significant decrease of these cells in the HIV^+ TB patients compared to healthy controls ($p = 0.046$*) (Figure 55). Furthermore, we found no statistically significant correlations between the CD4 counts of the HIV^+ TB patients and each of the T cell subsets. However, due to low sample numbers, there was limited power to detect differences.

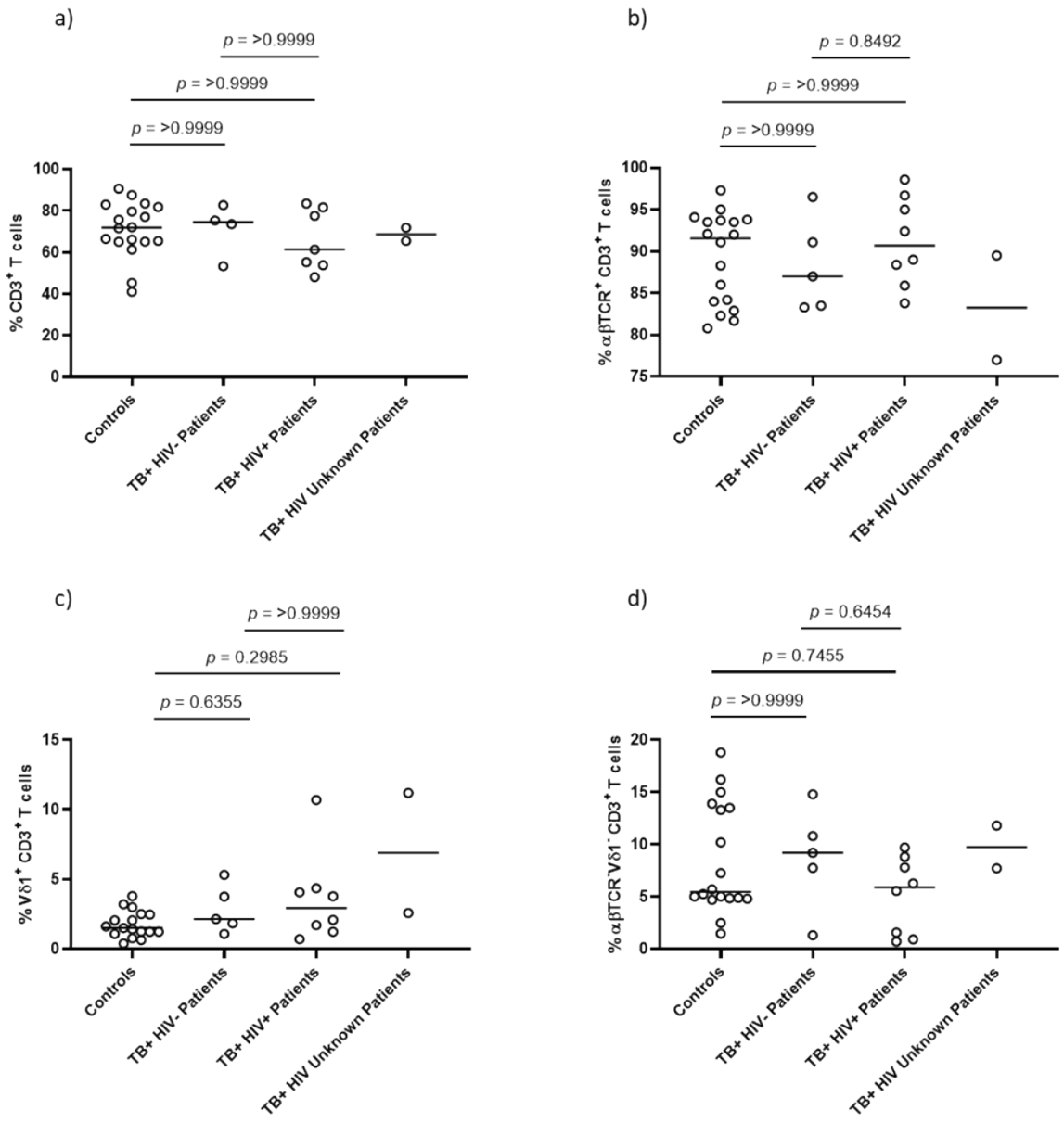

Figure 54: Comparison of T cell subsets between healthy controls and active HIV$^{+/-}$ TB patients
Cumulative staining data showing frequency of a) CD3^{+} T cells, b) αβTCR^{+} T cells, c) Vδ1^{+} T cells and D) αβTCR^{-}Vδ1^{-} T cells in the Live CD19^{-}CD14^{-} and Live CD19^{-}CD14^{-} CD3^{+} population in healthy control and active TB patients subdivided by HIV status. Statistical significance calculated using a Kruskal Wallis test.

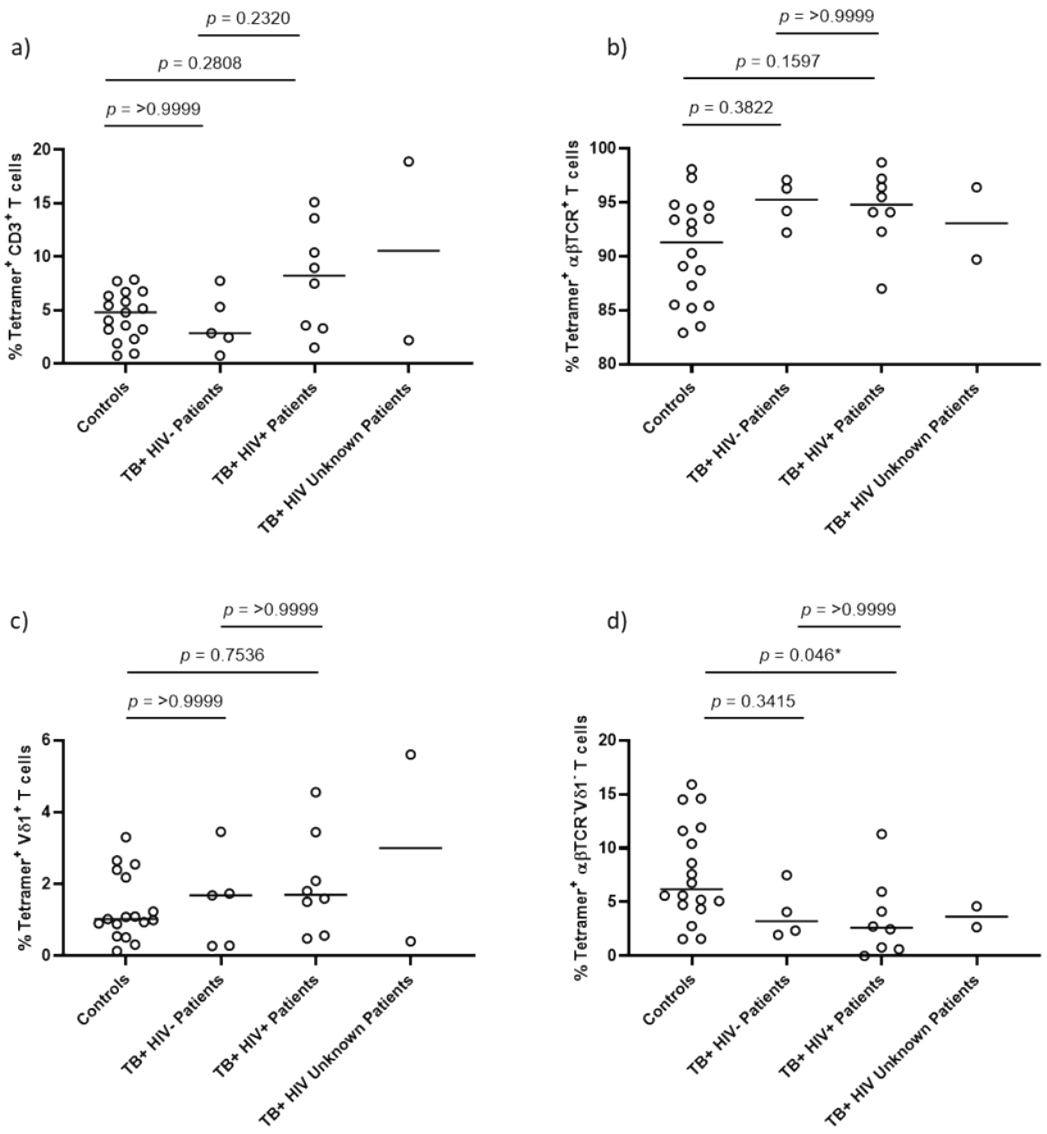

Figure 55: Comparison of CD1c tetramer$^+$ T cell subsets between healthy controls and active HIV$^{+/-}$ TB patients

Cumulative staining data showing frequency of a) CD1c tetramer$^+$ CD3$^+$ T cells, b) CD1c tetramer$^+$ αβTCR$^+$ T cells, c) CD1c tetramer$^+$ Vδ1$^+$ T cells and d) CD1c tetramer$^+$ αβTCR$^-$Vδ1$^-$ T cells in the Live CD19$^-$CD14$^-$ and Live CD19$^-$CD14$^-$ CD3$^+$ population in healthy controls and active TB patients subdivided by HIV status. Statistical significance calculated using a Kruskal Wallis test.

4.3.2 CD1c-restricted T cells in human tuberculosis lesions

TB is primarily a disease of the lung, with hallmark granulomas comprising a range of different populations including T cells. Although $CD1c^+$ DC are present in pleural effusions from TB patients (462), my work is the first to show CD1c expression in human lung granulomas, albeit with uneven distribution. It is not currently known whether CD1c restricted T cells are present within TB granulomas. Furthermore, $V\delta1^+$ T cells are predominantly resident in tissues, not in the circulation, and localised clonal expansions of this subset within the TB lung have recently been identified (200). Critically, we wanted to expand our initial investigation of circulating CD1c responses in TB patients by staining lung biopsy samples with our CD1c-SL tetramers to identify the CD1c-restricted T cell subsets at the site of disease.

4.3.2.1 Patient Cohort Demographics

Cryopreserved PBMCs and lung samples were obtained from fourteen South African patients that had confirmed active TB or had previous episodes of active TB. Patient samples were collected by colleagues at the Africa Health Research Institute, Durban, South Africa in 2019 following lung resection procedures carried out for TB related lung damage. All active TB patients were currently receiving treatment with Rifafour, while the remaining patients in the TB group without current infection had previously been confirmed to have an episode of severe pulmonary TB necessitating surgery for lung sequelae. Nine patients in the TB group were seropositive for HIV, with seven of these confirmed to be receiving anti-retroviral medication. Eleven healthy control donors were selected who were also undergoing surgical lung resection as treatment for non-TB related issues, primarily lung cancer. These donors were confirmed to be negative for active, or previous active TB infection, but HIV status for this group was less well characterised than the TB group. Five of the eleven participants in this group had an unknown HIV status, with treatment status of the two seropositive donors also remaining unknown. It is not known whether any participants in this study had a diagnosis of diabetes mellitus or any other autoimmune disease. The demographic and clinical information for this cohort can be found in Table 8.

Table 8: Demographics and clinical status of the TB group and healthy controls in the lung cohort

Characteristic	TB Group (n = 14)	Healthy Controls (n = 11)
Male (%)	56%	44%
Age (Mean ± S.D.)	39.54 ± 6.95	40.44 ± 15.12
Ethnicity	Black African (92.86%) Unknown (7.14%)	Black African (63.34%) Indian (9.09%) Coloured (9.09%) Unknown (18.18%)
Pulmonary TB (%)	Active (42.86%) Previous (57.14%)	Active (0%) Previous (0%)
HIV Status (%)	Positive (64.29%) Negative (28.57%) Unknown (7.14%)	Positive (18.18%) Negative (36.36%) Unknown (45.45%)

4.3.2.2 Staining Methodology

In accordance with the previous cohort, PBMC and lung sample cells were blocked with 50% human serum and 0.5% BSA before incubating with 50nM Dasatinib. The cells were stained with two CD1c-SL tetramers and the same antibody panel as the previous cohort, with the addition of an anti-Vδ2 to further investigate the $\alpha\beta TCR^-$ population. The addition of anti-CD69 and anti-CD103 antibodies enabled the identification of tissue resident cells, while anti-PD1 was included to assess exhaustion/activation status. Anti-CD11b was included to exclude ILT4 expressing DC. The gating strategy for this cohort can be viewed in Figure 56 and 57.

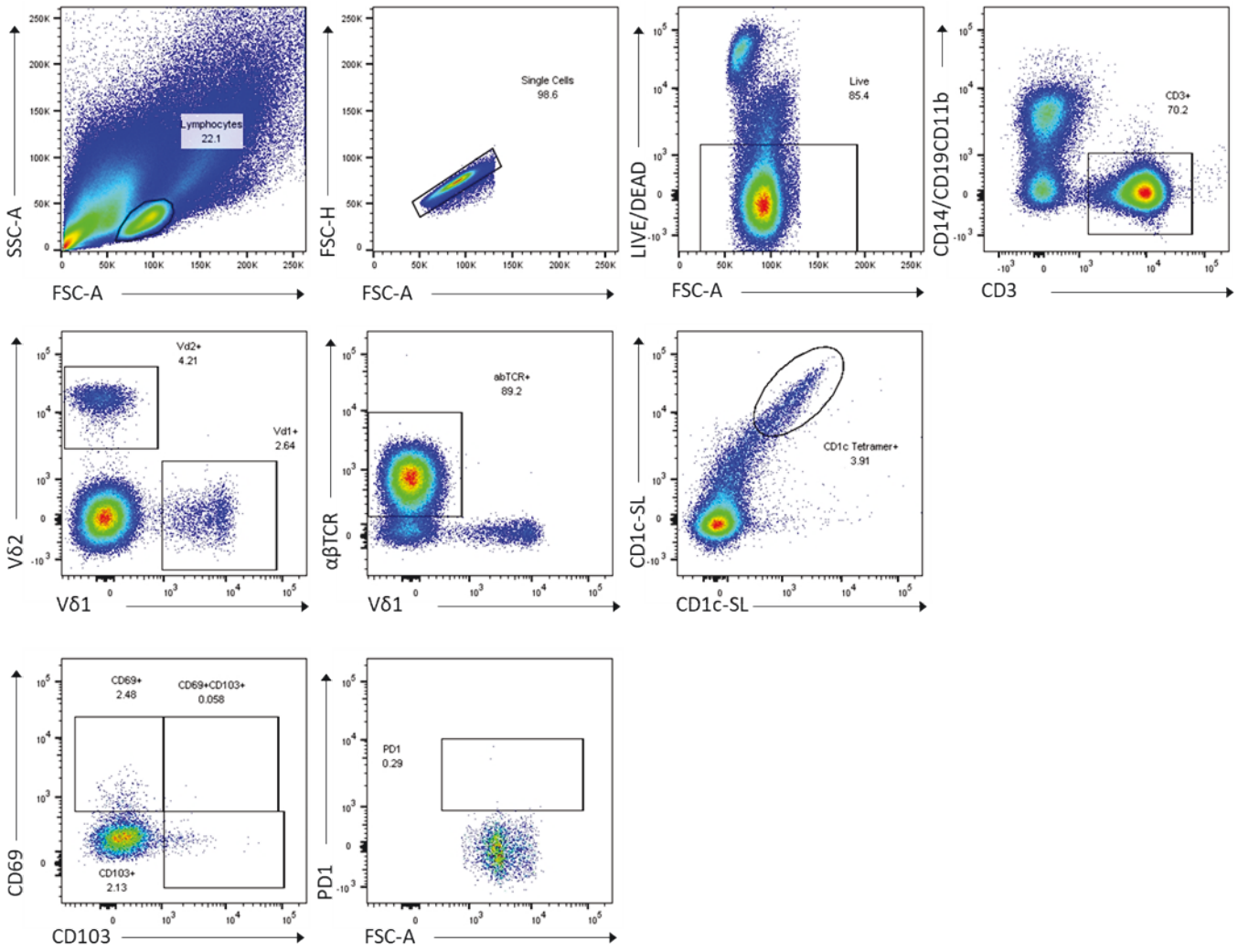

Figure 56: Gating strategy for T cell subsets in PBMC samples that were matched to lung samples

Flow cytometry dot plots representative of the gating strategy used to identify T cell subsets in PBMC samples. Lymphocytes were initially gated on before excluding doublets and dead cells. $CD19^+$, $CD14^+$ and $CD11b^+$ cells were excluded whilst selecting for $CD3^+$ T cells. $V\delta1^+$, $V\delta2^+$ or $\alpha\beta TCR^+$ T cells were then gated before identifying T cells that were double positive for CD1c-SL tetramers. Tissue residency and exhaustion/activation status was then analysed by expression of CD69/CD103 and PD1, respectively.

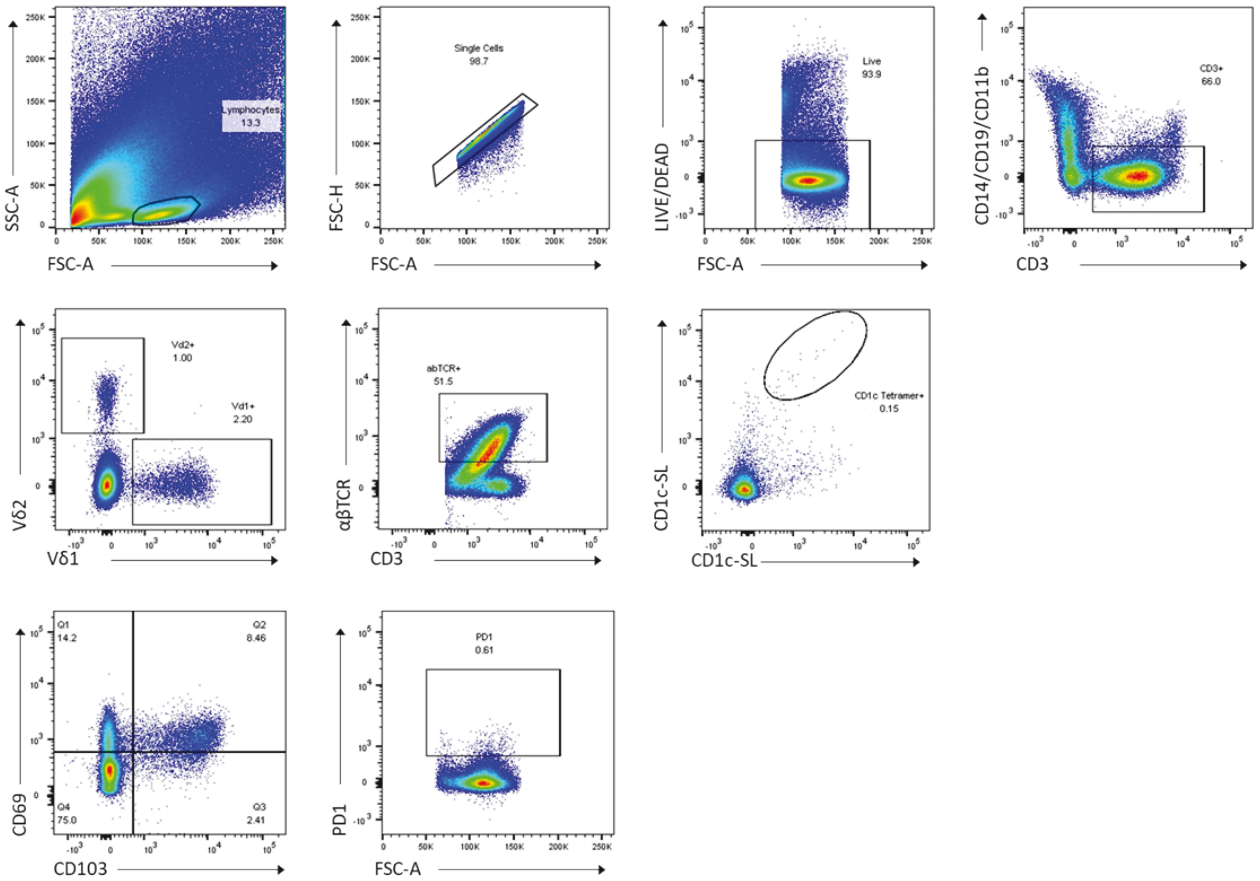

Figure 57: Gating strategy for T cell subsets in lung samples

Flow cytometry dot plots representative of the gating strategy used to identify T cell subsets in Lung samples. Lymphocytes were initially gated on before excluding doublets and dead cells. $CD19^+$, $CD14^+$ and $CD11b^+$ cells were excluded whilst selecting for $CD3^+$ T cells. $V\delta1^+$, $V\delta2^+$ or $\alpha\beta TCR^+$ T cells were then gated before identifying T cells that were double positive for CD1c-SL tetramers. Tissue residency and exhaustion/activation status was then analysed by expression of CD69/CD103 and PD1, respectively.

4.3.2.3 T cell subsets in peripheral blood

In contrast to the previous cohort, there was a trend towards a greater overall frequency of $CD3^+$ T cells in the peripheral blood of TB patients compared to controls, but this was not significant. Of the $CD3^+$ population, individual T cell subsets of $\alpha\beta TCR^+$, $V\delta1^+$ and $V\delta2^+$ γδ T cells were analysed. We found no differences between the T cell subsets in the peripheral blood of both TB patients and controls (Figure 58). Unlike the first cohort, not all individuals within the TB group were classified as having active disease but were included as they were undergoing surgical procedures for TB-mediated lung damage. Absence of active disease may therefore impact circulating T cell populations.

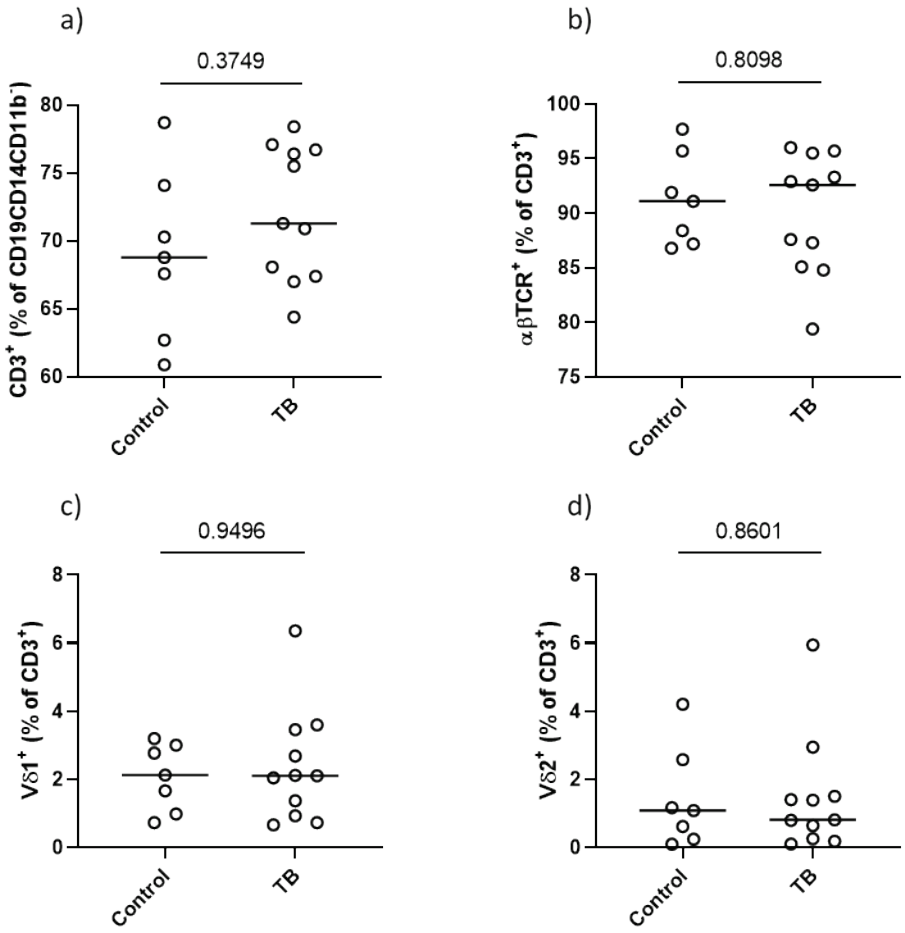

Figure 58: Comparison of circulating T cell subsets in TB patients and controls

Cumulative flow cytometry staining data showing frequency of a) $CD3^+$ T cells in the Live, $CD14^-$ $CD19^-CD11b^-$ population, b) $\alpha\beta TCR^+$ T cells, c) $V\delta1^+$ T cells and d) $V\delta2^+$ T cells in the Live, $CD19^-$ $CD14^-CD11b^-$ $CD3^+$ populations. Statistical significance calculated using a Mann-Whitney test.

4.3.2.4 Expression of $CD69^+CD103^+$ by T cells

Expression of both CD69 and CD103 by T cells has been reported to denote tissue residency with CD69 in particular distinguishing those from circulation (465, 466). We analysed the expression of CD69 and CD103 by each T cell subset and observed a significantly greater proportion of expression for both of these markers in lung samples compared to peripheral blood. This demonstrates that we have accurately defined lung cells in each sample despite potential blood contamination. While there were significantly greater frequencies of $CD69^+CD103^+$ $V\delta2^+$ T cells in the lungs of control patients compared to peripheral blood, the difference was more pronounced in TB patients (Figure 59).

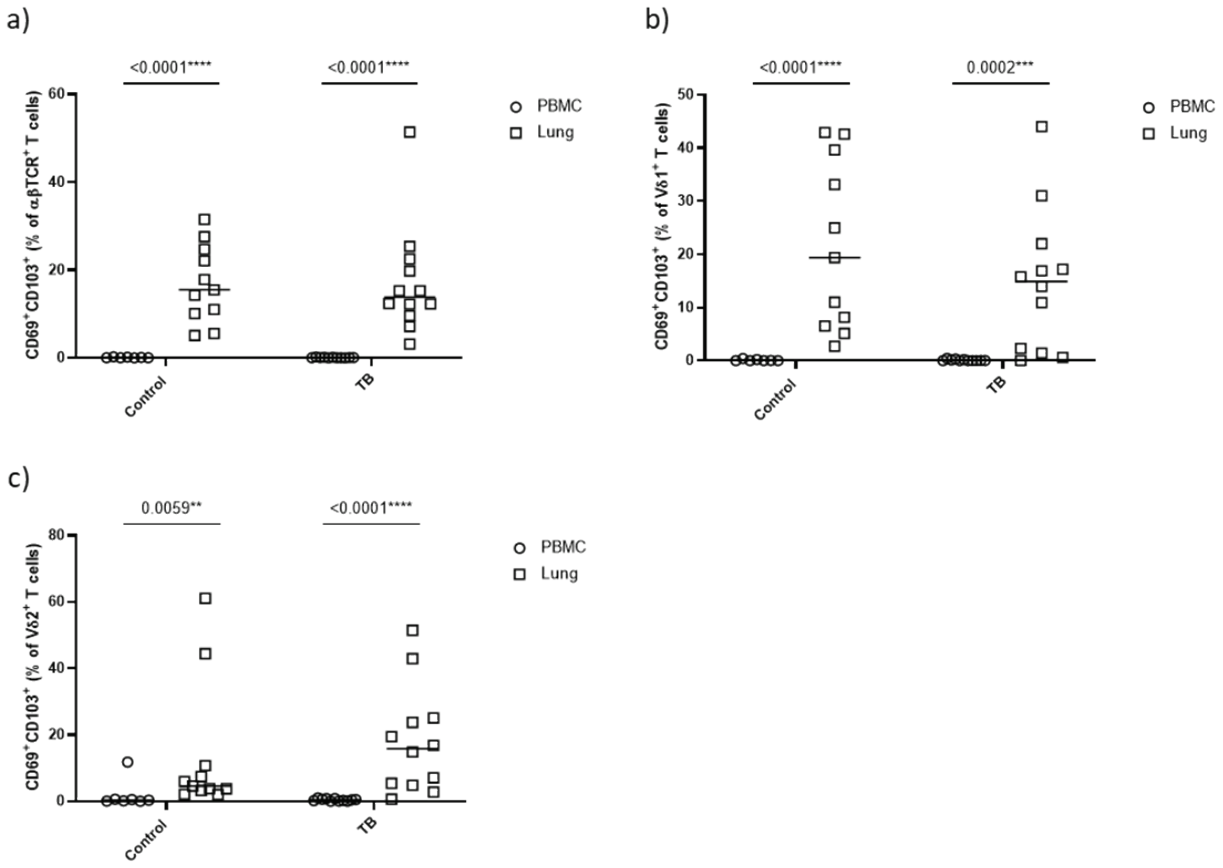

Figure 59: Comparison of CD69$^+$CD103$^+$ T cell subsets between PBMC and lung samples in TB patients and controls

Cumulative flow cytometry staining data showing frequency of a) CD69$^+$CD103$^+$ αβTCR$^+$ T cells, b) CD69$^+$CD103$^+$ Vδ1$^+$ T cells and c) CD69$^+$CD103$^+$ Vδ2$^+$ T cells in the live CD3$^+$ population in the TB and control groups. Statistical significance calculated using a Mann-Whitney test.

4.3.2.5 T cell subsets in the lung

Within the lung, the frequency of overall CD3$^+$ T cells was similar between TB patients and controls. Of CD3$^+$ T cells, there was a trend towards an increased frequency of αβTCR$^+$ T cells in TB patient lung samples compared to control lung. In contrast, there was a trend towards a lower frequency Vδ1$^+$ γδ T cells in TB patient lung samples, but this was not quite significant. Frequencies of lung Vδ2$^+$ γδ T cells was similar between TB patients and controls (Figure 60).

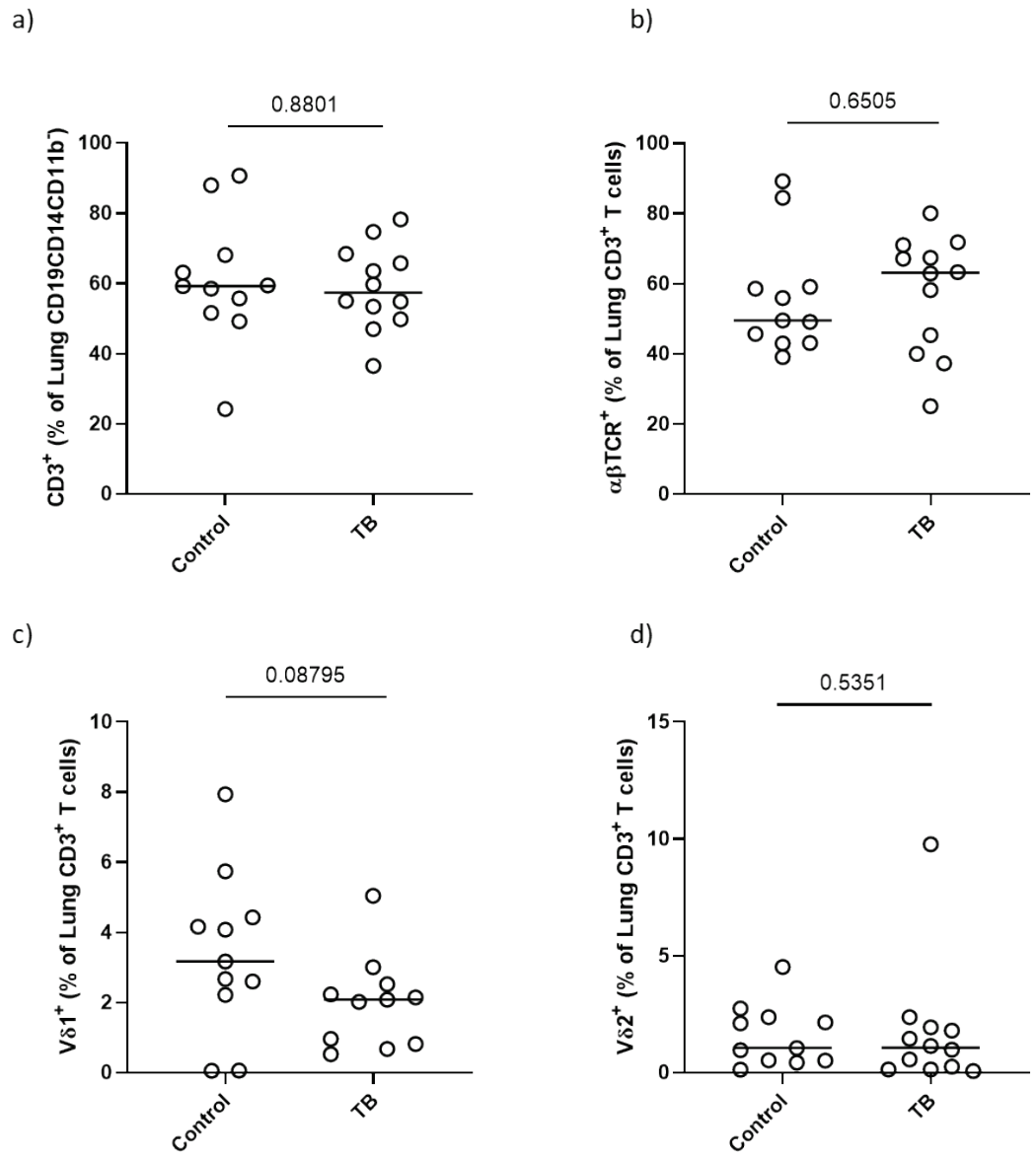

Figure 60: T cell subsets within the lungs of TB patients and controls

Cumulative flow cytometry staining data showing frequency of a) $CD3^+$ T cells, b) $\alpha\beta TCR^+$ T cells, c) $V\delta1^+$ T cells and D) $V\delta2^+$ T cells within the live $CD19^-CD14^-CD11b^-$ and live $CD19^-CD14^-CD11b^-$ $CD3^+$ populations in the lungs of the TB and control groups. Statistical significance calculated using a Mann-Whitney test.

4.3.2.6 T cell subsets in matched PBMC and lung samples

Matched samples of PBMCs and lung cells from each donor that had both samples were analysed together. In the control group, the frequency of overall $CD3^+$ T cells was not significantly different in the lung compared to matched PBMC samples, however lung cells of TB patients showed significantly less frequencies of $CD3^+$ T cells compared to matched blood. Frequencies of $\alpha\beta TCR^+$ T cells were significantly lower in the lungs of both TB and control groups compared to their

matched PBMC samples. In contrast, differences in Vδ1$^+$ γδ T cells between the lung and matching PBMC samples were surprisingly not consistent for either the TB group nor control group, despite this γδ T cell subset recognised as being predominantly tissue resident. There was a trend towards fewer Vδ2$^+$ γδ T cells in the lungs of both groups, but this was not significant (Figure 61). While all other T cell subsets show a reduced frequency in the lung compared to peripheral blood, the Vδ1$^+$ T cell population appears more donor dependent as frequencies of Vδ1$^+$ T cells are not consistently greater in one compartment.

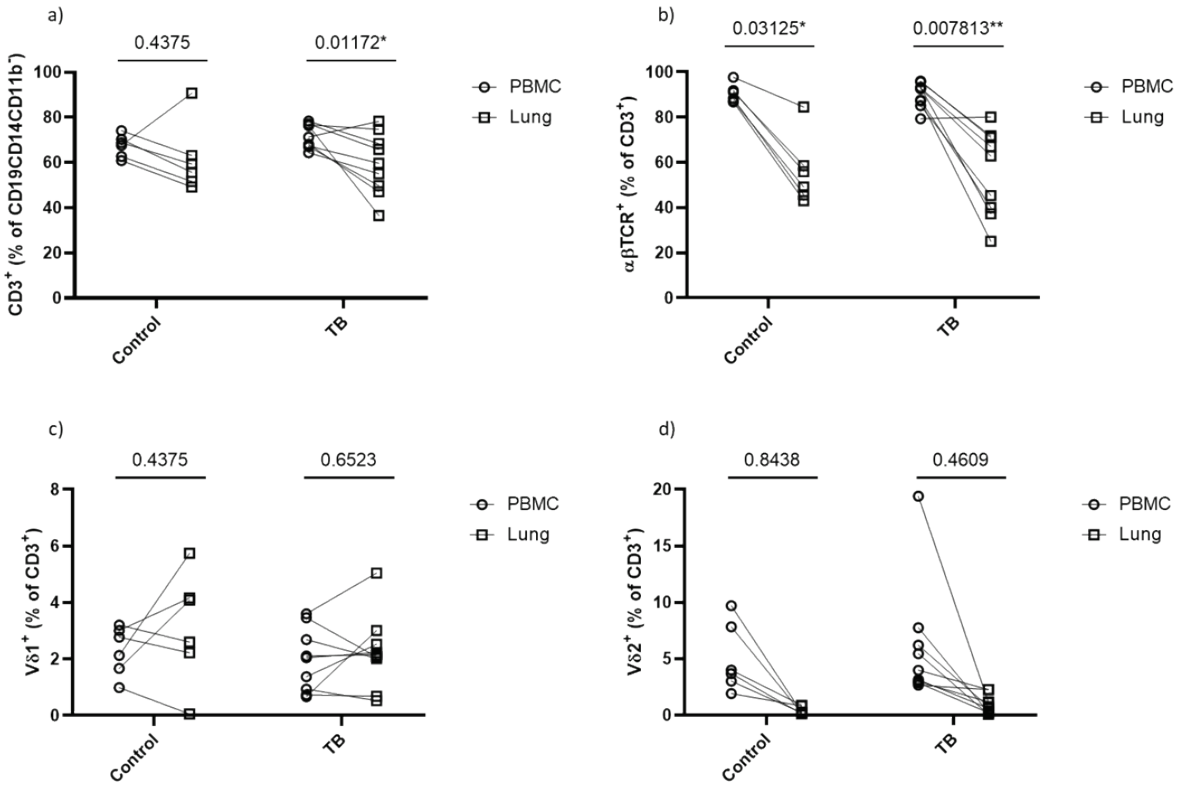

Figure 61: Comparison of T cell subsets between matched PBMC and lung samples in TB patients and controls

Cumulative flow cytometry staining data showing frequency of a) CD3$^+$ T cells, b) αβTCR$^+$ T cells, c) Vδ1$^+$ T cells and D) Vδ2$^+$ T cells within the live CD19$^-$CD14$^-$CD11b$^-$ and live CD19$^-$CD14$^-$CD11b$^-$ CD3$^+$ populations of matched PBMC and lung samples in the TB and control groups. Statistical significance calculated using a Wilcoxon matched pairs signed rank test.

4.3.2.7 PD1 expression by T cell subsets

Expression of PD1 is reported to be associated with activation and/or exhaustion status of T cells. Exposure to antigen leads to an increase in surface expression of PD1 which subsequently puts the 'brakes' on T cell activity to prevent excessive tissue damage (467). We analysed the expression of PD1 on each of the T cell subsets in both lung and PBMC samples from each donor. Similar frequencies of PD1 expression by $\alpha\beta TCR^+$ T cells were observed to be similar in the lungs of TB patients compared to the controls, but when looking at matched lung and PBMC samples within the groups, the frequency of $PD1^+$ $\alpha\beta TCR^+$ T cells was significantly greater in the lungs of the TB group compared to PBMCs (Figure 62). Of the $V\delta1^+$ T cell subset, there was a trend toward a lower frequency of PD1 expression in the lung samples of the control group compared to PBMCs. This was in contrast to the TB group where a greater frequency of $PD1^+$ $V\delta1^+$ T cells were observed in TB lungs compared to PBMC samples. Furthermore, a significantly greater frequency of PD1 expression by $V\delta1^+$ T cells was seen in the lungs of TB patients compared to those of the control group (Figure 63). PD1 expression by $V\delta2^+$ T cells was found to be significantly greater in the peripheral blood of both the control and TB groups compared to the lungs, but no difference in expression was seen in the lungs between the two groups (Figure 63). Therefore, the PD1 expression by $V\delta1^+$ T cells in the lungs suggests that they are activating in response to antigen during disease, suggesting a key role in the host-pathogen interaction.

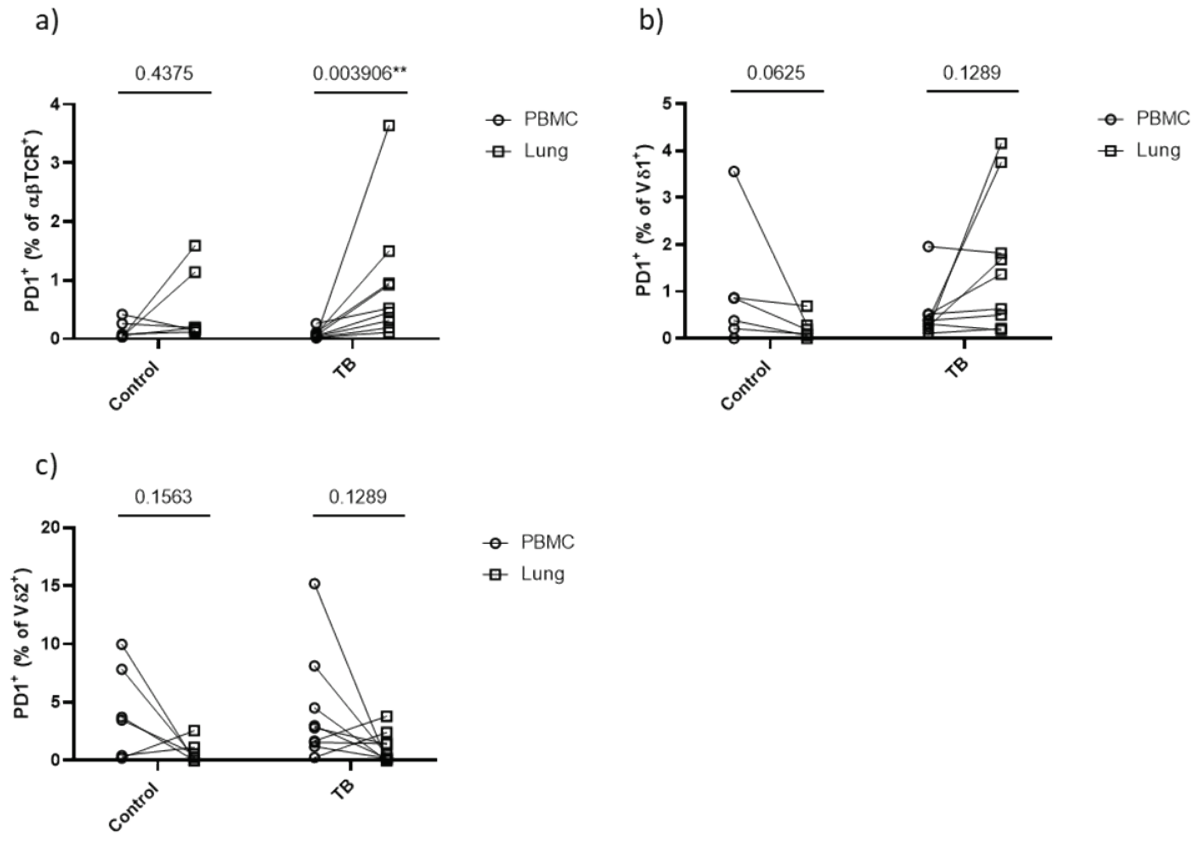

Figure 62: Comparison of PD1 expression by T cell subsets in matched PBMC and lung samples

Cumulative flow cytometry staining data showing frequency of a) $PD1^+$ $\alpha\beta TCR^+$ T cells. b) $PD1^+$ $V\delta1^+$ T cells. c) $PD1^+$ $V\delta2^+$ T cell within the live $CD19^-CD14^-CD11b^-CD3^+$ populations of matched PBMC and lung samples in the TB and control groups. Statistical significance calculated using a Wilcoxon matched pairs signed rank test.

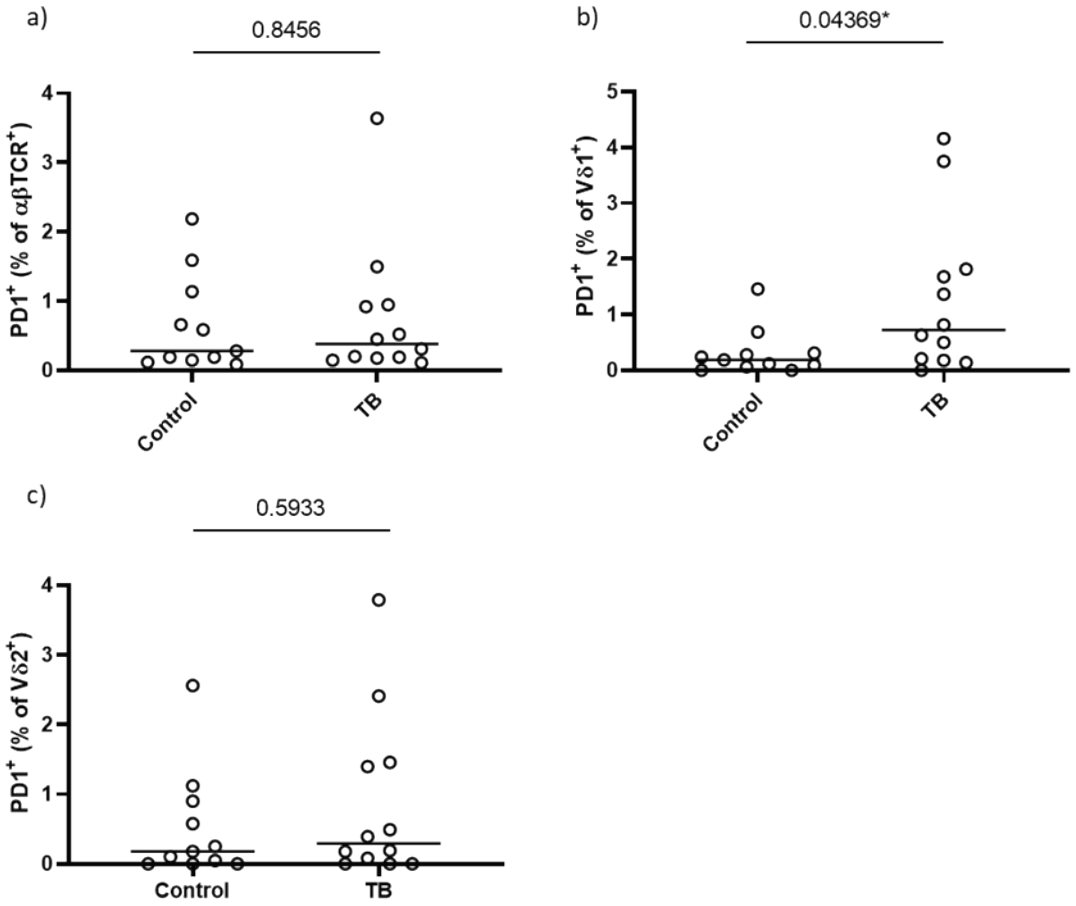

Figure 63: Comparison of PD1 expression by T cell subsets in the lungs of the TB and control groups

Cumulative flow cytometry staining data showing frequency of a) $PD1^+$ $\alpha\beta TCR^+$ T cells. b) $PD1^+$ $V\delta1^+$ T cells. c) $PD1^+$ $V\delta2^+$ T cell within the live $CD19^-CD14^-CD11b^-$ $CD3^+$ populations of lung samples in the TB and control groups. Statistical significance calculated using a Mann-Whitney test.

4.3.2.8 CD1c-SL Tetramer$^+$ T cell subsets

In contrast to the previous cohort, no differences in the frequency of CD1c tetramer$^+$ $CD3^+$, CD1c tetramer$^+$ $\alpha\beta TCR^+$ or CD1c tetramer$^+$ $V\delta1^+$ γδ T cell subsets were found in the peripheral blood between the TB and control groups. This may be due to many of the TB group not currently having active TB disease, but were included in the group as they were undergoing surgical resection of the lung for TB related issues. Within the lung, there was a trend toward a greater frequency of CD1c tetramer$^+$ $CD3^+$ T cells in the TB group compared to the controls. While the CD1c tetramer$^+$ $\alpha\beta TCR^+$ population was observed to be similar in the lungs of both the TB and

control groups, there was a significantly greater frequency of CD1c tetramer$^+$ Vδ1$^+$ T cells in TB lung samples compared to the controls (Figure 64).

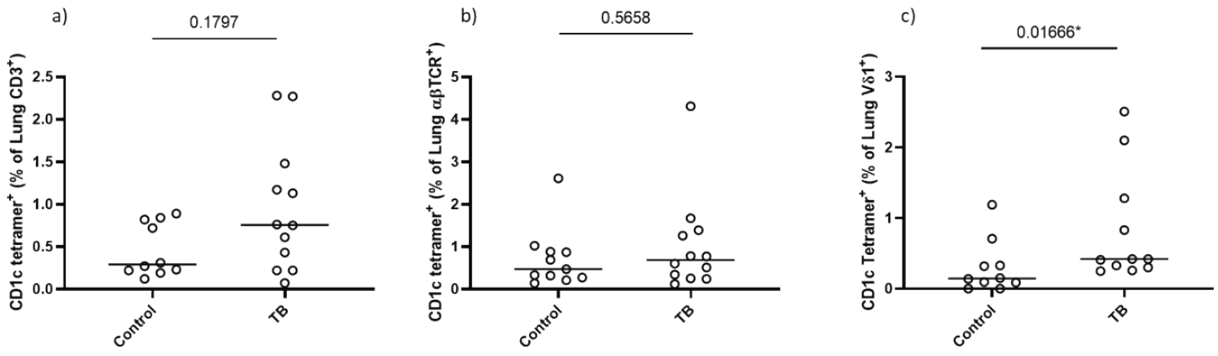

Figure 64: Comparison of CD1c tetramer$^+$ T cell subsets in the lungs of the TB and control groups
Cumulative flow cytometry staining data showing frequency of a) CD1c tetramer$^+$ CD3$^+$ T cells, b) CD1c tetramer$^+$ αβTCR$^+$ T cells and c) CD1c tetramer$^+$ Vδ1$^+$ T cells within the live CD19$^-$CD14$^-$ CD11b$^-$ and live CD19$^-$CD14$^-$CD11b$^-$ CD3$^+$ populations of lungs samples in the TB and control groups. Statistical significance calculated using a Mann-Whitney test.

When comparing the lung to matched PBMC samples, there was significantly fewer CD1c tetramer$^+$ CD3$^+$, αβTCR$^+$ and Vδ1$^+$ T cells in the lungs of both TB and control donors, with the difference being more pronounced in the TB group (Figure 65). Due to low cell numbers, it was not possible to accurately study expression of PD1 by CD1c tetramer$^+$ T cell subsets.

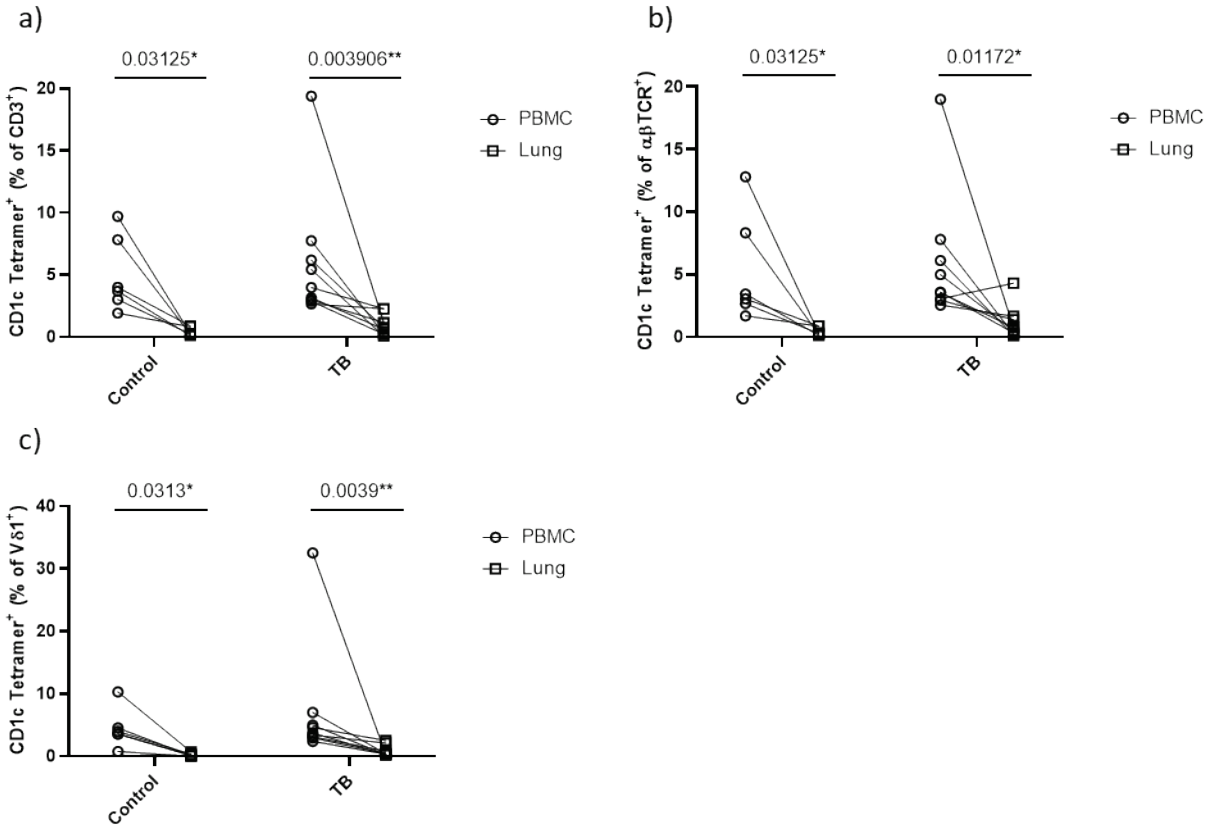

Figure 65: Comparison of CD1c tetramer$^+$ T cell subsets between matched PBMC and lung samples

a) Frequency of CD1c tetramer$^+$ T cells in the CD3$^+$ population. b) Frequency of CD1c tetramer$^+$ T cells in the αβTCR$^+$ population. c) Frequency of CD1c tetramer$^+$ T cells in the Vδ1$^+$ population. Statistical significance calculated using a Wilcoxon matched pairs signed rank test.

4.4 Discussion

4.4.1 Activation induced marker assay

CD1c autoreactive T cells are abundant in the peripheral blood of healthy humans, particularly in the $CD4^+$ and $CD4^-CD8^-$ DN subsets (304). CD1c-restricted T cell lines have also been characterised in human CD1 transgenic (hCD1Tg) mice following challenge with *Mycobacterium tuberculosis* (331). Interestingly, of the derived CD1c-restricted T cell lines, the majority were found to be autoreactive and therefore not specific for mycobacterial lipid antigens (331). The functional response of CD1c autoreactive T cells has previously been investigated by Vincent *et al* (300). Unique CD1-restricted T cell clones, of $\alpha\beta TCR^+$ lineage, were derived from a microbial antigen stimulated T cell population and were revealed to respond to their cognate CD1 antigen presenting molecule in the absence of exogenous antigen (300). However, these T cell clones were also shown to have dual reactivity as a greater response was observed when the CD1-restricted clones were exposed to microbial antigen. Furthermore, dual reactivity of γδ T cells has been reported by Roy *et al* (174) with data demonstrating that $V\delta1^+$ T cells isolated by CD1c-PM tetramers were also reactive to self-lipids such as sulfatide and lysophospholipids.

The use of tetramers to identify and isolate antigen-specific T cells has been gaining popularity in recent years and have been instrumental in the characterisation of many well-known CD1-restricted T cell clones. However, tetramer staining is not without issues as they are known to have higher rates of dissociation and a lower binding avidity than antibodies (287). Furthermore, TCR downregulation upon cognate antigen engagement reduces availability for further staining. In addition, T cells reactive to self-lipids have been reported to bind with lower affinity than to microbial antigens (287, 300, 447). In order to further characterise CD1c-autoreactive T cells irrespective of αβ or γδ lineage, we aimed to employ a tetramer-independent assay to follow T cell proliferation by APC and to gain further insights into their phenotype such as co-receptor status and T-helper phenotype. We optimised a short term expansion method to specifically expand CD1c-restricted T cells in the absence of exogenous antigen and analysed the expression of activation markers. AIM assays have been used as an alternative to, or in combination with classical cytokine based methods to assess antigen-specific T cell responses. Traditional methods employed to analyse the T cell response include the ELISPOT assay and ICS, both are highly sensitive methods commonly used to ascertain the functional response. However, the cytokines to be assessed need to be pre-determined which introduces bias towards the T cell phenotype that can be analysed. Additional T cell information such as co-receptor usage is also unable to be elucidated from the ELISPOT assay, thus preventing the total antigen-specific T cell response being analysed accurately.

The AIM assay overcomes these issues by analysing the expression of activation markers that are induced following TCR engagement. Furthermore, activated cells can then be sorted for further investigation which is not possible following the fixation and permeabilisation steps carried out as part of the ICS assay. We therefore aimed to assess the activation and subsequent expansion of CD1c-restricted T cells following a short term culture and re-stimulation with CD1c expressing antigen presenting cells. Overall, greater levels of T cell expansion, as measured by diminishing CTV signal, were observed in cultures that included APCs. Differences in levels of T cell expansion between those cultured with THP1-CD1c and THP1-KO were recognisable at day 16 of culture following overnight re-stimulation. Significant increases at day 16 in the expression of activation markers $CD69^{+}CD137^{+}$ and $CD25^{+}CD137^{+}$ were seen in T cells re-stimulated with THP1-CD1c compared to THP1-KO, indicating a CD1c-specific response. It has been reported that enrichment of antigen-specific T cells occurs following at least 12 days of culture with cognate antigen (337, 338), corroborating our data which showed a significant difference in levels of activation markers in the presence of CD1c at day 16 but not day 8.

To further characterise the phenotype of the responding T cells, we also stained for CD4 and CD8 co-receptors. The frequency of $CD4^{+}$ T cells increased for each donor over the time course when cultured with CD1c expressing cells, but as this was not seen in the WT APC co-culture or T cell only culture, this may suggest that the expansion of this subset was antigen specific. In contrast, the frequency of $CD8^{+}$ T cells remained relatively stable over the time course, with greater average frequencies being recorded in the T cell only condition. Interestingly, on day 16 when greater levels of expansion were observed, DN T cells were the predominant subset when expanded and stimulated with THP1-CD1c. This supports De Lalla *et al*'s findings of a large frequency of CD1c autoreactive T cells being of the DN T cell subset (304). Expression of activation markers for each of the three T cell subsets peaked at day 16, with slightly greater frequencies of $CD69^{+}CD137^{+}$ and $CD25^{+}CD137^{+}$ DN T cells being observed compared to activation marker positive $CD4^{+}$ and $CD8^{+}$ T cells. The role of co-receptors in thymic selection and functional differentiation has been characterised for MHC-restricted T cells, in addition to facilitating antigen recognition by the TCR (468). However, the functional role for CD4 and CD8 co-receptor involvement in CD1 lipid mediated recognition by T cells is not well described. James *et al* sought to define differences in recognition of CD1b presenting mycobacterial lipids by T cells expressing either the CD4 or CD8 co-receptor (456). They discovered that while both $CD4^{+}$ and $CD8^{+}$ T cells stained with CD1b-SGL tetramers, $CD4^{+}$ T cells bound the tetramers with higher affinity than both $CD8^{+}$ and DN T cells and *ex vivo* data suggested that lipid-specific $CD4^{+}$ T cells may have greater functional avidity (456). Previous studies have also shown that CD4 expression is associated with increased activation and TCR signalling of iNKT cells (469) and T cells recognising CD1b presenting GMM did

so with higher affinity when the CD4 co-receptor was expressed in contrast to $CD8^+$ or DN T cell clones (293). Investigations carried out by Guo *et al* to characterise CD1c autoreactive T cells revealed that stimulation by CD1c expressed on K562 APCs, in the absence of exogenous antigen, consistently activated a population of $CD4^+$ T cells (337). These T cells were of αβ lineage and preferentially expressed TRBV4-1 TCRs. In contrast, Vincent *et al* derived all $CD8^+$ autoreactive CD1-restricted T cell clones from T cells that had been previously stimulated with microbial antigen (300). Unlike the $CD4^+$ T cell clones previously described which had a conserved TRBV4-1 sequence, these $CD8^+$ αβ T cell clones were unique with diverse CDR3 regions (300). Combined with our results showing a larger frequency of activated DN T cells in response to CD1c, we can reason that the CD1c autoreactive T cell response is not restricted to a particular co-receptor subset.

The AIM assay is particularly useful for identifying these diverse populations of CD1-restricted T cells, as multiple phenotypic and functional markers can be analysed simultaneously. Furthermore, the cytokine profile of antigen-specific T cells responding to stimulus has been shown by numerous groups to be diverse, something that may not be accurately assessed by traditional methods (293, 300, 314, 470). Affinity for antigen has been reported to be associated with cytokine profile, with high affinity CD1-restricted $CD4^+$ T cells expressing Th1 cytokines and low affinity T cells expressing Th1 and Th17 cytokines (293). Additionally, although CD1-restricted $CD8^+$ T cell clones were cytolytic and predominantly expressed IFNγ, they were also found to produce Th2 cytokines IL-13 and IL-5 in large quantities (300). This demonstrates that although traditional cytokine based assays are advantageous for quantifying this functional response, they are more valuable when paired with methods such as the AIM assay which take a wider approach to the total population of antigen-specific T cells which may otherwise be underappreciated. In order to further characterise the responding T cells in our experiment, it would be pertinent to better understand these populations at the clonal level to interrogate phenotype and function including their T-helper cytokine profile. Our data suggests that this short term expansion method successfully expands CD1c specific T cells and will be used to derive clonal populations for further study.

We further subdivided our donors into those that were *M.tb* exposed or unexposed to assess whether prior exposure had an effect on the CD1c autoreactive T cell population. It has previously been demonstrated that CD1 tetramers loaded with mycobacterial lipids PM or GMM are able to detect mycobacteria-specific T cells at similar levels in donors with active or latent TB infection, but not in healthy controls (264, 292). Furthermore, studies have shown that T cells exposed to MPD proliferated in a CD1c-dependent manner in donors with LTBI to a significantly greater degree than uninfected control donors (313). However, the effects of *M.tb* infection on activation

and proliferation of CD1c autoreactive T cells is yet to be investigated. In this experiment, we observed greater levels of activation, as measured by CD69 and CD137 expression, in $CD4^+$, $CD8^+$ and DN T cell subsets of healthy *M.tb* unexposed donors when stimulated with CD1c compared to donors with prior *M.tb* exposure. This suggests that there may be a larger frequency of CD1c autoreactive T cells in the peripheral blood of those unexposed to *M.tb*, however, confirmation of this finding requires the study of a larger cohort.

In agreement with previous work, our results confirm the presence of circulating CD1c autoreactive T cells in healthy humans. The optimised methodology described here for short term expansion can now be employed to investigate T cell function. Future work will aim to enrich CD1c autoreactive T cells from *M.tb* exposed and unexposed donors with a view to clone T cells in order to investigate their autoreactive recognition mechanisms, functional prolife and overall phenotype as well as their role in the host pathogen interaction in TB using advanced *M.tb* cell culture models.

4.4.2 Immunohistochemistry staining for CD1c and γδ T cells in human TB granulomas

The cell envelope of *M.tb* has a characteristically high lipid content, with lipids comprising 40% of the total cell envelope weight (471). The ability of CD1 molecules to present lipids to T cells suggests that CD1-restricted T cells specific for *M.tb* lipids could be involved in the host immune response to *M.tb* infection. Of the four antigen presenting molecules of the CD1 family, CD1c surveys the full endocytic system and therefore has access to a broad range of lipids (317). Additionally, CD1c, which is highly expressed on activated B cells and the majority of DC subsets (472, 473), has been reported to present mycobacteria-derived lipids and subsequently activate CD1c-restricted T cells (174, 248). *In vitro* studies have reported that cellular *M.tb* infection is associated with the development of group 1 $CD1^-$ myeloid precursors into competent APCs expressing CD1 proteins (339), further indicating a role for CD1 in the host response to infection. Our group has previously demonstrated the expression of CD1b both within granulomas and adjacent to the caseous core (275), however there is yet no direct evidence of CD1c expression at the site of *M.tb* immunopathology. We therefore sought to investigate the expression of CD1c within TB lesions by using immunohistochemistry techniques to stain *M.tb* infected lung tissue from TB patients. In contrast to what has been demonstrated for CD1b, the majority of CD1c expression in TB lung tissue was observed to be more remote from the caseous core, with the majority of expression found within B cell follicles and areas of inflammatory tissue away from the centre of infection. Interestingly, expression of CD1c appeared low in comparison to the degree of inflammation within each tissue section. Low levels of CD1c expression were observed in a small

number of granulomas, but these were infrequent and not found within each patient tissue section.

Our findings appear to be contrary to other studies which have indicated that CD1c expression is induced or unaffected by *M.tb* infection (339, 474). However, there are also reports which have suggested that *M.tb* infection in fact downregulates expression of CD1c. Previous studies have demonstrated that while *M.tb* infected monocytes are still capable of differentiating into DC, CD1c expression appears to be absent (63, 458, 459). Further investigations into these reports have revealed that suppressed CD1c expression is associated with the upregulation of microRNA-381-3P by DC in TB patients (460). Additionally, BCG infection of DC also induced upregulation of microRNA-381-3P and the subsequent suppression of CD1c (460). However, Inhibition of microRNA-381-3P upregulation consequently prevented the suppression of CD1c and T cell responses against BCG were then promoted (460). These data suggest that the observed lack of CD1c immunohistochemistry staining within TB granulomas may be due to *M.tb* induced downregulation of expression by the cells directly adjacent to the area of infection, potentially as part of its immune evasion strategy. Higher levels of CD1c expression observed away from the focus of infection may indicate areas of a more intact immune response with T cells recognising CD1c presented lipids.

In addition to CD1c, we sought to investigate the presence of γδ T cells within the site of *M.tb* infection. Studies have reported that γδ T cells secreting Th1 cytokines, such as TNFα and IFNγ, accumulate in early mycobacterial lesions (475). *M.tb* infected macrophages secrete MCP-1 and IL-8 which has been shown to induce chemotaxis of γδ T cells; the infected macrophages are then subsequently eliminated by the γδ T cells *in vitro* (475, 476). Furthermore, as γδ T cells recognising mycobacterial lipids presented by CD1c have been characterised it is therefore plausible that CD1c-restricted γδ T cells may respond to *M.tb* at the site of infection within the lungs. We utilised immunohistochemistry staining of lung sections taken from TB patients to visualise γδ T cells at the site of infection. We observed scanty expression of γδ T cells in inflammatory tissues surrounding areas of caseous necrosis, but clusters of γδ T cells were only detected in a minority of granulomas but were not observed in every TB patient. It has been recently reported that individuals with active TB have localised clonal expansions of $V\delta1^+$ γδ T cells in the lungs, a feature which is not observed in healthy control subjects (200). In addition to this, NHP studies have demonstrated that while Vγ2Vδ2 T cells are almost undetectable in the lung tissue of uninfected macaques, increased numbers of Vγ2Vδ2 are observed in the lungs of *M.tb* infected macaques and are present within granulomas in the case of severe disease (477). Further to these conclusions, both of these studies describe how γδ T cell repertoires are highly heterogeneous between granulomas both within one individual, and between individuals (200, 477). These

results are in support of our data, as we did not observe staining of γδ T cells in control lungs, but within the TB lung we confirmed localisation in some granulomas but noted that areas of expression were not homogeneous within one patient or between patients.

Granulomas formed in response to *M.tb* infection are known to be of heterogeneous composition and different types are often found within one individual (200, 478, 479). NHP models of *M.tb* immunopathology have demonstrated that systemic T cell responses differ from those at the site of infection (479). Additionally, while only a small proportion of localised T cells are reported to secrete cytokines, they still demonstrate the ability to control infection (479). Taken together, it is likely that the outcome to *M.tb* infection is dependent upon the granuloma local environment and while small numbers of γδ T cells may be present, they may contribute to anti-*M.tb* immunity. The lack of expression of CD1c within the focus of infection and a tendency for γδ T cells to also reside away from this area may suggest that *M.tb* suppression of CD1c may contribute to a reduction of recruitment and activation of γδ T cells and therefore greater immunopathology.

4.4.3 CD1c-restricted T cells in *M.tb* infected humans

4.4.3.1 CD1c-restricted T cells in the peripheral blood of Tuberculosis patients

Mycobacteria-specific lipids such as MA and PM are known to be presented by CD1 molecules, and have been demonstrated to induce expansion of lipid-specific T cells both *in vivo* and *in vitro* (307, 429, 431). It has recently been reported by Liu *et al* that there is an increase in DC expressing CD1c in both the peripheral blood and pleural effusions of TB patients (312) which raises the question as to whether there is also a simultaneous increase in CD1c-restricted T cells. CD1c is known to present lipid antigens to TCRs of both αβ and γδ lineage, with reports of these T cells recognising either self-phospholipids or mycobacteria-specific lipids (174, 268, 436). However, the effect of *M.tb* infection on the frequency and subset distribution of CD1c autoreactive T cells compared to healthy individuals has not been extensively studied. We therefore set out to characterise the CD1c autoreactive T cell subset distribution in South African TB patients using CD1c tetramers.

We observed a trend towards an increased frequency of $CD3^+$ T cells bound to CD1c tetramers in the TB group compared to the healthy controls. However, the TB group frequencies of CD1c $tetramer^+$ T cells appeared to be on a spectrum, with some demonstrating much higher frequencies than others. This may be due to individual differences and the clinical status of each patient, such as HIV status or stage of TB disease which was unknown. However, when the TB group was divided into those that were HIV^+ or HIV^-, we observed a trend towards an increased frequency of CD1c-restricted T cells in HIV^+ TB patients compared to HIV^- patients and the healthy

controls. There are few reports on the CD1c-restricted T cell population in HIV infection, but a downregulation of CD1c expression by HIV infected cells has been described (480). The modulation of CD1c expression was observed alongside a concurrent reduction in CD1c-restricted T cell stimulation (480).

However, conflicting results from this same study describe a limitation of CD1c downregulation in accordance with HIV induced upregulation of cholesterol synthesis (480, 481). The increased cholesterol production was also shown to induce IFNγ in CD1c-restricted T cells (480). Cholesterol plays a crucial role in successful HIV infection. Cholesterol is involved in maintaining the function of plasma membrane lipid rafts which facilitates entry of the virion and viral budding, and depletion of cholesterol is linked to a reduction in HIV virion production (480, 482, 483). In addition to this, cholesterol is also a key component in the survival and persistence of *M.tb* infection. Cholesterol has been reported as both a requirement of *M.tb* entry into macrophages as well as being used as an important source of carbon to facilitate growth and persistence (484-486). It has been demonstrated in mice that high levels of cholesterol are associated with higher rates of *M.tb* growth and tissue destruction in the lung (487, 488). Cholesterol is also demonstrated to accumulate in human granulomas, where a large population of T cells are also known to congregate (485). It is therefore possible that coinfection with both HIV and TB may lead to increased levels of cholesterol over those with a singular infection, leading to a greater frequency of CD1c-restricted T cells, either from increased expression of CD1c on macrophages or the presentation of cholesterol/cholesteryl esters to T cells. This is further evidenced by reports demonstrating that not only do cholesteryl esters stabilise CD1c, but that they are also presented and recognised by CD1c autoreactive T cells (265).

Investigating circulating T cell subsets of the South African cohort revealed a significantly increased population of Vδ1$^+$ T cells in the TB patients, as well as a trend towards an increased population of Vδ1$^+$ T cells that were CD1c-reactive. Again, a spread of frequencies within the TB group was observed, in both the CD1c-reactive Vδ1$^+$ subset, and the Vδ1$^+$ T cell population as a whole. Separating the TB patients by HIV status did not reveal any substantial differences in Vδ1$^+$ T cells frequencies between HIV seropositivity and seronegativity of the TB patients or to the healthy controls. The subset known to be most notably affected by *M.tb* infection is Vδ2$^+$ T cells, but one study has reported an increase in Vδ1$^+$ T cells in TB patients presenting with anergy to the tuberculin skin test (173, 489, 490). This is in contrast to our results which demonstrate an increase in Vδ1$^+$ T cells in TB patients with a demonstrable reaction to tuberculin.

Vδ1$^+$ T cells are known to be predominantly tissue resident cells; this may suggest that higher frequencies seen within these data could be due to extravasation of these T cells from the lung

into the peripheral blood. It is possible that severity of TB disease for each patient, which was unknown, may have influenced the spread of Vδ1$^+$ T cell frequencies of the TB group. It was expected that HIV seropositivity would have influenced a higher Vδ1$^+$ frequency as it has been demonstrated by Carvalho and colleagues that HIV$^+$ TB patients had higher levels of Vδ1$^+$ T cells in the peripheral blood than healthy controls (491). However, in our study, Vδ1$^+$ T cell frequencies did not appear to be affected by HIV status. This is in contrast to our findings as we did not see an observable difference in Vδ1$^+$ T cells levels between HIV$^+$ TB patients, HIV$^-$ TB patients and healthy controls. As previously discussed, greater levels of CD1c tetramer staining seen in HIV$^+$ patients and the TB group as a whole may be due to greater lipid accumulation, leading to an expansion of CD1c-restricted T cells. Vδ1$^+$ T cells have also been demonstrated to recognise mycobacterial lipids presented by CD1c (174), which could lead to an expansion of CD1c-restricted lipid reactive T cells in the TB patients. However, there are also reports that γδ T cells may respond to CD1 molecules that are absent of pathogenic lipid and instead react to self-lipids presented by CD1c (174, 179). Furthermore, data by Roy *et al* indicates that Vδ1 TCR binding may be mainly directed towards the CD1c molecule itself (174).

Taken together with the knowledge that Vδ1$^+$ T cells can bind CD1c loaded with mycobacterial PM, predominantly CD1c-centric TCR binding may explain why TB patients in our study had an increased level of binding to our CD1c tetramers that were not loaded with any specific lipid. However, binding to our spacer lipid loaded CD1c tetramers is indicative of autoreactive T cells which may be driving TB-related autoreactivity. This is also supported by our observation of a significantly increased population of αβTCR$^+$ T cells in the TB group binding the CD1c-SL tetramers, regardless of HIV status. Vincent and colleagues demonstrated that CD1-restricted T cells that had dual reactivity to self-lipids and mycobacteria-specific lipids were composed of an αβ TCR, were CD8$^+$ and had cytotoxic function (300). As HIV infection predominantly affects the CD4$^+$ T cell population, we can assume that elevated CD1c-restricted αβTCR$^+$ T cell populations seen in both the HIV$^+$ and HIV$^-$ TB patients were CD8$^+$ or DN and were reacting to the CD1c molecule itself as the protein was not refolded in the presence of mycobacterial lipid. Autoreactivity has been suggested as a mechanism of *M.tb* associated pathology as autoimmune-associated antibodies have been detected in a large percentage of TB patients, as well as the occurrence of autoimmune phenome such as erythema nodosum and uveitis (457). Additionally, granulomas are commonly seen in the autoimmune disease sarcoidosis, and are almost indistinguishable from those seen in TB patients, despite the absence of *M.tb* (457). Interestingly, an expansion of Vδ1$^+$ T cells has been found in the lungs of patients with pulmonary sarcoidosis, suggesting these cells are also involved in the tissue destruction seen in autoimmune disease (210). To further investigate this potential CD1c-restricted autoreactive T cell hypothesis, we would need to expand this study to

analyse the CD1c-restricted T cell subsets in the lung lesions of TB patients using our CD1c-SL tetramers.

Finally, an unexpected finding emerged from this data: there was a significantly reduced frequency of T cells in the TB group that were neither TCRαβ$^+$ nor Vδ1$^+$. A large spectrum in frequencies of this particular subset was also noted for the healthy controls. This may be due to individual differences in immune system composition or underlying morbidities, as it is not known whether the healthy controls were indeed completely healthy. No tests were conducted to investigate LTBI, presence of CMV or other diseases and infections which may have had an effect on frequencies of this subset of T cells for particular individuals in the healthy control group. However, even though flow cytometric analysis determined these cells were neither TCRαβ$^+$ nor Vδ1$^+$, we do not know the exact phenotype of this population of T cells. It is possible that these T cells may have also carried the TCRδ chain, but it is currently only the Vδ1$^+$ T cell subset that is known to recognise CD1c. As this TCRαβ$^-$ Vδ1$^-$ subset of the healthy controls was significantly greater than TB patients within the CD1c tetramer$^+$ population, it suggests that there may be another TCRδ subset which recognise CD1c and are diminished in TB disease. There are only three true Vδ genes in humans: Vδ1, Vδ2 and Vδ3. Although Vδ genes 4-8 exist, they are formed from the inclusion of Vα genes in Vδ rearrangement and therefore can be distinguished as Vδ or Vα (184). The available literature has thus far determined that Vδ2 cells recognise phosphoantigens in the presence of butyrophilin 3.1 but independently of CD1, and Vδ3 cells recognise CD1d but not the group 1 molecules (184, 206, 492), however specific evidence against these cells binding to CD1c is lacking. In addition, there has as of yet been no investigation into whether T cells with Vδ4-8 chains are able to recognise CD1 molecules or whether they are bound by anti-TCRαβ antibodies as their rearrangement includes Vα genes. As this finding of decreased CD1c tetramer$^+$ TCRαβ$^-$ Vδ1$^-$ T cells was also found in TB patients with or without HIV coinfection, we can conclude that this result was not a result of HIV coinfection but was driven by TB. To investigate the identity of this population, staining with antibodies for other TCRδ chains could be included as well as antibodies for Ig-like transcript 4 (ILT4). ILT4 is the only other molecule, besides the TCR, which is known to bind CD1c (450). Although ILT4 is expressed primarily by APCs, blocking this molecule or positive antibody staining would reveal whether it has contributed to the CD1c tetramer$^+$ TCRαβ$^-$ Vδ1$^-$ T cell frequencies observed here.

Although useful information has been garnered from this study, we could expand upon this data in a variety of aspects. Before testing a greater number of patients to improve and reliably identify statistical significance of the T cell subset frequencies, we need to confirm the specificity of our CD1c tetramers. The addition of a third tetramer that is either irrelevant or composed of another CD1 molecule could be included. Negative staining of the double CD1c tetramer$^+$ cells

with this third tetramer would provide more confidence that these cells are CD1c specific. Additionally, T cells binding the CD1c tetramers could also be tested for IFNγ release, a measure of T cell activation through binding its cognate antigen (236, 493). Further investigations could also include CD1c tetramers refolded in the presence of mycobacteria specific lipids such as PM, and lipids shared by both the bacterium and the host such as PG. This would allow us to investigate the presence of lipid specific T cells in both healthy controls and TB patients and whether T cells with dual reactivity to shared lipids are associated with pathology. However, our key goal includes utilisation of our CD1c tetramer in lung lesion samples from TB patients. The collection of data including increased CD1c expression in TB patient pleural effusions (462), accumulation of lipids in TB-associated granulomas (485), and an expansion of the tissue resident $V\delta1^+$ T cells in lung granulomas of pulmonary sarcoidosis patients (210) leads us to hypothesise that there may be an increase of CD1c-restricted $V\delta1^+$ T cells in the lungs of TB patients. Evidence of this, along with the knowledge of whether these T cells prevent or exacerbate damage, would allow us to design agents to augment the response.

4.4.3.2 CD1c-restricted T cells in tuberculosis lung lesions

TB is primarily a disease of the lung, with hallmark granulomas being formed by an array of cells including T cells, B cells and fibroblasts surrounding infected macrophages to prevent the spread of the pathogen (2, 15). It is therefore logical to study the immune response to *M.tb* infection at the site of disease in addition to immunological markers in the periphery. It has been reported that CD1-restricted T cells, MAIT and γδ T cells may be involved in the early stages of the response to *M.tb* infection (494) with IL-17 producing γδ T cells being reported as an essential player in the formation and maturation of granulomas (197, 198). CD1c has been shown to present a variety of lipids, including mycobacterial PM, cholesteryl esters and phospholipids obtained from the host and/or pathogen (264-266). In addition to a TB-specific increase in pleural $CD1c^+$ DC (462), this suggests that CD1c-restricted T cells are involved in the host response to TB. T cells restricted to CD1b and CD1d have been demonstrated in the lungs during TB infection (200), but as of yet, CD1c-restricted T cells have not been described in this context.

As CD1c-restricted T cells can be of either αβ or γδ lineage, we aimed to investigate the frequency and phenotype of CD1c-autoreactive T cell subsets within the lungs and matched blood samples of TB patients. To further expand upon the data obtained from our previous South African cohort, we analysed the T cell subsets within the PBMC samples from both the TB and healthy control groups. Compared to the previous cohort, we found that circulating frequencies of each T cell subset were similar between the TB and control groups. The variation in peripheral blood T cell subsets may be explained by differences in the TB group included within this second cohort. The

TB group in the previous study was comprised of donors that were confirmed to be suffering with active TB disease, while in this second cohort, we aimed to include PBMCs that were from donors that had matching lung samples. Lung samples were acquired from patients that were undergoing surgical lung resection associated with TB related issues and were not necessarily suffering from active disease at that time, therefore several of the patients had previously treated TB, not active disease. We demonstrated in our previous work that HIV status of the donors did not affect the spread of the data, so we can assume in this cohort that similar frequencies of T cell subsets may have been affected by lack of TB disease and not HIV coinfection.

In this second cohort, we also investigated frequencies of Vδ2$^+$ T cells in the peripheral blood and observed similar circulating frequencies between the TB group and controls. This is in contrast to published data reporting a reduction in circulating Vδ2$^+$ T cells in active TB patients (200, 201). However, as the TB group in our study comprised those with past active TB and not necessarily current active TB, this may have contributed to the similar frequencies seen to the control group. Data from both humans and NHP studies have demonstrated an elevation in the circulating Vδ2$^+$ T cell subset in BCG vaccinated individuals or those who are household contacts of active TB patients (203-206). South Africa has one of the highest incidence rates of TB worldwide and BCG vaccination is routinely given (1, 495, 496), so it is not unreasonable to assume that donors in the TB or control group may have been exposed to TB through household contacts or vaccination and therefore may have an elevated frequency of Vδ2$^+$ to a comparable level.

Within the lungs, while we observed a trend for reduced Vδ1$^+$ T cells in the TB group, there was a significantly increased frequency of CD1c tetramer$^+$ Vδ1$^+$ T cells in the lungs of the TB group compared to controls. Ogongo and colleagues had previously demonstrated that CD1b- and CD1d-restricted T cells are present in the lungs of TB infected patients, but our work demonstrates that frequencies of CD1c-restricted T cells are also elevated (200). Data from this group further probes the Vδ1$^+$ T cell population in the lungs, reporting that the repertoire of δ chain bearing T cells in TB patients were dominated by the Vδ1$^+$ subtype with a significantly higher degree of localised clonal expansions (200). They also found that clonality of Vδ1$^+$ T cells was greater in the lungs than in peripheral blood samples, and only 7% of the lung clonotypes were found in the blood (200). These non-overlapping populations of γδ T cells may suggest that antigen-specific T cells in the context of TB may be localised to the lung. A reduction of Vδ2$^+$ T cells has been reported in the peripheral blood of active TB patients and it has been suggested that these cells may have been recruited to the lung (200, 201). However, in support of our observations, Ogongo and colleagues also found similar frequencies of Vδ2$^+$ T cells in the lungs of both TB patients and controls, indicating that any loss of Vδ2$^+$ T cells from the blood was not associated with lung recruitment (200).

To assess tissue residency of the T cell subsets, we also analysed expression of CD69 and CD103. It has been reported that TB-specific T cells that are resident in the lung could have protective activity (200). In contrast to our expectations, we observed a trend for a decreased $CD69^{+}CD103^{+}$ $V\delta1^{+}$ T cell subset in the lungs of TB patients but an increase in tissue resident $V\delta2^{+}$ T cells compared to controls. In contrast to our findings, a reduction in tissue resident $V\delta2^{+}$ T cells, specifically the Vγ9Vδ2 subset, has been reported in the BAL fluid of TB patients, coupled with an impaired response to antigen stimulation (497). However in support of our data, a specific clonal expansion of $V\delta2^{+}$ T cells has been reported in the lungs of TB patients which may explain the increase we observed in the lungs of TB patients (200).

Unfortunately, due to low frequencies, we were unable to accurately assess frequencies of CD69 and CD103 expression by CD1c $tetramer^{+}$ populations. Studies involving adoptive transfer of CD1-restricted αβ and γδ T cells in transgenic mice and NHPs, respectively, have revealed migration of these cells back to the lungs and attenuation of *M.tb* infection, demonstrating a protective function of these lung-resident CD1-restricted T cells (148, 209). Although we were unable to properly assess function of lung resident CD1c-restricted T cell subsets in our cohort, these studies suggest a similar role for CD1c-restricted T cells in human TB.

The work by Ogongo *et al* suggests that expansion of antigen-specific T cells in the lung at the site of disease gives rise to the observed populations of clonally expanded T cells (200). While we were able to elucidate frequencies of CD1c-restricted T cell populations, we also aimed to assess activation phenotype of these cells through expression of PD1. PD1 is expressed by cells in response to persistent antigen-induced activation and acts as a suppressor to the adaptive immune response (498). We observed significantly greater frequencies of $PD1^{+}$ $V\delta1^{+}$ T cells in the lungs of the TB group compared to the controls, indicating that these cells are likely to have been responding to antigen. Negash *et al* has previously demonstrated a significant increase in the frequency of peripheral blood $V\delta1^{+}$ T cells expressing PD1 and the activation marker CD38 in TB patients compared to healthy controls (212), with the expression of PD1 demonstrated in the lungs of active TB patients by various groups (499, 500). Immunohistochemical staining has revealed expression of PD1 within human TB granulomas (499, 500), but is absent at sites of immunopathology such as caseating necrosis (500).

Expression of PD1 by T cells has been revealed as being an important component in controlling the immune response and preventing excessive immunopathology. Reports have emerged of patients developing TB following treatment for cancer with PD1 checkpoint inhibitors (501-504). The binding of PD1 to its ligand PD-L1 expressed by T cells, B cells and antigen presenting cells, triggers the PD1 expressing cell to ignore TCR mediated signalling and therefore the adaptive

immune response is inhibited (505). This mechanism prevents an excessive immune response and promotes self-tolerance and thus avoids autoimmunity. PD1 checkpoint inhibitors prevent the binding of PD-L1 to PD1, thus removing the brakes of the previously controlled T cell response to their cognate antigen (498). In the context of cancer, checkpoint inhibitors allow for the destruction of the tumour by activated and unsuppressed T cells. However, it has been shown that in the context of TB, expression of PD1 is critical for control of the disease. $PD1^{-/-}$ mice have been observed to be highly susceptible to TB and succumb to the disease faster than mice with intact PD1 expression (79, 506). Findings from Tezera *et al* also demonstrate that PD1 is necessary for regulation of the immune response to TB, with inhibition of PD1 expression leading to an increase in *M.tb* growth through excessive cytokine secretion (500). Their group also found that PD1 expression by $CD4^+$ and $CD8^+$ T cells was increased in the lungs when compared to matched blood samples (500). This supports our observation of significantly increased frequencies of PD1 expressing αβ T cells in the lungs of TB patients compared to matched blood samples, a finding which was not seen in the control group. We also observed increased PD1 expression by $V\delta1^+$ T cells in the lungs of TB patients compared to matched blood. In contrast, there was a decrease in $PD1^+$ $V\delta1^+$ T cells in lung samples of the control group compared to their matched blood, suggesting less activation of these cells within the healthy lung. In addition to our other findings, this further supports the hypothesis that $V\delta1^+$ T cells play a protective function in the response to TB.

Whilst acquiring peripheral blood and lung samples by flow cytometry, we sorted single CD1c $tetramer^+$ and CD1c $tetramer^-$ and $V\delta1^+$ T cells from both the TB and control groups into PCR plates. We intended to employ the same method of separating and amplifying the γ and δ TCR chains that we previously used to sequence γδTCRs from our γδ enriched T cell lines. However, following sorting and storage of the sorted cells, we were then unable to undertake the RT-PCR required before shipping the cDNA back to the UK from Durban, South Africa due to the COVID-19 pandemic. Viability of cells following long term storage at -80°C is poor, thus when the sorted samples were subjected to RT-PCR following 9 months of storage, no bands were visible on an agarose electrophoresis gel. Successful separation, amplification and sequencing of CD1c $tetramer^{+/-}$ $V\delta1^+$ T cells from both peripheral blood and lung samples would have revealed more information on whether TCR chain usage differed between CD1c-restricted $V\delta1^+$ T cells, and whether CD1c-restricted clonotypes differed between the lung and blood. However, despite unsuccessfully identifying specific CD1c-restricted TCR chain usage, we did observe significantly increased frequencies of PD1 expression by $V\delta1^+$ T cells in the lungs of the TB group, indicating an antigen specific response. In addition to this, we also observed a significant increase in CD1c $tetramer^+$ $V\delta1^+$ T cell population in the lungs of the TB group, indicating that this subset may be

specifically expanded in response to *M.tb* infection. To further investigate the CD1c autoreactive immune response in TB, it would be pertinent to identify specific CD1c-restricted TCRs in the lung and peripheral blood of active TB patients and interrogate their response to lipid antigens shared between the host and pathogen such as PG and PI.

Chapter 5 CD1-restricted T cells in the macaque model

The impact of *M.tb* on the profile and function of responding T cells from the point of initial infection and the subsequent course of disease is almost impossible to monitor accurately in humans. The physiology and immunology of the macaque is nearly identical to that of humans and with high levels of conservation in the genes encoding the CD1 proteins, making them an ideal model in which to investigate the CD1-restricted immune response to *M.tb* infection. In human TB patients, decreased levels of CD1d-restricted iNKT cells have been observed, but with an increased population in those with latent infection (169, 507), suggesting a role for these cells in immune defence. iNKT cells have been demonstrated in a variety of macaque species and have been shown to produce IFNγ in response to stimulation (31, 508). However, the frequency and function of these cells has not been closely studied from pre-infection and through the course of subsequent active and latent disease following *M.tb* challenge. While the association between macaque iNKTs and outcome of *M.tb* infection is starting to be explored, the role of CD1c-restricted T cells in the macaque model is even less well understood. Two studies have touched upon the recognition of macaque CD1c by T cells (377, 378), but as of yet the frequency and function of these T cells in disease remains largely unexplored. Furthermore, while CD1d tetramers have been validated as a useful tool in identifying and isolating CD1d-restricted T cells in the macaque, there is as of yet just one recent report of the use of macaque CD1c tetramers (376). This study built upon work by Morita and colleagues by using GMM pulsed macaque CD1c tetramer to isolate and investigate cross-species reactivity of macaque CD1c-restricted T cells (376, 378). However, as the function and phenotype of CD1 autoreactive T cells in humans are beginning to be unravelled, the presence of these T cells in the macaque remain completely unknown.

5.1 Macaque CD1d-restricted T cells

5.1.1 *Ex vivo* iNKT staining

We have previously shown that iNKT cells in macaque can be specifically stained with human CD1d-α-GalCer tetramers (31). Furthermore, iNKT phenotypes are seemingly associated with outcome as we have shown previously that there is a trend between an increased $CD8^+$ iNKT subset and reduced total lung pathology following *M.tb* challenge (31). To further investigate whether iNKT numbers and function changed with time during *M.tb* infection, blood samples were collected from three Rhesus macaques from the day of infection and every 2 weeks following until necropsy. Uninfected samples from the day of challenge were used to study the

change in iNKTs from pre- to post-infection, and to determine whether sample fixation would affect CD1d tetramer staining efficiency. We found that fixation of the PBMCs in 2% paraformaldehyde for 15 minutes following antibody staining did not significantly alter iNKT staining for any of the animals. The gating strategy can be viewed in Figure 66.

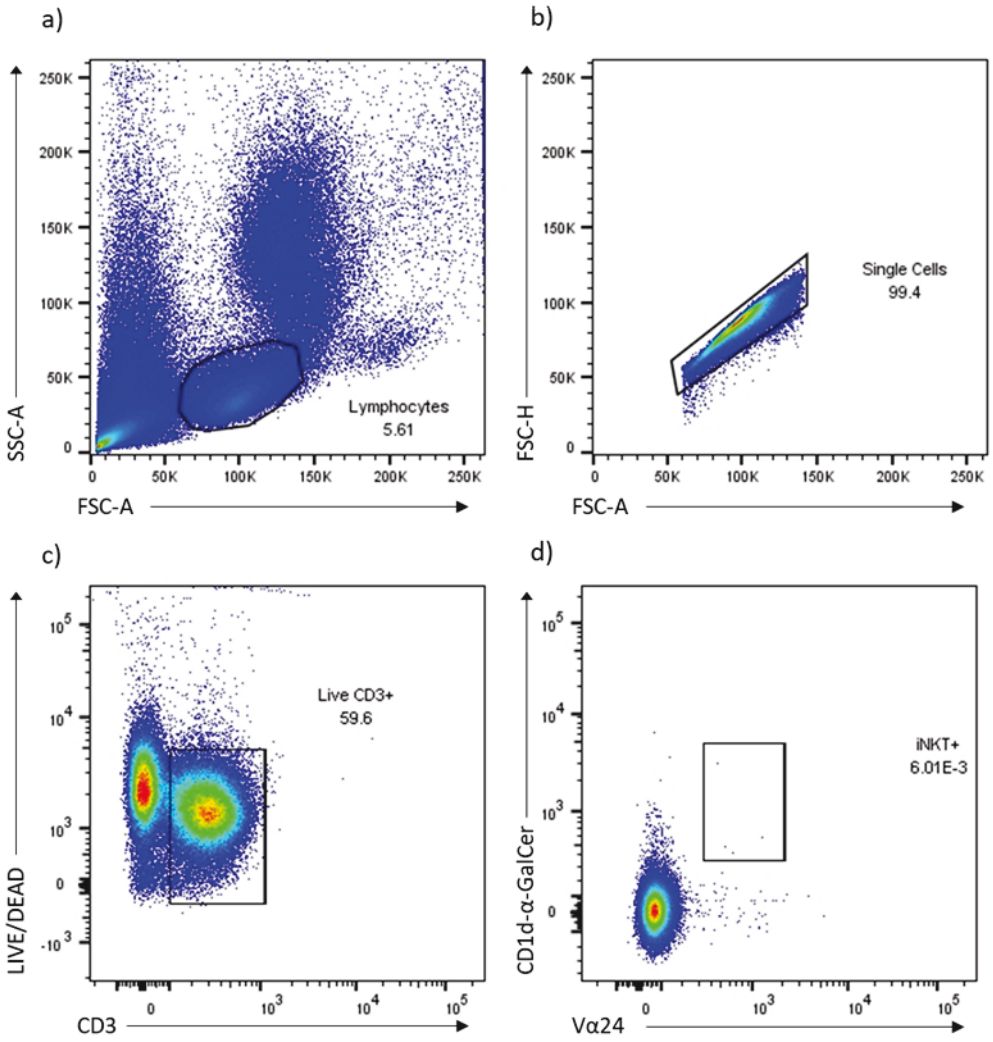

Figure 66: Gating strategy for macaque iNKTs

Flow cytometry dot plots depicting the gating strategy using FlowJo VX for CD1d-α-GalCer$^+$ Vα24$^+$ iNKTs. a) Lymphocytes, b) Single cells, c) Live CD3$^+$ lymphocytes and d) CD1d-α-GalCer$^+$ Vα24$^+$ iNKTs.

The frequency of iNKTs, as a percentage of live CD3$^+$ lymphocytes, was found to remain relatively stable for all animals up to 4 weeks post *M.tb* challenge but with small, inconsistent increases and decreases for each animal (Figure 67). Results from week 6 post challenge were removed as staining at this time point appeared to be ineffective. We observed an increase in iNKT frequencies for each animal at weeks 7 and 8 when necropsies were carried out. Animal 27W had the greatest frequency of iNKTs at necropsy with 0.13% whereas animal 56W had the lowest

frequency of just 0.00516%. These animals also had the largest (27W) and smallest (56W) iNKT frequency before *M.tb* challenge of 0.00348% and 0%, respectively.

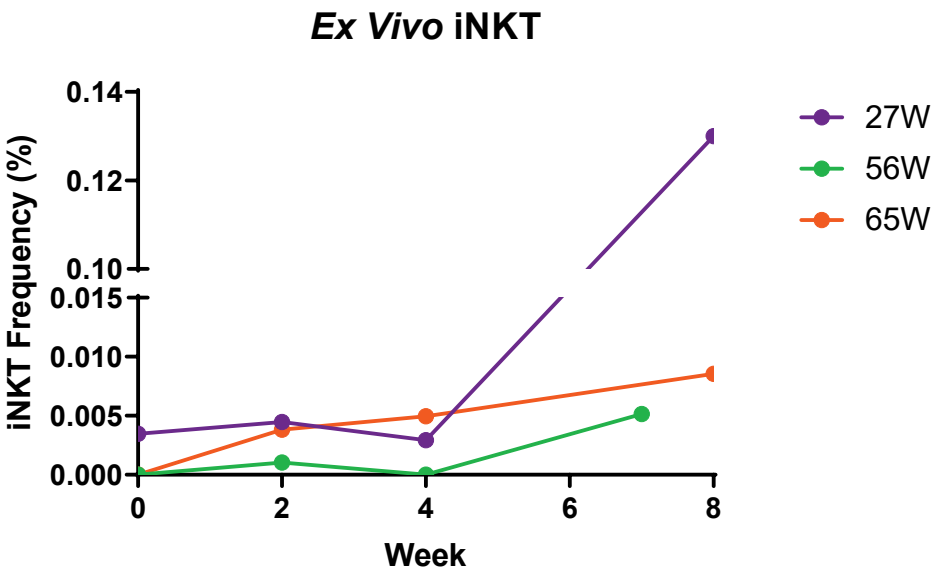

Figure 67: Time course of macaque *ex vivo* iNKT frequency

Graph demonstrating the frequency of CD1d-α–GalCer$^+$ Vα24$^+$ iNKTs for each animal from the beginning to the end of the study.

5.1.2 Expansion of iNKTs

To investigate iNKT function, we employed α–GalCer mediated expansion of iNKTs to measure iNKT proliferative responses. α-GalCer, originally isolated from a marine sponge, is a potent iNKT agonist (509), inducing activation and proliferation (510, 511) Therefore, α-GalCer is commonly used to measure iNKT proliferative response in challenge models (512). To this end, PBMCs isolated from each macaque were cultured with vehicle control or with α–GalCer for 14 days before measuring iNKT expansion by CD1d tetramer staining. Expansion of iNKTs mediated by α-GalCer was assessed by comparing the numbers of expanded CD1d-α-GalCer$^+$ Vα24$^+$ T cells after two weeks in culture to iNKT numbers *ex vivo* as a functional measure of iNKT proliferative response. For all samples, excluding animal 27W at week 4, expansion of iNKTs was observed after 2 weeks in culture from the *ex vivo* frequency determined on the day of blood collection. The fold expansion of iNKTs from animal 27W declined each week, suggesting the iNKT population is becoming defective with the progression of TB. Animals 56W and 65W however, had a decrease in iNKT fold expansion at week 2 before proliferation recuperated at week 4 (Figure 68).

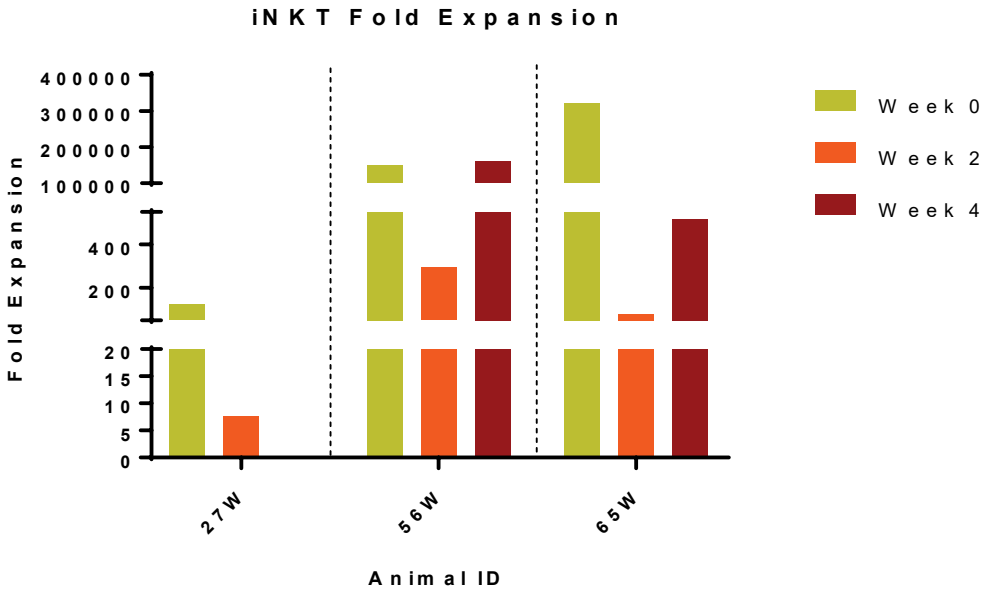

Figure 68: *In vitro* antigen induced iNKT expansion in macaques

Graph representing the fold expansion of iNKTs at each time point. Peripheral blood derived T cells were stimulated with the strong iNKT agonist α-GalCer. Data showing fold expansion (ratio of *in vitro* grown iNKT/*ex vivo* frequency) of iNKT cells in response to α-GalCer.

5.1.3 Lung biopsy iNKTs

The iNKT population in different lung lobes was assessed to observe any trends between iNKT numbers and disease status as determined by PHE pathology and bacteriology assessments. Processed biopsy samples were stained with CD1d tetramers and fixed in 2% paraformaldehyde before flow cytometry analysis. Frequencies of iNKTs were representative of the percentage from live $CD3^+$ lymphocytes acquired from each processed lung sample (Figure 69). For animals 56W and 65W, the greatest iNKT frequencies were observed in the right upper lung lobes, but in contrast the lowest frequency of iNKTs for animal 27W was observed in this lobe. Animal 65W had the greatest total frequency of iNKTs in the lungs whereas animal 56W had the lowest total frequency. There was little consistency observed in the frequency of iNKTs stained in each lung lobe between each animal.

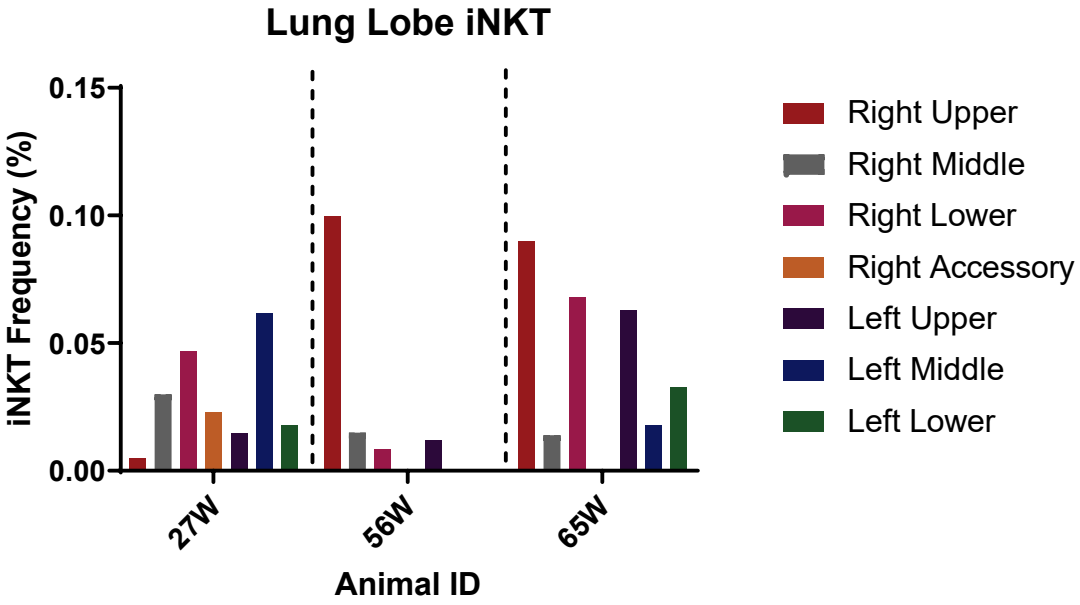

Figure 69: iNKT cells in macaque lung lobe biopsies

Lung biopsy samples of seven lobes were processed and stained with anti-Vα24 and CD1d-α-GalCer tetramers to quantify tissue iNKT cell frequencies. Graph depicting the CD1d-α–GalCer^{+} Vα24^{+} iNKT frequencies of lung lobe biopsies from each macaque after necropsy at weeks 7/8 post *M.tb* challenge.

Lung biopsy samples were also sent for bacteriological and pathological analysis carried out at PHE, Porton Down (details of scoring system in Table 5). Total pathology of the lungs was greatest for animal 56W with a score of 11 (Figure 70). The upper left lobe and lower right lobe of this animal were the greatest affected, both having a pathology score of 3. Animal 27W had the lowest total pathology score of 5, but the greatest affected lobes in this animal were right middle and right upper lobes which both had a score of 2. For all animals, the total pathology score of the right lobes was greater than that of the left, but there were no trends for either the upper or lower lobes having more severe pathology in any animal.

Bacteriology analysis was carried out on three different biopsy samples: a randomised punch biopsy sample (as previously described by Luciw *et al* (427)), standard tissue samples containing lesion, and standard tissue samples without lesion (Figure 70). Of the randomised punch biopsy samples, animal 27W had the highest total CFU when all lobes were combined, and animal 65W had the lowest total CFU. There were no consistencies between the animals in which lobe had the greatest CFU/tissue in the randomised punch biopsy samples. Both animals 27W and 56W had the lowest CFU/tissue in the right accessory lobe, but this sample was not available for analysis from animal 65W which had the lowest CFU in the left middle lobe. When looking at the standard lung

tissue samples, all animals predictably had higher CFU counts for samples containing lesion compared to samples without lesion from the same lobe. 56W had the greatest CFU count when all lobe samples, with and without lesion, were combined, whereas 65W again had the lowest total CFU count. There were no consistencies between the animals as to which lobe had the greatest CFU count when using the standard tissue sampling method. Both 27W and 56W had the lowest CFU counts in the right lower lobe with lesions but this was the only similarity.

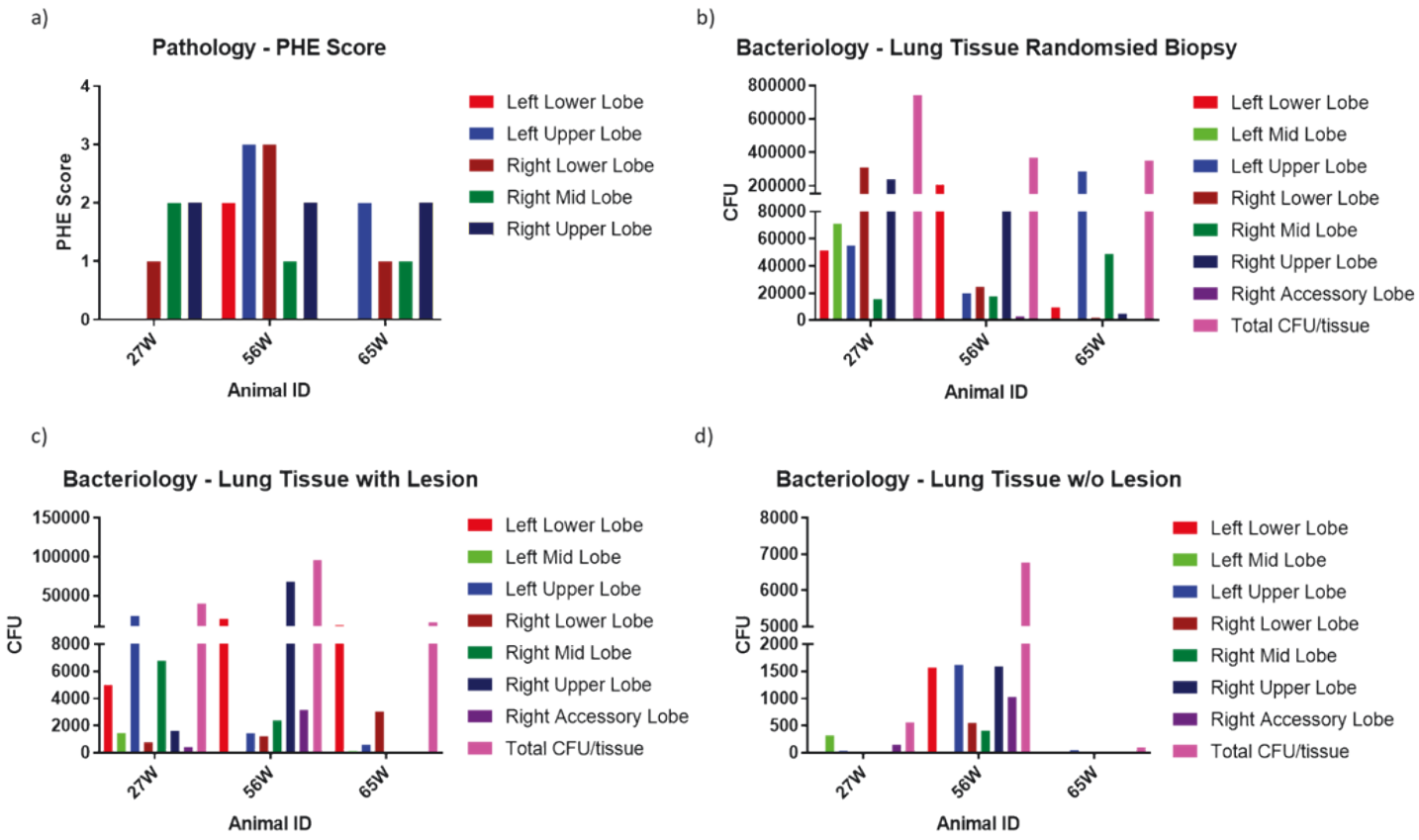

Figure 70: Pathological and bacteriological results of lung lobe samples

Graphs representing the pathological and bacteriological data for different lung lobe biopsies from each animal. a) Pathology scores using the PHE scoring system for lung lobes biopsy samples. b) CFU/tissue results for lung tissue biopsies. c) CFU/tissue results for lung tissue samples with lesions present. d) CFU/tissue results for lung tissue samples without lesions. Samples of the left mid lobe for 56W and right accessory lobe for 65W were not available for bacteriology analysis.

5.2 Macaque CD1c-restricted T cells

5.2.1 Cross-reactivity of human CD1c tetramers

Unlike other animal models, the macaque has retained the full set of CD1 molecules with only slight sequence alterations from that of human CD1 genes. It has previously been demonstrated that macaque CD1b presenting GMM can be recognised *in vitro* by human CD1b-restricted GEM T cells (377). However, in the macaque it has been found that both CD1b and CD1c-restricted T cells recognise mycobacterial derived GMM (376, 378). The combination of antibody blocking experiments, IFNγ ELISPOT assay and tetramer studies have demonstrated that GMM specific T cells exist in BCG vaccinated macaques and activation is dependent upon the presence of lipid in addition to CD1b or CD1c. Despite this, there has as of yet been no evidence of CD1c autoreactive T cells in the macaque.

As human CD1d-αGalCer tetramers have been validated for the detection of iNKT cells in macaque (31, 513, 514), we investigated the potential for species cross-reactivity of human CD1c tetramers refolded in the absence of exogenous antigen on PBMCs from a variety of species of macaque. Cryopreserved PBMCs from 12 TB-naïve Rhesus and Cynomolgus macaques were either single stained with CD1c-SL tetramers composed of Streptavidin-PE or Streptavidin-APC, or were stained with both tetramers. The frequency of either single or double CD1c tetramer$^+$ staining cells as a percentage of CD3$^+$ cells was compared to that of PBMCs stained with negative control tetramers. Despite 79% of the tested macaque samples staining positively with CD1c tetramer, there was no significant difference between PBMCs stained with CD1c tetramers and those stained with negative control tetramers (Figure 71). The lowest frequency of CD1c tetramer staining of CD3$^+$ T cells was found when two CD1c-SL tetramers (CD1c-SL PE and CD1c-SL APC) were used simultaneously. In comparison, the greatest levels of staining were observed when CD1c-SL PE was used as a single stain which may indicate greater levels of background staining with this tetramer (Figure 72). Due to the negligible difference in staining, it is difficult to conclude whether the human CD1c protein is truly cross-reactive with each species of macaque.

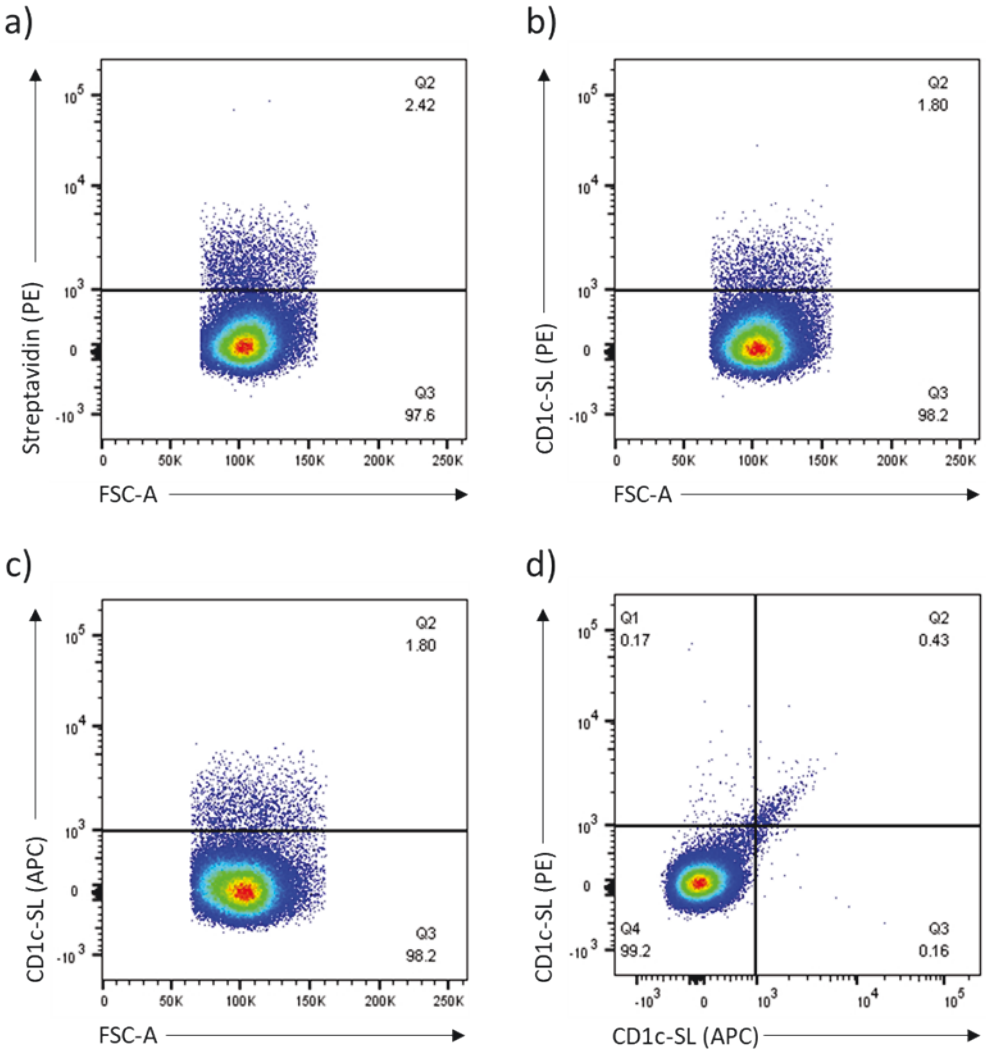

Figure 71: CD1c-SL tetramer staining of macaque PBMCs

Cryopreserved macaque PBMCs were resuscitated and stained with human CD1c-SL tetramers conjugated to Streptavidin-PE or Streptavidin-APC to identify species cross-reactive CD1c-restricted T cells. Representative flow cytometry dot plots show tetramer staining of macaque PBMCs with a) Streptavidin (PE) only, b) CD1c-SL (PE), c) CD1c-SL (APC) and d) CD1c-SL (PE) and CD1c-SL (APC).

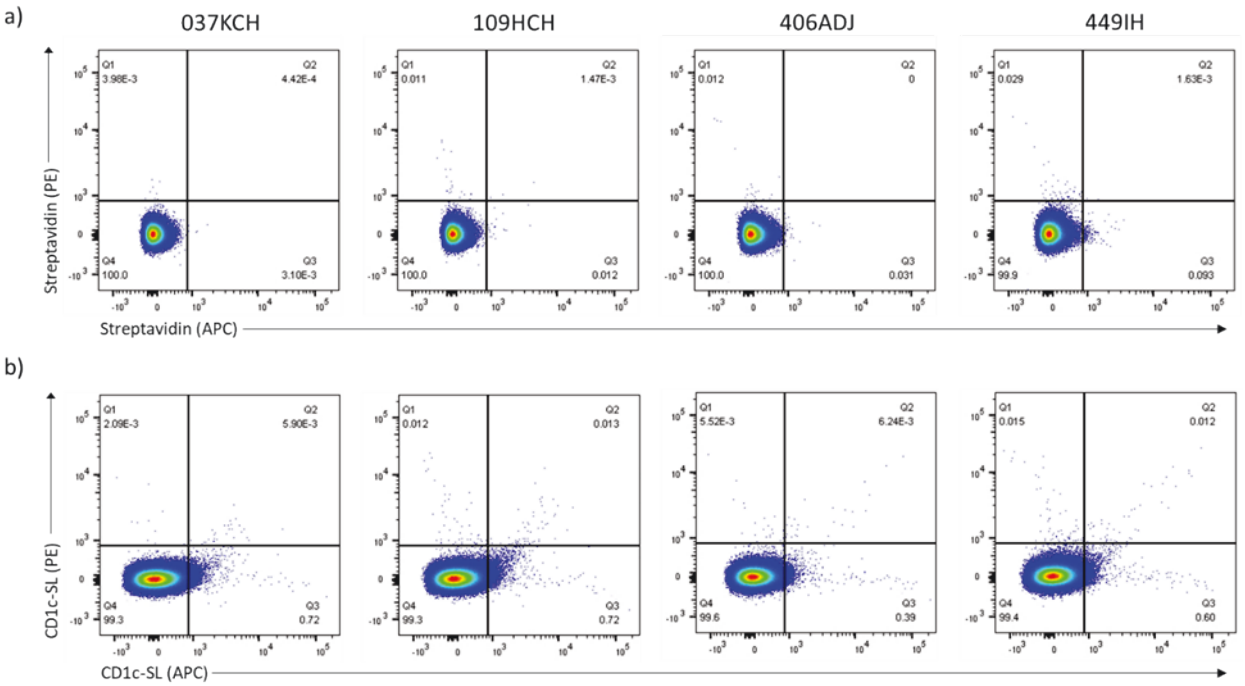

Figure 72: Double streptavidin and CD1c-SL tetramer staining of macaque PBMCs

Representative flow cytometry dot plots demonstrating double staining of four macaque PBMC samples with a) Streptavidin (PE) and Streptavidin (APC) or b) CD1c-SL (PE) and CD1c-SL (APC). Positive staining with both Streptavidin reagents or both CD1c-SL tetramers can be viewed in Q2.

5.2.2 Macaque CD1c tetramers

In order to validate the use of CD1c tetramers as tools for the detection and isolation of macaque CD1c-restricted T cells, it would be pertinent to refold and tetramerise macaque CD1c protein to compare to that of human CD1c. Validation of this tetramer would be of significant value for tracking CD1c-restricted T cells over the TB disease course and enable the investigation of the role of host- or mycobacteria derived lipids. Furthermore, the use of CD1c tetramers refolded in the absence of exogenous lipid would allow for the investigation of CD1c autoreactive T cells in the macaque. CD1c-restricted T cells have been demonstrated in the macaque but only those specific for CD1c-presented GMM have been demonstrated (376, 378). As of yet, there have been no reports of CD1c autoreactive T cells in the macaque, therefore we aimed to develop tools and assays to investigate the presence of these cells.

The protein sequence of human CD1c has been aligned and compared with that of both the Rhesus and Cynomolgus macaque. While the protein sequence of the α1-α2 domains of the human and Cynomolgus macaque CD1c is the same in length, there are variations in 18 amino acids. In comparison, the α1-α2 protein sequence of the Rhesus macaque is shorter than both the human and Cynomolgus macaque by 2 amino acids, and has variations in 21 amino acids (Figure 73). Due to the greater differences in CD1c sequence between the Rhesus macaque and human, the macaque CD1c plasmid was designed from the Cynomolgus macaque α1-α2 protein sequence.

```
Cyno            MLFLQFLLLAV-LSGGDNADAAQEHVSFYTIQILSFANQSWAQSQGSGWL
Human           MLFLQFLLLALLLPGGDNADASQEHVSFHVIQIFSFVNQSWARGQGSGWL
Rhesus          MLFLQFLLLAV-LSGGDNADA-QEHVSFYTIQILSFANQSWAQSQGSGWL
                **********: *.******* ******:.***:**.*****:.******

Cyno            DELQTHGWESESGRIIFLHTWSKSNFSNEELSDLELLFRVYFFGLTREIQ
Human           DELQTHGWDSESGTIIFLHNWSKGNFSNEELSDLELLFRFYLFGLTREIQ
Rhesus          DELQTHGWESESGRIIFLHTWSKSNFSNEELSDLELLFRVYFFGLTREIQ
                ********:**** *****.***.***************.*:********

Cyno            DHASQDYSKYPFEVQVKAGCELHSGKSPEGFFRVAFNGLDLLSFQNTTWV
Human           DHASQDYSKYPFEVQVKAGCELHSGKSPEGFFQVAFNGLDLLSFQNTTWV
Rhesus          DHASQDYSKYPFEVQVKAGCELHSGKNPEGFFRVAFNGLDLLSFQNTTWV
                **************************.*****:*****************

Cyno            PSPDGGSLAPGVCHLLNHQYEGVTETVYNLIRSTCPRFLLGLLDAGKMYL
Human           PSPGCGSLAQSVCHLLNHQYEGVTETVYNLIRSTCPRFLLGLLDAGKMYV
Rhesus          P-PDGGSLAPGVCHLLNHQYEGVTETVYNLIRSTCPRFLLGLLDAGKMYL
                * *. **** .*************************************:

Cyno            HRQVRPEAWLSSRRSLGSGRLLLVCHASGFYPKPVWVTWMRNEQEQLGTK
Human           HRQVRPEAWLSSRPSLGSGQLLLVCHASGFYPKPVWVTWMRNEQEQLGTK
Rhesus          HRQVRPEAWLSSRRSLGSGRLLLVCHASGFYPKPVWVTWMRNEQEQVGTK
                ************* *****:**************************:***

Cyno            HGDVLPNADGTWYLQVILEVAAEETAGLSCRVRHSSLGGQDIILYWGHHF
Human           HGDILPNADGTWYLQVILEVASEEPAGLSCRVRHSSLGGQDIILYWGHHF
Rhesus          HGDVLPNADGTWYLQVILEVASEETAGLSCRVRHSSLGGQDIILYWGHHF
                ***:******************:**.**************************

Cyno            SMNWIALIVLVSLVILIVLVLRFKKHCSYQDIL
Human           SMNWIALVVIVPLVILIVLVLWFKKHCSYQDIL
Rhesus          SMNWIALIVLVSLVILIVLVLRFKKHCSYQDIL
                *******:*:*.********* ***********
```

Figure 73: Polypeptide sequence of human and macaque CD1c

Aligned CD1c polypeptide sequence from Cynomolgus macaque (Cyno), human, and Rhesus macaque (Rhesus). Dark highlighting indicates an amino acid residue deletion and light shading indicates residue alterations in the macaque sequence from that of the human CD1c protein.

Following synthesis of the extracellular mCD1c sequence and cloning into the pMK-RQ holding vector by GeneArt, we removed the mCD1c sequence from this vector by restriction digest and ligated it to our pET23d expression vector (Figure 74).

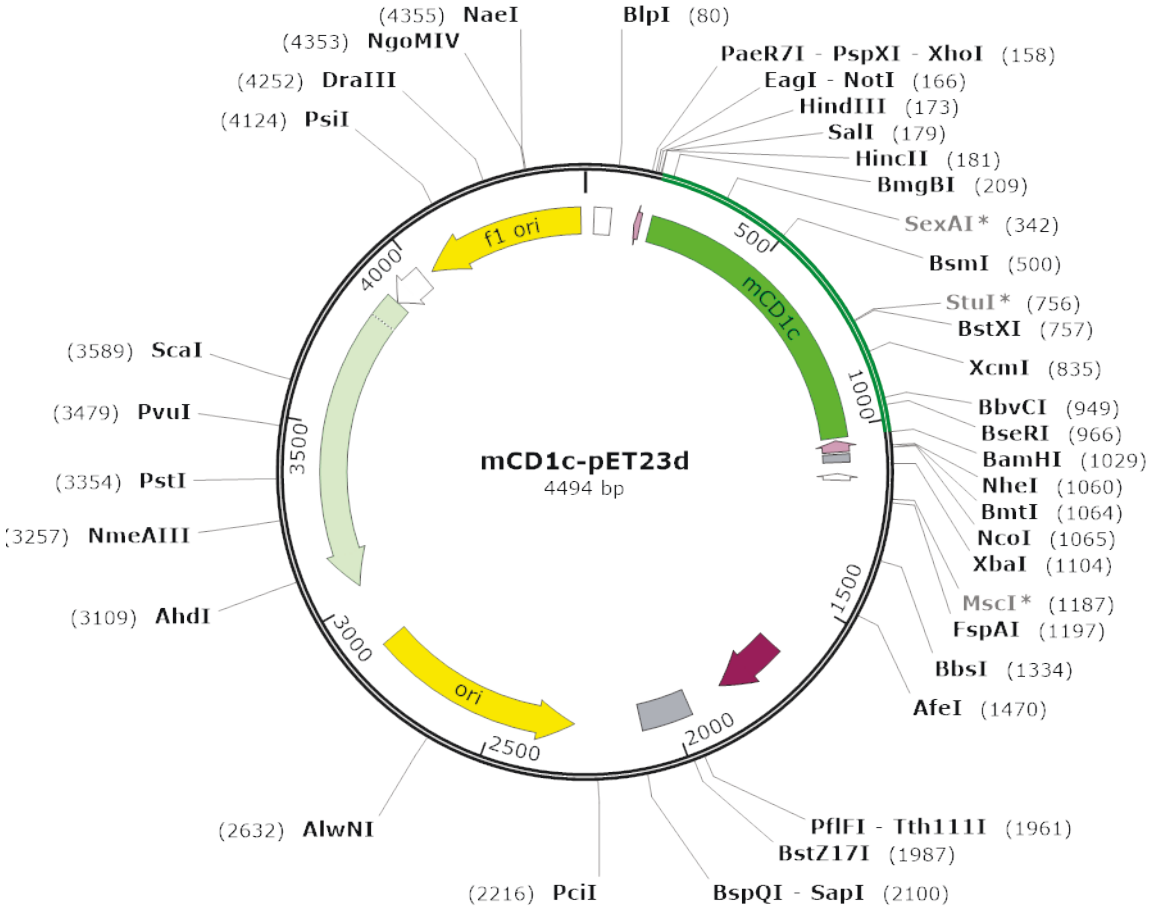

Figure 74: Vector map of mCD1c

A visual representation of the synthesised mCD1c insert cloned into the expression vector pET23d.

The mCD1c protein was expressed as inclusion bodies and then subsequently refolded with human β_2m and purified by FPLC. The resulting, purified monomer was run on SDS-PAGE and the protein was visualised at the expected molecular weight. Following tetramerisation with Streptavidin-PE, the mCD1c tetramer was used to stain the human CD1c-restricted TCR, NM4 expressed by J.RT3-T3.5 Jurkat cells. When compared to the TCR negative J.RT3-T3.5 parental line, no positive staining with the mCD1c tetramer was observed (Figure 75). This may be due to the NM4 TCR being of human origin and may only recognise the corresponding human CD1c protein.

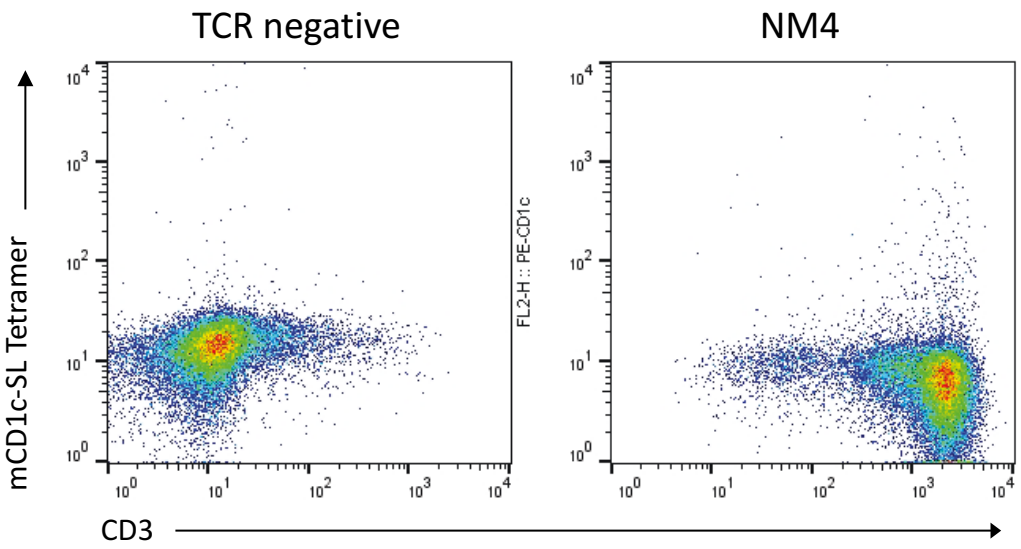

Figure 75: mCD1c-SL tetramer staining of a human CD1c-restricted TCR

Flow cytometry dot plots depicting mD1c-SL tetramer and anti-CD3 staining of the parental J.RT3-T3.5 TCR negative Jurkat T cell line (left) and J.RT3-T3.5 Jurkat T cells expressing the human CD1c autoreactive TCR, NM4 (right).

To further investigate this protein, the mCD1c tetramer was used to stain PBMCs from three Rhesus macaques (8X, 20X, 37X) and three Cynomolgus macaques (M651BE, M139FE, M7012ED). Staining was also performed with human CD1c tetramers and a Streptavidin-PE only negative control. Out of the six animals used, only Cynomolgus macaque M139FE showed obvious positive staining with the mCD1c tetramer. The remaining animals had little to no staining with the mCD1c tetramer and no distinct populations of cells were visible with the human CD1c tetramer (Figure 76).

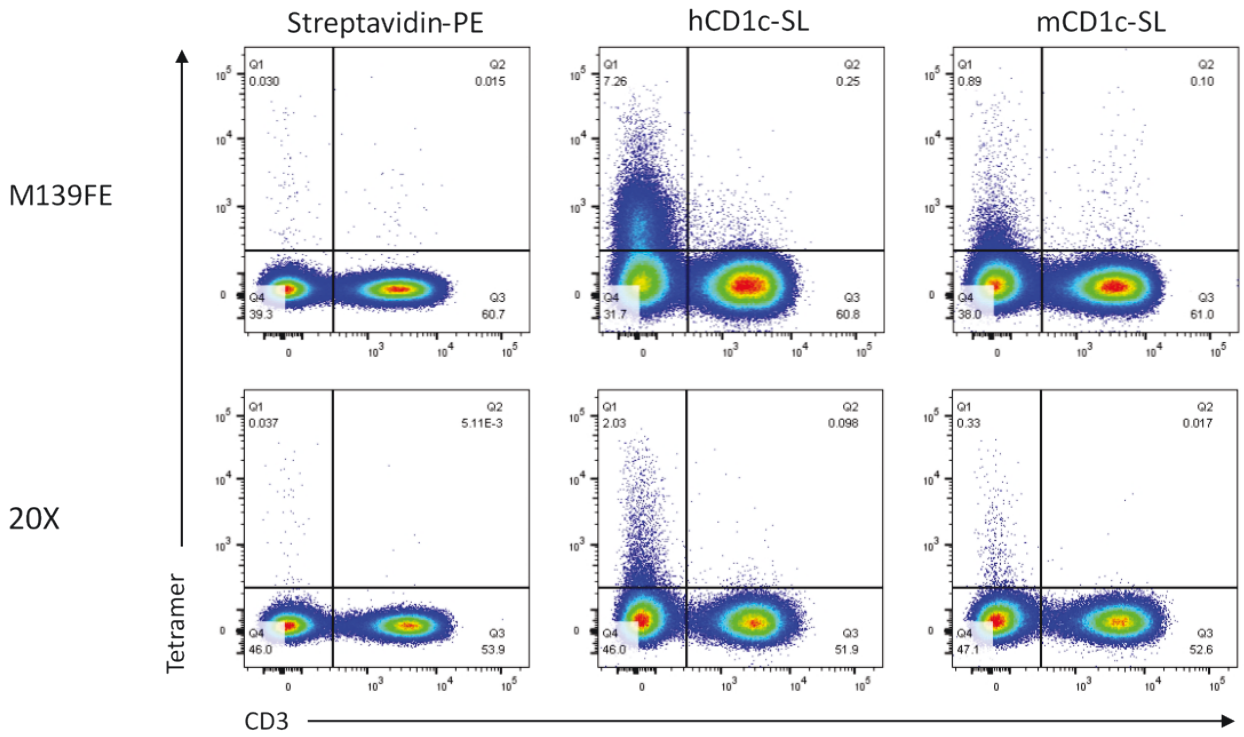

Figure 76: mCD1c-SL tetramer staining of macaque PBMCs

Representative flow cytometry dot plots demonstrating staining of one Cynomolgus macaque (M139FE) and one Rhesus macaque (20X) with human and macaque CD1c-SL tetramers. Streptavidin-PE alone was also used to stain PBMCs as a negative control for tetramer staining.

5.2.3 Expansion of Macaque CD1c-restricted T cells

To investigate CD1c autoreactive T cells in macaques and whether they are cross-reactive to the human CD1c protein, we employed the AIM assay described previously to analyse activation and expansion of this T cell population in a tetramer-independent way. $CD3^+$ T cells were isolated from three Rhesus macaques (20X, 37X and 58Y) and cultured with parental WT THP1 cells (THP1-KO) or THP1-CD1c. As in the AIM assay described previously, no exogenous antigen was added in order to stimulate expansion of macaque CD1c autoreactive T cells. In contrast to the previous human AIM assay, macaque cells were only cultured for a total of 9 days. On day 8, the T cells were stimulated with irradiated THP1-CD1c or THP1-KO cells and were analysed the following day by flow cytometry for their expression of activation markers CD25 and CD137. Proliferative response of T cells was indicated by diminishing signal of CTV. Of the three macaques, only one animal demonstrated a greater frequency of proliferated T cells (CTV^- $CD3^+$ cells) in the THP1-CD1c stimulated cultures compared to those stimulated with THP1-KO. Increased frequencies of proliferated T cells in the THP1-KO stimulated cultures for the remaining animals seemingly suggests that the presence of APCs may drive T cell proliferation. Antigen specific responses

within the short term cultures were assessed by comparing frequency of T cells double positive for activation markers CD25 and CD137 following overnight stimulation with THP1-CD1c or THP1-KO. Our data revealed that T cells from all animals demonstrated greater frequencies of $CD25^{+}CD137^{+}$ cells in the CTV^{-} gate compared to the CTV^{+} gate, indicating that the proliferated T cells are indeed activated (Figure 77).

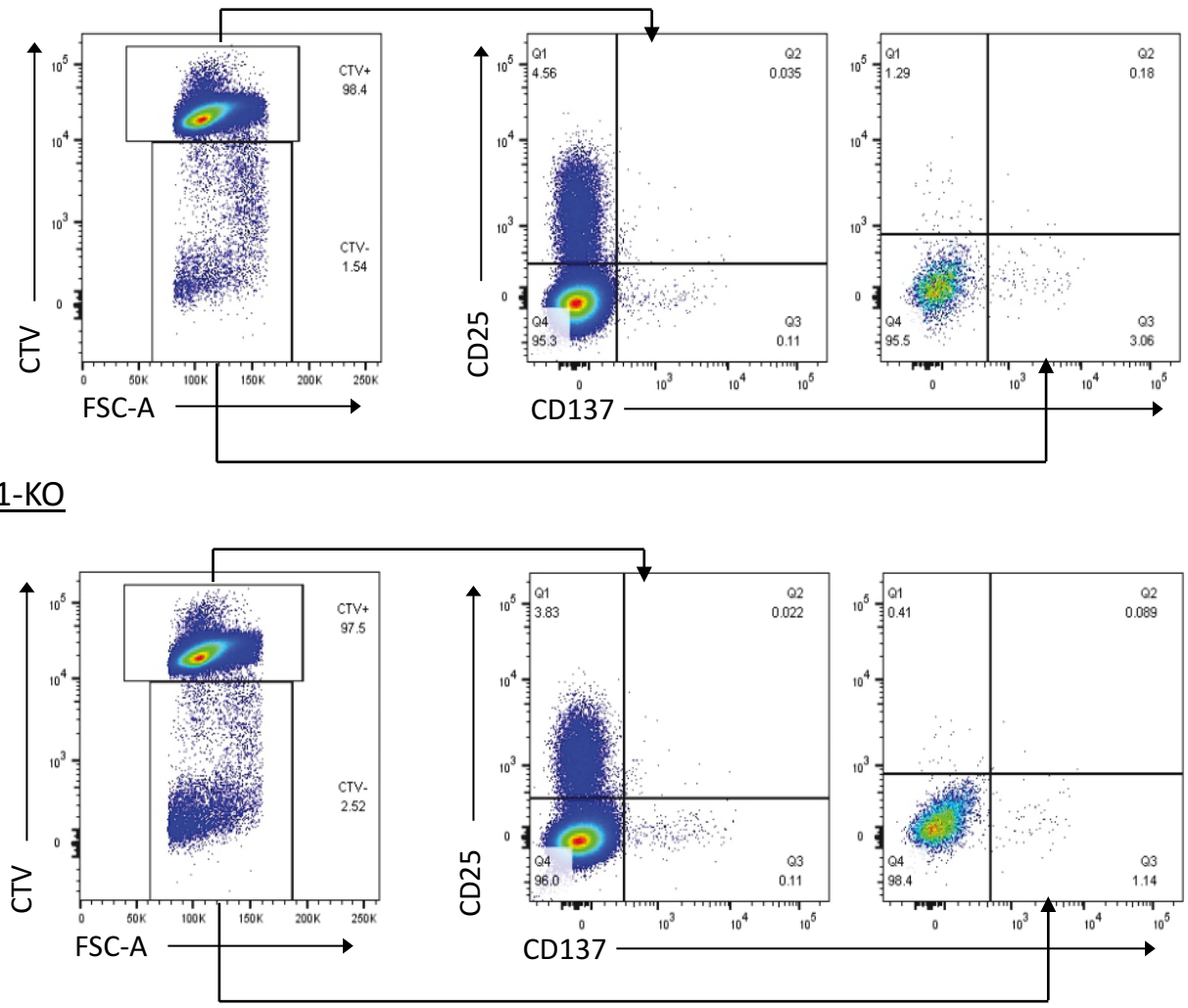

Figure 77: Expansion of CD1c autoreactive macaque T cells in the absence of exogenous antigen

Representative flow cytometry dot plots of purified macaque T cells expanded in the presence of THP1 cells. T cell activation markers CD25 and CD137 were analysed following overnight stimulation with THP1-KO or THP1-CD1c in the absence of exogenous lipid antigen.

Two macaques had greater frequencies of $CD25^{+}CD137^{+}$ T cells in the CTV^{-} gate following stimulation with THP1-CD1c compared to stimulation with THP1-KO, seemingly suggesting an antigen specific response. However, populations of $CD25^{+}CD137^{+}$ T cells from all cultures were low in number and not well defined. It has since been observed in our AIM assay involving human T cells that cultures for longer periods of time are associated with greater levels of proliferation and antigen-specific activation of T cells. As the proliferation of macaque T cells following 8 days of culture did not appear to be as substantial as expected, it may indicate that a longer duration of culture is required in order to observe CD1c mediated activation and proliferation of CD1c autoreactive T cells.

5.3 Discussion

5.3.1 CD1d-restricted iNKTs

iNKTs are thought to have a crucial role in the immune response to pathogens; secreting cytokines such as IFNγ that contribute to host defence. The population of iNKTs has been reported to be decreased in patients with active TB (169-171), but higher frequencies have shown to be associated with decreased pathology in macaque studies (31). The anti-mycobacterial function of iNKTs has been indicated as depending upon expression of CD1d, with CD1d-knockout mice succumbing to mycobacterial infection faster than those with CD1d intact (149, 150). The aim of this investigation was to track *ex vivo* CD1d restricted iNKT numbers in Rhesus macaques over the course of *M.tb* infection, from pre-exposure to 7-8 weeks post challenge. Fold expansion of iNKTs as a function of α-GalCer stimulus at each time point was also examined, as well as the iNKT frequency in various lung lobe biopsies. This investigation builds upon previous work carried out by this group which discovered trends for an increased $CD8^{+}$ iNKT population with improved clinical outcomes in both the Chinese Cynomolgus macaque and the Indian Rhesus macaque (31). The data in this study demonstrated low numbers of iNKTs staining positively with the CD1d-α–GalCer tetramer at pre-infection through the course of infection until the week of necropsy where counts increased for all animals. Despite subtle changes throughout the time course, the iNKT count at the beginning and end of the study appeared to be linked. For example, animals with the highest frequency of iNKTs at the beginning of the time course were observed to have the lowest iNKT frequencies at the final time point, and *vice versa.*

Data generated previously from this group demonstrated a large variance in α–GalCer mediated iNKT expansion between both individuals and species, ranging between <10 and >1000 fold difference in expansion (31). Expansion of iNKTs was observed for each animal at each time point, with the exception of 27W which demonstrated a lack of expansion at week 4 post *M.tb*

challenge. Between weeks 2 and 4, there was a CO_2 supply failure to the incubators containing the iNKT cells in culture. Furthermore, contamination of the cultures was observed at week 6. Due to these factors, we were unable to assess iNKT fold expansion between weeks 2 and 6. Repetition of the experiment using cryopreserved samples from each time point would be possible, although cryopreservation and thawing is known to reduce PBMC viability and functionality (515). The effects of α–GalCer are important to investigate as mice treated with α–GalCer have demonstrated CD1d specific activation of iNKTs with decreased tissue damage and an increase in protection from TB (512). Animals 56W and 65W demonstrated the greatest expansion of iNKTs at all time points, with both animals showing a similar pattern of reduced expansion at week 2 before an increase in fold expansion at week 4. Perhaps coincidentally, these animals had lower total bacterial burden in their randomised lung punch biopsy samples. In contrast, 27W demonstrated diminishing iNKT fold expansion each week but demonstrated the highest total CFU in the lungs. The defective iNKT population of this animal may have contributed to an inability to control the bacterial burden within the lungs.

Lung biopsies taken at necropsy from each of the animals allowed for the investigation of iNKT numbers in different lobes which could be analysed alongside pathological and bacteriological data. This novel investigation aimed to examine whether iNKT levels in both the peripheral blood and different lung lobes could be an indicator of disease severity and outcome. Peripheral blood iNKT levels have been found to be lower in patients with active TB (171), and in macaques, increased levels of $CD8^+$ iNKTs are associated with better outcomes (31). During active TB disease, it has been suggested that iNKT cells home to areas of infection within the lung (170), but as of yet the iNKT population in different lung lobes has not been investigated. Although small animal numbers in this experiment made it challenging to find consistencies within such a small group, the animal with the lowest level of total lung and peripheral blood iNKTs (animal 56W) also demonstrated the highest total pathology score. Additionally, this animal also had the greatest bacterial load in the lung when the CFU/tissue counts for each lung lobe with lesions were combined. In contrast, a high level of iNKTs in the right lower lobe of animal 27W was also found alongside high CFU/tissue in the biopsy of the same lung lobe. This was also true for the left upper lobe of animal 65W.

The concurrent findings of higher quantities of iNKTs and high pathology scores but with low bacteriology may indicate that the larger amount of iNKTs are causing destruction to the tissue in particular segments of the lung. The worsened pathology but lower bacteriology may be due to iNKTs homing to the site of infection (170) and attempting to eradicate the pathogen, with tissue destruction being a by-product of bacterial killing. It has been demonstrated that Jα18 knockout mice lacking iNKTs have higher bacterial burden in the lungs when infected with *Streptococcus*

pneumoniae or *Chlamydophila pneumoniae* (516, 517). Bacterial clearance is thought to occur from an increased iNKT-mediated Th1 response as transfer of iNKTs from wild type mice lead to a reduction in bacterial load (516). This effect has also been shown for mice challenged with *M.tb* as adoptive transfer of iNKTs into Jα18 deficient mice reveals a reduction in bacterial numbers within the lungs (150). However, although an association has been indicated between iNKTs and bacterial burden in the lungs, there is as of yet no published data linking to lung pathology.

As only three animals were used in this study, statistical analysis could not be accurately carried out, and as individual variations are more pronounced in such a small population size it is not possible to draw trends or associations from the data. To improve upon this data, more animals would need to be included in future studies to be able to make associations between data sets. Furthermore, increasing the staining panel would be beneficial to elucidate activation status of the iNKTs as well as co-receptor surface expression.

5.3.2 CD1c-restricted T cells

CD1c-restricted T cells have been demonstrated as highly prominent in the peripheral blood of humans, with up to 7% of self-reactive $CD4^+$ T cells estimated to be reactive to CD1c (304). The ability of T cells to recognise CD1c presenting mycobacterial lipids such as PM suggests that these cells may have a key role in the immune response to TB. Due to the similarities in physiology and immunology to that of humans, the macaque model is ideal for studying the changes in immune cells over time in response to mycobacterial challenge. While the macaque model has already been utilised to uncover more information about the role of iNKTs in TB infection, there has been little research into the frequency and function of the CD1c-restricted T cell population in the context of *M.tb* infection. Both human and macaque CD1d tetramers have already been used successfully to stain macaque CD1d-restricted T cells (31, 518), but use of CD1c tetramers are scarce with only one study describing the use of a macaque specific tetramer (376).

We set out to test our human CD1c-SL tetramers in the macaque and to investigate cross-reactivity between species. In the majority of macaque samples tested, positive staining with the CD1c-SL tetramer was observed after subtracting background from the negative control tetramer. As background staining for some animals was very high, a second CD1c-SL tetramer was used to increase our confidence in specific binding of the tetramers to CD1c-restricted T cells. For the samples stained with two tetramers, there was a substantial amount of single staining with the CD1c-SL PE tetramer but not the CD1c-SL APC tetramer which indicated non-specific binding. The validation of an assay requires the assessment of various parameters, including accuracy, specificity, repeatability, intermediate precision, limit of detection and quantification, linearity and range (493, 519). As the CD1c-SL tetramer was only tested on 10 Cynomolgus and 2 Rhesus

macaques, we cannot accurately assess any of these validation parameters. To continue to validate the use of human CD1c tetramers, a greater number of samples from both the Cynomolgus and Rhesus macaque species would first need to be tested, acquiring at least $1x10^6$ cells during flow cytometric analysis. CD1c tetramer staining of samples from the same animals should also be repeated using both the same and new batches of tetramer to assess repeatability. The specificity and sensitivity of the CD1c tetramers for macaque CD1c-restricted T cells could be investigated by serially diluting macaque PBMCs with a CD1c-specific T cell line and quantifying levels of positive staining compared to that of a negative control tetramer. To assess the accuracy of tetramer staining, we would need to compare the data to the true value which would have been determined from a gold standard reference assay (519). However, as there is no standard reference assay to assess the true value of the frequency of CD1c-restricted T cells so we will not be able to evaluate this parameter (493, 520).

We also wish to test tetramers comprised of the macaque CD1c protein and compare this to staining levels seen from the human CD1c tetramers to assess trans-species cross-reactivity. Currently, there are only a few reports into cross-reaction of CD1c between humans and macaque. One study identified that although human anti-CD1c monoclonal antibodies bind Rhesus macaque CD1c, the human CD1c-restricted T cell line CD8-1 that recognises MPM in the context of human CD1c does not show reactivity to CD1c of Rhesus macaque origin (377). However, a recently published study detailed the one-sided cross-reactivity of human T cells to macaque CD1b- and CD1c-GMM tetramers, but macaque T cells failed to stain with human CD1b- and CD1c-GMM tetramers (376).

Our alignment of the human and Rhesus macaque CD1c amino acid sequence shows a high degree of conservation, in agreement with the 90.4% homology demonstrated by Morita *et al* (377). This may suggest that the lack of reactivity of the human T cell line to macaque CD1c may either be due to differences in amino acid sequences occurring in a crucial area for TCR binding, or the macaque protein has an altered antigen presenting function. The small differences in amino acid sequence may have a large contribution to antigen presenting capabilities, as in the macaque it has been found that CD1c can successfully present GMM to GMM specific human T cells, whereas in the human only CD1b is known to be able to present this lipid (378). The α1 and α2 helices of CD1 proteins make up the antigen presenting domain and many solved TCR footprints map to this area of human CD1 molecules (165, 263, 267). Differences in the amino acid sequence between human and macaque CD1c are mainly found within the α1 and α2 helices; as this area is commonly reported to be involved in the TCR binding footprint, any differences in the CD1c molecule may prevent cross-species recognition of CD1c by macaque T cells. Furthermore, the only report of T cells recognising macaque CD1c is in the context of a lipid (GMM) (378).

As our CD1c tetramers were refolded in the absence of any specific lipid, it may be that CD1c-restricted T cells in the macaque are lipid specific and are unable to recognise human CD1c refolded with spacer lipids. To investigate both of these suggestions, we would need to test macaque CD1c refolded with and without specific lipids and compare the tetramer staining profiles to that of human CD1c tetramers on a large number of macaque PBMC samples. Furthermore, to confirm specificity of both human and macaque CD1c tetramers, we would need to use tetramer guided sorting of CD1c-restricted T cells from the macaque with the aim of cloning the TCRs. These TCRs would then be expressed on Jurkat cells to confirm binding and specificity to the CD1c tetramers. Following the successful validation of CD1c tetramers in the macaque, we can then go on to investigate the frequency and function of CD1c-restricted T cells in response to BCG vaccination and over the course of *M.tb* infection.

5.3.3 Macaque CD1c tetramers

Until recently, there had been no reports of macaque CD1c tetramers or their use in identifying macaque CD1c-restricted T cells. Layton and colleagues have recently published reports of macaque CD1c-GMM tetramers detecting GMM specific, CD1c-restricted T cells in Rhesus macaques that have been BCG vaccinated (376). However, we aimed to investigate the presence of CD1c autoreactive T cells in the macaque by constructing and refolding our own macaque CD1c tetramers. The CD1 locus is highly conserved between humans and macaques (376) and our alignment analysis showed that the Cynomolgus macaque CD1c sequence was more similar than that of the Rhesus macaque to the human protein. The extracellular portion of the Cynomolgus macaque CD1c protein (mCD1c) was synthesised by Geneart and we subsequently cloned this into our expression vector. We refolded mCD1c with human β_2m in the absence of exogenous lipid in order to mirror production of our human CD1c-SL tetramer which has been used successfully to isolate CD1c autoreactive T cells from human donors (265).

In contrast to our human CD1c-SL tetramer which consistently stains our isolated and cloned CD1c autoreactive TCR, NM4, the mCD1c-SL tetramer did not show any staining of this TCR expressed by Jurkat T cells. As we were confident that the protein had stably refolded, as demonstrated by SDS-PAGE gels, lack of staining may indicate a lack of species cross-reactivity of this TCR. This is in contrast to the macaque CD1c tetramer used by Layton *et al,* which demonstrated staining of human CD1c-restricted T cell lines (376). However, in this study the GMM-specific CD1c-restricted human T cell lines did not recognise human CD1c tetramers in the absence of loaded GMM, indicating that the presence of GMM is a requirement for binding to CD1c and the protein itself may be of secondary importance (376).

We also aimed to investigate whether our mCD1c-SL tetramers could be used to identify CD1c autoreactive T cells in macaques. We stained PBMCs from three Rhesus and three Cynomolgus macaques with our mCD1c-SL tetramer and compared this to staining with our human CD1c-SL tetramer. Out of the six, no animals were observed to have convincing staining with the human CD1c-SL tetramer and only one animal was observed to have clear staining with the mCD1c-SL tetramer. This may further demonstrate species specificity, as the animal with positive staining was a Cynomolgus macaque and our mCD1c-SL tetramer comprises the Cynomolgus CD1c sequence. However, this hypothesis needs to be further tested to confirm this level of extreme species specificity.

The observation of staining with our mCD1c-SL tetramer in the Cynomolgus macaque indicates that CD1c autoreactive T cells may be present in the peripheral blood of naïve macaques. In the Layton study, macaque CD1c tetramers without the addition of exogenous lipid were also employed (referred to as mock tetramers). Although isolated human and macaque CD1c-GMM specific T cells were not reactive to mock CD1c tetramers, initial staining of PBMC samples did reveal a small frequency of cells binding to the macaque CD1c tetramers in the absence of GMM (376). This population of mock CD1c tetramer$^+$ cells was more pronounced in the human PBMC sample, but still observable in that of the macaque, further suggesting the existence of CD1c autoreactive T cells in the macaque. It is possible that any CD1c autoreactive T cells may not be as visible using tetramer staining as it has been reported that in humans, T cells reactive to self-antigen bind with lower affinity than to microbial antigen (287, 300, 447).

Layton *et al* also investigated recognition in a tetramer-independent assay and reported that while CD1c-GMM specific macaque T cells did not recognise the human CD1c-GMM tetramer, these T cells did show some level of activation following culture with GMM and the APC line K562 expressing human CD1c molecule (376). This suggests that although recognition was not observable through tetramer staining, release of IFNγ may be a more sensitive measure of recognition for low affinity binding. Overall, to further validate our mCD1c-SL tetramers and investigate the presence of CD1c autoreactive T cells in macaques, we need to assess the responses on a greater range of macaques and include tetramer-independent studies to better detect low affinity CD1c-restricted T cells.

5.3.4 Expansion of macaque CD1c-restricted T cells

In order to assess the recognition of CD1c by autoreactive T cells in the macaque, we employed a short term culture assay to activate and expand these cells. CD3$^+$ T cells were isolated from three Rhesus macaques and cultured in the absence of exogenous antigen for 8 days with a human

myelomonocytic leukaemia cell line (THP1) with or without expression of human CD1c. At day 8 the T cells were re-stimulated with THP1 cells before analysing the cells the following day for activation and expansion. Of the three animals tested, only one was observed to have a greater frequency of expanded T cells following culture with THP1-CD1c compared to the parental CD1c$^-$ THP1 line, but two out of three animals had greater expression of both activation markers CD25 and CD137 following culture with THP1-CD1c. However, both findings were minimal and it cannot be concluded that expansion or activation of T cells was specific to the presence of CD1c.

More information could have been garnered from this experiment if it were employed on a larger number of samples and if the conditions had been optimised to the level of the AIM assay discussed in Chapter 2. The human AIM assay was carried out at a much more recent time point than the macaque assay, thus specific details of the experiment which were found to be advantageous for antigen-specific proliferation were not included when attempting to assess CD1c autoreactive T cells in the macaque. For example, it has been reported that longer periods of culture for at least 12 days in the presence of antigen leads to greater expansion of antigen specific T cells (337, 338). This suggests that we may not have observed convincing levels of expanded T cells in the macaque study as they were in culture with antigen for just 8 days. Furthermore, addition of IL-2 was not included in this experiment, despite being commonly used in short-term expansion cultures to promote survival and expansion (337, 338).

Another issue with this experiment was the lack of appropriate conditions to accurately assess activation of T cells by CD1c. While CD1c-mediated expansion is analysed by comparing T cell frequency following culture with THP1 with or without expression of CD1c, to properly assess activation we should have included a condition where THP1-CD1c expanded T cells were re-stimulated with the CD1c$^-$ parental line. This would have allowed us to assess whether activation markers were upregulated specifically by further stimulation, as currently the only T cells that were re-stimulated with the CD1c$^-$ THP1 line were those that were originally expanded with this line.

To further investigate specific recognition of CD1c it would have been pertinent to include antibodies for CD69 as this is a marker of early activation (433, 434). It may have been the case that CD1c-restricted T cells in Rhesus macaques are unable to recognise the human CD1c protein, or are unable to bind in the absence of exogenous antigen. Data from Layton *et al* suggests that during NHP evolution, the genes encoding group 1 CD1 protein have undergone diversifying selection which may alter their ability to present antigen to T cells (376). However, in contrast to our findings, Layton and colleagues did observe some activation of sorted macaque CD1c-restricted T cells by human CD1c expressed by K562 cells (376). Morita and colleagues also

observed activation of the human CD1b-restricted TCR LDN5 in the presence of T2 cells expressing human or macaque CD1b (377). However, no activation of human CD1a- or CD1c-restricted TCRs were observed with cognate macaque CD1 proteins. While some level of cross-species activation has been reported, a broader approach may be required to identify CD1c autoreactive T cells in the macaque. This may involve the use of lipid pulsed tetramers alongside those without exogenous antigen, short term expansion protocols with a greater range of parameters to be assessed, and cytokine assays to more closely monitor T cell response to CD1c.

Chapter 6 Future work and concluding remarks

6.1 Future work

6.1.1 Investigating the molecular basis underpinning TCR recognition of CD1c-lipid complexes

Mutational studies of CD1c interacting with a CD1c autoreactive αβTCR produced contradictory results and it was unclear whether the mutations generated, including those at the F' roof, had an effect on recognition by the TCR. To further probe the mechanisms of CD1c recognition, additional residues surrounding and distal to the F' roof would need to be mutated in order to gain insights into the binding footprint of this particular TCR. In addition to tetramer studies and SPR, mutant CD1c recognition by the TCR can also be assessed through activation assays that offer greater sensitivity to low affinity interactions when compared to tetramer staining. This would also provide further information on the interaction between the TCR and CD1c loaded with specific lipids. As we have revealed that the NM4 TCR promiscuously recognises an array of host derived lipids, it would be pertinent to observe whether mycobacteria derived lipids are also recognised. More importantly, co-crystallisation of CD1c with this TCR would provide unequivocal information on the binding footprint between the two molecules and how loaded lipids augment this interaction.

CD1c autoreactive γδ T cells were identified and isolated from the peripheral blood of healthy human donors. Our initial investigations into cloned γδTCRs confirmed recognition of CD1c loaded with endogenous lipids, but further characterisation is required to understand the mechanisms of interaction. Similar methods should be employed to investigate these CD1c autoreactive γδTCRs as for the αβTCR, NM4, to assess important CD1c residues involved in the TCR binding footprint and whether specific lipids inhibit the interaction. This would include mutational analyses, lipid loaded CD1c tetramer studies and activation assays. Further to this, primary T cells can be transduced with these CD1c autoreactive γδTCRs and incorporated into the 3D cell culture model to investigate function in the context of the immune response to TB. These studies together would provide an insight into the mechanisms involved in T cell autoreactivity to CD1c and how these cells are involved in the immune response to TB. This improved understanding would then inform the development of future therapeutics harnessing unconventional CD1c-restricted T cells.

6.1.2 CD1c autoreactive T cells in healthy and *M.tb* infected patients

Autoreactive T cells have been suggested to be involved in the immune response to TB, but as of yet little is understood about these populations and their role in disease. Our results corroborate previous reports that CD1c autoreactive T cells are abundant in the periphery of healthy individuals. To further characterise the purpose of these T cells in the absence of disease, short-term expansion cultures should be applied to a much larger cohort of healthy donors. The analysis of activation induced marker expression in response to CD1c stimulation can be coupled with tetramer studies to specifically evaluate expansion of CD1c-restricted T cells. Luminex assays could also be employed to evaluate the cytokine profile of CD1c stimulated cells, providing information on the role of CD1c autoreactive T cells within the healthy individual. The functional phenotype of these CD1c autoreactive T cells could then be compared to individuals with known LTBI or active TB to assess whether these populations are modulated in response to infection.

Our studies of South African TB patients indicate that CD1c autoreactive T cell populations are amplified in comparison to uninfected individuals. It would therefore be pertinent to further our understanding of the specific populations that expand in response to *M.tb* infection in order to develop more targeted therapeutics. Comparable to our tetramer-guided isolation of CD1c autoreactive γδ T cells from healthy individuals, CD1c autoreactive populations could also be sorted and sequenced from both the periphery and site of disease in the lung. TCR sequencing would provide information on whether there are clonal expansions of CD1c autoreactive T cells at the site of disease and if these differ from circulating T cells. These data could also be compared to that of healthy individuals to assess whether specific populations of CD1c autoreactive T cells are shared between healthy individuals and TB patients. The functional role of these T cells would then require investigation. Assessment of their cytokine profile in response to stimulation would provide information on the function of these T cells, but also their use within the 3D cell culture model would demonstrate their relevance in the context of *M.tb* infection. This would benefit our understanding of whether CD1c autoreactive T cells are indeed involved in the immune response to TB and whether they have a protective or deleterious role.

6.1.3 CD1-restricted T cells in the macaque model

The macaque model of *M.tb* infection allows the immune response to be precisely followed from pre-infection to necropsy, enabling the assessment of immune correlates in therapeutic development. Our group observed fluctuations in iNKT frequency and proliferative ability following *M.tb* challenge. However, to acquire a greater understanding of how this population is impacted by infection, a larger cohort of animals over a longer time course is required for a more

in-depth study of iNKT function in disease. As different species of macaque display varying levels of susceptibility or resistance to infection, it would be advantageous to analyse frequency, phenotype and functional parameters across species of both Rhesus and Cynomolgus macaques. The effect of additional conditions such as vaccination and anti-TB treatment on iNKT function can also be evaluated and correlated with infection outcomes for each animal. This would further inform our understanding of the iNKT response to infection and if these cells are a potential target for future vaccines or diagnostic indicators.

For the first time we have demonstrated the generation of Cynomolgus macaque CD1c tetramers which could be invaluable in evaluating the CD1c-restricted T cell response in *M.tb* challenge studies. However, further validation of this tool is required in order for it to be confidently used for quantitative studies. This would require testing on a much larger cohort of macaque samples from a variety of species. Loading of these macaque CD1c tetramers with specific lipids would also demonstrate whether a lipid is a requirement for recognition by macaque T cells. It has so far not been confirmed whether macaques indeed harbour CD1c autoreactive T cells, thus loading tetramers with specific lipids may allow for the isolation of CD1c-restricted T cell clones which could then be further functionally characterised. Following confirmation of the aptitude of macaque CD1c tetramers to identify CD1c-restricted T cells in the macaque, this tool could then be used in longitudinal studies to investigate the functional role of these cells in response to *M.tb* challenge, vaccination and novel therapeutics.

6.2 Conclusions

Unconventional T cells have been an understudied facet of human immunity, but a critical role for these populations in response to *M.tb* infection is beginning to be appreciated. Before these T cells can be utilised for the development of future anti-TB therapeutics, we must develop a greater understanding of their mechanistic interactions with their cognate ligands. Using molecular techniques and tetramer studies, we revealed that isolated CD1c autoreactive αβ and γδ T cells promiscuously recognise CD1c presenting an array of host-derived lipids. Furthermore, we have demonstrated that CD1c autoreactive T cells are elevated within the circulating αβ T cell subset and lung resident $V\delta1^+$ T cell subset of TB patients compared to healthy individuals. Additionally, elevated PD1 expression by lung resident $V\delta1^+$ T cells of TB patients suggest activation in response to antigen. Our results therefore indicate a role for CD1c autoreactive T cells in the immune response to *M.tb* infection and perhaps the exacerbation of tissue destruction following recognition of both host and pathogen derived lipids.

We also utilised the macaque model of TB to investigate iNKT frequency and function within the peripheral blood and lung lobe biopsies following *M.tb* challenge. We revealed in a small cohort of Rhesus macaques the acute impact of *M.tb* infection on the proliferative function of iNKT cells. We also laid out the potential of correlating iNKT frequency and proliferative response with bacteriology and pathology scores from individual lung lobes following necropsy. In addition, we demonstrated the generation of a novel Cynomolgus macaque CD1c tetramer with a preliminary investigation into the functional ability to identify CD1c-restricted T cells in a small set of macaque PBMC samples. The success of constructing this macaque CD1c tetramer paves the way for future validation and use in longitudinal challenge studies, with implications for the development of unconventional T cell based therapeutics.

The immune response to *M.tb* is a complex process involving the interplay between many facets of both innate and adaptive immunity. While knockout models have been invaluable in demonstrating the absolute requirement of an intact immune response for the control of infection, it remains unclear what is involved in maintaining the balance between pathogen elimination and destruction of host tissue. The development of new preventative therapeutics must take into account the wider interactions between various components of the immune system and provide protection for the global population. Lipid-based vaccines may address this requirement due to the non-polymorphic nature of their cognate antigen presenting molecules. It is however imperative that new lipid-based vaccines stimulate a targeted anti-*M.tb* response and do not initiate autoreactive responses which may occur from the recognition of shared lipids. Further understanding is therefore required of TCR mediated recognition of CD1 molecules presenting host and pathogen derived lipids, in addition to how *M.tb* infection modulates lipid-specific autoreactive T cell responses.

List of References

1. World Health Organisation. Global tuberculosis report 2020 France: World Health Organisation; 2020 [Available from: https://www.who.int/publications/i/item/9789240013131.
2. O'Garra A, Redford PS, McNab FW, Bloom CI, Wilkinson RJ, Berry MP. The immune response in tuberculosis. Annu Rev Immunol. 2013;31:475-527.
3. Elkington PT, Friedland JS. Permutations of time and place in tuberculosis. The Lancet Infectious diseases. 2015;15(11):1357-60.
4. Ndiaye BP, Thienemann F, Ota M, Landry BS, Camara M, Dièye S, et al. Safety, immunogenicity, and efficacy of the candidate tuberculosis vaccine MVA85A in healthy adults infected with HIV-1: a randomised, placebo-controlled, phase 2 trial. The Lancet Respiratory Medicine.3(3):190-200.
5. Tameris MD, Hatherill M, Landry BS, Scriba TJ, Snowden MA, Lockhart S, et al. Safety and efficacy of MVA85A, a new tuberculosis vaccine, in infants previously vaccinated with BCG: a randomised, placebo-controlled phase 2b trial. The Lancet. 2013;381(9871):1021-8.
6. Koch R. The etiology of tuberculosis. Zentralblatt fur Bakteriologie, Mikrobiologie und Hygiene 1 Abt Originale A, Medizinische Mikrobiologie, Infektionskrankheiten und Parasitologie = International journal of microbiology and hygiene A, Medical microbiology, inf. 1882;15:221-30.
7. Ghazaei C. Mycobacterium tuberculosis and lipids: Insights into molecular mechanisms from persistence to virulence. Journal of research in medical sciences : the official journal of Isfahan University of Medical Sciences. 2018;23:63.
8. Jackson M. The mycobacterial cell envelope-lipids. Cold Spring Harbor perspectives in medicine.4(10):a021105.
9. Russell DG. Mycobacterium tuberculosis and the intimate discourse of a chronic infection. Immunological reviews. 2011;240(1):252-68.
10. Colombo MI, Gutierrez MG, Romano PS. The two faces of autophagy: Coxiella and Mycobacterium. Autophagy. 2006;2(3):162-4.
11. Gutierrez MG, Master SS, Singh SB, Taylor GA, Colombo MI, Deretic V. Autophagy is a defense mechanism inhibiting BCG and Mycobacterium tuberculosis survival in infected macrophages. Cell. 2004;119(6):753-66.
12. Behar SM, Martin CJ, Booty MG, Nishimura T, Zhao X, Gan HX, et al. Apoptosis is an innate defense function of macrophages against Mycobacterium tuberculosis. Mucosal immunology. 2011;4(3):279-87.
13. Sturgill-Koszycki S, Schlesinger PH, Chakraborty P, Haddix PL, Collins HL, Fok AK, et al. Lack of acidification in Mycobacterium phagosomes produced by exclusion of the vesicular proton-ATPase. Science (New York, NY). 1994;263(5147):678-81.
14. Ramachandra L, Smialek JL, Shank SS, Convery M, Boom WH, Harding CV. Phagosomal Processing of Mycobacterium tuberculosis Antigen 85B Is Modulated Independently of Mycobacterial Viability and Phagosome Maturation. Infection and immunity. 2005;73(2):1097-105.
15. Silva Miranda M, Breiman A, Allain S, Deknuydt F, Altare F. The Tuberculous Granuloma: An Unsuccessful Host Defence Mechanism Providing a Safety Shelter for the Bacteria? Clinical and Developmental Immunology. 2012;2012:139127.
16. Adams DO. The granulomatous inflammatory response. A review. The American journal of pathology. 1976;84(1):164-92.
17. Sandor M, Weinstock JV, Wynn TA. Granulomas in schistosome and mycobacterial infections: a model of local immune responses. Trends in immunology. 2003;24(1):44-52.
18. Barry CE, 3rd, Boshoff HI, Dartois V, Dick T, Ehrt S, Flynn J, et al. The spectrum of latent tuberculosis: rethinking the biology and intervention strategies. Nature reviews Microbiology. 2009;7(12):845-55.
19. Ramakrishnan L. Revisiting the role of the granuloma in tuberculosis. Nature Reviews Immunology. 2012;12(5):352-66.

20. Wolf AJ, Linas B, Trevejo-Nunez GJ, Kincaid E, Tamura T, Takatsu K, et al. Mycobacterium tuberculosis infects dendritic cells with high frequency and impairs their function in vivo. J Immunol. 2007;179(4):2509-19.
21. Schluger NW, Rom WN. The Host Immune Response to Tuberculosis. American journal of respiratory and critical care medicine. 1998;157(3):679-91.
22. Law KF, Jagirdar J, Weiden MD, Bodkin M, Rom WN. Tuberculosis in HIV-positive patients: cellular response and immune activation in the lung. American journal of respiratory and critical care medicine. 1996;153(4):1377-84.
23. Sakai S, Mayer-Barber KD, Barber DL. Defining Features of Protective CD4 T cell responses to Mycobacterium tuberculosis. Current opinion in immunology. 2014;0:137-42.
24. Caruso AM, Serbina N, Klein E, Triebold K, Bloom BR, Flynn JL. Mice deficient in CD4 T cells have only transiently diminished levels of IFN-gamma, yet succumb to tuberculosis. J Immunol. 1999;162(9):5407-16.
25. Havlir DV, Barnes PF. Tuberculosis in patients with human immunodeficiency virus infection. The New England journal of medicine. 1999;340(5):367-73.
26. Serbina NV, Lazarevic V, Flynn JL. CD4+ T Cells Are Required for the Development of Cytotoxic CD8+ T Cells During Mycobacterium tuberculosis Infection. The Journal of Immunology. 2001;167(12):6991.
27. Stenger S, Mazzaccaro RJ, Uyemura K, Cho S, Barnes PF, Rosat JP, et al. Differential effects of cytolytic T cell subsets on intracellular infection. Science (New York, NY). 1997;276(5319):1684-7.
28. Tascon RE, Stavropoulos E, Lukacs KV, Colston MJ. Protection against Mycobacterium tuberculosis Infection by CD8+ T Cells Requires the Production of Gamma Interferon. Infection and immunity. 1998;66(2):830.
29. van Pinxteren LA, Cassidy JP, Smedegaard BH, Agger EM, Andersen P. Control of latent Mycobacterium tuberculosis infection is dependent on CD8 T cells. European journal of immunology. 2000;30(12):3689-98.
30. Flynn JL, Goldstein MM, Triebold KJ, Koller B, Bloom BR. Major histocompatibility complex class I-restricted T cells are required for resistance to Mycobacterium tuberculosis infection. Proceedings of the National Academy of Sciences. 1992;89(24):12013.
31. Chancellor A, White A, Tocheva AS, Fenn JR, Dennis M, Tezera L, et al. Quantitative and qualitative iNKT repertoire associations with disease susceptibility and outcome in macaque tuberculosis infection. Tuberculosis (Edinburgh, Scotland). 2017;105:86-95.
32. Tezera LB, Bielecka MK, Chancellor A, Reichmann MT, Shammari BA, Brace P, et al. Dissection of the host-pathogen interaction in human tuberculosis using a bioengineered 3-dimensional model. eLife. 2017;6.
33. Elkington PT, D'Armiento JM, Friedland JS. Tuberculosis immunopathology: the neglected role of extracellular matrix destruction. Science translational medicine. 2011;3(71):71ps6.
34. Al Shammari B, Shiomi T, Tezera L, Bielecka MK, Workman V, Sathyamoorthy T, et al. The Extracellular Matrix Regulates Granuloma Necrosis in Tuberculosis. The Journal of infectious diseases. 2015;212(3):463-73.
35. Buchheit CL, Rayavarapu RR, Schafer ZT. The regulation of cancer cell death and metabolism by extracellular matrix attachment. Seminars in cell & developmental biology. 2012;23(4):402-11.
36. Mueller-Klieser W. Three-dimensional cell cultures: from molecular mechanisms to clinical applications. The American journal of physiology. 1997;273(4 Pt 1):C1109-23.
37. Berrington WR, Hawn TR. Mycobacterium tuberculosis, macrophages, and the innate immune response: does common variation matter? Immunological reviews. 2007;219:167-86.
38. Ehrt S, Schnappinger D. Mycobacterial survival strategies in the phagosome: defence against host stresses. Cellular microbiology. 2009;11(8):1170-8.
39. Jo EK. Mycobacterial interaction with innate receptors: TLRs, C-type lectins, and NLRs. Current opinion in infectious diseases. 2008;21(3):279-86.

40. Jo EK, Yang CS, Choi CH, Harding CV. Intracellular signalling cascades regulating innate immune responses to Mycobacteria: branching out from Toll-like receptors. Cellular microbiology. 2007;9(5):1087-98.
41. Reiling N, Ehlers S, Hölscher C. MyDths and un-TOLLed truths: sensor, instructive and effector immunity to tuberculosis. Immunology letters. 2008;116(1):15-23.
42. Nicholson S, Bonecini-Almeida Mda G, Lapa e Silva JR, Nathan C, Xie QW, Mumford R, et al. Inducible nitric oxide synthase in pulmonary alveolar macrophages from patients with tuberculosis. The Journal of experimental medicine. 1996;183(5):2293-302.
43. Dorhoi A, Iannaccone M, Maertzdorf J, Nouailles G, Weiner J, 3rd, Kaufmann SHE. Reverse translation in tuberculosis: neutrophils provide clues for understanding development of active disease. Frontiers in immunology. 2014;5:36-.
44. Gleeson LE, Sheedy FJ, Palsson-McDermott EM, Triglia D, O'Leary SM, O'Sullivan MP, et al. Cutting Edge: Mycobacterium tuberculosis Induces Aerobic Glycolysis in Human Alveolar Macrophages That Is Required for Control of Intracellular Bacillary Replication. J Immunol. 2016;196(6):2444-9.
45. Silver RF, Walrath J, Lee H, Jacobson BA, Horton H, Bowman MR, et al. Human alveolar macrophage gene responses to Mycobacterium tuberculosis strains H37Ra and H37Rv. Am J Respir Cell Mol Biol. 2009;40(4):491-504.
46. Noss EH, Pai RK, Sellati TJ, Radolf JD, Belisle J, Golenbock DT, et al. Toll-like receptor 2-dependent inhibition of macrophage class II MHC expression and antigen processing by 19-kDa lipoprotein of Mycobacterium tuberculosis. J Immunol. 2001;167(2):910-8.
47. Wang J, Gigliotti F, Maggirwar S, Johnston C, Finkelstein JN, Wright TW. Pneumocystis carinii activates the NF-kappaB signaling pathway in alveolar epithelial cells. Infection and immunity. 2005;73(5):2766-77.
48. Sreejit G, Ahmed A, Parveen N, Jha V, Valluri VL, Ghosh S, et al. The ESAT-6 protein of Mycobacterium tuberculosis interacts with beta-2-microglobulin (β2M) affecting antigen presentation function of macrophage. PLoS pathogens. 2014;10(10):e1004446-e.
49. Awuh JA, Flo TH. Molecular basis of mycobacterial survival in macrophages. Cellular and Molecular Life Sciences. 2017;74(9):1625-48.
50. Flynn JL, Chan J. Immune evasion by Mycobacterium tuberculosis: living with the enemy. Current opinion in immunology. 2003;15(4):450-5.
51. Chen M, Gan H, Remold HG. A mechanism of virulence: virulent Mycobacterium tuberculosis strain H37Rv, but not attenuated H37Ra, causes significant mitochondrial inner membrane disruption in macrophages leading to necrosis. J Immunol. 2006;176(6):3707-16.
52. Fratazzi C, Arbeit RD, Carini C, Balcewicz-Sablinska MK, Keane J, Kornfeld H, et al. Macrophage apoptosis in mycobacterial infections. Journal of leukocyte biology. 1999;66(5):763-4.
53. Keane J, Balcewicz-Sablinska MK, Remold HG, Chupp GL, Meek BB, Fenton MJ, et al. Infection by Mycobacterium tuberculosis promotes human alveolar macrophage apoptosis. Infection and immunity. 1997;65(1):298-304.
54. Lee J, Hartman M, Kornfeld H. Macrophage apoptosis in tuberculosis. Yonsei Med J. 2009;50(1):1-11.
55. Marino S, Pawar S, Fuller CL, Reinhart TA, Flynn JL, Kirschner DE. Dendritic cell trafficking and antigen presentation in the human immune response to Mycobacterium tuberculosis. J Immunol. 2004;173(1):494-506.
56. Mihret A. The role of dendritic cells in Mycobacterium tuberculosis infection. Virulence. 2012;3(7):654-9.
57. Demangel C, Bertolino P, Britton WJ. Autocrine IL-10 impairs dendritic cell (DC)-derived immune responses to mycobacterial infection by suppressing DC trafficking to draining lymph nodes and local IL-12 production. European journal of immunology. 2002;32(4):994-1002.
58. Khader SA, Partida-Sanchez S, Bell G, Jelley-Gibbs DM, Swain S, Pearl JE, et al. Interleukin 12p40 is required for dendritic cell migration and T cell priming after Mycobacterium tuberculosis infection. The Journal of experimental medicine. 2006;203(7):1805-15.

59. Young D, Stark J, Kirschner D. Systems biology of persistent infection: tuberculosis as a case study. Nature reviews Microbiology. 2008;6(7):520-8.
60. Gonzalez-Juarrero M, Orme IM. Characterization of murine lung dendritic cells infected with Mycobacterium tuberculosis. Infection and immunity. 2001;69(2):1127-33.
61. Tian T, Woodworth J, Sköld M, Behar SM. In Vivo Depletion of CD11c⁺ Cells Delays the CD4⁺ T Cell Response to Mycobacterium tuberculosis and Exacerbates the Outcome of Infection. The Journal of Immunology. 2005;175(5):3268.
62. Henderson RA, Watkins SC, Flynn JL. Activation of human dendritic cells following infection with Mycobacterium tuberculosis. J Immunol. 1997;159(2):635-43.
63. Stenger S, Niazi KR, Modlin RL. Down-regulation of CD1 on antigen-presenting cells by infection with Mycobacterium tuberculosis. J Immunol. 1998;161(7):3582-8.
64. van der Wel N, Hava D, Houben D, Fluitsma D, van Zon M, Pierson J, et al. M. tuberculosis and M. leprae translocate from the phagolysosome to the cytosol in myeloid cells. Cell. 2007;129(7):1287-98.
65. Winau F, Weber S, Sad S, de Diego J, Hoops SL, Breiden B, et al. Apoptotic vesicles crossprime CD8 T cells and protect against tuberculosis. Immunity. 2006;24(1):105-17.
66. Juffermans NP, Paxton WA, Dekkers PE, Verbon A, de Jonge E, Speelman P, et al. Up-regulation of HIV coreceptors CXCR4 and CCR5 on CD4(+) T cells during human endotoxemia and after stimulation with (myco)bacterial antigens: the role of cytokines. Blood. 2000;96(8):2649-54.
67. Khan N, Vidyarthi A, Pahari S, Agrewala JN. Distinct Strategies Employed by Dendritic Cells and Macrophages in Restricting Mycobacterium tuberculosis Infection: Different Philosophies but Same Desire. International reviews of immunology. 2016;35(5):386-98.
68. Ladel CH, Blum C, Dreher A, Reifenberg K, Kaufmann SH. Protective role of gamma/delta T cells and alpha/beta T cells in tuberculosis. European journal of immunology. 1995;25(10):2877-81.
69. Mayer-Barber KD, Andrade BB, Barber DL, Hieny S, Feng CG, Caspar P, et al. Innate and adaptive interferons suppress IL-1α and IL-1β production by distinct pulmonary myeloid subsets during Mycobacterium tuberculosis infection. Immunity. 2011;35(6):1023-34.
70. Cooper AM. Cell-mediated immune responses in tuberculosis. Annual review of immunology. 2009;27:393-422.
71. Ottenhoff TH, Kumararatne D, Casanova JL. Novel human immunodeficiencies reveal the essential role of type-I cytokines in immunity to intracellular bacteria. Immunology today. 1998;19(11):491-4.
72. Mohagheghpour N, van Vollenhoven A, Goodman J, Bermudez LE. Interaction of Mycobacterium avium with human monocyte-derived dendritic cells. Infection and immunity. 2000;68(10):5824-9.
73. Hanekom WA, Mendillo M, Manca C, Haslett PA, Siddiqui MR, Barry C, 3rd, et al. Mycobacterium tuberculosis inhibits maturation of human monocyte-derived dendritic cells in vitro. The Journal of infectious diseases. 2003;188(2):257-66.
74. Bhatt K, Hickman SP, Salgame P. Cutting edge: a new approach to modeling early lung immunity in murine tuberculosis. J Immunol. 2004;172(5):2748-51.
75. Mihret A, Mamo G, Tafesse M, Hailu A, Parida S. Dendritic Cells Activate and Mature after Infection with Mycobacterium tuberculosis. BMC Res Notes. 2011;4:247-.
76. Geijtenbeek TB, Krooshoop DJ, Bleijs DA, van Vliet SJ, van Duijnhoven GC, Grabovsky V, et al. DC-SIGN-ICAM-2 interaction mediates dendritic cell trafficking. Nature immunology. 2000;1(4):353-7.
77. Balboa L, Romero MM, Yokobori N, Schierloh P, Geffner L, Basile JI, et al. Mycobacterium tuberculosis impairs dendritic cell response by altering CD1b, DC-SIGN and MR profile. Immunol Cell Biol. 2010;88(7):716-26.
78. Motta A, Schmitz C, Rodrigues L, Ribeiro F, Teixeira C, Detanico T, et al. Mycobacterium tuberculosis heat-shock protein 70 impairs maturation of dendritic cells from bone marrow precursors, induces interleukin-10 production and inhibits T-cell proliferation in vitro. Immunology. 2007;121(4):462-72.

79. Barber DL, Mayer-Barber KD, Feng CG, Sharpe AH, Sher A. CD4 T cells promote rather than control tuberculosis in the absence of PD-1-mediated inhibition. Journal of immunology (Baltimore, Md : 1950). 2011;186(3):1598-607.
80. Wolf AJ, Desvignes L, Linas B, Banaiee N, Tamura T, Takatsu K, et al. Initiation of the adaptive immune response to Mycobacterium tuberculosis depends on antigen production in the local lymph node, not the lungs. The Journal of experimental medicine. 2008;205(1):105-15.
81. Eum SY, Kong JH, Hong MS, Lee YJ, Kim JH, Hwang SH, et al. Neutrophils are the predominant infected phagocytic cells in the airways of patients with active pulmonary TB. Chest. 2010;137(1):122-8.
82. Tan BH, Meinken C, Bastian M, Bruns H, Legaspi A, Ochoa MT, et al. Macrophages acquire neutrophil granules for antimicrobial activity against intracellular pathogens. J Immunol. 2006;177(3):1864-71.
83. Appelberg R. Neutrophils and intracellular pathogens: beyond phagocytosis and killing. Trends in microbiology. 2007;15(2):87-92.
84. Martin CJ, Booty MG, Rosebrock TR, Nunes-Alves C, Desjardins DM, Keren I, et al. Efferocytosis is an innate antibacterial mechanism. Cell host & microbe. 2012;12(3):289-300.
85. Blomgran R, Desvignes L, Briken V, Ernst JD. Mycobacterium tuberculosis inhibits neutrophil apoptosis, leading to delayed activation of naive CD4 T cells. Cell host & microbe. 2012;11(1):81-90.
86. Blomgran R, Ernst JD. Lung neutrophils facilitate activation of naive antigen-specific CD4+ T cells during Mycobacterium tuberculosis infection. J Immunol. 2011;186(12):7110-9.
87. Martineau AR, Newton SM, Wilkinson KA, Kampmann B, Hall BM, Nawroly N, et al. Neutrophil-mediated innate immune resistance to mycobacteria. J Clin Invest. 2007;117(7):1988-94.
88. Kroon EE, Coussens AK, Kinnear C, Orlova M, Möller M, Seeger A, et al. Neutrophils: Innate Effectors of TB Resistance? Front Immunol. 2018;9:2637.
89. Dorhoi A, Desel C, Yeremeev V, Pradl L, Brinkmann V, Mollenkopf HJ, et al. The adaptor molecule CARD9 is essential for tuberculosis control. The Journal of experimental medicine. 2010;207(4):777-92.
90. Mishra BB, Lovewell RR, Olive AJ, Zhang G, Wang W, Eugenin E, et al. Nitric oxide prevents a pathogen-permissive granulocytic inflammation during tuberculosis. Nat Microbiol. 2017;2:17072-.
91. Nair S, Huynh JP, Lampropoulou V, Loginicheva E, Esaulova E, Gounder AP, et al. Irg1 expression in myeloid cells prevents immunopathology during M. tuberculosis infection. The Journal of experimental medicine. 2018;215(4):1035-45.
92. Zhang Y, Zhou Y, Lou J, Li J, Bo L, Zhu K, et al. PD-L1 blockade improves survival in experimental sepsis by inhibiting lymphocyte apoptosis and reversing monocyte dysfunction. Critical care (London, England). 2010;14(6):R220.
93. Mogues T, Goodrich ME, Ryan L, LaCourse R, North RJ. The relative importance of T cell subsets in immunity and immunopathology of airborne Mycobacterium tuberculosis infection in mice. The Journal of experimental medicine. 2001;193(3):271-80.
94. Scanga CA, Mohan VP, Yu K, Joseph H, Tanaka K, Chan J, et al. Depletion of CD4(+) T cells causes reactivation of murine persistent tuberculosis despite continued expression of interferon gamma and nitric oxide synthase 2. The Journal of experimental medicine. 2000;192(3):347-58.
95. Volkman HE, Pozos TC, Zheng J, Davis JM, Rawls JF, Ramakrishnan L. Tuberculous granuloma induction via interaction of a bacterial secreted protein with host epithelium. Science (New York, NY). 2010;327(5964):466-9.
96. Repique CJ, Li A, Brickey WJ, Ting JPY, Collins FM, Morris SL. Susceptibility of Mice Deficient in the MHC Class II Transactivator to Infection with Mycobacterium tuberculosis. Scandinavian Journal of Immunology. 2003;58(1):15-22.
97. Srivastava S, Ernst JD. Cutting edge: Direct recognition of infected cells by CD4 T cells is required for control of intracellular Mycobacterium tuberculosis in vivo. J Immunol. 2013;191(3):1016-20.

98. Chang ST, Linderman JJ, Kirschner DE. Multiple mechanisms allow Mycobacterium tuberculosis to continuously inhibit MHC class II-mediated antigen presentation by macrophages. Proceedings of the National Academy of Sciences of the United States of America. 2005;102(12):4530-5.
99. Harding CV, Boom WH. Regulation of antigen presentation by Mycobacterium tuberculosis: a role for Toll-like receptors. Nature reviews Microbiology. 2010;8(4):296-307.
100. Sia JK, Rengarajan J. Immunology of Mycobacterium tuberculosis Infections. Microbiol Spectr. 2019;7(4):10.1128/microbiolspec.GPP3-0022-2018.
101. Khader SA, Pearl JE, Sakamoto K, Gilmartin L, Bell GK, Jelley-Gibbs DM, et al. IL-23 compensates for the absence of IL-12p70 and is essential for the IL-17 response during tuberculosis but is dispensable for protection and antigen-specific IFN-gamma responses if IL-12p70 is available. J Immunol. 2005;175(2):788-95.
102. Andreasen SO, Christensen JE, Marker O, Thomsen AR. Role of CD40 ligand and CD28 in induction and maintenance of antiviral CD8+ effector T cell responses. J Immunol. 2000;164(7):3689-97.
103. Clarke SR. The critical role of CD40/CD40L in the CD4-dependent generation of CD8+ T cell immunity. Journal of leukocyte biology. 2000;67(5):607-14.
104. Kalams SA, Walker BD. The critical need for CD4 help in maintaining effective cytotoxic T lymphocyte responses. The Journal of experimental medicine. 1998;188(12):2199-204.
105. Sia JK, Bizzell E, Madan-Lala R, Rengarajan J. Engaging the CD40-CD40L pathway augments T-helper cell responses and improves control of Mycobacterium tuberculosis infection. PLoS Pathog. 2017;13(8):e1006530.
106. Flynn JL, Chan J, Triebold KJ, Dalton DK, Stewart TA, Bloom BR. An essential role for interferon gamma in resistance to Mycobacterium tuberculosis infection. The Journal of experimental medicine. 1993;178(6):2249-54.
107. Cadena AM, Flynn JL, Fortune SM. The Importance of First Impressions: Early Events in Mycobacterium tuberculosis Infection Influence Outcome. mBio. 2016;7(2):e00342-16.
108. Feng CG, Bean AG, Hooi H, Briscoe H, Britton WJ. Increase in gamma interferon-secreting CD8(+), as well as CD4(+), T cells in lungs following aerosol infection with Mycobacterium tuberculosis. Infection and immunity. 1999;67(7):3242-7.
109. Serbina NV, Liu CC, Scanga CA, Flynn JL. CD8+ CTL from lungs of Mycobacterium tuberculosis-infected mice express perforin in vivo and lyse infected macrophages. J Immunol. 2000;165(1):353-63.
110. Tascon RE, Stavropoulos E, Lukacs KV, Colston MJ. Protection against Mycobacterium tuberculosis infection by CD8+ T cells requires the production of gamma interferon. Infection and immunity. 1998;66(2):830-4.
111. Cowley SC, Elkins KL. CD4+ T cells mediate IFN-gamma-independent control of Mycobacterium tuberculosis infection both in vitro and in vivo. J Immunol. 2003;171(9):4689-99.
112. Gallegos AM, van Heijst JW, Samstein M, Su X, Pamer EG, Glickman MS. A gamma interferon independent mechanism of CD4 T cell mediated control of M. tuberculosis infection in vivo. PLoS Pathog. 2011;7(5):e1002052.
113. Darrah PA, Patel DT, De Luca PM, Lindsay RWB, Davey DF, Flynn BJ, et al. Multifunctional TH1 cells define a correlate of vaccine-mediated protection against Leishmania major. Nature medicine. 2007;13(7):843-50.
114. Soares AP, Scriba TJ, Joseph S, Harbacheuski R, Murray RA, Gelderbloem SJ, et al. Bacillus Calmette-Guérin vaccination of human newborns induces T cells with complex cytokine and phenotypic profiles. J Immunol. 2008;180(5):3569-77.
115. Winkler S, Necek M, Winkler H, Adegnika AA, Perkmann T, Ramharter M, et al. Increased specific T cell cytokine responses in patients with active pulmonary tuberculosis from Central Africa. Microbes and infection. 2005;7(9-10):1161-9.
116. Harari A, Rozot V, Bellutti Enders F, Perreau M, Stalder JM, Nicod LP, et al. Dominant TNF-α+ Mycobacterium tuberculosis-specific CD4+ T cell responses discriminate between latent infection and active disease. Nature medicine. 2011;17(3):372-6.

117. Chakravarty SD, Xu J, Lu B, Gerard C, Flynn J, Chan J. The chemokine receptor CXCR3 attenuates the control of chronic Mycobacterium tuberculosis infection in BALB/c mice. J Immunol. 2007;178(3):1723-35.
118. de Martino M, Lodi L, Galli L, Chiappini E. Immune Response to Mycobacterium tuberculosis: A Narrative Review. Frontiers in pediatrics. 2019;7:350.
119. Behar SM. Antigen-specific CD8(+) T cells and protective immunity to tuberculosis. Advances in experimental medicine and biology. 2013;783:141-63.
120. Mohagheghpour N, Gammon D, Kawamura LM, van Vollenhoven A, Benike CJ, Engleman EG. CTL response to Mycobacterium tuberculosis: identification of an immunogenic epitope in the 19-kDa lipoprotein. J Immunol. 1998;161(5):2400-6.
121. Silva CL, Lowrie DB. Identification and characterization of murine cytotoxic T cells that kill Mycobacterium tuberculosis. Infection and immunity. 2000;68(6):3269-74.
122. Zhu X, Stauss HJ, Ivanyi J, Vordermeier HM. Specificity of CD8+ T cells from subunit-vaccinated and infected H-2b mice recognizing the 38 kDa antigen of Mycobacterium tuberculosis. Int Immunol. 1997;9(11):1669-76.
123. Caminero JA, Pena MJ, Campos-Herrero MI, Rodríguez JC, Afonso O, Martin C, et al. Exogenous reinfection with tuberculosis on a European island with a moderate incidence of disease. American journal of respiratory and critical care medicine. 2001;163(3 Pt 1):717-20.
124. Lalvani A, Brookes R, Wilkinson RJ, Malin AS, Pathan AA, Andersen P, et al. Human cytolytic and interferon gamma-secreting CD8+ T lymphocytes specific for Mycobacterium tuberculosis. Proceedings of the National Academy of Sciences of the United States of America. 1998;95(1):270-5.
125. Pathan AA, Wilkinson KA, Wilkinson RJ, Latif M, McShane H, Pasvol G, et al. High frequencies of circulating IFN-gamma-secreting CD8 cytotoxic T cells specific for a novel MHC class I-restricted Mycobacterium tuberculosis epitope in M. tuberculosis-infected subjects without disease. European journal of immunology. 2000;30(9):2713-21.
126. Urdahl KB, Liggitt D, Bevan MJ. CD8+ T cells accumulate in the lungs of Mycobacterium tuberculosis-infected Kb-/-Db-/- mice, but provide minimal protection. J Immunol. 2003;170(4):1987-94.
127. Serbina NV, Flynn JL. Early emergence of CD8(+) T cells primed for production of type 1 cytokines in the lungs of Mycobacterium tuberculosis-infected mice. Infection and immunity. 1999;67(8):3980-8.
128. Canaday DH, Wilkinson RJ, Li Q, Harding CV, Silver RF, Boom WH. CD4(+) and CD8(+) T cells kill intracellular Mycobacterium tuberculosis by a perforin and Fas/Fas ligand-independent mechanism. J Immunol. 2001;167(5):2734-42.
129. Lin PL, Flynn JL. CD8 T cells and Mycobacterium tuberculosis infection. Seminars in Immunopathology. 2015;37(3):239-49.
130. Sud D, Bigbee C, Flynn JL, Kirschner DE. Contribution of CD8+ T cells to control of Mycobacterium tuberculosis infection. J Immunol. 2006;176(7):4296-314.
131. Stenger S, Hanson DA, Teitelbaum R, Dewan P, Niazi KR, Froelich CJ, et al. An antimicrobial activity of cytolytic T cells mediated by granulysin. Science (New York, NY). 1998;282(5386):121-5.
132. Behar SM, Dascher CC, Grusby MJ, Wang CR, Brenner MB. Susceptibility of mice deficient in CD1D or TAP1 to infection with Mycobacterium tuberculosis. The Journal of experimental medicine. 1999;189(12):1973-80.
133. Orme IM. The kinetics of emergence and loss of mediator T lymphocytes acquired in response to infection with Mycobacterium tuberculosis. J Immunol. 1987;138(1):293-8.
134. Sousa AO, Mazzaccaro RJ, Russell RG, Lee FK, Turner OC, Hong S, et al. Relative contributions of distinct MHC class I-dependent cell populations in protection to tuberculosis infection in mice. Proceedings of the National Academy of Sciences of the United States of America. 2000;97(8):4204-8.
135. Green AM, Difazio R, Flynn JL. IFN-γ from CD4 T cells is essential for host survival and enhances CD8 T cell function during Mycobacterium tuberculosis infection. J Immunol. 2013;190(1):270-7.

136. Godfrey DI, Uldrich AP, McCluskey J, Rossjohn J, Moody DB. The burgeoning family of unconventional T cells. Nature immunology. 2015;16(11):1114-23.
137. Rossjohn J, Gras S, Miles JJ, Turner SJ, Godfrey DI, McCluskey J. T cell antigen receptor recognition of antigen-presenting molecules. Annu Rev Immunol. 2015;33:169-200.
138. Huang S. Targeting Innate-Like T Cells in Tuberculosis. Frontiers in Immunology. 2016;7:594.
139. Van Rhijn I, Moody DB. CD1 and mycobacterial lipids activate human T cells. Immunological reviews. 2015;264(1):138-53.
140. Pellicci DG, Koay H-F, Berzins SP. Thymic development of unconventional T cells: how NKT cells, MAIT cells and γδ T cells emerge. Nature Reviews Immunology. 2020;20(12):756-70.
141. Chua WJ, Truscott SM, Eickhoff CS, Blazevic A, Hoft DF, Hansen TH. Polyclonal mucosa-associated invariant T cells have unique innate functions in bacterial infection. Infection and immunity. 2012;80(9):3256-67.
142. Winslow GM, Cooper A, Reiley W, Chatterjee M, Woodland DL. Early T-cell responses in tuberculosis immunity. Immunological reviews. 2008;225:284-99.
143. Keane J, Gershon S, Wise RP, Mirabile-Levens E, Kasznica J, Schwieterman WD, et al. Tuberculosis associated with infliximab, a tumor necrosis factor alpha-neutralizing agent. The New England journal of medicine. 2001;345(15):1098-104.
144. Selwyn PA, Hartel D, Lewis VA, Schoenbaum EE, Vermund SH, Klein RS, et al. A prospective study of the risk of tuberculosis among intravenous drug users with human immunodeficiency virus infection. The New England journal of medicine. 1989;320(9):545-50.
145. Sperber SJ, Gornish N. Reactivation of Tuberculosis During Therapy with Corticosteroids. Clinical Infectious Diseases. 1992;15(6):1073-4.
146. Busch M, Herzmann C, Kallert S, Zimmermann A, Höfer C, Mayer D, et al. Lipoarabinomannan-Responsive Polycytotoxic T Cells Are Associated with Protection in Human Tuberculosis. American journal of respiratory and critical care medicine. 2016;194(3):345-55.
147. Shen L, Frencher J, Huang D, Wang W, Yang E, Chen CY, et al. Immunization of Vgamma2Vdelta2 T cells programs sustained effector memory responses that control tuberculosis in nonhuman primates. Proceedings of the National Academy of Sciences of the United States of America. 2019;116(13):6371-8.
148. Zhao J, Siddiqui S, Shang S, Bian Y, Bagchi S, He Y, et al. Mycolic acid-specific T cells protect against Mycobacterium tuberculosis infection in a humanized transgenic mouse model. eLife. 2015;4.
149. Rothchild AC, Jayaraman P, Nunes-Alves C, Behar SM. iNKT Cell Production of GM-CSF Controls Mycobacterium tuberculosis. PLOS Pathogens. 2014;10(1):e1003805.
150. Sada-Ovalle I, Chiba A, Gonzales A, Brenner MB, Behar SM. Innate Invariant NKT Cells Recognize Mycobacterium tuberculosis–Infected Macrophages, Produce Interferon-γ, and Kill Intracellular Bacteria. PLOS Pathogens. 2008;4(12):e1000239.
151. Lepore M, Mori L, De Libero G. The Conventional Nature of Non-MHC-Restricted T Cells. Frontiers in Immunology. 2018;9:1365.
152. Bienemann K, Iouannidou K, Schoenberg K, Krux F, Reuther S, Feyen O, et al. iNKT Cell Frequency in Peripheral Blood of Caucasian Children and Adolescent: The Absolute iNKT Cell Count is Stable from Birth to Adulthood. Scandinavian Journal of Immunology. 2011;74(4):406-11.
153. Bendelac A, Savage PB, Teyton L. The biology of NKT cells. Annu Rev Immunol. 2007;25:297-336.
154. Berzins SP, Smyth MJ, Baxter AG. Presumed guilty: natural killer T cell defects and human disease. Nature reviews Immunology. 2011;11(2):131-42.
155. Godfrey DI, Stankovic S, Baxter AG. Raising the NKT cell family. Nature immunology. 2010;11(3):197-206.
156. Kovalovsky D, Uche OU, Eladad S, Hobbs RM, Yi W, Alonzo E, et al. The BTB-zinc finger transcriptional regulator PLZF controls the development of invariant natural killer T cell effector functions. Nature immunology. 2008;9(9):1055-64.
157. Lazarevic V, Zullo AJ, Schweitzer MN, Staton TL, Gallo EM, Crabtree GR, et al. The gene encoding early growth response 2, a target of the transcription factor NFAT, is required for the development and maturation of natural killer T cells. Nature immunology. 2009;10(3):306-13.

158. Savage AK, Constantinides MG, Han J, Picard D, Martin E, Li B, et al. The transcription factor PLZF directs the effector program of the NKT cell lineage. Immunity. 2008;29(3):391-403.
159. Seiler MP, Mathew R, Liszewski MK, Spooner CJ, Barr K, Meng F, et al. Elevated and sustained expression of the transcription factors Egr1 and Egr2 controls NKT lineage differentiation in response to TCR signaling. Nature immunology. 2012;13(3):264-71.
160. Crosby CM, Kronenberg M. Tissue-specific functions of invariant natural killer T cells. Nature reviews Immunology. 2018;18(9):559-74.
161. Matsuda JL, Mallevaey T, Scott-Browne J, Gapin L. CD1d-restricted iNKT cells, the 'Swiss-Army knife' of the immune system. Current opinion in immunology. 2008;20(3):358-68.
162. Middendorp S, Nieuwenhuis EE. NKT cells in mucosal immunity. Mucosal immunology. 2009;2(5):393-402.
163. Gapin L. iNKT cell autoreactivity: what is 'self' and how is it recognized? Nature reviews Immunology. 2010;10(4):272-7.
164. Natori T, Morita M, Akimoto K, Koezuka Y. Agelasphins, novel antitumor and immunostimulatory cerebrosides from the marine sponge Agelas mauritianus. Tetrahedron. 1994;50(9):2771-84.
165. Schiefner A, Wilson IA. Presentation of lipid antigens by CD1 glycoproteins. Current pharmaceutical design. 2009;15(28):3311-7.
166. Siddiqui S, Visvabharathy L, Wang C-R. Role of Group 1 CD1-Restricted T Cells in Infectious Disease. Frontiers in Immunology. 2015;6:337.
167. Mori L, Lepore M, Libero GD. The Immunology of CD1- and MR1-Restricted T Cells. Annual Review of Immunology. 2016;34(1):479-510.
168. de Jong A. Activation of human T cells by CD1 and self-lipids. Immunological reviews. 2015;267(1):16-29.
169. Sutherland JS, Jeffries DJ, Donkor S, Walther B, Hill PC, Adetifa IMO, et al. High granulocyte/lymphocyte ratio and paucity of NKT cells defines TB disease in a TB-endemic setting. Tuberculosis. 2009;89(6):398-404.
170. Montoya CJ, Cataño JC, Ramirez Z, Rugeles MT, Wilson SB, Landay AL. Invariant NKT cells from HIV-1 or Mycobacterium tuberculosis-infected patients express an activated phenotype. Clinical Immunology. 2008;127(1):1-6.
171. Kee SJ, Kwon YS, Park YW, Cho YN, Lee SJ, Kim TJ, et al. Dysfunction of natural killer T cells in patients with active Mycobacterium tuberculosis infection. Infection and immunity. 2012;80(6):2100-8.
172. Gansert JL, Kieβler V, Engele M, Wittke F, Röllinghoff M, Krensky AM, et al. Human NKT Cells Express Granulysin and Exhibit Antimycobacterial Activity. The Journal of Immunology. 2003;170(6):3154.
173. Szereday L, Baliko Z, Szekeres-Bartho J. Gamma/delta T cell subsets in patients with active Mycobacterium tuberculosis infection and tuberculin anergy. Clinical and experimental immunology. 2003;131(2):287-91.
174. Roy S, Ly D, Castro CD, Li NS, Hawk AJ, Altman JD, et al. Molecular Analysis of Lipid-Reactive Vdelta1 gammadelta T Cells Identified by CD1c Tetramers. J Immunol. 2016;196(4):1933-42.
175. Luoma AM, Castro CD, Adams EJ. γδ T cell surveillance via CD1 molecules. Trends in immunology. 2014;35(12):613-21.
176. Sardinha LR, Elias RM, Mosca T, Bastos KR, Marinho CR, D'Império Lima MR, et al. Contribution of NK, NK T, gamma delta T, and alpha beta T cells to the gamma interferon response required for liver protection against Trypanosoma cruzi. Infection and immunity. 2006;74(4):2031-42.
177. Tikhonov I, Deetz CO, Paca R, Berg S, Lukyanenko V, Lim JK, et al. Human Vgamma2Vdelta2 T cells contain cytoplasmic RANTES. International immunology. 2006;18(8):1243-51.
178. Costa G, Loizon S, Guenot M, Mocan I, Halary F, de Saint-Basile G, et al. Control of Plasmodium falciparum erythrocytic cycle: γδ T cells target the red blood cell-invasive merozoites. Blood. 2011;118(26):6952-62.

179. Spada FM, Grant EP, Peters PJ, Sugita M, Melian A, Leslie DS, et al. Self-recognition of CD1 by gamma/delta T cells: implications for innate immunity. The Journal of experimental medicine. 2000;191(6):937-48.
180. Sparrow E, Bodman-Smith MD. Granulysin: The attractive side of a natural born killer. Immunology letters. 2020;217:126-32.
181. Todaro M, D'Asaro M, Caccamo N, Iovino F, Francipane MG, Meraviglia S, et al. Efficient killing of human colon cancer stem cells by gammadelta T lymphocytes. J Immunol. 2009;182(11):7287-96.
182. Wrobel P, Shojaei H, Schittek B, Gieseler F, Wollenberg B, Kalthoff H, et al. Lysis of a broad range of epithelial tumour cells by human gamma delta T cells: involvement of NKG2D ligands and T-cell receptor- versus NKG2D-dependent recognition. Scand J Immunol. 2007;66(2-3):320-8.
183. He Y, Wu K, Hu Y, Sheng L, Tie R, Wang B, et al. γδ T cell and other immune cells crosstalk in cellular immunity. Journal of immunology research. 2014;2014:960252.
184. Lawand M, Déchanet-Merville J, Dieu-Nosjean M-C. Key Features of Gamma-Delta T-Cell Subsets in Human Diseases and Their Immunotherapeutic Implications. Frontiers in immunology. 2017;8:761-.
185. Vantourout P, Hayday A. Six-of-the-best: unique contributions of γδ T cells to immunology. Nature reviews Immunology. 2013;13(2):88-100.
186. Bonneville M, O'Brien RL, Born WK. Gammadelta T cell effector functions: a blend of innate programming and acquired plasticity. Nature reviews Immunology. 2010;10(7):467-78.
187. Hayday AC. γδ T Cell Update: Adaptate Orchestrators of Immune Surveillance. J Immunol. 2019;203(2):311-20.
188. Kabelitz D, Lettau M, Janssen O. Immunosurveillance by human γδ T lymphocytes: the emerging role of butyrophilins. F1000Research. 2017;6:F1000 Faculty Rev-782.
189. Witherden DA, Havran WL. EPCR: a stress trigger for gammadelta T cells. Nature immunology. 2012;13(9):812-4.
190. Kabelitz D, Déchanet-Merville J. Recent advances in gamma/delta T cell biology: new ligands, new functions, and new translational perspectives. Frontiers in Immunology. 2015;6(371).
191. Harly C, Guillaume Y, Nedellec S, Peigne CM, Monkkonen H, Monkkonen J, et al. Key implication of CD277/butyrophilin-3 (BTN3A) in cellular stress sensing by a major human gammadelta T-cell subset. Blood. 2012;120(11):2269-79.
192. Gu S, Nawrocka W, Adams EJ. Sensing of Pyrophosphate Metabolites by Vγ9Vδ2 T Cells. Frontiers in Immunology. 2014;5:688.
193. Harly C, Peigne CM, Scotet E. Molecules and Mechanisms Implicated in the Peculiar Antigenic Activation Process of Human Vgamma9Vdelta2 T Cells. Front Immunol. 2014;5:657.
194. Groh V, Steinle A, Bauer S, Spies T. Recognition of stress-induced MHC molecules by intestinal epithelial gammadelta T cells. Science (New York, NY). 1998;279(5357):1737-40.
195. Willcox CR, Pitard V, Netzer S, Couzi L, Salim M, Silberzahn T, et al. Cytomegalovirus and tumor stress surveillance by binding of a human gammadelta T cell antigen receptor to endothelial protein C receptor. Nature immunology. 2012;13(9):872-9.
196. Janis EM, Kaufmann SH, Schwartz RH, Pardoll DM. Activation of gamma delta T cells in the primary immune response to Mycobacterium tuberculosis. Science (New York, NY). 1989;244(4905):713-6.
197. Lockhart E, Green AM, Flynn JL. IL-17 production is dominated by gammadelta T cells rather than CD4 T cells during Mycobacterium tuberculosis infection. J Immunol. 2006;177(7):4662-9.
198. Okamoto Yoshida Y, Umemura M, Yahagi A, O'Brien RL, Ikuta K, Kishihara K, et al. Essential role of IL-17A in the formation of a mycobacterial infection-induced granuloma in the lung. J Immunol. 2010;184(8):4414-22.
199. Li B, Rossman MD, Imir T, Oner-Eyuboglu AF, Lee CW, Biancaniello R, et al. Disease-specific changes in gammadelta T cell repertoire and function in patients with pulmonary tuberculosis. J Immunol. 1996;157(9):4222-9.
200. Ogongo P, Porterfield JZ, Leslie A. Lung Tissue Resident Memory T-Cells in the Immune Response to Mycobacterium tuberculosis. Front Immunol. 2019;10:992.

201. Gioia C, Agrati C, Casetti R, Cairo C, Borsellino G, Battistini L, et al. Lack of CD27-CD45RA-V gamma 9V delta 2+ T cell effectors in immunocompromised hosts and during active pulmonary tuberculosis. J Immunol. 2002;168(3):1484-9.
202. Follows GA, Munk ME, Gatrill AJ, Conradt P, Kaufmann SH. Gamma interferon and interleukin 2, but not interleukin 4, are detectable in gamma/delta T-cell cultures after activation with bacteria. Infection and immunity. 1992;60(3):1229-31.
203. Hoft DF, Brown RM, Roodman ST. Bacille Calmette-Guérin vaccination enhances human gamma delta T cell responsiveness to mycobacteria suggestive of a memory-like phenotype. J Immunol. 1998;161(2):1045-54.
204. Rojas RE, Chervenak KA, Thomas J, Morrow J, Nshuti L, Zalwango S, et al. Vdelta2+ gammadelta T cell function in Mycobacterium tuberculosis- and HIV-1-positive patients in the United States and Uganda: application of a whole-blood assay. The Journal of infectious diseases. 2005;192(10):1806-14.
205. Shen Y, Zhou D, Qiu L, Lai X, Simon M, Shen L, et al. Adaptive immune response of Vgamma2Vdelta2+ T cells during mycobacterial infections. Science (New York, NY). 2002;295(5563):2255-8.
206. Vorkas CK, Wipperman MF, Li K, Bean J, Bhattarai SK, Adamow M, et al. Mucosal-associated invariant and gammadelta T cell subsets respond to initial Mycobacterium tuberculosis infection. JCI insight. 2018;3(19).
207. Fowler DW, Copier J, Dalgleish AG, Bodman-Smith MD. Tripartite immune cell co-operation in the Bacillus Calmette Guérin-induced activation of γδ T cells. Immunol Cell Biol. 2013;91(7):461-8.
208. Fowler DW, Copier J, Wilson N, Dalgleish AG, Bodman-Smith MD. Mycobacteria activate γδ T-cell anti-tumour responses via cytokines from type 1 myeloid dendritic cells: a mechanism of action for cancer immunotherapy. Cancer Immunol Immunother. 2012;61(4):535-47.
209. Qaqish A, Huang D, Chen CY, Zhang Z, Wang R, Li S, et al. Adoptive Transfer of Phosphoantigen-Specific γδ T Cell Subset Attenuates Mycobacterium tuberculosis Infection in Nonhuman Primates. J Immunol. 2017;198(12):4753-63.
210. Forrester JM, Newman LS, Wang Y, King TE, Kotzin BL. Clonal expansion of lung V delta 1+ T cells in pulmonary sarcoidosis. Journal of Clinical Investigation. 1993;91(1):292-300.
211. Uyemura K DR, Band H, et al. Evidence for clonal selection of gamma/delta T cells in response to a human pathogen. The Journal of experimental medicine. 1991;174(3):683-92.
212. Negash M, Tsegaye A, Wassie L, Howe R. Phenotypic and functional heterogeneity of peripheral γδ T cells in pulmonary TB and HIV patients in Addis Ababa, Ethiopia. BMC Infectious Diseases. 2018;18(1):464.
213. La Manna MP, Orlando V, Tamburini B, Badami GD, Dieli F, Caccamo N. Harnessing Unconventional T Cells for Immunotherapy of Tuberculosis. Front Immunol. 2020;11:2107.
214. Rahimpour A, Koay HF, Enders A, Clanchy R, Eckle SB, Meehan B, et al. Identification of phenotypically and functionally heterogeneous mouse mucosal-associated invariant T cells using MR1 tetramers. The Journal of experimental medicine. 2015;212(7):1095-108.
215. Reantragoon R, Corbett AJ, Sakala IG, Gherardin NA, Furness JB, Chen Z, et al. Antigen-loaded MR1 tetramers define T cell receptor heterogeneity in mucosal-associated invariant T cells. The Journal of experimental medicine. 2013;210(11):2305-20.
216. Dusseaux M, Martin E, Serriari N, Péguillet I, Premel V, Louis D, et al. Human MAIT cells are xenobiotic-resistant, tissue-targeted, CD161hi IL-17-secreting T cells. Blood. 2011;117(4):1250-9.
217. Gold MC, Cerri S, Smyk-Pearson S, Cansler ME, Vogt TM, Delepine J, et al. Human mucosal associated invariant T cells detect bacterially infected cells. PLoS biology. 2010;8(6):e1000407.
218. Le Bourhis L, Martin E, Péguillet I, Guihot A, Froux N, Coré M, et al. Antimicrobial activity of mucosal-associated invariant T cells. Nature immunology. 2010;11(8):701-8.
219. Corbett AJ, Eckle SB, Birkinshaw RW, Liu L, Patel O, Mahony J, et al. T-cell activation by transitory neo-antigens derived from distinct microbial pathways. Nature. 2014;509(7500):361-5.
220. Hinks TSC, Marchi E, Jabeen M, Olshansky M, Kurioka A, Pediongco TJ, et al. Activation and In Vivo Evolution of the MAIT Cell Transcriptome in Mice and Humans Reveals Tissue Repair Functionality. Cell Rep. 2019;28(12):3249-62.e5.

221. Kjer-Nielsen L, Patel O, Corbett AJ, Le Nours J, Meehan B, Liu L, et al. MR1 presents microbial vitamin B metabolites to MAIT cells. Nature. 2012;491(7426):717-23.
222. Legoux F, Salou M, Lantz O. Unconventional or Preset αβ T Cells: Evolutionarily Conserved Tissue-Resident T Cells Recognizing Nonpeptidic Ligands. Annual review of cell and developmental biology. 2017;33:511-35.
223. Serriari NE, Eoche M, Lamotte L, Lion J, Fumery M, Marcelo P, et al. Innate mucosal-associated invariant T (MAIT) cells are activated in inflammatory bowel diseases. Clinical and experimental immunology. 2014;176(2):266-74.
224. Hashimoto K, Hirai M, Kurosawa Y. A gene outside the human MHC related to classical HLA class I genes. Science (New York, NY). 1995;269(5224):693-5.
225. Riegert P, Wanner V, Bahram S. Genomics, isoforms, expression, and phylogeny of the MHC class I-related MR1 gene. J Immunol. 1998;161(8):4066-77.
226. Gold MC, Eid T, Smyk-Pearson S, Eberling Y, Swarbrick GM, Langley SM, et al. Human thymic MR1-restricted MAIT cells are innate pathogen-reactive effectors that adapt following thymic egress. Mucosal immunology. 2013;6(1):35-44.
227. Jiang J, Wang X, An H, Yang B, Cao Z, Liu Y, et al. Mucosal-associated invariant T-cell function is modulated by programmed death-1 signaling in patients with active tuberculosis. American journal of respiratory and critical care medicine. 2014;190(3):329-39.
228. Sakala IG, Kjer-Nielsen L, Eickhoff CS, Wang X, Blazevic A, Liu L, et al. Functional Heterogeneity and Antimycobacterial Effects of Mouse Mucosal-Associated Invariant T Cells Specific for Riboflavin Metabolites. J Immunol. 2015;195(2):587-601.
229. Kwon YS, Cho YN, Kim MJ, Jin HM, Jung HJ, Kang JH, et al. Mucosal-associated invariant T cells are numerically and functionally deficient in patients with mycobacterial infection and reflect disease activity. Tuberculosis (Edinburgh, Scotland). 2015;95(3):267-74.
230. Van Kaer L, Wu L, Joyce S. Mechanisms and Consequences of Antigen Presentation by CD1. Trends in immunology. 2016;37(11):738-54.
231. Scharf L, Li NS, Hawk AJ, Garzon D, Zhang T, Fox LM, et al. The 2.5 A structure of CD1c in complex with a mycobacterial lipid reveals an open groove ideally suited for diverse antigen presentation. Immunity. 2010;33(6):853-62.
232. Moody DB, Suliman S. CD1: From Molecules to Diseases. F1000Research. 2017;6:1909.
233. Ly D, Moody DB. The CD1 size problem: lipid antigens, ligands, and scaffolds. Cellular and molecular life sciences : CMLS. 2014;71(16):3069-79.
234. Garzón D, Anselmi C, Bond PJ, Faraldo-Gómez JD. Dynamics of the Antigen-binding Grooves in CD1 Proteins: REVERSIBLE HYDROPHOBIC COLLAPSE IN THE LIPID-FREE STATE. The Journal of Biological Chemistry. 2013;288(27):19528-36.
235. Moody DB, Cotton RN. Four pathways of CD1 antigen presentation to T cells. Current opinion in immunology. 2017;46:127-33.
236. Adams EJ. Lipid presentation by human CD1 molecules and the diverse T cell populations that respond to them. Current opinion in immunology. 2014;26(Supplement C):1-6.
237. Dougan SK, Kaser A, Blumberg RS. CD1 expression on antigen-presenting cells. Current topics in microbiology and immunology. 2007;314:113-41.
238. Moody DB, Porcelli SA. Intracellular pathways of CD1 antigen presentation. Nature Reviews Immunology. 2003;3(1):11-22.
239. Sugita M, Grant EP, van Donselaar E, Hsu VW, Rogers RA, Peters PJ, et al. Separate pathways for antigen presentation by CD1 molecules. Immunity. 1999;11(6):743-52.
240. Barral DC, Cavallari M, McCormick PJ, Garg S, Magee AI, Bonifacino JS, et al. CD1a and MHC class I follow a similar endocytic recycling pathway. Traffic (Copenhagen, Denmark). 2008;9(9):1446-57.
241. Salamero J, Goud B, Bausinger H, Mieke Mommaas A, Lipsker D, Proamer F, et al. CD1a Molecules Traffic Through the Early Recycling Endosomal Pathway in Human Langerhans Cells11Presented in part at the 6th International Workshop on Langerhans Cells, New York, NY, U.S.A., 8–10 October 1999 (J Invest Dermatol 114:228 2000). Journal of Investigative Dermatology. 2001;116(3):401-8.

242. Sugita M, Cernadas M, Brenner MB. New insights into pathways for CD1-mediated antigen presentation. Current opinion in immunology. 2004;16(1):90-5.
243. Zajonc DM, Elsliger MA, Teyton L, Wilson IA. Crystal structure of CD1a in complex with a sulfatide self antigen at a resolution of 2.15 A. Nature immunology. 2003;4(8):808-15.
244. Fredman P, Månsson JE, Rynmark BM, Josefsen K, Ekblond A, Halldner L, et al. The glycosphingolipid sulfatide in the islets of Langerhans in rat pancreas is processed through recycling: possible involvement in insulin trafficking. Glycobiology. 2000;10(1):39-50.
245. Sandhoff R, Hepbildikler ST, Jennemann R, Geyer R, Gieselmann V, Proia RL, et al. Kidney sulfatides in mouse models of inherited glycosphingolipid disorders: determination by nano-electrospray ionization tandem mass spectrometry. J Biol Chem. 2002;277(23):20386-98.
246. Shamshiev A, Gober HJ, Donda A, Mazorra Z, Mori L, De Libero G. Presentation of the same glycolipid by different CD1 molecules. The Journal of experimental medicine. 2002;195(8):1013-21.
247. Vos JP, Lopes-Cardozo M, Gadella BM. Metabolic and functional aspects of sulfogalactolipids. Biochimica et biophysica acta. 1994;1211(2):125-49.
248. Rosat JP, Grant EP, Beckman EM, Dascher CC, Sieling PA, Frederique D, et al. CD1-restricted microbial lipid antigen-specific recognition found in the CD8+ alpha beta T cell pool. J Immunol. 1999;162(1):366-71.
249. Moody DB, Young DC, Cheng TY, Rosat JP, Roura-Mir C, O'Connor PB, et al. T cell activation by lipopeptide antigens. Science (New York, NY). 2004;303(5657):527-31.
250. Van Rhijn I, Zajonc DM, Wilson IA, Moody DB. T-cell activation by lipopeptide antigens. Current opinion in immunology. 2005;17(3):222-9.
251. Zajonc DM, Crispin MD, Bowden TA, Young DC, Cheng TY, Hu J, et al. Molecular mechanism of lipopeptide presentation by CD1a. Immunity. 2005;22(2):209-19.
252. Olivier M, Foret B, Le Vern Y, Kerboeuf D, Guilloteau LA. Plasticity of migrating CD1b+ and CD1b- lymph dendritic cells in the promotion of Th1, Th2 and Th17 in response to Salmonella and helminth secretions. PLoS One. 2013;8(11):e79537.
253. Sugita M, Jackman RM, van Donselaar E, Behar SM, Rogers RA, Peters PJ, et al. Cytoplasmic tail-dependent localization of CD1b antigen-presenting molecules to MIICs. Science (New York, NY). 1996;273(5273):349-52.
254. Briken V, Jackman RM, Watts GF, Rogers RA, Porcelli SA. Human CD1b and CD1c isoforms survey different intracellular compartments for the presentation of microbial lipid antigens. The Journal of experimental medicine. 2000;192(2):281-8.
255. Sugita M, Cao X, Watts GF, Rogers RA, Bonifacino JS, Brenner MB. Failure of trafficking and antigen presentation by CD1 in AP-3-deficient cells. Immunity. 2002;16(5):697-706.
256. Cheng TY, Relloso M, Van Rhijn I, Young DC, Besra GS, Briken V, et al. Role of lipid trimming and CD1 groove size in cellular antigen presentation. The EMBO journal. 2006;25(13):2989-99.
257. Shamshiev A, Donda A, Prigozy TI, Mori L, Chigorno V, Benedict CA, et al. The αβ T Cell Response to Self-Glycolipids Shows a Novel Mechanism of CD1b Loading and a Requirement for Complex Oligosaccharides. Immunity. 2000;13(2):255-64.
258. Gadola SD, Zaccai NR, Harlos K, Shepherd D, Castro-Palomino JC, Ritter G, et al. Structure of human CD1b with bound ligands at 2.3 A, a maze for alkyl chains. Nature immunology. 2002;3(8):721-6.
259. Moody DB, Zajonc DM, Wilson IA. Anatomy of CD1-lipid antigen complexes. Nature reviews Immunology. 2005;5(5):387-99.
260. Beckman EM, Porcelli SA, Morita CT, Behar SM, Furlong ST, Brenner MB. Recognition of a lipid antigen by CD1-restricted alpha beta+ T cells. Nature. 1994;372(6507):691-4.
261. Layre E, Collmann A, Bastian M, Mariotti S, Czaplicki J, Prandi J, et al. Mycolic acids constitute a scaffold for mycobacterial lipid antigens stimulating CD1-restricted T cells. Chemistry & biology. 2009;16(1):82-92.
262. Moody DB, Briken V, Cheng TY, Roura-Mir C, Guy MR, Geho DH, et al. Lipid length controls antigen entry into endosomal and nonendosomal pathways for CD1b presentation. Nature immunology. 2002;3(5):435-42.

263. Batuwangala T, Shepherd D, Gadola SD, Gibson KJ, Zaccai NR, Fersht AR, et al. The crystal structure of human CD1b with a bound bacterial glycolipid. J Immunol. 2004;172(4):2382-8.
264. Ly D, Kasmar AG, Cheng TY, de Jong A, Huang S, Roy S, et al. CD1c tetramers detect ex vivo T cell responses to processed phosphomycoketide antigens. The Journal of experimental medicine. 2013;210(4):729-41.
265. Mansour S, Tocheva AS, Cave-Ayland C, Machelett MM, Sander B, Lissin NM, et al. Cholesteryl esters stabilize human CD1c conformations for recognition by self-reactive T cells. Proceedings of the National Academy of Sciences of the United States of America. 2016;113(9):E1266-75.
266. Adams EJ. Diverse antigen presentation by the Group 1 CD1 molecule, CD1c. Molecular Immunology. 2013;55(2):182-5.
267. Roy S, Ly D, Li NS, Altman JD, Piccirilli JA, Moody DB, et al. Molecular basis of mycobacterial lipid antigen presentation by CD1c and its recognition by alphabeta T cells. Proceedings of the National Academy of Sciences of the United States of America. 2014;111(43):E4648-57.
268. Wun KS, Reijneveld JF, Cheng TY, Ladell K, Uldrich AP, Le Nours J, et al. T cell autoreactivity directed toward CD1c itself rather than toward carried self lipids. Nature immunology. 2018.
269. Mangtani P, Abubakar I, Ariti C, Beynon R, Pimpin L, Fine PE, et al. Protection by BCG vaccine against tuberculosis: a systematic review of randomized controlled trials. Clinical infectious diseases : an official publication of the Infectious Diseases Society of America. 2014;58(4):470-80.
270. Brutkiewicz RR. CD1d Ligands: The Good, the Bad, and the Ugly. The Journal of Immunology. 2006;177(2):769.
271. Lefèvre F, Rémy M-H, Masson J-M. Alanine-stretch scanning mutagenesis: a simple and efficient method to probe protein structure and function. Nucleic Acids Research. 1997;25(2):447-8.
272. Lee PUY, Churchill HRO, Daniels M, Jameson SC, Kranz DM. Role of 2c T Cell Receptor Residues in the Binding of Self–And Allo–Major Histocompatibility Complexes. The Journal of experimental medicine. 2000;191(8):1355.
273. Manning TC, Schlueter CJ, Brodnicki TC, Parke EA, Speir JA, Garcia KC, et al. Alanine scanning mutagenesis of an alphabeta T cell receptor: mapping the energy of antigen recognition. Immunity. 1998;8(4):413-25.
274. Borg NA, Ely LK, Beddoe T, Macdonald WA, Reid HH, Clements CS, et al. The CDR3 regions of an immunodominant T cell receptor dictate the 'energetic landscape' of peptide-MHC recognition. Nature immunology. 2005;6(2):171-80.
275. Chancellor A, Tocheva AS, Cave-Ayland C, Tezera L, White A, Al Dulayymi JR, et al. CD1b-restricted GEM T cell responses are modulated by Mycobacterium tuberculosis mycolic acid meromycolate chains. Proceedings of the National Academy of Sciences of the United States of America. 2017.
276. Gras S, Van Rhijn I, Shahine A, Cheng TY, Bhati M, Tan LL, et al. T cell receptor recognition of CD1b presenting a mycobacterial glycolipid. Nature communications. 2016;7:13257.
277. Wun KS, Borg NA, Kjer-Nielsen L, Beddoe T, Koh R, Richardson SK, et al. A minimal binding footprint on CD1d-glycolipid is a basis for selection of the unique human NKT TCR. The Journal of experimental medicine. 2008;205(4):939.
278. Smyth MS, Martin JH. x ray crystallography. Molecular pathology : MP. 2000;53(1):8-14.
279. Birkinshaw RW, Pellicci DG, Cheng TY, Keller AN, Sandoval-Romero M, Gras S, et al. alphabeta T cell antigen receptor recognition of CD1a presenting self lipid ligands. Nature immunology. 2015;16(3):258-66.
280. Shahine A, Reinink P, Reijneveld JF, Gras S, Holzheimer M, Cheng TY, et al. A T-cell receptor escape channel allows broad T-cell response to CD1b and membrane phospholipids. Nature communications. 2019;10(1):56.
281. Zuiderweg ERP. Mapping Protein−Protein Interactions in Solution by NMR Spectroscopy. Biochemistry. 2002;41(1):1-7.

282. Varani L, Bankovich AJ, Liu CW, Colf LA, Jones LL, Kranz DM, et al. Solution mapping of T cell receptor docking footprints on peptide-MHC. Proceedings of the National Academy of Sciences of the United States of America. 2007;104(32):13080-5.
283. Saline M, Rödström KEJ, Fischer G, Orekhov VY, Karlsson BG, Lindkvist-Petersson K. The structure of superantigen complexed with TCR and MHC reveals novel insights into superantigenic T cell activation. Nature communications. 2010;1:119.
284. Doherty PC, Topham DJ, Tripp RA. Establishment and persistence of virus-specific CD4+ and CD8+ T cell memory. Immunological reviews. 1996;150:23-44.
285. Altman JD, Moss PA, Goulder PJ, Barouch DH, McHeyzer-Williams MG, Bell JI, et al. Phenotypic analysis of antigen-specific T lymphocytes. Science (New York, NY). 1996;274(5284):94-6.
286. Sidobre S, Kronenberg M. CD1 tetramers: a powerful tool for the analysis of glycolipid-reactive T cells. Journal of Immunological Methods. 2002;268(1):107-21.
287. Wooldridge L, Lissina A, Cole DK, van den Berg HA, Price DA, Sewell AK. Tricks with tetramers: how to get the most from multimeric peptide–MHC. Immunology. 2009;126(2):147-64.
288. Nepom GT. MHC class II tetramers. Journal of immunology (Baltimore, Md : 1950). 2012;188(6):2477-82.
289. Matsuda JL, Naidenko OV, Gapin L, Nakayama T, Taniguchi M, Wang CR, et al. Tracking the response of natural killer T cells to a glycolipid antigen using CD1d tetramers. The Journal of experimental medicine. 2000;192(5):741-54.
290. Sidobre S, Kronenberg M. CD1 tetramers: a powerful tool for the analysis of glycolipid-reactive T cells. J Immunol Methods. 2002;268(1):107-21.
291. Altamirano MM, Woolfson A, Donda A, Shamshiev A, Briseño-Roa L, Foster NW, et al. Ligand-independent assembly of recombinant human CD1 by using oxidative refolding chromatography. Proceedings of the National Academy of Sciences. 2001;98(6):3288.
292. Kasmar AG, van Rhijn I, Cheng TY, Turner M, Seshadri C, Schiefner A, et al. CD1b tetramers bind alphabeta T cell receptors to identify a mycobacterial glycolipid-reactive T cell repertoire in humans. The Journal of experimental medicine. 2011;208(9):1741-7.
293. Van Rhijn I, Gherardin NA, Kasmar A, de Jager W, Pellicci DG, Kostenko L, et al. TCR bias and affinity define two compartments of the CD1b-glycolipid-specific T Cell repertoire. J Immunol. 2014;192(9):4054-60.
294. Van Rhijn I, Ly D, Moody DB. CD1a, CD1b, and CD1c in immunity against mycobacteria. Advances in experimental medicine and biology. 2013;783:181-97.
295. de Jong A, Cheng TY, Huang S, Gras S, Birkinshaw RW, Kasmar AG, et al. CD1a-autoreactive T cells recognize natural skin oils that function as headless antigens. Nature immunology. 2014;15(2):177-85.
296. Melandri D, Zlatareva I, Chaleil RAG, Dart RJ, Chancellor A, Nussbaumer O, et al. The gammadeltaTCR combines innate immunity with adaptive immunity by utilizing spatially distinct regions for agonist selection and antigen responsiveness. Nature immunology. 2018;19(12):1352-65.
297. Shahine A, Van Rhijn I, Cheng TY, Iwany S, Gras S, Moody DB, et al. A molecular basis of human T cell receptor autoreactivity toward self-phospholipids. Science immunology. 2017;2(16).
298. Cotton RN, Cheng TY, Wegrecki M, Le Nours J, Orgill DP, Pomahac B, et al. Human skin is colonized by T cells that recognize CD1a independently of lipid. J Clin Invest. 2021;131(1).
299. Reijneveld JF, Ocampo TA, Shahine A, Gully BS, Vantourout P, Hayday AC, et al. Human γδ T cells recognize CD1b by two distinct mechanisms. Proceedings of the National Academy of Sciences of the United States of America. 2020;117(37):22944-52.
300. Vincent MS, Xiong X, Grant EP, Peng W, Brenner MB. CD1a-, b-, and c-restricted TCRs recognize both self and foreign antigens. J Immunol. 2005;175(10):6344-51.
301. Van Rhijn I, van Berlo T, Hilmenyuk T, Cheng TY, Wolf BJ, Tatituri RV, et al. Human autoreactive T cells recognize CD1b and phospholipids. Proceedings of the National Academy of Sciences of the United States of America. 2016;113(2):380-5.

302. Porcelli S, Brenner MB, Greenstein JL, Balk SP, Terhorst C, Bleicher PA. Recognition of cluster of differentiation 1 antigens by human CD4-CD8-cytolytic T lymphocytes. Nature. 1989;341(6241):447-50.
303. Cardell S, Tangri S, Chan S, Kronenberg M, Benoist C, Mathis D. CD1-restricted CD4+ T cells in major histocompatibility complex class II-deficient mice. The Journal of experimental medicine. 1995;182(4):993-1004.
304. de Lalla C, Lepore M, Piccolo FM, Rinaldi A, Scelfo A, Garavaglia C, et al. High-frequency and adaptive-like dynamics of human CD1 self-reactive T cells. European journal of immunology. 2011;41(3):602-10.
305. Sieling PA, Jullien D, Dahlem M, Tedder TF, Rea TH, Modlin RL, et al. CD1 expression by dendritic cells in human leprosy lesions: correlation with effective host immunity. J Immunol. 1999;162(3):1851-8.
306. Ulrichs T, Moody DB, Grant E, Kaufmann SHE, Porcelli SA. T-Cell Responses to CD1-Presented Lipid Antigens in Humans with Mycobacterium tuberculosis Infection. Infection and immunity. 2003;71(6):3076-87.
307. Gilleron M, Stenger S, Mazorra Z, Wittke F, Mariotti S, Bohmer G, et al. Diacylated sulfoglycolipids are novel mycobacterial antigens stimulating CD1-restricted T cells during infection with Mycobacterium tuberculosis. The Journal of experimental medicine. 2004;199(5):649-59.
308. Moody DB, Reinhold BB, Guy MR, Beckman EM, Frederique DE, Furlong ST, et al. Structural requirements for glycolipid antigen recognition by CD1b-restricted T cells. Science (New York, NY). 1997;278(5336):283-6.
309. Sieling PA, Chatterjee D, Porcelli SA, Prigozy TI, Mazzaccaro RJ, Soriano T, et al. CD1-restricted T cell recognition of microbial lipoglycan antigens. Science (New York, NY). 1995;269(5221):227-30.
310. Lopez K, Iwany SK, Suliman S, Reijneveld JF, Ocampo TA, Jimenez J, et al. CD1b Tetramers Broadly Detect T Cells That Correlate With Mycobacterial Exposure but Not Tuberculosis Disease State. Frontiers in immunology. 2020;11:199-.
311. Montamat-Sicotte DJ, Millington KA, Willcox CR, Hingley-Wilson S, Hackforth S, Innes J, et al. A mycolic acid–specific CD1-restricted T cell population contributes to acute and memory immune responses in human tuberculosis infection. The Journal of Clinical Investigation. 2011;121(6):2493-503.
312. Beckman EM, Melián A, Behar SM, Sieling PA, Chatterjee D, Furlong ST, et al. CD1c restricts responses of mycobacteria-specific T cells. Evidence for antigen presentation by a second member of the human CD1 family. The Journal of Immunology. 1996;157(7):2795.
313. Moody DB, Ulrichs T, Muhlecker W, Young DC, Gurcha SS, Grant E, et al. CD1c-mediated T-cell recognition of isoprenoid glycolipids in Mycobacterium tuberculosis infection. Nature. 2000;404(6780):884-8.
314. Li S, Choi HJ, Felio K, Wang CR. Autoreactive CD1b-restricted T cells: a new innate-like T-cell population that contributes to immunity against infection. Blood. 2011;118(14):3870-8.
315. Raberger J, Schebesta A, Sakaguchi S, Boucheron N, Blomberg KEM, Berglöf A, et al. The transcriptional regulator PLZF induces the development of CD44 high memory phenotype T cells. Proceedings of the National Academy of Sciences of the United States of America. 2008;105(46):17919-24.
316. de Jong A, Peña-Cruz V, Cheng TY, Clark RA, Van Rhijn I, Moody DB. CD1a-autoreactive T cells are a normal component of the human αβ T cell repertoire. Nature immunology. 2010;11(12):1102-9.
317. Sugita M, Brenner MB. T lymphocyte recognition of human group 1 CD1 molecules: Implications for innate and acquired immunity. Seminars in Immunology. 2000;12(6):511-6.
318. Bai L, Picard D, Anderson B, Chaudhary V, Luoma A, Jabri B, et al. The majority of CD1d-sulfatide-specific T cells in human blood use a semiinvariant Vδ1 TCR. European journal of immunology. 2012;42(9):2505-10.

319. Luoma AM, Castro CD, Mayassi T, Bembinster LA, Bai L, Picard D, et al. Crystal structure of Vdelta1 T cell receptor in complex with CD1d-sulfatide shows MHC-like recognition of a self-lipid by human gammadelta T cells. Immunity. 2013;39(6):1032-42.
320. Uldrich AP, Le Nours J, Pellicci DG, Gherardin NA, McPherson KG, Lim RT, et al. CD1d-lipid antigen recognition by the gammadelta TCR. Nature immunology. 2013;14(11):1137-45.
321. Bukowski JF, Morita CT, Tanaka Y, Bloom BR, Brenner MB, Band H. V gamma 2V delta 2 TCR-dependent recognition of non-peptide antigens and Daudi cells analyzed by TCR gene transfer. The Journal of Immunology. 1995;154(3):998.
322. Jack F Bukowski CM, Hamid Band, Michael Brenner. Crucial Role of TCRγ Chain Junctional Region in Prenyl Pyrophosphate Antigen Recognition by γδ T Cells. J Immunol. 1998;161(1):286-93.
323. Xi X, Han X, Li L, Zhao Z. gammadelta T cells response to Mycobacterium tuberculosis in pulmonary tuberculosis patients using preponderant complementary determinant region 3 sequence. The Indian journal of medical research. 2011;134:356-61.
324. Faure F, Jitsukawa S, Miossec C, Hercend T. CD1c as a target recognition structure for human T lymphocytes: analysis with peripheral blood gamma/delta cells. European journal of immunology. 1990;20(3):703-6.
325. Russano AM, Bassotti G, Agea E, Bistoni O, Mazzocchi A, Morelli A, et al. CD1-restricted recognition of exogenous and self-lipid antigens by duodenal gammadelta+ T lymphocytes. J Immunol. 2007;178(6):3620-6.
326. Duhen T, Geiger R, Jarrossay D, Lanzavecchia A, Sallusto F. Production of interleukin 22 but not interleukin 17 by a subset of human skin-homing memory T cells. Nature immunology. 2009;10(8):857-63.
327. Trifari S, Kaplan CD, Tran EH, Crellin NK, Spits H. Identification of a human helper T cell population that has abundant production of interleukin 22 and is distinct from T(H)-17, T(H)1 and T(H)2 cells. Nature immunology. 2009;10(8):864-71.
328. Wolk K, Kunz S, Witte E, Friedrich M, Asadullah K, Sabat R. IL-22 increases the innate immunity of tissues. Immunity. 2004;21(2):241-54.
329. Wolk K, Sabat R. Interleukin-22: a novel T- and NK-cell derived cytokine that regulates the biology of tissue cells. Cytokine & growth factor reviews. 2006;17(5):367-80.
330. Boniface K, Guignouard E, Pedretti N, Garcia M, Delwail A, Bernard FX, et al. A role for T cell-derived interleukin 22 in psoriatic skin inflammation. Clinical and experimental immunology. 2007;150(3):407-15.
331. Felio K, Nguyen H, Dascher CC, Choi H-J, Li S, Zimmer MI, et al. CD1-restricted adaptive immune responses to Mycobacteria in human group 1 CD1 transgenic mice. The Journal of experimental medicine. 2009;206(11):2497-509.
332. Bagchi S, Li S, Wang CR. CD1b-autoreactive T cells recognize phospholipid antigens and contribute to antitumor immunity against a CD1b(+) T cell lymphoma. Oncoimmunology. 2016;5(9):e1213932.
333. Bagchi S, He Y, Zhang H, Cao L, Van Rhijn I, Moody DB, et al. CD1b-autoreactive T cells contribute to hyperlipidemia-induced skin inflammation in mice. J Clin Invest. 2017;127(6):2339-52.
334. Josefowicz SZ, Niec RE, Kim HY, Treuting P, Chinen T, Zheng Y, et al. Extrathymically generated regulatory T cells control mucosal Th2 inflammation. Nature. 2012;482(7385):395-9.
335. O'Donnell VB, Rossjohn J, Wakelam MJ. Phospholipid signaling in innate immune cells. J Clin Invest. 2018;128(7):2670-9.
336. Kaufmann SHE. Immunity to Intracellular Bacteria. Annual Review of Immunology. 1993;11(1):129-63.
337. Guo T, Koo MY, Kagoya Y, Anczurowski M, Wang CH, Saso K, et al. A Subset of Human Autoreactive CD1c-Restricted T Cells Preferentially Expresses TRBV4-1(+) TCRs. J Immunol. 2017.
338. Lepore M, Kalinichenko A, Calogero S, Kumar P, Paleja B, Schmaler M, et al. Functionally diverse human T cells recognize non-microbial antigens presented by MR1. eLife. 2017;6:e24476.

339. Roura-Mir C, Catálfamo M, Cheng T-Y, Marqusee E, Besra GS, Jaraquemada D, et al. CD1a and CD1c Activate Intrathyroidal T Cells during Graves' Disease and Hashimoto's Thyroiditis. The Journal of Immunology. 2005;174(6):3773.
340. Lebre MC, Jongbloed SL, Tas SW, Smeets TJ, McInnes IB, Tak PP. Rheumatoid arthritis synovium contains two subsets of CD83-DC-LAMP- dendritic cells with distinct cytokine profiles. The American journal of pathology. 2008;172(4):940-50.
341. Vincent MS, Leslie DS, Gumperz JE, Xiong X, Grant EP, Brenner MB. CD1-dependent dendritic cell instruction. Nature immunology. 2002;3:1163.
342. Sekiya M, Osuga J-i, Igarashi M, Okazaki H, Ishibashi S. The Role of Neutral Cholesterol Ester Hydrolysis in Macrophage Foam Cells. Journal of Atherosclerosis and Thrombosis. 2011;18(5):359-64.
343. Russell DG, Cardona P-J, Kim M-J, Allain S, Altare F. Foamy macrophages and the progression of the human tuberculosis granuloma. Nature immunology. 2009;10:943.
344. Pickl WF, Majdic O, Kohl P, Stöckl J, Riedl E, Scheinecker C, et al. Molecular and functional characteristics of dendritic cells generated from highly purified CD14+ peripheral blood monocytes. J Immunol. 1996;157(9):3850-9.
345. Zhou LJ, Tedder TF. CD14+ blood monocytes can differentiate into functionally mature CD83+ dendritic cells. Proceedings of the National Academy of Sciences of the United States of America. 1996;93(6):2588-92.
346. Leslie DS, Dascher CC, Cembrola K, Townes MA, Hava DL, Hugendubler LC, et al. Serum lipids regulate dendritic cell CD1 expression and function. Immunology. 2008;125(3):289-301.
347. Smed-Sörensen A, Moll M, Cheng T-Y, Loré K, Norlin A-C, Perbeck L, et al. IgG regulates the CD1 expression profile and lipid antigen-presenting function in human dendritic cells via FcgammaRIIa. Blood. 2008;111(10):5037-46.
348. Singh AK, Gupta UD. Animal models of tuberculosis: Lesson learnt. The Indian journal of medical research. 2018;147(5):456-63.
349. Vandamme TF. Use of rodents as models of human diseases. J Pharm Bioallied Sci. 2014;6(1):2-9.
350. Franzblau SG, DeGroote MA, Cho SH, Andries K, Nuermberger E, Orme IM, et al. Comprehensive analysis of methods used for the evaluation of compounds against Mycobacterium tuberculosis. Tuberculosis (Edinburgh, Scotland). 2012;92(6):453-88.
351. Irwin SM, Driver E, Lyon E, Schrupp C, Ryan G, Gonzalez-Juarrero M, et al. Presence of multiple lesion types with vastly different microenvironments in C3HeB/FeJ mice following aerosol infection with Mycobacterium tuberculosis. Dis Model Mech. 2015;8(6):591-602.
352. Apt A, Kramnik I. Man and mouse TB: contradictions and solutions. Tuberculosis (Edinburgh, Scotland). 2009;89(3):195-8.
353. Seok J, Warren HS, Cuenca AG, Mindrinos MN, Baker HV, Xu W, et al. Genomic responses in mouse models poorly mimic human inflammatory diseases. Proceedings of the National Academy of Sciences of the United States of America. 2013;110(9):3507-12.
354. Young D. Animal models of tuberculosis. European journal of immunology. 2009;39(8):2011-4.
355. Helke KL, Mankowski JL, Manabe YC. Animal models of cavitation in pulmonary tuberculosis. Tuberculosis. 2006;86(5):337-48.
356. Ordonez AA, Tasneen R, Pokkali S, Xu Z, Converse PJ, Klunk MH, et al. Mouse model of pulmonary cavitary tuberculosis and expression of matrix metalloproteinase-9. Dis Model Mech. 2016;9(7):779-88.
357. Hoff DR, Ryan GJ, Driver ER, Ssemakulu CC, De Groote MA, Basaraba RJ, et al. Location of intra- and extracellular M. tuberculosis populations in lungs of mice and guinea pigs during disease progression and after drug treatment. PloS one. 2011;6(3):e17550-e.
358. Kramnik I, Beamer G. Mouse models of human TB pathology: roles in the analysis of necrosis and the development of host-directed therapies. Seminars in immunopathology. 2016;38(2):221-37.
359. Eckhardt E, Bastian M. Animal models for human group 1 CD1 protein function. Mol Immunol. 2021;130:159-63.

360. Sada-Ovalle I, Sköld M, Tian T, Besra GS, Behar SM. Alpha-galactosylceramide as a therapeutic agent for pulmonary Mycobacterium tuberculosis infection. American journal of respiratory and critical care medicine. 2010;182(6):841-7.
361. Cambau E, Drancourt M. Steps towards the discovery of Mycobacterium tuberculosis by Robert Koch, 1882. Clinical microbiology and infection : the official publication of the European Society of Clinical Microbiology and Infectious Diseases. 2014;20(3):196-201.
362. Sakamoto K. The pathology of Mycobacterium tuberculosis infection. Veterinary pathology. 2012;49(3):423-39.
363. Lenaerts AJ, Hoff D, Aly S, Ehlers S, Andries K, Cantarero L, et al. Location of persisting mycobacteria in a Guinea pig model of tuberculosis revealed by r207910. Antimicrob Agents Chemother. 2007;51(9):3338-45.
364. Manabe YC, Dannenberg AM, Jr., Tyagi SK, Hatem CL, Yoder M, Woolwine SC, et al. Different strains of Mycobacterium tuberculosis cause various spectrums of disease in the rabbit model of tuberculosis. Infection and immunity. 2003;71(10):6004-11.
365. Kjellsson MC, Via LE, Goh A, Weiner D, Low KM, Kern S, et al. Pharmacokinetic evaluation of the penetration of antituberculosis agents in rabbit pulmonary lesions. Antimicrob Agents Chemother. 2012;56(1):446-57.
366. Dascher CC, Hiromatsu K, Naylor JW, Brauer PP, Brown KA, Storey JR, et al. Conservation of a CD1 multigene family in the guinea pig. J Immunol. 1999;163(10):5478-88.
367. Hiromatsu K, Dascher CC, Sugita M, Gingrich-Baker C, Behar SM, LeClair KP, et al. Characterization of guinea-pig group 1 CD1 proteins. Immunology. 2002;106(2):159-72.
368. Dascher CC, Hiromatsu K, Xiong X, Morehouse C, Watts G, Liu G, et al. Immunization with a mycobacterial lipid vaccine improves pulmonary pathology in the guinea pig model of tuberculosis. Int Immunol. 2003;15(8):915-25.
369. Larrouy-Maumus G, Layre E, Clark S, Prandi J, Rayner E, Lepore M, et al. Protective efficacy of a lipid antigen vaccine in a guinea pig model of tuberculosis. Vaccine. 2017;35(10):1395-402.
370. Kaushal D, Mehra S, Didier PJ, Lackner AA. The non-human primate model of tuberculosis. Journal of medical primatology. 2012;41(3):191-201.
371. Sharpe SA, Eschelbach E, Basaraba RJ, Gleeson F, Hall GA, McIntyre A, et al. Determination of lesion volume by MRI and stereology in a macaque model of tuberculosis. Tuberculosis. 2009;89(6):405-16.
372. Sharpe S, White A, Gleeson F, McIntyre A, Smyth D, Clark S, et al. Ultra low dose aerosol challenge with Mycobacterium tuberculosis leads to divergent outcomes in rhesus and cynomolgus macaques. Tuberculosis. 2016;96:1-12.
373. Javed S, Marsay L, Wareham A, Lewandowski KS, Williams A, Dennis MJ, et al. Temporal Expression of Peripheral Blood Leukocyte Biomarkers in a Macaca fascicularis Infection Model of Tuberculosis; Comparison with Human Datasets and Analysis with Parametric/Non-parametric Tools for Improved Diagnostic Biomarker Identification. PLoS One. 2016;11(5):e0154320.
374. Pena JC, Ho WZ. Monkey models of tuberculosis: lessons learned. Infection and immunity. 2015;83(3):852-62.
375. Lin PL, Rodgers M, Smith L, Bigbee M, Myers A, Bigbee C, et al. Quantitative comparison of active and latent tuberculosis in the cynomolgus macaque model. Infection and immunity. 2009;77(10):4631-42.
376. Layton ED, Barman S, Wilburn DB, Yu KKQ, Smith MT, Altman JD, et al. T Cells Specific for a Mycobacterial Glycolipid Expand after Intravenous Bacillus Calmette–Guérin Vaccination. The Journal of Immunology. 2021:ji2001065.
377. Morita D, Katoh K, Harada T, Nakagawa Y, Matsunaga I, Miura T, et al. Trans-species activation of human T cells by rhesus macaque CD1b molecules. Biochemical and Biophysical Research Communications. 2008;377(3):889-93.
378. Morita D, Hattori Y, Nakamura T, Igarashi T, Harashima H, Sugita M. Major T cell response to a mycolyl glycolipid is mediated by CD1c molecules in rhesus macaques. Infection and immunity. 2013;81(1):311-6.
379. Renshaw SA, Trede NS. A model 450 million years in the making: zebrafish and vertebrate immunity. Dis Model Mech. 2012;5(1):38-47.

380. Swaim LE, Connolly LE, Volkman HE, Humbert O, Born DE, Ramakrishnan L. Mycobacterium marinum infection of adult zebrafish causes caseating granulomatous tuberculosis and is moderated by adaptive immunity. Infection and immunity. 2006;74(11):6108-17.
381. Traver D, Herbomel P, Patton EE, Murphey RD, Yoder JA, Litman GW, et al. The zebrafish as a model organism to study development of the immune system. Advances in immunology. 2003;81:253-330.
382. Meijer AH, Spaink HP. Host-pathogen interactions made transparent with the zebrafish model. Current drug targets. 2011;12(7):1000-17.
383. Takaki K, Davis JM, Winglee K, Ramakrishnan L. Evaluation of the pathogenesis and treatment of Mycobacterium marinum infection in zebrafish. Nature protocols. 2013;8(6):1114-24.
384. Davis JM, Clay H, Lewis JL, Ghori N, Herbomel P, Ramakrishnan L. Real-time visualization of mycobacterium-macrophage interactions leading to initiation of granuloma formation in zebrafish embryos. Immunity. 2002;17(6):693-702.
385. Myllymäki H, Bäuerlein CA, Rämet M. The Zebrafish Breathes New Life into the Study of Tuberculosis. Frontiers in immunology. 2016;7:196-.
386. Benard EL, van der Sar AM, Ellett F, Lieschke GJ, Spaink HP, Meijer AH. Infection of zebrafish embryos with intracellular bacterial pathogens. J Vis Exp. 2012(61):3781.
387. Cosma CL, Swaim LE, Volkman H, Ramakrishnan L, Davis JM. Zebrafish and frog models of Mycobacterium marinum infection. Current protocols in microbiology. 2006;Chapter 10:Unit 10B.2.
388. Adams KN, Takaki K, Connolly LE, Wiedenhoft H, Winglee K, Humbert O, et al. Drug tolerance in replicating mycobacteria mediated by a macrophage-induced efflux mechanism. Cell. 2011;145(1):39-53.
389. Cronan MR, Tobin DM. Fit for consumption: zebrafish as a model for tuberculosis. Dis Model Mech. 2014;7(7):777-84.
390. Dascher CC. Evolutionary biology of CD1. Current topics in microbiology and immunology. 2007;314:3-26.
391. Wang C, Perera TV, Ford HL, Dascher CC. Characterization of a divergent non-classical MHC class I gene in sharks. Immunogenetics. 2003;55(1):57-61.
392. Luca S, Mihaescu T. History of BCG Vaccine. Mædica. 2013;8(1):53-8.
393. McShane H. Tuberculosis vaccines: beyond bacille Calmette–Guérin. Philosophical Transactions of the Royal Society B: Biological Sciences. 2011;366(1579):2782-9.
394. Calmette A. Preventive Vaccination Against Tuberculosis with BCG. Proc R Soc Med. 1931;24(11):1481-90.
395. Brosch R, Gordon SV, Garnier T, Eiglmeier K, Frigui W, Valenti P, et al. Genome plasticity of BCG and impact on vaccine efficacy. Proceedings of the National Academy of Sciences of the United States of America. 2007;104(13):5596-601.
396. Mostowy S, Tsolaki AG, Small PM, Behr MA. The in vitro evolution of BCG vaccines. Vaccine. 2003;21(27-30):4270-4.
397. Li J, Zhao A, Tang J, Wang G, Shi Y, Zhan L, et al. Tuberculosis vaccine development: from classic to clinical candidates. European Journal of Clinical Microbiology & Infectious Diseases. 2020;39(8):1405-25.
398. Glaziou P, Sismanidis C, Floyd K, Raviglione M. Global Epidemiology of Tuberculosis. Cold Spring Harbor Perspectives in Medicine. 2015;5(2):a017798.
399. Roy A, Eisenhut M, Harris RJ, Rodrigues LC, Sridhar S, Habermann S, et al. Effect of BCG vaccination against Mycobacterium tuberculosis infection in children: systematic review and meta-analysis. BMJ : British Medical Journal. 2014;349.
400. Trunz BB, Fine PEM, Dye C. Effect of BCG vaccination on childhood tuberculous meningitis and miliary tuberculosis worldwide: a meta-analysis and assessment of cost-effectiveness. The Lancet. 2006;367(9517):1173-80.
401. Rodrigues LC, Mangtani P, Abubakar I. How does the level of BCG vaccine protection against tuberculosis fall over time? BMJ (Clinical research ed). 2011;343:d5974.

402. Andersen P, Doherty TM. The success and failure of BCG - implications for a novel tuberculosis vaccine. Nature reviews Microbiology. 2005;3(8):656-62.
403. Kagina BM, Abel B, Scriba TJ, Hughes EJ, Keyser A, Soares A, et al. Specific T cell frequency and cytokine expression profile do not correlate with protection against tuberculosis after bacillus Calmette-Guerin vaccination of newborns. American journal of respiratory and critical care medicine. 2010;182(8):1073-9.
404. Andersen P, Kaufmann SHE. Novel vaccination strategies against tuberculosis. Cold Spring Harbor perspectives in medicine. 2014;4(6):a018523.
405. White AD, Sarfas C, West K, Sibley LS, Wareham AS, Clark S, et al. Evaluation of the Immunogenicity of Mycobacterium bovis BCG Delivered by Aerosol to the Lungs of Macaques. Clinical and vaccine immunology : CVI. 2015;22(9):992-1003.
406. Darrah PA, Zeppa JJ, Maiello P, Hackney JA, Wadsworth MH, 2nd, Hughes TK, et al. Prevention of tuberculosis in macaques after intravenous BCG immunization. Nature. 2020;577(7788):95-102.
407. Gallant CJ, Cobat A, Simkin L, Black GF, Stanley K, Hughes J, et al. Impact of age and sex on mycobacterial immunity in an area of high tuberculosis incidence. The international journal of tuberculosis and lung disease : the official journal of the International Union against Tuberculosis and Lung Disease. 2010;14(8):952-9.
408. Aguilo N, Gonzalo-Asensio J, Alvarez-Arguedas S, Marinova D, Gomez AB, Uranga S, et al. Reactogenicity to major tuberculosis antigens absent in BCG is linked to improved protection against Mycobacterium tuberculosis. Nature communications. 2017;8:16085.
409. Gonzalo-Asensio J, Aguilo N, Marinova D, Martin C. Breaking Transmission with Vaccines: The Case of Tuberculosis. Microbiol Spectr. 2017;5(4).
410. Marinova D, Gonzalo-Asensio J, Aguilo N, Martin C. MTBVAC from discovery to clinical trials in tuberculosis-endemic countries. Expert review of vaccines. 2017;16(6):565-76.
411. Spertini F, Audran R, Chakour R, Karoui O, Steiner-Monard V, Thierry AC, et al. Safety of human immunisation with a live-attenuated Mycobacterium tuberculosis vaccine: a randomised, double-blind, controlled phase I trial. The Lancet Respiratory medicine. 2015;3(12):953-62.
412. Hawkridge T, Scriba TJ, Gelderbloem S, Smit E, Tameris M, Moyo S, et al. Safety and immunogenicity of a new tuberculosis vaccine, MVA85A, in healthy adults in South Africa. The Journal of infectious diseases. 2008;198(4):544-52.
413. Stylianou E, Griffiths KL, Poyntz HC, Harrington-Kandt R, Dicks MD, Stockdale L, et al. Improvement of BCG protective efficacy with a novel chimpanzee adenovirus and a modified vaccinia Ankara virus both expressing Ag85A. Vaccine. 2015;33(48):6800-8.
414. Wilkie M, Satti I, Minhinnick A, Harris S, Riste M, Ramon RL, et al. A phase I trial evaluating the safety and immunogenicity of a candidate tuberculosis vaccination regimen, ChAdOx1 85A prime - MVA85A boost in healthy UK adults. Vaccine. 2020;38(4):779-89.
415. Perez-Martinez AP, Ong E, Zhang L, Marrs CF, He Y, Yang Z. Conservation in gene encoding Mycobacterium tuberculosis antigen Rv2660 and a high predicted population coverage of H56 multistage vaccine in South Africa. Infection, genetics and evolution : journal of molecular epidemiology and evolutionary genetics in infectious diseases. 2017;55:244-50.
416. Lin PL, Dietrich J, Tan E, Abalos RM, Burgos J, Bigbee C, et al. The multistage vaccine H56 boosts the effects of BCG to protect cynomolgus macaques against active tuberculosis and reactivation of latent Mycobacterium tuberculosis infection. J Clin Invest. 2012;122(1):303-14.
417. Luabeya AK, Kagina BM, Tameris MD, Geldenhuys H, Hoff ST, Shi Z, et al. First-in-human trial of the post-exposure tuberculosis vaccine H56:IC31 in Mycobacterium tuberculosis infected and non-infected healthy adults. Vaccine. 2015;33(33):4130-40.
418. Suliman S, Luabeya AKK, Geldenhuys H, Tameris M, Hoff ST, Shi Z, et al. Dose Optimization of H56:IC31 Vaccine for Tuberculosis-Endemic Populations. A Double-Blind, Placebo-controlled, Dose-Selection Trial. American journal of respiratory and critical care medicine. 2019;199(2):220-31.
419. Homolka S, Ubben T, Niemann S. High Sequence Variability of the ppE18 Gene of Clinical Mycobacterium tuberculosis Complex Strains Potentially Impacts Effectivity of Vaccine Candidate M72/AS01E. PloS one. 2016;11(3):e0152200-e.

420. Nabavinia MS, Naderi Nasab M, Meshkat Z, Derakhshan M, Khaje-Karamadini M. Construction of an Expression Vector Containing Mtb72F of Mycobacterium tuberculosis. Cell journal. 2012;14(1):61-6.
421. Skeiky YA, Alderson MR, Ovendale PJ, Guderian JA, Brandt L, Dillon DC, et al. Differential immune responses and protective efficacy induced by components of a tuberculosis polyprotein vaccine, Mtb72F, delivered as naked DNA or recombinant protein. J Immunol. 2004;172(12):7618-28.
422. Wood PL, Tippireddy S, Feriante J. Plasma lipidomics of tuberculosis patients: altered phosphatidylcholine remodeling. Future Science OA. 2017:FSO255.
423. Weiner J, 3rd, Parida SK, Maertzdorf J, Black GF, Repsilber D, Telaar A, et al. Biomarkers of inflammation, immunosuppression and stress with active disease are revealed by metabolomic profiling of tuberculosis patients. PLoS One. 2012;7(7):e40221.
424. Feng S, Du YQ, Zhang L, Zhang L, Feng RR, Liu SY. Analysis of serum metabolic profile by ultra-performance liquid chromatography-mass spectrometry for biomarkers discovery: application in a pilot study to discriminate patients with tuberculosis. Chinese medical journal. 2015;128(2):159-68.
425. Altamirano MM, Garcia C, Possani LD, Fersht AR. Oxidative refolding chromatography: folding of the scorpion toxin Cn5. Nature biotechnology. 1999;17(2):187-91.
426. Sharpe SA, McShane H, Dennis MJ, Basaraba RJ, Gleeson F, Hall G, et al. Establishment of an aerosol challenge model of tuberculosis in rhesus macaques and an evaluation of endpoints for vaccine testing. Clinical and vaccine immunology : CVI. 2010;17(8):1170-82.
427. Luciw PA, Oslund KL, Yang X-w, Adamson L, Ravindran R, Canfield DR, et al. Stereological analysis of bacterial load and lung lesions in nonhuman primates (rhesus macaques) experimentally infected with Mycobacterium tuberculosis. American Journal of Physiology - Lung Cellular and Molecular Physiology. 2011;301(5):L731-L8.
428. Aquino A, Graziani G, Franzese O, Prete SP, Bonmassar E, Bonmassar L, et al. Exogenous Control of the Expression of Group I CD1 Molecules Competent for Presentation of Microbial Nonpeptide Antigens to Human T Lymphocytes. Clinical and Developmental Immunology. 2011;2011:790460.
429. DeWitt WS, Yu KKQ, Wilburn DB, Sherwood A, Vignali M, Day CL, et al. A Diverse Lipid Antigen-Specific TCR Repertoire Is Clonally Expanded during Active Tuberculosis. J Immunol. 2018.
430. Riordan JF, McElvany KD, Borders CL, Jr. Arginyl residues: anion recognition sites in enzymes. Science (New York, NY). 1977;195(4281):884-6.
431. Rötzschke O, Lau JM, Hofstätter M, Falk K, Strominger JL. A pH-sensitive histidine residue as control element for ligand release from HLA-DR molecules. Proceedings of the National Academy of Sciences. 2002;99(26):16946.
432. Yin Y, Li Y, Mariuzza RA. Structural basis for self-recognition by autoimmune T-cell receptors. Immunological reviews. 2012;250(1):32-48.
433. Simms PE, Ellis TM. Utility of flow cytometric detection of CD69 expression as a rapid method for determining poly- and oligoclonal lymphocyte activation. Clinical and diagnostic laboratory immunology. 1996;3(3):301-4.
434. Cibrián D, Sánchez-Madrid F. CD69: from activation marker to metabolic gatekeeper. European journal of immunology. 2017;47(6):946-53.
435. Butler MO, Lee JS, Ansen S, Neuberg D, Hodi FS, Murray AP, et al. Long-lived antitumor CD8+ lymphocytes for adoptive therapy generated using an artificial antigen-presenting cell. Clinical cancer research : an official journal of the American Association for Cancer Research. 2007;13(6):1857-67.
436. José ES, Borroto A, Niedergang F, Alcover A, Alarcón B. Triggering the TCR Complex Causes the Downregulation of Nonengaged Receptors by a Signal Transduction-Dependent Mechanism. Immunity. 2000;12(2):161-70.
437. Van Rhijn I, Iwany SK, Fodran P, Cheng TY, Gapin L, Minnaard AJ, et al. CD1b-mycolic acid tetramers demonstrate T-cell fine specificity for mycobacterial lipid tails. European journal of immunology. 2017;47(9):1525-34.

438. de Jong A, Arce EC, Cheng TY, van Summeren RP, Feringa BL, Dudkin V, et al. CD1c presentation of synthetic glycolipid antigens with foreign alkyl branching motifs. Chemistry & biology. 2007;14(11):1232-42.
439. Matsunaga I, Bhatt A, Young DC, Cheng T-Y, Eyles SJ, Besra GS, et al. Mycobacterium tuberculosis pks12 Produces a Novel Polyketide Presented by CD1c to T Cells. The Journal of experimental medicine. 2004;200(12):1559-69.
440. Haig NA, Guan Z, Li D, McMichael A, Raetz CR, Xu XN. Identification of self-lipids presented by CD1c and CD1d proteins. J Biol Chem. 2011;286(43):37692-701.
441. Burugupalli S, Richardson MB, Williams SJ. Total synthesis and mass spectrometric analysis of a Mycobacterium tuberculosis phosphatidylglycerol featuring a two-step synthesis of (R)-tuberculostearic acid. Organic & biomolecular chemistry. 2017;15(35):7422-9.
442. Horvath SE, Daum G. Lipids of mitochondria. Progress in lipid research. 2013;52(4):590-614.
443. Porcelli SA, Modlin RL. The CD1 system: antigen-presenting molecules for T cell recognition of lipids and glycolipids. Annu Rev Immunol. 1999;17:297-329.
444. Dolton G, Tungatt K, Lloyd A, Bianchi V, Theaker SM, Trimby A, et al. More tricks with tetramers: a practical guide to staining T cells with peptide–MHC multimers. Immunology. 2015;146(1):11-22.
445. Kao C, Daniels MA, Jameson SC. Loss of CD8 and TCR binding to Class I MHC ligands following T cell activation. International Immunology. 2005;17(12):1607-17.
446. Sadeghi A, Ullenhag G, Wagenius G, Tötterman TH, Eriksson F. Rapid expansion of T cells: Effects of culture and cryopreservation and importance of short-term cell recovery. Acta Oncologica. 2013;52(5):978-86.
447. Rius C, Attaf M, Tungatt K, Bianchi V, Legut M, Bovay A, et al. Peptide-MHC Class I Tetramers Can Fail To Detect Relevant Functional T Cell Clonotypes and Underestimate Antigen-Reactive T Cell Populations. J Immunol. 2018;200(7):2263-79.
448. Lissina A, Ladell K, Skowera A, Clement M, Edwards E, Seggewiss R, et al. Protein kinase inhibitors substantially improve the physical detection of T-cells with peptide-MHC tetramers. J Immunol Methods. 2009;340(1):11-24.
449. Chattopadhyay N, Zastre J, Wong HL, Wu XY, Bendayan R. Solid lipid nanoparticles enhance the delivery of the HIV protease inhibitor, atazanavir, by a human brain endothelial cell line. Pharmaceutical research. 2008;25(10):2262-71.
450. Li D, Hong A, Lu Q, Gao GF, Jin B, Screaton GR, et al. A novel role of CD1c in regulating CD1d-mediated NKT cell recognition by competitive binding to Ig-like transcript 4. Int Immunol. 2012;24(11):729-37.
451. Rinne A, Blatter LA. A fluorescence-based assay to monitor transcriptional activity of NFAT in living cells. J Physiol. 2010;588(Pt 17):3211-6.
452. Di Marco Barros R, Roberts NA, Dart RJ, Vantourout P, Jandke A, Nussbaumer O, et al. Epithelia Use Butyrophilin-like Molecules to Shape Organ-Specific γδ T Cell Compartments. Cell. 2016;167(1):203-18.e17.
453. Bowyer G, Rampling T, Powlson J, Morter R, Wright D, Hill AVS, et al. Activation-induced Markers Detect Vaccine-Specific CD4$^+$ T Cell Responses Not Measured by Assays Conventionally Used in Clinical Trials. Vaccines (Basel). 2018;6(3):50.
454. Reiss S, Baxter AE, Cirelli KM, Dan JM, Morou A, Daigneault A, et al. Comparative analysis of activation induced marker (AIM) assays for sensitive identification of antigen-specific CD4 T cells. PloS one. 2017;12(10):e0186998-e.
455. Barham MS, Whatney WE, Khayumbi J, Ongalo J, Sasser LE, Campbell A, et al. Activation-Induced Marker Expression Identifies Mycobacterium tuberculosis-Specific CD4 T Cells in a Cytokine-Independent Manner in HIV-Infected Individuals with Latent Tuberculosis. ImmunoHorizons. 2020;4(10):573-84.
456. James CA, Xu Y, Aguilar MS, Jing L, Layton ED, Gilleron M, et al. CD4 and CD8 co-receptors modulate functional avidity of CD1b-restricted T cells. bioRxiv. 2020:2020.10.17.332072.
457. Elkington P, Tebruegge M, Mansour S. Tuberculosis: An Infection-Initiated Autoimmune Disease? Trends in immunology. 2016;37(12):815-8.

458. Gagliardi MC, Lemassu A, Teloni R, Mariotti S, Sargentini V, Pardini M, et al. Cell wall-associated alpha-glucan is instrumental for Mycobacterium tuberculosis to block CD1 molecule expression and disable the function of dendritic cell derived from infected monocyte. Cellular microbiology. 2007;9(8):2081-92.
459. Mariotti S, Teloni R, Iona E, Fattorini L, Giannoni F, Romagnoli G, et al. Mycobacterium tuberculosis subverts the differentiation of human monocytes into dendritic cells. European journal of immunology. 2002;32(11):3050-8.
460. Wen Q, Zhou C, Xiong W, Su J, He J, Zhang S, et al. MiR-381-3p Regulates the Antigen-Presenting Capability of Dendritic Cells and Represses Antituberculosis Cellular Immune Responses by Targeting CD1c. J Immunol. 2016;197(2):580-9.
461. Kawashima T, Norose Y, Watanabe Y, Enomoto Y, Narazaki H, Watari E, et al. Cutting edge: major CD8 T cell response to live bacillus Calmette-Guérin is mediated by CD1 molecules. J Immunol. 2003;170(11):5345-8.
462. Liu Y, Wang R, Jiang J, Cao Z, Zhai F, Sun W, et al. A subset of CD1c(+) dendritic cells is increased in patients with tuberculosis and promotes Th17cell polarization. Tuberculosis (Edinburgh, Scotland). 2018;113:189-99.
463. Del Gallo F, Lombardi G, Piccolella E, Gilardini Montani MS, Del Porto P, Pugliese O, et al. Increased autoreactive T cell frequency in tuberculous patients. International archives of allergy and applied immunology. 1990;91(1):36-42.
464. Tagirasa R, Parmar S, Barik MR, Devadas S, Basu S. Autoreactive T Cells in Immunopathogenesis of TB-Associated Uveitis. Investigative ophthalmology & visual science. 2017;58(13):5682-91.
465. Kumar BV, Ma W, Miron M, Granot T, Guyer RS, Carpenter DJ, et al. Human Tissue-Resident Memory T Cells Are Defined by Core Transcriptional and Functional Signatures in Lymphoid and Mucosal Sites. Cell reports. 2017;20(12):2921-34.
466. Yang Q, Zhang M, Chen Q, Chen W, Wei C, Qiao K, et al. Cutting Edge: Characterization of Human Tissue-Resident Memory T Cells at Different Infection Sites in Patients with Tuberculosis. The Journal of Immunology. 2020;204(9):2331.
467. Jubel JM, Barbati ZR, Burger C, Wirtz DC, Schildberg FA. The Role of PD-1 in Acute and Chronic Infection. Frontiers in immunology. 2020;11:487-.
468. Van Laethem F, Tikhonova AN, Singer A. MHC restriction is imposed on a diverse T cell receptor repertoire by CD4 and CD8 co-receptors during thymic selection. Trends in immunology. 2012;33(9):437-41.
469. Thedrez A, de Lalla C, Allain S, Zaccagnino L, Sidobre S, Garavaglia C, et al. CD4 engagement by CD1d potentiates activation of CD4+ invariant NKT cells. Blood. 2007;110(1):251-8.
470. Vincent MS, Gumperz JE, Brenner MB. Understanding the function of CD1-restricted T cells. Nature immunology. 2003;4(6):517-23.
471. Brennan PJ. Structure, function, and biogenesis of the cell wall of Mycobacterium tuberculosis. Tuberculosis (Edinburgh, Scotland). 2003;83(1-3):91-7.
472. Allan LL, Stax AM, Zheng DJ, Chung BK, Kozak FK, Tan R, et al. CD1d and CD1c expression in human B cells is regulated by activation and retinoic acid receptor signaling. J Immunol. 2011;186(9):5261-72.
473. Dzionek A, Fuchs A, Schmidt P, Cremer S, Zysk M, Miltenyi S, et al. BDCA-2, BDCA-3, and BDCA-4: three markers for distinct subsets of dendritic cells in human peripheral blood. J Immunol. 2000;165(11):6037-46.
474. Felio K, Nguyen H, Dascher CC, Choi HJ, Li S, Zimmer MI, et al. CD1-restricted adaptive immune responses to Mycobacteria in human group 1 CD1 transgenic mice. The Journal of experimental medicine. 2009;206(11):2497-509.
475. Stenger S, Modlin RL. T cell mediated immunity to Mycobacterium tuberculosis. Current opinion in microbiology. 1999;2(1):89-93.
476. Ferrero E, Biswas P, Vettoretto K, Ferrarini M, Uguccioni M, Piali L, et al. Macrophages exposed to Mycobacterium tuberculosis release chemokines able to recruit selected leucocyte subpopulations: focus on gammadelta cells. Immunology. 2003;108(3):365-74.

477. Huang D, Shen Y, Qiu L, Chen CY, Shen L, Estep J, et al. Immune Distribution and Localization of Phosphoantigen-Specific Vγ2Vδ2 T Cells in Lymphoid and Nonlymphoid Tissues in Mycobacterium tuberculosis Infection. Infection and immunity. 2008;76(1):426.
478. Flynn JL, Chan J, Lin PL. Macrophages and control of granulomatous inflammation in tuberculosis. Mucosal immunology. 2011;4(3):271-8.
479. Gideon HP, Phuah J, Myers AJ, Bryson BD, Rodgers MA, Coleman MT, et al. Variability in tuberculosis granuloma T cell responses exists, but a balance of pro- and anti-inflammatory cytokines is associated with sterilization. PLoS Pathog. 2015;11(1):e1004603.
480. Kelly H, Mandraju R, Coelho-dos-Reis JGA, Tsuji M. Effects of HIV-1-induced CD1c and CD1d modulation and endogenous lipid presentation on CD1c-restricted T-cell activation. BMC immunology. 2013;14:4-.
481. van 't Wout AB, Swain JV, Schindler M, Rao U, Pathmajeyan MS, Mullins JI, et al. Nef induces multiple genes involved in cholesterol synthesis and uptake in human immunodeficiency virus type 1-infected T cells. Journal of virology. 2005;79(15):10053-8.
482. Ono A, Freed EO. Plasma membrane rafts play a critical role in HIV-1 assembly and release. Proceedings of the National Academy of Sciences of the United States of America. 2001;98(24):13925-30.
483. Chazal N, Gerlier D. Virus entry, assembly, budding, and membrane rafts. Microbiology and molecular biology reviews : MMBR. 2003;67(2):226-37, table of contents.
484. Miner MD, Chang JC, Pandey AK, Sassetti CM, Sherman DR. Role of cholesterol in Mycobacterium tuberculosis infection. Indian journal of experimental biology. 2009;47(6):407-11.
485. Kim M-J, Wainwright HC, Locketz M, Bekker L-G, Walther GB, Dittrich C, et al. Caseation of human tuberculosis granulomas correlates with elevated host lipid metabolism. EMBO molecular medicine. 2010;2(7):258-74.
486. Nesbitt NM, Yang X, Fontan P, Kolesnikova I, Smith I, Sampson NS, et al. A thiolase of Mycobacterium tuberculosis is required for virulence and production of androstenedione and androstadienedione from cholesterol. Infection and immunity. 2010;78(1):275-82.
487. Martens GW, Arikan MC, Lee J, Ren F, Vallerskog T, Kornfeld H. Hypercholesterolemia impairs immunity to tuberculosis. Infection and immunity. 2008;76(8):3464-72.
488. Pandey AK, Sassetti CM. Mycobacterial persistence requires the utilization of host cholesterol. Proceedings of the National Academy of Sciences of the United States of America. 2008;105(11):4376-80.
489. Chen ZW. Immune regulation of γδ T cell responses in mycobacterial infections. Clinical immunology (Orlando, Fla). 2005;116(3):202-7.
490. Falini B, Flenghi L, Pileri S, Pelicci P, Fagioli M, Martelli MF, et al. Distribution of T cells bearing different forms of the T cell receptor gamma/delta in normal and pathological human tissues. J Immunol. 1989;143(8):2480-8.
491. Carvalho AC, Matteelli A, Airo P, Tedoldi S, Casalini C, Imberti L, et al. gammadelta T lymphocytes in the peripheral blood of patients with tuberculosis with and without HIV co-infection. Thorax. 2002;57(4):357-60.
492. Mangan BA, Dunne MR, O'Reilly VP, Dunne PJ, Exley MA, O'Shea D, et al. Cutting edge: CD1d restriction and Th1/Th2/Th17 cytokine secretion by human Vδ3 T cells. Journal of immunology (Baltimore, Md : 1950). 2013;191(1):30-4.
493. Layton ED, Yu KKQ, Smith MT, Scriba TJ, De Rosa SC, Seshadri C. Validation of a CD1b tetramer assay for studies of human mycobacterial infection or vaccination. Journal of Immunological Methods. 2018;458:44-52.
494. Prezzemolo T, Guggino G, La Manna MP, Di Liberto D, Dieli F, Caccamo N. Functional Signatures of Human CD4 and CD8 T Cell Responses to Mycobacterium tuberculosis. Front Immunol. 2014;5:180.
495. Wood R, Lawn SD, Caldwell J, Kaplan R, Middelkoop K, Bekker LG. Burden of new and recurrent tuberculosis in a major South African city stratified by age and HIV-status. PLoS One. 2011;6(10):e25098.

496. VACFA Vaccines for Africa. BCG & COVID-19 Implifactions for South Africa: University of Cape Town; 2020 [Available from: http://www.vacfa.uct.ac.za/news/bcg-vaccine-covid-19-implications-south-africa.
497. El Daker S, Sacchi A, Montesano C, Altieri AM, Galluccio G, Colizzi V, et al. An abnormal phenotype of lung Vγ9Vδ2 T cells impairs their responsiveness in tuberculosis patients. Cell Immunol. 2013;282(2):106-12.
498. Qin W, Hu L, Zhang X, Jiang S, Li J, Zhang Z, et al. The Diverse Function of PD-1/PD-L Pathway Beyond Cancer. Frontiers in Immunology. 2019;10(2298).
499. Elkington PT, Bateman AC, Thomas GJ, Ottensmeier CH. Implications of Tuberculosis Reactivation after Immune Checkpoint Inhibition. American journal of respiratory and critical care medicine. 2018;198(11):1451-3.
500. Tezera LB, Bielecka MK, Ogongo P, Walker NF, Ellis M, Garay-Baquero DJ, et al. Anti-PD-1 immunotherapy leads to tuberculosis reactivation via dysregulation of TNF-α. eLife. 2020;9:e52668.
501. Barber DL, Sakai S, Kudchadkar RR, Fling SP, Day TA, Vergara JA, et al. Tuberculosis following PD-1 blockade for cancer immunotherapy. Science translational medicine. 2019;11(475).
502. Elkington P, Lerm M, Kapoor N, Mahon R, Pienaar E, Huh D, et al. In Vitro Granuloma Models of Tuberculosis: Potential and Challenges. The Journal of infectious diseases. 2019;219(12):1858-66.
503. Fujita K, Terashima T, Mio T. Anti-PD1 Antibody Treatment and the Development of Acute Pulmonary Tuberculosis. Journal of thoracic oncology : official publication of the International Association for the Study of Lung Cancer. 2016;11(12):2238-40.
504. Tsai C-C, Chen J-H, Wang Y-C, Chang F-Y. Re-activation of pulmonary tuberculosis during anti-programmed death-1 (PD-1) treatment. QJM: An International Journal of Medicine. 2018;112(1):41-2.
505. Freeman GJ, Long AJ, Iwai Y, Bourque K, Chernova T, Nishimura H, et al. Engagement of the PD-1 immunoinhibitory receptor by a novel B7 family member leads to negative regulation of lymphocyte activation. The Journal of experimental medicine. 2000;192(7):1027-34.
506. Lázár-Molnár E, Scandiuzzi L, Basu I, Quinn T, Sylvestre E, Palmieri E, et al. Structure-guided development of a high-affinity human Programmed Cell Death-1: Implications for tumor immunotherapy. EBioMedicine. 2017;17:30-44.
507. Paquin-Proulx D, Costa PR, Terrassani Silveira CG, Marmorato MP, Cerqueira NB, Sutton MS, et al. Latent Mycobacterium tuberculosis Infection Is Associated With a Higher Frequency of Mucosal-Associated Invariant T and Invariant Natural Killer T Cells. Frontiers in Immunology. 2018;9(1394).
508. Li X, Polacino P, Garcia-Navarro R, Hu S-L, Tsuji M. Peripheral Blood Invariant Natural Killer T Cells of Pig-Tailed Macaques. PLOS ONE. 2012;7(10):e48166.
509. Kawano T, Cui J, Koezuka Y, Toura I, Kaneko Y, Motoki K, et al. CD1d-restricted and TCR-mediated activation of valpha14 NKT cells by glycosylceramides. Science (New York, NY). 1997;278(5343):1626-9.
510. Burdin N, Brossay L, Koezuka Y, Smiley ST, Grusby MJ, Gui M, et al. Selective ability of mouse CD1 to present glycolipids: alpha-galactosylceramide specifically stimulates V alpha 14+ NK T lymphocytes. J Immunol. 1998;161(7):3271-81.
511. Spada FM, Koezuka Y, Porcelli SA. CD1d-restricted recognition of synthetic glycolipid antigens by human natural killer T cells. The Journal of experimental medicine. 1998;188(8):1529-34.
512. Chackerian A, Alt J, Perera V, Behar SM. Activation of NKT Cells Protects Mice from Tuberculosis. Infection and immunity. 2002;70(11):6302-9.
513. Rout N, Else JG, Yue S, Connole M, Exley MA, Kaur A. Paucity of CD4+ Natural Killer T (NKT) Lymphocytes in Sooty Mangabeys Is Associated with Lack of NKT Cell Depletion after SIV Infection. PLOS ONE. 2010;5(3):e9787.
514. Rout N, Greene J, Yue S, O'Connor D, Johnson RP, Else JG, et al. Loss of Effector and Anti-Inflammatory Natural Killer T Lymphocyte Function in Pathogenic Simian Immunodeficiency Virus Infection. PLOS Pathogens. 2012;8(9):e1002928.

515. Ramachandran H, Laux J, Moldovan I, Caspell R, Lehmann PV, Subbramanian RA. Optimal Thawing of Cryopreserved Peripheral Blood Mononuclear Cells for Use in High-Throughput Human Immune Monitoring Studies. Cells. 2012;1(3):313-24.
516. Kawakami K, Yamamoto N, Kinjo Y, Miyagi K, Nakasone C, Uezu K, et al. Critical role of Valpha14+ natural killer T cells in the innate phase of host protection against Streptococcus pneumoniae infection. European journal of immunology. 2003;33(12):3322-30.
517. Joyee AG, Qiu H, Wang S, Fan Y, Bilenki L, Yang X. Distinct NKT cell subsets are induced by different Chlamydia species leading to differential adaptive immunity and host resistance to the infections. J Immunol. 2007;178(2):1048-58.
518. Motsinger A, Azimzadeh A, Stanic AK, Johnson RP, Van Kaer L, Joyce S, et al. Identification and simian immunodeficiency virus infection of CD1d-restricted macaque natural killer T cells. Journal of virology. 2003;77(14):8153-8.
519. group IEW. Validation of Analytical Procedures: Text and Methology Q2(R1) [PDF]. 2005 [updated November 2005. Available from: http://www.ich.org/fileadmin/Public_Web_Site/ICH_Products/Guidelines/Quality/Q2_R1/Step4/Q2_R1__Guideline.pdf.
520. Xu Y, Theobald V, Sung C, DePalma K, Atwater L, Seiger K, et al. Validation of a HLA-A2 tetramer flow cytometric method, IFNgamma real time RT-PCR, and IFNgamma ELISPOT for detection of immunologic response to gp100 and MelanA/MART-1 in melanoma patients. Journal of translational medicine. 2008;6:61-.